INVESTIGATIONS ON BEHAVIOUR OF PREFORMED FOAM CONCRETE USING TWO SYNTHETIC SURFACTANTS

A THESIS

submitted by

G. INDU SIVA RANJANI

for the award of the degree

of

DOCTOR OF PHILOSOPHY

BUILDING TECHNOLOGY AND CONSTRUCTION MANAGEMENT DIVISION
DEPARTMENT OF CIVIL ENGINEERING
INDIAN INSTITUTE OF TECHNOLOGY MADRAS
CHENNAI 600 036

APRIL 2011

THESIS CERTIFICATE

This is to certify that the thesis entitled "**INVESTIGATIONS ON THE BEHAVIOUR OF PREFORMED FOAM CONCRETE USING TWO SYNTHETIC SURFACTANTS "** submitted by **G. Indu Siva Ranjani** to the Indian Institute of Technology; Madras for the award of the degree of **Doctor of Philosophy** is a bonafide record of research work carried out by her under my supervision. The contents of this thesis, in full or in parts, have not been submitted to any other Institute or University for the award of any degree or diploma.

Chennai 600 036
Date:

Dr. K.Ramamurthy
(Research Guide)
Professor
B.T.&C.M. Division
Department of Civil Engineering
I.I.T. Madras

ACKNOWLEDGEMENTS

I am very happy to have worked as a doctoral research scholar at I.I.T Madras. I have great pleasure to warmly thank my research guide Prof. K. Ramamurthy for his guidance and support, which have enabled me in the completion of this research work. His enthusiasm, integral view, analytical skills and mission for providing only high quality work and not less have made a deep impression on me. I owe him for his dedication, generosity, patience in correcting and directing me in the path of research. I would like to place on record, my sincere appreciation to Dr. S.R. Gandhi, Head of the Department of Civil Engineering for all the administrative support and encouraging words. Also I extend my sincere thanks to Prof. K. Rajagopal former head of the department for all his valuable supports.

I also wish to place on record my sincere gratitude to Dr. C.P.Vendhan, Dr.Pratap Haridoss, and Dr. S.R. Satish Kumar who apart being members of my doctoral committee, have been most helpful in offering very useful and encouraging comments at various stages of my research work.

All the faculty members of the BT&CM Division – Prof. M.S. Mathews, Prof. A. Ramachandraiah, Prof. Ravindra Gettu, Dr. Manu Santhanam and Prof. K. N. Satyanarayana, Prof. Koshy Varghese and Dr. K. Ananthanarayanan have been very co-operative and displayed keen interest in my progress. I express my sincere thanks to all of them.

The staff of concrete lab will always have a special place in my heart for all the efforts they have put in towards the successful completion of my experimental work. Messers M. Soundarapandiyan, Murthy, Krishnan, Dhanasekaran, Ms. A. Malarvizhi, all have contributed their might. I am also thankful to all the staff members of the Civil Engineering Department Office, Stores section and DCF for their excellent cooperation.

I wish to thank Krishna, Premkumar, Palani, Premraj and Durga Prasad who admirably and unstintingly helped me physically through all the laboratory work.

I am also thankful to all my fellow research scholars Dr. E.K.K Nambiar, Dr. Glory joseph, Dr.Manikandan, Dr.Prakash, Dr.Ramesh, Dr.Jayasree, Dr.Senthil, Dr.Venkatesan, Dr. Uma, Geetha, Paul, Ganesh, Ashok Kumar, Rakesh, Rajesh, Rajasekar, Muthu Kumar, Vasugi, Manju Nair and many others- for all their encouragement and moral support. I wish to express special thanks to Sathyanarayanan for his timely help in my research.

Finally, I wish to express my indebtedness to my family members who have supported me in all possible ways. In particular, I wish to record my deepest appreciation for the important contribution made by my mother Surya, father Gandhi, my husband Saravanan and my son Surya Kailash by way of their boundless support, patience and understanding, during the course of this research work.

G. INDU SIVA RANJANI

ABSTRACT

KEYWORDS: Foam concrete, surfactants, compressive strength, density, water absorption, sorptivity, drying shrinkage, consistence, stability, response surface methodology, density ratio, air-void parameters, image analysis.

Foam concrete is a type of lightweight cellular concrete produced by introducing sufficient quantities of stable air pores into a neat cement paste, or fresh mortar consisting of cement paste and filler material. Most of the investigations on foamed concrete in the past have been confined to the evaluation of foamed concrete properties alone rather than on the foam itself which is more important to attain the desired properties of foamed concrete. The need for identifying affordable foaming agent and foam generator is essential to facilitate wider use of foamed concrete in India. Review of literature also reveals the fact that the availability of information on physical, mechanical and durability related properties of foamed concrete are limited. It is in this context that in depth studies on the evaluation of locally available materials which can constitute efficient foaming agents and on the effect of foaming agents on the foamed concrete properties are deemed necessary.

Foam was produced by aerating four commercially available synthetic surfactants viz; Sodium lauryl sulfate, Sodium lauryl ether sulfate, Sulfanol (ionic surfactants) and Cocodiethanolamide (non-ionic surfactant) using a laboratory-scale foam generator designed and developed at IIT Madras.

The first phase of the studies comprised of evaluation of characteristics of foam produced with four commercially available synthetic surfactants. Their suitability for producing foamed concrete was assessed with foamed cement paste as per ASTM C 796-97. Out of these, Sodium lauryl sulfate and Sodium lauryl ether sulfate have yielded relatively good results. Having identified their potential basic foaming characteristics, as a next step, the relative workability and strength behaviour of foam concrete produced using these two surfactants were studied.

To study the fresh state behaviour, as a first step, the narrow range of water-solids ratio and optimum dosage of superplasticiser (sp) required to produce a stable and workable foam concrete within ± 50 kg/m^3 of the design density was determined. As a next step, the workability of the mixes within the above range of water-solids ratio

(0.36 to 0.47 for mixes without sp and 0.315 to 0.46 for mixes with sp) was evaluated by spread in a flow table and flow in modified marsh cone. It is observed that for a constant water-solids ratio, the spread reduces and flow time increases with an increase in foam volume. A systematic study on the influence of variation in density of foam concrete on its mechanical properties namely compressive strength, split tensile strength and flexural strength of foam concrete was carried out. Though the addition of superplasticiser resulted in considerable reduction in water-solids ratio, it did not result in proportionate enhancement in strength indicating that the strength of foam concrete is mainly influenced by the characteristics and the volume of entrained air voids.

The air voids in foam concrete are characterized on the basis of volume, size distribution, shape and spacing and the influence of these parameters on density and strength of foam concrete are studied. The shape of the air voids as characterized based on its circularity were found to be the order of 0.8 indicating that practically most of the air-voids are nearly spherical. When compared to bubble size distribution in foam the void size distribution in foam concrete did not deviate significantly. Modified Rosin-Rammler distribution can be evaluated as a method providing easy means of describing the size distribution of air void and bubble in foam concrete and foam. All the air void parameters studied viz., size factors, shape factors and spacing factors are found to correlate well with strength and density. It is observed that the smaller and circular the voids, and larger the spacing between voids, the greater is the strength of foam concrete.

The movement of moisture through any porous building material has an important bearing on the durability of the material. Water absorption by complete immersion, sorptivity and shrinkage behavior was studied for mixes with different design densities. Sorption and shrinkage are observed to be lower than the corresponding base mixes (mortar without foam) for both the surfactants, the reduction being proportional to the amount of foam added. Hence the moisture movement in foam concrete depends on the pores in the paste content and not on the entrained air voids which are not interconnected. Also the effect of curing on the sorption behavior has been investigated and concluded that the sorptivity of air cured foam concrete is 2.5 times higher than that of water cured concrete.

Studies on exposure of foam concrete to sulphate environment (0.5 mass percent sodium sulphate and 0.424 mass percent magnesium sulphate representing severe exposure condition and 5 mass percent sodium sulphate and 4.24 mass percent magnesium sulphate representing very severe exposure condition as per ACI 318-99) were carried out. The effects of different concentrations of sodium and magnesium sulphate solutions on the durability of foam concrete were evaluated through the measurements of change in length, mass, strength and through chemical analysis. Irrespective of the concentration and type of sulphate environment, the expansion, strength and mass loss of foam concrete were observed to be lower than that of base mix (mortar without foam). The higher deterioration of base mix can be attributed to higher paste content which is more susceptible to permeation mechanism of sulphate ions. These results still need to be correlated with full scale, long term durability tests.

TABLE OF CONTENTS

Title **Page No.**

CHAPTER 1 INTRODUCTION

CHAPTER 2 REVIEW OF LITERATURE

Table of Contents (Contd.,) Page No.

CHAPTER 3 OBJECTIVES AND SCOPE OF THE PRESENT STUDY

CHAPTER 4 RELATIVE PERFORMANCE EVALUATION OF FOUR SYNTHETIC SURFACTANTS AS FOAMING AGENTS

Table of Contents (Contd.,) **Page No.**

CHAPTER 5 FRESH AND HARDENED PROPERTIES OF FOAM CONCRETE

CHAPTER 6 ANALYSIS OF AIR VOID SYSTEM IN FOAM CONCRETE USING IMAGE ANALYSIS TECHNIQUE

CHAPTER 7 SORPTION AND SHRINKAGE BEHAVIOUR OF FOAM CONCRETE

CHAPTER 8 BEHAVIOUR OF FOAM CONCRETE UNDER SULPHATE ENVIRONMENT

Table of Contents (Contd.,) **Page No.**

CHAPTER 9 CONCLUSIONS AND SCOPE FOR FURTHER WORK

LIST OF TABLES

List of Tables (Contd.) **Page No.**

LIST OF FIGURES

Figure No. **Title** **Page No.**

List of Figures (Contd.,) **Page No.**

List of Figures (Contd.,) **Page No.**

List of Figures (Contd.,) **Page No.**

List of Figures (Contd.,) **Page No.**

List of Figures (Contd.,) **Page No.**

List of Figures (Contd.,) **Page No.**

List of Figures (Contd.,) **Page No.**

List of Figures (Contd.,) **Page No.**

List of Figures (Contd.,) **Page No.**

List of Figures (Contd.,) **Page No.**

List of Figures (Contd.,) **Page No.**

List of Figures (Contd.,) **Page No.**

List of Figures (Contd.,) **Page No.**

NOTATIONS

$\overline{S}$	SO_3
i	cumulative volume absorbed per unit area of inflow surface,
l_2	final reading of length after 100 days
l_1	first reading of length
A	Al_2O_3
C	calcite ($CaCO_3$)
C_3S	tricalcium silicate
d	depth of penetration
Dexp	experimental density of foam concrete
do	constant
Dth	theoretical density of foam concrete
E	modulus of elasticity
f_c	compressive strength
f_t	split tensile strength
G	gypsum ($CaSO_4. 2H_2O$)
H	H_2O
L_d	original length of the specimen
M	MgO
$MgSO_4$	magnesium sulphate
N	Na_2O
n	slope
Na_2SO_4	sodium sulphate
P	portlandite ($Ca (OH)_2$)
p	probability
Q	quartz (SiO_2)
RR	cumulative % oversize
S	SiO_2
SO_4^{2-}	sulphate ion
Va	volume of air
V_f	volume of foam
Wc	weight of cement

W_f	weight of foam
Ws	weight of sand
w-s	water – solids ratio
W_{tw}	weight of total water including the water present in the foam
Wuf	unit weight of foam
x	bubble size
x_o	the position parameter
Yi	predicted response
β_1, β_2	regression coefficients
β_{11}, $\beta 22$	quadratic effects
β_{12}	interaction effect
βo	offset term
Δw	increase in weight with time
ρ	density of water
pi	constant (3.14)
γ_{dry}	dry density
γ_{cast}	cast density

CHAPTER 1

INTRODUCTION

1.1 GENERAL

In concrete construction a reduction in self weight of the structure is undoubtedly considered an advantage, if not a necessity in some cases. A saving of dead weight for a given live load capacity not only results in reduction of stresses through the life time of the structure but also creates additional saving through ease of handling and working, speed of fabrication and thus results in a reduced demand on energy during construction. Further more, lightweight concrete offers better thermal insulation, seismic resistance and fire protection than normal weight concrete.

1.2 LIGHTWEIGHT CONCRETE

Lightweight concrete can be made with a wide range of densities ranging from 300 kg/m^3 to 1850 kg/m^3. This offers ample scope for its selective use in modern building construction. The concrete can be made lighter only by including air in its composition. There are three different possibilities by which air can be entrained in concrete viz., (i) by replacing ordinary aggregate with porous aggregate (lightweight aggregate concrete), (ii) no fines concrete in which the finer sizes from the aggregate grading are omitted, and (iii) concrete with porous matrix by introducing gas/air bubbles in the mix (cellular concrete) (Lohaus and Pott, 2003). Out of these lightweight aggregate concrete and cellular concrete are most widely used. Natural light weight aggregates have limited applications because its production and marketing are largely local in scope. Artificial lightweight aggregates again involve heavy investment in terms of plant and equipment and high temperature (1300^{o}C) furnace for sintering. This would in addition mean substantial energy consumption. Also, it is possible to produce this material within a limited range of densities (1200 – 1800 kg/m^3). The cellular concrete which is characterised by incorporation of a homogenous void or cell structure throughout the material has low self weight (300 to 1800 kg/m^3), high workability (flowing and self compacting) and excellent thermal insulation properties which makes it attractive for many construction applications.

1.3 CELLULAR CONCRETE

There are a number of methods for producing the cell structure in cellular concrete. These include;

(i) Mechanical methods, where by air is entrained in the mixture by the high speed mixing of a cementitious slurry with a foaming agent (Mix foamed concrete) or where a stable, preformed air foam is blended into a pre-mixed slurry (Preformed foamed concrete).

(ii) Chemical methods, which depend upon admixtures that react chemically with each other or with certain compounds already present in the cementitious slurry to generate uniformly distributed gas bubbles throughout the mix. The most widely used agents in the commercial production of this “gas” concrete are Aluminium powder and hydrogen peroxide.

(iii) Excess water method where in pores are introduced by using excessive water proportion in the mortar, which after setting acquires a low density by evaporation of excess water and consequent formation of finely divided voids (microporites).

A subsequent disadvantage of gas concrete and microporites is the requirement of very expensive and inflexible autoclaved hardening process for better strength and low drying shrinkage and this limits its usage as precast units (Lohaus and Pott, 2003). The pore structure of gas concrete is also characterized by number of drawbacks viz.,; (i) presence of crack and connectivity and thus loss of structural closed porosity; (ii) ellipticity of gas pores which leads to an anisotropy of properties; (iii) disorganized matrix of different sizes of bubbles due either to agglomeration of aluminium powder paricles or to instability of cells; and (iv) difficulty in attaining precise control of density (Valore, 1954b; Malou et.al., 2002; Cabrillac, 2006). Hence when we need insitu concrete with porous matrix it is most promising to use foamed concrete which is a much more versatile material than aerated concrete.

1.4 FOAM CONCRETE

The most basic definition of foamed concrete is that it is “mortar with air bubbles in it”. The incorporation of air bubbles can be achieved by prefoaming or by mix foaming method. Prefoaming type foam concrete is mixed by preformed foams in cement slurry while mixed foaming type foamed concrete is mixed with surface active agent into cement slurry during mixing (Byun et. al., 1998). The advantages of preformed foaming method are (i) much lower foaming agent requirement and (ii) a close relationship between the amount of foaming agent used and air content in the mix (Valore 1954a; Byun et. al., 1998). Thus with preformed foam it is easier to reach a required air content than by foaming the mix (Weigler and Karl, 1980).

1.5 HISTORICAL BACKGROUND OF FOAM CONCRETE

Foam concrete has a surprisingly long history and was first patented in 1923, mainly for use as an insulation material. Although there is evidence that the Romans used air entrainers to decrease density, this was not really true foam concrete (Jones and McCarthy, 2005a). However, the lack of specialized materials and equipments, limited its use to small-scale projects. Significant improvements over the past 20 years in production equipment and better quality surfactants has enabled the use of foam concrete on a larger scale. It is now extensively used in Netherland, Sweden, Germany, Switzerland, USA and UK (Cox and VanDijk, 2002). In India, foam concrete manufactured based on technology of Neopor of Germany is being utilized for making cellular lightweight blocks and panels for the construction of load bearing cum partition walls (Singh, 2002).

1.6 APPLICATIONS OF FOAM CONCRETE

Foamed concrete finds application in many areas, generally as a function of its relatively lightweight and its beneficial properties of ease in placement and manufacture (Beningfield et al., 2005). The most obvious advantage of foam concrete is its low density which economises the design of supporting structures including the foundation and walls of lower floors and thus finds application in earthquake proof structures (Hamidah et al., 2005). Foam concrete can be produced right on the spot of construction, which is attributed to the available portable foam generators

(Liew, 2005). Proper exercise of control in accurate dosage of foam enables production of wide range of controlled densities of foamed concrete from 400 to 1800 kg/m^3 (Basiurski and Wells, 2001) thereby offering flexibility in manufacturing products for specific applications viz., structural, partition, insulation and filling grades. Foam concrete has excellent thermal insulation properties due to its porous system which make it an ideal material for roofing insulation. Thus, foam concrete is an energy-efficient material and for this reason, it is a potential material in cases where strength is required along with thermal insulation. Another significant advantage of foam concrete is its ability to absorb industrial waste, like fly ash as one of its constituent material, in large quantities. It thus serves as an effective and efficient method of waste utilization. Moreover, acting as a highly competitive substitute for the clay bricks, it is helping to save depletion of fertile top soil being used for brick making.

1.7 MOTIVATION FOR RESEARCH

Currently foam concrete production is one of the most prospective and energy saving development direction in building materials industry. Therefore forming new ways for further development of foam concrete production and overcoming the available difficulties predetermine the necessity of this research. The need for identifying affordable foaming agent and foam generator is essential to facilitate wider use of foamed concrete in India. Also for the identified foaming agents, the optimization of foam production parameters is essential since the quality of foam will have considerable bearing on final strength of foamed concrete. The use of foam concrete for structural application has not gained the confidence of the industry because of the limited data available in this direction and this necessitates studies on properties of foam concrete which could affect its structural behaviour. Review of literature also reveals the fact that the availability of information on physical, mechanical and durability related properties of foamed concrete are limited. It is in this context that in depth studies on the evaluation of a few locally available materials which can constitute efficient foaming agents and on the effect of foaming agents on the foamed concrete properties are deemed necessary.

1.8 ORGANISATION OF THE THESIS

A general introduction of lightweight concrete and its classification, highlighting foam concrete and its applications along with motivation for present study have been presented in the preceding sections. A critical review of literature on foam concrete with a special emphasis on materials, production methods, physical, mechanical and functional properties is presented in Chapter 2. Chapter 3 defines the objectives and scope of the present study.

Chapter 4 describes the assessment of relative performance of four synthetic surfactants in terms of suitability for use in foam concrete production based on ASTM test method using Response Surface Methodology. The surfactant concentration and foam generation pressure required to produce stable foam is presented first. As a next step, the behaviour of the foam in cement slurry is reported, which established the stability of the foam in the mix. Two surfactants viz., Sodium lauryl sulfate and Sodium lauryl ether sulfate yielded relatively good results. Having identified the two potential foaming agents, the relative workability and strength characteristics of foam concrete produced using these two surfactants are reported in Chapter 5. An extensive study made on the influence of parameters namely foam volume and water-solids ratio on various fresh and hardened state properties namely stability, consistence and strength behavior of foam concrete produced with two synthetic surfactants is also presented in this chapter. Investigations on the air-void structures of foam concrete using image analysis technique form the first part of Chapter 6. Characterization of air-void parameters and its influence on strength and density are also discussed in this chapter. Experimental investigations on the moisture movement related characteristics like water absorption, hydraulic sorptivity and shrinkage of foam concrete are presented in Chapter 7. The behaviour of foam concrete under sulphate environment through variation in length, compressive strength and mass with duration of exposure are presented in Chapter 8. The conclusions of this research work and scope for further studies forms Chapter 9.

CHAPTER 2

REVIEW OF LITERATURE

2.1 GENERAL

Foam concrete is either a cement paste or mortar, classified as lightweight concrete, in which air-voids are entrapped in the mortar mix by means of suitable foaming agent. Broadly speaking foam concrete falls into the group of cellular concrete. Its key attributes are its high flowability, low self weight, minimal consumption of aggregate, low strength and excellent thermal insulation properties. Since the entrained air with the help of foam reduces the density of concrete, the foamed concrete density would naturally depend on the extent of foam injected into the slurry. By proper exercise of control in accurate dosage of foam wide range of controlled densities of foamed concrete from 400 to 1800 kg/m^3 can be obtained and thereby offering flexibility in manufacturing products for specific applications (structural, partition, insulation and filling grades). Foam concrete is relatively homogeneous when compared to normal concrete, as it does not contain the coarse aggregate phase, yet shows a vast variation in its properties. The properties of foam concrete depend on its composition and air-void system. Although the material was first patented in 1923 (Valore 1954a), its construction applications as lightweight non- or semi structural material are increasing during the last few years. The first comprehensive review on cellular concrete was presented by Valore (1954a, 1954b) and a detailed treatment by Rudnai (1963) and Short and Kinniburgh (1963), summerising the composition, properties and uses of cellular concrete, irrespective of the method of formation of the cell structure. Recently, Jones and McCarthy (2005a) have reviewed the history of use of foam concrete, constituent materials used, its properties, and construction application including some projects carried out worldwide. The functional properties like fire resistance, thermal conductivity and acoustical properties are also included in these reviews while the data on fresh state properties, durability and air-void system of foam concrete are rather limited. The production of stable foam concrete mix depends on many factors viz., selection of foaming agent, method of foam preparation and addition for uniform air-voids distribution, materials selection and mixture design strategies, production of foam concrete, and performance with respect to fresh and hardened state are of greater significance (Ramamurthy et al., 2009). With the above aspects in view, this chapter classifies the studies on foam concrete related to its constituent materials, mix proportioning, production and fresh state and hardened properties.

2.2 CONSTITUENT MATERIALS

2.2.1 Base Mix Constituents

In addition to Ordinary Portland cement, Rapid hardening Portland cement (De Rose and Morris, 1999; Kearsley and Wainwright, 2001a), high alumina and calcium sulfoaluminate (Turner, 2001) have been used for reducing the setting time and to improve early strength of foam concrete. Fly ash (Kearsley and Wainwright, 2001a; Papayianni and Milud, 2005; Jones and McCarthy, 2005 a, b, c, 2006) and ground granulated blast furnace slag have been used in the range of 30-70% and 10-50%, respectively (Pickford and Crompton, 1996; Wee et al., 2006) as cement replacement to reduce cost, enhance consistence of mix and to reduce heat of hydration while contributing towards long term strength. Silica fume up to 10% by mass of cement has been added to intensify the strength of cement (Kearsley, 1996; Byun et al., 1998; Fujiwara et al., 1995). Alternate fine aggregates, viz., fly ash (Jones et. al., 2003; Durack and Weiqing, 1998; Nambiar and Ramamurthy, 2006a), lime (De Rose and Morris, 1999) , chalk and crushed concrete (Aldridge and Ansell, 2001), incinerator bottom ash, recycled glass, foundry sand and quarry finer (Jones et. al., 2005), expanded polystyrene and Lytag fines (Van Deijk, 1991; Lee et al, 2005) were used either to reduce the density of foam concrete and/or to use waste/recycled materials. Concrete with densities between 800 and 1200 kg/m^3 have been produced using lightweight coarse aggregate in foamed cement matrix (Regan and Arasteh, 1990).

The water requirement for a mix depends upon the composition and use of admixtures and is governed by the consistency and stability of the mix (Karl and Worner, 1993). At lower water content, the mix is too stiff causing bubbles to break while a high water content make the mix too thin to hold the bubbles leading to separation of bubbles from the mix and thus segregation (Nambiar and Ramamurthy, 2006a). Water-cement ratio used ranges from 0.4 to 1.25 (Srivastava, 1977; Kearsley, 1996). Though superplasticisers are also sometimes used (Jones, 2001), its use in foamed concrete can be a possible reason for instability in the foam (Jones and McCarthy, 2006) and hence compatibility of admixtures with foam concrete is of importance.

Chopped polypropylene fibres of 12 mm length in the dosage of 1-3 kg/m^3 have been reported to enhance the shear behavior of foam concrete equivalent to that of normal concrete. Also the usage of fibres is reported to mitigate brittleness, while reducing its weight and cost (Kearsley and Mostert, 1997; Kearsley, 1999; Jones and McCarthy, 2005a). Optimum combinations of strength, ductility, density, workability and also cost can be obtained by selecting a suitable fiber type, air content and w/c ratio of base mortar (Yamamoto et al., 1999).

2.2.2 Foam

The importance of foam within any foamed material cannot be over emphasized and is of particular importance when producing foamed materials for structural uses and mass void infills. The foam that is added to the base material must be capable of remaining stable and not collapsing during pumping, placement and curing (Aldridge, 2005). It is therefore important to understand the basic characteristics of foam to attain the desired properties of foamed concrete. An overview of salient literature pertaining to various properties of foam and foaming agents are presented.

Foaming agents can be either natural or synthetic based. Natural material-based foaming agents commonly used are vegetable or animal glue, hydrolysed protein such as keratin, cattle hooves and fish scales, saponified wood resin stabilised with animal glue, soy protein foaming agents and glues, dried animal blood proteins that hydrolyse and saponin and easein. Some of the synthetical agents are detergents, alkylated naphthalene sulfonate and degenerated glue, butylated naphthalene sulfonate and water glass, and isopropylated naphthalene sulfonate, certain sulphates of petroleum derivatives and calcium chloride (Valore, 1954a). Sodium lauryl sulfate is one of the commonly used surfactant in detergent industry. This has been used in the concentration range of 0.1 to 0.4% in the production of foamed gypsum of density less than 1000 kg/m^3 (Colak, 2000). When Sodium lauryl sulfate is ethoxylated it forms Sodium lauryl ether sulfate with enhanced foaming properties. Cocodiethanolamide is an alkanolamide and imparts excellent viscosity enhancing and foam stabilization in anionic based system. Surfactant mixture of 2% Sulfonol as foaming agent and 0.3% bone glue hydrosolution as stabilizer in the ratio 1:0.15 can produce stable foam (Laukaitis et al, 2005). The relative performance of foam produced with the four synthetic surfactants viz., Sodium lauryl sulfate, Sodium lauryl ether sulfate, Sulfanol, Cocodiethanolamide have been assessed in terms of suitability for use in foam concrete production based on ASTM test method (Ranjani and Ramamurthy, 2010). Foam produced with high purity hydoxy silicon ester has been used in the manufacture of low density cement composites (Park et al, 1999a). Apart from above mentioned agents, alkaline tar solution (ATS) produced by dissolving the tar obtained from pyrolyzed baggase in sodium hydroxide solution exhibited surface active properties (Perez and Cortez, 1997).

Most of the earlier studies have used proprietary foaming agents, viz., Neopor (Hunaiti, 1996, 97), Mearlcrete (McCormick, 1967), Elastizell (Richard 1975, 77), and Foamtech (Kearsley and Wainwright, 2001a, b, 02a, b). All the surfactants used are basically amphiphiles having both hydrophilic and hydrophobic group. This bifunctionality in one molecule provides the basic properties to act as foaming agent. The hydrophilic group may be charged (ionic surfactants) or uncharged (nonionic surfactants). Depending on the nature of hydrophilic group (charge), the surfactants can be classified as anion active foaming agents and cation active foaming agents. Ionic surfactants can contribute to foam formation and stabilization as a result of the presence at the interface of an electrical double layer that can interact with the opposing interface in the form of the disjoining pressure. Nonionic surfactants generally produce less initial foam and less stable foam than ionics in aqueous solution (Myers, 1998).

Foam concrete is produced either by pre-foaming method or mixed foaming method. Pre-foaming method comprises of producing base mix and stable preformed aqueous foam separately and then thoroughly blending foam into base mix. In mixed foaming, the surface active agent is mixed along with base mix ingredients and during the process of mixing, foam is produced resulting in cellular structure in concrete (Byun et al., 1998). The foam must be firm and stable so that it resists the pressure of the mortar until the cement takes its initial set and a strong skeleton of concrete is built up around the void filled with air (Koudriashoff, 1949). The preformed foam that is blended with the base materials can be either wet or dry foam, the method of production and stability characteristics of such foams are discussed by Aldridge (2005). The wet foam is produced by spraying a solution of foaming agent over a fine mesh, has 2-5 mm bubble size and is relatively less stable. Dry foam is produced by forcing a diluted foaming agent through a series of high-density restrictions and forcing compressed air simultaneously into a mixing chamber. Compared to wet foam, the dry foam is extremely stable and has size smaller than 1 mm, which makes it easier for blending with the base materials for producing a pump able foam concrete.

Based on kinetics (degree of stability) there are three classes of foam namely unstable, metastable and solid foams. Unstable (low persistence) foams as their name implies, remain for a very short time .The lifetime of these foams ranges from several seconds to about 20 seconds. Metastable foam possess a persistence from few seconds to months. They are stabilized by the presence of surface active materials at the liquid/gas interface. Solid foams could be considered as thermodynamically stable since they possess a mechanically rigid structure formed as a result of irreversible chemical process during or just after foam formation (Myers, 1998).

Factors influencing foam stability as identified by various researchers are:
i) high viscosity of liquid phase which retards drainage of the liquid from between the bubble interfaces as well as provides a cushion effect to absorb the shock resulting from random or induced motion (Pugh, 1996; Hutzler et al., 2005).

ii) a high surface viscosity which also retard drainage by a viscous drag type of mechanism and dampens the film deformation prior to bubble collapse (Myers, 1998).

iii) Surface effects such as Gibbs and Marangoni effects which act to “heal” areas of film thinning due to liquid loss. The surface tension will decrease as the concentration of the surface active material in solution increases up to its Critical Micelle Concentration (the Gibbs effect). Second, there is a finite time requirement during which the surface active molecules in the bulk solution must diffuse to the interface in order to lower the surface tension (the Marangoni effect). Not only the concentration of surfactants and their rate of diffusion at the air water interface influence foam stability, but also their ability to attach water molecules (Tan et al., 2005).

iv) disjoining pressure between adjacent interfaces due to adsorption of ionic and nonionic surfactants, polymers etc. When the two sides of the lamellar film are in sufficiently close proximity, interaction can occur involving the dispersion, electrostatic and steric forces Such forces acting normal to lamellar film are collectively exhibited so called disjoining pressure of system which can oppose the loss of liquid or drainage (Jalmes et al., 2005).

2.3 PROPORTIONING AND PREPARATION OF FOAM CONCRETE

Often trial and error process is adopted to achieve foam concrete with desired properties (Nehdi et.al., 2001). For a given mix proportion and density, a rational proportioning method based on solid volume calculations was proposed by McCormick (1967). Based on this work, the design aid of ACI 523-1975 relates plastic density and compressive strength, using which the cement content and water-cement ratio can be chosen for a given strength and density. ASTM C 796-97 provides a method of calculation of foam volume required to make cement slurry of known water-cement ratio and target density. Kearsley and Mostert (2005a) have proposed a set of equations (density and volume of foam concrete), which are written in terms of the mixture composition, for calculating the foam volume and cement content. For a given 28-day compressive strength, filler-cement ratio and fresh density, typical mix design equations of Nambiar and Ramamurthy (2006b) determines mixture constituents viz., percentage foam volume, net water content, cement content and percentage fly ash replacement. Most of the methods proposed, help in calculation of batch quantities if the mix proportions are known. Even though the strength of foam concrete depends on its density, for a given density, the strength can be increased by changing the constituent materials. Also, for a given density, the foam volume requirement depends on the constituent materials (Nambiar and Ramamurthy 2006b). Hence for a given strength and density requirement, the mix design strategy should be able to determine the batch quantities.

Pre-formed foaming is preferred to mix-forming technique due to the following advantages i) lower foaming agent requirement and ii) a close relationship between amount of foaming agent used and air content of mix (Valore 1954a; Byun et. al., 1998). Most common types of mixers (tilt drum or pan mixer used for concrete or mortar) are suitable for foam concrete. The type of mixer and batching and mixing sequences of foam concrete depends upon pre-formed foam method or mix-foaming method (Karl and Worner, 1993). For production of foam concrete with preformed foam, the following batching sequence was reported. To the base mix prepared the necessary volume of preformed foam is introduced and thereafter mixed for at least two minutes in order to gain uniform distribution of the foam (Karl and Worner, 1993). The compressive strength, drying shrinkage, and absorption properties directly depend on the method and duration of curing. Moist-curing and autoclaving are the two commonly adopted methods.

2.4 PROPERTIES OF FOAM CONCRETE

Table 2.1 summarizes the fresh and hardened properties studied by researchers. The hardened properties are classified into physical (drying shrinkage, density, porosity and air void system, sorption), mechanical (compressive and tensile strength, modulus of elasticity, prediction models), durability properties and functional characteristics (thermal conductivity, fire resistance and acoustical properties).

2.4.1 Fresh State Properties

As foam concrete cannot be subjected to compaction or vibration the foam concrete should have flowability and self-compactibility. These two properties are evaluated in terms of consistency and stability of foam concrete, which are affected by the water content in the base mix, amount of foam added along with the other solid ingredients in the mix (Nambiar and Ramamurthy 2008a).

2.4.1.1 Consistency

Flow time using marsh cone and flow cone spread tests are adopted to assess the consistency of foam concrete (Jones and McCarthy, 2005a). These measurements were also related to rheology and it was observed that coarse fly ash as filler exhibited 2.5 times higher spread compared to cement-sand mix. This enhanced consistence and rheology is attributed to difference in particle shape and size of fine aggregate. When replacing sand with fine fly ash by mass, the consistency of the mix is reduced due to higher fines content. Hence to satisfy the consistency requirement an increase in water-solids ratio is required with an increase in fly ash replacement level.

Table 2.1 Tabulation showing literature and properties of foam concrete investigated

Authors (Year)	Ingredients	Fresh state properties	Physical and mechanical properties						Durability	Functional properties
			Shrinkage	sorption	Porosity	Density	Strength	Models		
Valore (1954)	C/L/CM		√	√	√	√	√			Thermal, fire and acoustical properties
Mc Cormick (1967)	CM					√	√	√		
Hoff G C (1972)]	C				√		√	√		
Richard T G (1975,77)	C					√	√			Thermal properties, Cryogenic applications
Prim & Wittmann (1983)	CM			√	√					
Tada and Nakano (1983)	CM			√	√					
Tada S (1986)	C					√	√	√		Optimum acoustical performance design
Tam et. al (1987)	CM						√			
Regan & Arasteh(1990)	LWA		√			√	√			
Karl and Worner (1993)	-	√								
Hunaiti (1996,'97)	CM						√			
Kearsley E P (1996,1999)	CM		√				√	√		
Kearsley & Mostert(1997)	C/CF®					√	√			Thermal properties
Kearsley & Booyens (1998)	-			√			√		√	
Durack and Weiqing (1998)	CM/ CFM				√		√	√		
Kearsley & Visagie (1999)	C/CF®				√ **(AV)**	√	√			
De Ross & Morris (1999)	C/CF/L®		√				√			Thermal conductivity
Nehdi M et al (2001)	-					√	√	√		
Jones M R (2001)	CM		√				√		√	
Turner M (2001)	CM	√								
Kyle (2001)	CM						√			
Kearsley & Wainwright	C/CF®			√	√	√	√			
Jones & Giannakou (2002,2004)	-									Energy efficient foundation -thermal analysis
Madjoudj et al (2002)	-			√						
Jones M R et.al (2003)	CM	√	√				√			
Tikaisky P J et al (2004)	CM								√	
Kearsley & Mostert (2005b)	CM/CFM									Fire resistance, use in refractory
Proshin et ai. (2005)	-									Thermal protective foam concrete & energy
Jones M R & McCarthy (2005a)	CM	√	√				√			Comparison of Thermal conductivity
Jones M R & McCarthy (2005b)	CM		√				√	√	√	
Wee et.al. (2006)	CG®				√**(AV)**		√			
Laukitis and Fiks (2006)	CM				√					Comparison of acoustical properties
Nambiar & Ramamurthy (2006,2007, 2008 & 2009)	CM/CFM	√	√	√	√**(AV)**	√	√	√		

CM- Cement Mortar, C – Neat Cement, L – Lime, CFM – Cement Fly ash Mortar, CF® - Cement with fly ash replacement, ac – autoclaving, mc – moist curing , LWA- Lightweight aggregate, CG®- cement with GGBS replacement, AV- Air-void characterization (system)

However fly ash mixes were also reported to affect foam stability and necessitating larger foam volume to achieve the design plastic density, which was attributed to the high fluid consistency in the base mix and high residual carbon in the ash (Jones and McCarthy, 2005c). The consistency reduces with an increase in volume of foam in the mix, which may be attributed to the i) reduced self-weight and greater cohesion resulting from higher air content (Karl and Worner, 1993), and ii) adhesion between the bubbles and solid particles in the mix increases the stiffness of the mix.

2.4.1.2 Stability

The stability of foam concrete is the consistency at which the density ratio is nearly one (the measured fresh density/design density), without any segregation and bleeding (Nambiar and Ramamurthy, 2006a, 2008a). This ratio is higher than unity at both lower and higher consistencies due to either stiffer mix or segregation. For each foam volume there exists an optimal superplasticiser dosage which results in a mix of desired density (± 50 kg/m^3) with a reduction in water-solids ratio. This optimum dosage of superplasticiser reduces with increase in foam volume as the mixes become unstable at higher dosages of superplasticiser. The stability of test mixes can also be assessed by comparing the (i) calculated and actual quantities of foam required to achieve a plastic density within 50 kg/m^3 of the design value (ii) The calculated and actual w/c ratios .The additional free water contents resulting from the foam collapse corresponded to an increase in actual w/c ratios (Jones and McCarthy, 2005c). Thus the consistency of the base mix to which foam is added is an important factor, which affects the stability of mix. This consistency reduces considerably when foam is added and depends on the filler type also.

Hence there is a need for determining the water-solids ratio, which would satisfy both stability and consistence of the mix. Regression equations based on the experimental results, for predicting the spread flow value of foam concrete, knowing the proportion of the other ingredients, will help in arriving at this water content for the production of a stable and workable foam concrete mix. For typical materials used, an appropriate workability value has been arrived at as 45% of spread at which a foam concrete mix of good stability and consistency can be produced (Nambiar and Ramamurthy, 2008a).

2.4.2 Physical Properties

2.4.2.1 Drying shrinkage

Foam concrete possesses high drying shrinkage due to the absence of coarse aggregates, i.e., up to 10 times greater than those observed on normal weight concrete (Valore, 1954b; Jones et al., 2003). Autoclaving is reported to reduce the drying shrinkage significantly by 12 to 50% of that of moist cured concrete (due to a change in mineralogical compositions) and is essential if the products are required within acceptable level of strength and shrinkage (Valore, 1954a, Schubert, 1983). The shrinkage of foam concrete reduces with density (Tada and Nakano, 1983; Schubert, 1983; Nmai et al., 1997; Jones et. al., 2003; Nambiar and Ramamurthy, 2009) which is attributed to the lower paste content affecting the shrinkage in low-density mixes.

In a comparative study on the shrinkage behaviour with sand and fly ash as filler, foam concrete with sand exhibited smaller drying shrinkage which is attributed to the higher shrinkage restraining capacity of sand as compared to fly ash particles (Jones et. al., 2003; Nambiar and Ramamurthy, 2009). It is reported that lightweight aggregate could be used to reduce the shrinkage of foam concrete (Weigler and Karl, 1980; Regan and Arasteh, 1990).

2.4.2.2 Air-void systems

The pore structure of cementitious material, predetermined by its porosity, permeability and pore size distribution, is a very important characteristic as it influences the properties such as strength and durability. The pore structure of foam concrete consists of gel pores, capillary pores as well as air voids (air entrained and entrapped pores) (Visagie and Kearsely, 2002). As foam concrete being a self-flowing and self-compacting concrete and without coarse aggregate, the possibility of entrapped air is negligible. The air-voids in the foam concrete can be characterized by a few parameters like volume, size, size distribution, shape and spacing between air-voids.

The air-void distribution is one of the most important micro-properties influencing strength of foam concrete. Foam concrete with narrower air-void distributions shows higher strength. The use of fly ash as filler helps in achieving more uniform distribution of air-voids by providing uniform coating on each bubble and thereby prevents merging of bubbles. At higher foam volume, merging of bubbles results in wide distribution of void sizes leading to lower strength. In addition to the air-void size and its distribution, the compressive strength of foam concrete is also be influenced by the void/paste ratio, spacing of air voids, number (frequency) of air voids. Because of the uniform shape (characterized by shape factor) of air voids, its influence on strength is negligible (Kearsely and Visagie, 1999; Wee et al., 2006; Nambiar and Ramamurthy, 2006c). At the same time, for gas concrete, another type of aerated concrete, the expansion of concrete during gas formation result in the development of ellipsoidal oriented pores (Cabrillac et al., 2006). In a study on air-void system of foam concrete made of cement-ground granulated blast furnace slag mixture, for achieving a high strength-to-weight ratio, an air-void system with a spacing factor, air-void size and air content of 0.04mm, 0.12mm and 42% respectively were reported to be optimal (Wee et al., 2006). Finer filler material helps in uniform distribution of air-voids.

The ratio of connected pores to total pores in foam concrete is lower resulting in lower air permeability compared to gas concrete (Laukitis and Fiks, 2006), which leads to comparatively lower sound and water absorption in foam concrete. The entrained air-voids create an increasingly tortuous path for the capillary flow in proportion to foam volume and dampen the transport phenomenon. Higher air-void volume results in lesser pore wall thickness and paste volume causing lower shrinkage (Tada and Nakano, 1983). The larger pores in aerated concrete can be treated as aggregate of zero density and a transition zone exists in the void-paste interface of such concrete analogous to the one in aggregate-paste interface of normal concrete (Narayanan and Ramamurthy, 2000). Thus understanding the air-void system is essential for producing foam concrete with a high strength-to-weight ratio with advantageous properties.

2.4.2.3 Density

Density can be either in fresh or hardened state. Fresh density is required for mix design and casting control purposes. A theoretical equation for finding fresh density may not be applicable as there can be scatter in the results caused by a number of factors including continued expansion of the foam after its discharge, loss of foam during mixing (Regan and Arasteh, 1990). Many physical properties of foam concrete related to/depend upon its density in hardened state. While specifying the density, the moisture condition needs to be indicated as the comparison of properties of foam concrete from different sources can have little meaning without a close definition of the degree of dryness (Valore, 1954b). As the properties are expressed in terms of dry density, a few relationships between dry density and fresh density are summarized in Table 2.2.

Greater the proportion of aggregate, higher will be the density. McCormick (1967) studied the effect of types of fine aggregate, aggregate gradation, type of foam and sand-cement ratio on the wet density of foam concrete and reported that wet densities within about 5% of the design densities can be achieved by using solid volume calculations. The cement-sand based non-autoclaved preformed foam concrete has relatively higher density and higher requirement of cement content. Compared to a product based on sand (specific gravity 2.6) as fine aggregate, it is observed that when sand is replaced with same quantum of fly ash (specific gravity 2.2) by weight, the density is reduced due to its lower specific gravity (Durack and Weiqing, 1998). Alternately, to achieve a particular density of foam concrete, use of fly ash results in a reduction in foam volume requirement due to its lower specific gravity (Nambiar and Ramamurthy, 2006b), thereby resulting in higher strength.

2.4.3 Mechanical Properties

2.4.3.1 Compressive strength

Table 2.3 presents an overview of compressive strength of foam concrete of various mixture composition and densities reported in literature. The compressive strength decreases exponentially with a reduction in density of foam concrete (Kearsley, 1996). The range of applications for which foam concrete of different densities and compressive strengths are used are presented in Table 2.4. The specimen size and shape, the method of pore formation, direction of loading, age, water content, characteristics of ingredients used and the method of curing are reported to influence the strength of cellular concrete in total (Valore, 1954b). Other parameters affecting the strength of foam concrete are cement-sand and water-cement ratios, curing regime, type and particle size distribution of sand and type of foaming agent used (Hamidah et. al., 2005; Aldridge, 2005).

Table 2.2 Empirical models for density determination

Reference	Equation	Remarks
ASTM C 796-97	Dry density $=(W_c+0.2W_c)/V_{batch}$	W_c and V_{batch} are weight of cement and volume of batch respectively
ACI committee 523 (1992)	Dry density$=1.2C+A$	C and A are weight of cement and aggregate in kg per cubic meter of concrete
Kearsley (1999)	$\gamma_{dry} = 0.868\gamma_{cast} - 55.07$	Casting density range of 700 kg/m^3 to 1500 kg/m^3.Cement-fly ash mixture of varying ash-cement ratio (a/c= 0 to 4).

For dry density of foam concrete between 500 and 1000 kg/m^3, the compressive strength decreases with an increase in void diameter. For densities higher than 1000 kg/m^3, since the air void content is lower, the air-voids are far apart and thus its influence on the compressive strength is not predominant. And the composition of the paste content which is the major component in such cases determines the compressive strength (Visagie and Kearsely, 2002). It has been reported that the small changes in the water-cement ratio does not influence the strength of foam concrete as in the case of normal weight concrete (Jones and McCarthy 2006). At higher water-cement ratios (within the consistency and stability limit) an increase in strength is observed with an increase in water-cement ratio (De Rose and Morris, 1999; Tam et al., 1987), just opposite to the trend usually noted for conventional concrete/mortar where the entrapped air content is only a few percentage by volume. It has been concluded by Tam et al (1987), that (i) the strength of moist-cured foam concrete depends on water-cement ratio and air-cement ratio and (ii) the combined effect should be considered when volumetric composition of air-voids approaches that of water voids.

A study on the effect of replacing large volumes of cement (up to 75 % by weight) with both classified and unclassified fly ash on strength of foam concrete reports that up to 67% of the cement could be replaced with ungraded and graded fly ash without any significant reduction in strength (Kearsley and Wainwright 2001a).

Table 2.3 A review of mixes used and compressive strengths of foam concrete

Author (s),& year	Proportion of Cement kg/m^3 or	Ratios			Density range Kg/m^3	Comp. strength MPa (28 days)
		S/C	w/c	F/C		
McCormick (1967)	335-446	0.79-2.8	0.35-0.57		800-1800	1.8-17.6
Tam et al. (1987)	390	1.58-1.73	0.6-0.8		1300-1900	1.81-16.72
Regan and Arasteh (1990)		0.6 (LAC/C)	0.45-0.6		800-1200	4-16
Van Deijk (1991)	Cement-sand/fly ash				280-1200	0.6-10(91-d)
ACI 523.1R-1992	Neat cement paste				240-640 (DD)	0.48-3.1
	Cement- sand mix				400-560(DD)	0.9-1.72
Hunaiti (1997)		3			1667	12.11
Kearsley and Booyens (1998)	Cement – fly ash replacement				1000-1500	2.8-19.9
Durack and Weiqing (1998)	270-398	1.23-2.5	0.61-0.82		982-1185 (DD)	1-6
	137-380		0.48-0.7	1.48-2.5	541-1003 (DD)	3-15(77-d)
Aldridge D (2000)	Cement- sand mix				400-1600	0.5-10
Kearsley and Wainwright (2001a)	Cement-flyash replacement				1000-1500	2-18
	193-577		0.6-1.17			
Tikaisky P J et al. (2004)	Neat cement				490-660	0.71-2.07
	149-420		0.4-0.45			
	Cement –sand/fly ash				1320-1500	0.23-1.1
	57-149		0.5-0.57			
Jones and McCarthy (2005c)	300	1.83-3.17	0.5		1000-1400	1-2
			1.11-1.56	1.22-2.11	1000-1400	3.9-7.3
Jones and McCarthy (2005b)	500	1.5-2.3	0.3		1400-1800	10-26
	500		0.65-0.83	1.15-1.77	1400-1800	20-43
Nambiar and Ramamurthy (2006b)	Cement–sand mix (coarse)	With filler cement ratio varied from 1 to 3 and fly ash replacement for sand varied from 0 to 100 %			800-1350 (DD)	1-7
	Cement–sand mix (fine)				800-1350 (DD)	2-11
	Cement-sand-flyash mix				650-1200 (DD)	4-19
S/C: sand-cement ratio; F/C: Fly ash-cement ratio; w/c: water-cement ratio; a/c: ash-cement ratio; LAC: lightweight aggregate content, DD: dry density; d-days						

The results indicate that the compressive strength of foam concrete is primarily a function of dry density, and foam concrete mixes with high fly ash content needed a longer time to reach their maximum strength which was observed to be higher than that achieved using only cement. When the cement is replaced with silica fume, higher compressive strength is obtained in the long term, due to their pozzolanic reaction and filler characteristics, with a more marked effect at high foam concrete densities.

For a given density, the mix with fine sand resulted in higher strength than the mix with coarse sand and the variation is higher at higher density. This higher strength to density ratio is attributed to the comparatively uniform distribution of pore in foam concrete with fine sand, while the pores were larger and irregular for mixes with coarse sand (McCormick 1967; Nambiar and Ramamurthy, 2006a). Similar behaviour was observed when sand was replaced with fine fly ash (Nambiar and Ramamurthy, 2006b). Compressive strength of foam concrete using fly ash, as a partial/complete replacement for filler, resulted in higher strength to density ratio (Durack and Weiqing, 1998; Jones and McCarthy, 2005a, b; Nambiar and Ramamurthy, 2006b). The enhancement of strength with fly ash as filler is not pronounced at lower density range (higher % of foam volume) especially at lower ages. This is due to the fact that at lower density range it is the foam volume that controls the strength rather than the material properties (Nambiar and Ramamurthy, 2006b). The combined effect of high water retentivity and pozzolanic activity of fly ash has been attributed to contribute to the good performance of fly ash as binder in foam concrete (Papayianni et. al., 2005). Mixes containing expanded shale aggregate produced higher strength value than those containing sand as aggregate for the same wet density. The use of lime, demolition fines, recycled glass as fine aggregate has little or no effect on compressive strength, while some reduction in strength has been noted when crumb rubber, used foundry sand, china clay sand and quarry fines were employed (De Rose and Morris, 1999; Jones et. al., 2005) .

In terms of curing regime, autoclaving increases the compressive strength. In general, compressive strength of water-cured foamed concrete is reported to be higher than that cured in air (Hamidah et. al., 2005). But higher strengths are reported for humid air curing at a temperature around 40°C as compared to normal water-cured specimens (Kearsley and Booyens, 1998). The low cost of moist-curing is an attractive and viable alternative in many applications (Tam et al., 1987), though the strength development is rather slow. Autoclaving is generally used for pre-cast structural cellular concrete elements.

Table 2.4 Typical dry densities and compressive strengths of foam concrete for a range of applications (Basiurski and Wells, 2001)

Application	Dry density, kg/m^3	Compressive strength, MPa
Roof insulation screed	400-600	1.0-2.5
Structural walls	1200-1600	6.5-12
Non structural walls	800-1600	3-10
Floor slabs	1200-1600	4.5-10
Raising floor level	400-1200	1.0-4.5
Fire breaks	400-1200	1.0-3.5
Decorative panels	1000	3.5-5.5
Trench reinstatement	1200	4.5-5.5
Road sub-base	400-1000	1.0-3.0
Bridge abutments	400-1650	1.5-10
Void fill	400-1600	1.0-10.0
Ground stabilisation	600-1000	2.0-5.5
Harbour fill	400-1600	1.0-10.0

2.4.3.2 Flexural and tensile strengths

The ratio of flexural strength to compressive strength of cellular concrete is in the range of 0.25 to 0.35 (Valore, 1954b). Splitting tensile strengths of foam concrete are lower than those of equivalent normal weight and lightweight aggregate concrete with higher values observed for mixes with sand than those with fly ash. This increase is attributed to the improved shear capacity between sand particle and the paste phase (Jones and McCarthy, 2005b). Use of Polypropylene fibers has been reported to enhance the performance with respect to tensile and flexural strength of foam concrete, provided it is not affecting fresh concrete behaviour and self-compaction (Kearsley and Mostert, 1997).

2.4.3.3 Modulus of Elasticity

The static modulus of elasticity of foam concrete is reported to be significantly lower than that of normal weight and lightweight concrete, with values typically varying from 1.0 to 8.0 kN/mm^2, for dry densities between 500 and 1500 kg/m^3 respectively (Jones and McCarthy, 2005b). The E-values of normal weight concrete exhibited values up to 4 times larger than that of equivalent strength foam concrete. Foam concrete with fly ash as fine aggregate is reported to exhibit lower E-value than that of foam concrete with sand. This variation is attributed to the high amount of fine aggregate in sand mix compared to fly ash mix, which contains entirely paste with no aggregate (Jones, 2001). Use of Polypropylene fibers has been observed to increase the E-value between two and four times (Jones and McCarthy, 2005b). At low temperature, an increase in compressive strength is accompanied by an increase in stiffness, which was observed to be more in higher density range (Richard 1977). A few relations reported for Modulus of Elasticity with density and compressive strength are shown in Table 2.5.

Table 2.5 A few relations for Modulus of Elasticity (E)

Author(s)& year	Relationship	Remarks
Tada (1986)	$E = 5.31 * W - 853$	Density from 200 to 800 kg/m^3
McCormick (1967)	$E = 33\ W^{1.5}\sqrt{f_c}$	Pauw's equation
Jones and McCarthy (2005b)	$E = 0.42\ f_c^{1.18}$	Sand as fine aggregate
	$E = 0.99\ f_c^{0.67}$	Fly ash as fine aggregate
W- Density of concrete, f_c – Compressive strength		

2.4.4 Strength Prediction Models

A few researchers developed expressions for predicting strength of foam concrete, which contain large amount of air voids. Hoff (1972) proposed a single strength-porosity model for foam concrete with cement paste by combining space occupied by evaporable water and air voids. Strength prediction models on foam concrete proposed by Kearsely and Wainwright (2002b) states that Hoff's model can be effectively used to predict the compressive strength of foam concrete at different ages and different densities prepared from cement paste with and without fly ash replacement. These strength-porosity models based on cement paste cannot be directly extended to foam concrete with fillers like sand/fly ash.

For limited set of operating conditions Tam et al. (1987) reported a model for strength of foam concrete based on Feret's equations. This equation was improved by incorporating the degree of hydration through Power's gel-space ratio concept. Based on the same concept, strength prediction models for foam concrete made of cement mortar (with sand and fly ash as fine aggregate) was proposed by Durack and Weiqing (1998) for mixes of lower density ranges. For a range of mixture compositions but with wide range of densities, Nambiar and Ramamurthy (2008b) have proposed similar relations based on Balshin's model and Power's gel-space ratio concept. Out of these, model based on Balshin stands out as (i) correlated well with measured values (ii) ease in application since it employs composition of constituents and easily measurable parameters. Also Balshin's equation provides a good fit to the plot of compressive strength against total porosity for i) slate based autoclaved aerated concretes (Watson 1980), ii) at all ages of foam concrete made of cement paste containing high percentage of ash (Kearsley and Wainwright, 2002b), and iii) foam concrete containing high amount of fly ash as replacement to sand (Nambiar and Ramamurthy 2008b).

As there is a possibility of change in actual foam volume in hardened stage due to loss of foam in mixing and expansion of the foam after its discharge (Regan and Arasteh, 1990), dry density cannot be used as a basis for aiming at the exact composition of foam concrete mixes. Hence it would be preferable to include fresh density in such models, which can easily be measured in the field. Otherwise, models relating dry density and fresh density as given in Table 2.2 may be used for arriving the fresh density for a specified dry density. For evaluating the modulus of elasticity from density and strength, the models presented in Table 2.5 may be used.

Empirical models for predicting the strength and density of foam concrete from mixture composition details like filler-cement ratio, fly ash percentage as filler and foam volume, through statistically designed experiments (Response Surface Methodology) have been developed (Nambiar and Ramamurthy 2006b). These models can act as a guideline in the mixture proportioning of foam concrete.

2.4.5 Durability of Foam Concrete

2.4.5.1 Permeation characteristics

Water absorption: Water absorption of foam concrete decreases with a reduction in density, which is attributed to lower paste volume phase and thus to the lower capillary pore volume. The water absorption of foam concrete is mainly influenced by the paste phase and not all artificial pores are taking part in water absorption, as they are not interconnected (Kearsley and Wainwright, 2001b; Nambiar and Ramamurthy 2006a). Expressing water absorption as percentage by mass can lead to misleading results when foam concrete is concerned because of larger differences in density. The oxygen and water vapour permeability of foam concrete have been observed to increase with increasing porosity and fly ash content (Kearsley and Booyen, 1998). Permeability coefficient of lightweight foamed concrete is proportional to unit weight and inversely proportional to pore ratio (Byun et. al., 1998).

Sorptivity: The moisture transport phenomenon in porous materials has been defined by an easily measurable property called sorptivity (absorbing and transmitting water by capillarity), which is based on unsaturated flow theory (Hall, 1989; Wilson et al., 1991). It has been shown that the water transmission property can be better explained by sorptivity than by permeability. Sorptivity of foam concrete is reported to be lower than the corresponding base mix and the values reduce with an increase in foam volume (Giannakou and Jones, 2002; Madjoudj et al., 2002; Nambiar and Ramamurthy, 2007). Also, the sorption characteristic of foam concrete is observed to depend upon the filler type, pore structure and permeation mechanisms. A comparison of the sorptivity of foam concrete with sand and fly ash as aggregate exhibited that the mixes with fly ash resulted in marginally higher sorptivity than mixes with sand (Jones and McCarthy, 2005c).

2.4.5.2 Resistance to aggressive environment

Foam concrete mixture designed at low density taking into consideration of depth of initial penetration, absorption and absorption rate, provided good freeze-thaw resistance (Jones, 2001; Tikalsky et al., 2004). Sulphate resistance of foam concrete, studied by Jones and McCarthy (2005c) for 12 months, reveals that foam concrete has good resistance to aggressive chemical attack. A study on accelerated carbonation of foam concrete by Jones and McCarthy (2005b) indicate that lower density concrete appears to carbonate at a relatively higher rate. Comparing the performance of mixes with sand and fly ash, mixes with fly ash exhibited higher carbonation than that with sand. An accelerated chloride ingress tests suggested that foam concrete performance is equivalent to that of normal concrete, with enhanced corrosion resistance at lower density (Kearsley and Booyens, 1998). The cell-like structure of foam concrete and possible porosity of cell wall do not necessarily make the foam concrete less resistant to penetration of moisture than dense concrete; the air-voids appears to act as a buffer preventing rapid penetration.

2.4.6 Functional Characteristics

2.4.6.1 Thermal insulation

Foam concrete has excellent thermal insulating properties due to its cellular microstructure. The thermal conductivity of foam concrete of density 1000 kg/m^3 is reported to be one-sixth the value of typical cement-sand mortar. In comparison with a cement-sand screed, foam concrete of density 1000 kg/m^3 is reported to be 5 times more thermally efficient (Aldridge and Ansell, 2001). A study by Giannakau and Jones (2002) exploring the potential of foam concrete to enhance the thermal performance of low rise building has shown that the foam concrete ground supported slab foundation is thermally efficient with good permeation properties while producing satisfactory strength.

Comparison with normal concrete: The thermal conductivity values are 5% to 30% of those measured on normal weight concrete and range from between 0.1 and 0.7 W/mK for dry densities values of 600 to 1600 kg/m^3, reducing with decreasing densities (Jones and McCarthy, 2005a). Insulation of brick wall can be increased by 23% when inner leaf is replaced with foamed concrete of unit weight 800 kg/m^3 (Taylor, 1969).

Effect of density variation on thermal conductivity: Insulation is more or less inversely proportional to density of concrete (Shrivastava, 1977). A decrease of concrete dry density by 100 kg/m^3 results in a reduction of thermal conductivity by 0.04 W/mK of lightweight aggregate foam concrete (Weigler and Karl, 1980). Altering the mortar/foam ratio affects density which has enormous impact on insulation capacity (Van Deijk, 1991).

Influence of fly ash, light weight aggregate: 12 to 38% reduction in thermal conductivity of foam concrete with 30% PFA (Pulverized Fuel Ash) as compared to mixes with only Portland cement as binder is attributed to the lower density and cenospheric particle morphology of fly ash particles, which increases the heat flow path (Giannakou and Jones, 2002). Jones and McCarthy (2006) report that foam concrete exhibited typical thermal conductivity between 0.23 and 0.42 W/mK at 1000 and 1200 kg/m^3 dry densities. The replacement of cement by finer fly ash (30% by weight of cement) helped to reduce temperature development during heat of hydration. The use of lightweight aggregates with low particle density in combination with artificially introduced air-voids in mortar matrix has been observed to be advantageous in reducing thermal conductivity (Weigler and Karl, 1980). By moderate filling of porous mortar with polystyrene granules, foam concrete of density range 200–650 kg/m^3 with thermal conductivity 0.06–0.16 W/mK can be produced (Proshin et al., 2005).

Effect of temperature on thermal conductivity: Thermal insulation is reported to improve with a reduction in temperature (Richard, 1977). While studying the potential of cellular concrete for load bearing insulations for cryogenic applications, Richard et al. (1975) reviewed the thermal and mechanical characteristics of foam concrete. Influence of temperature variations from 22^oC to -196^oC is reported for selected densities between 640 kg/m^3 and 1440 kg/m^3. An apparent reduction of 26% in thermal conductivity of foam concrete has been reported when temperature was lowered from 22°C to -196°C. Based on the thermal performance requirements for buildings, an optimum material design has been proposed by Tada(1986).

2.4.6.2 Acoustical properties

Valore (1954b) states that cellular concrete does not possess unique or significant sound insulation characteristics. Foamed concrete is stated to be less effective than dense concrete in resisting the transmission of air borne sound (Taylor, 1969), the reason attributed is that the Transmission Loss (TL) of air-borne sound is dependant on mass law, which is a product of frequency and surface density of the component. Tada (1986) attributed the TL to the rigidity and internal resistance of the wall, in addition to the mass law and gives an acoustical performance design of cellular concrete based on bulk density and thickness. Sound transmission of a cellular concrete wall, over most of the audible frequency range may be higher by 2 to 3% as compared to normal weight concrete. While dense concrete tends to deflect sound, foam concrete absorbs it and hence the foam concrete has higher sound absorption capacity (Taylor, 1969).

2.4.6.3 Fire resistance

At high temperature heat transfer through porous materials is influenced by radiation, which is an inverse function of the number of air-solid interfaces traversed. Hence along with its lower thermal conductivity and diffusivity the foam concrete may result in better fire resistance properties (Valore, 1954b). Fire resistance tests on different densities of foam concrete indicated that the fire endurance enhanced with reductions in density. While reviewing the earlier studies on fire resistance, Jones and McCarthy (2005b) summarize that, for lower densities of foam concrete, the proportional strength loss was less when compared to normal concrete. As compared to vermiculite concrete, lower densities of foam concrete is reported to have exhibited better fire resistance, while with higher densities increases, this trend is stated to be reversed (Aldridge, 2005). Kearsley and Mostert (2005b) studied the effect of cement composition on the behaviour of foam concrete at high temperature and concluded that foam concrete containing hydraulic cement with an Al_2O_3/CaO ratio higher than 2 can withstand temperatures as high as 1450°C without showing any sign of damage.

2.5 BRIEF SUMMARY OF EARLIER RESEARCH IN FOAM CONCRETE AT IIT MADRAS

Extensive research on various properties of preformed foam concrete made with a natural based foaming agent was carried out by Dr.Nambiar during the period of 2002-2006 at IIT Madras. The first phase of Dr. Nambiar’s work comprised of manufacture of natural foaming agent using natural organic materials stabilized by a protein stabilizer. A laboratory model foam generator which works on the principle of compressed air method was developed. Systematic studies on various fresh and hardened state properties namely consistency, compressive strength, drying shrinkage, sorption and air void parameters were made. Significant contribution to utilization of high volume of fly ash in foam concrete was made by carrying out investigations on influence of filler-cement ratio and fly ash replacement level on various properties of foam concrete (Nambiar, 2006).

2.6 NEED FOR PRESENT STUDY

The review shows that the foam concrete is a versatile material with attractive characteristics and advantages; as a result the acceptance of it as realistic options for a number of lightweight non and semi-structural applications has now increased. However its wider use in structural applications has been inhibited by its technical and engineering unfamiliarity and non-availability of affordable foaming agents in India. Most of the investigations on foam concrete have been confined to evaluation of its properties rather than on foam characteristics which has bearing on the strength of the foamed material. Hence the need for identifying affordable foaming agent and foam generator and evaluation of foam properties is essential. For enhancing the potential of foam concrete as a structural material, more investigations on mixture proportioning, compatibility between foaming agent and chemical admixtures, the influence of composition and air-void parameters on the fresh and hardened properties and durability related studies is necessary. This will open up new tracks for further developing this energy efficient, environmental friendly and cost effective building material. It is in this context, that an in-depth study in the manufacture and properties of foam concrete are deemed necessary.

CHAPTER 3

OBJECTIVES AND SCOPE OF THE PRESENT STUDY

3.1 GENERAL

From the review of earlier research and development in the field of foam concrete, the need for an in-depth study on the identification of affordable foaming agents and its effect on concrete properties has been brought out in the previous chapter. The objectives and scope for the present study have been defined as outlined in the following sections.

3.2 OBJECTIVES

Following are the objectives of the present study:

i. To evaluate the relative performance of foam produced with identified four synthetic surfactants viz., Sodium lauryl sulfate, Sodium lauryl ether sulfate, Sulfanol and Cocodiethanolamide using statistically designed experiments and to select the potential foaming agents for use in foam concrete production.

ii. To study the relative performance of these synthetic foaming agents on workability, strength behavior and air void parameters of foam concrete.

iii. To investigate the sorption, shrinkage characteristics of foam concrete and its resistance to sulphate environment.

3.3 SCOPE

The scope of the study is limited to the following with respect to raw materials used and methods adopted:

i. The study is restricted to moist cured foam concrete made of preformed foaming method with the identified foaming agents viz,; Sodium lauryl sulfate, Sodium lauryl ether sulfate, Sulfanol (ionic surfactants) and Cocodiethanolamide (non ionic surfactant).

ii. A constant cement-sand ratio of 1:1 and foam volume range of 18% to 46% have been adopted. Ordinary Portland Cement conforming to IS 12269-1987 and pulverized river sand finer than 300 µm (specific gravity = 2.52) were used.

iii. Studies on exposure to different concentrations of sulphate environment (Sodium sulphate (Na_2SO_4)) and Magnesium sulphate ($MgSO_4$)) as per ACI 318-99 were carried out.

CHAPTER 4

RELATIVE PERFORMANCE EVALUATION OF FOUR SYNTHETIC SURFACTANTS AS FOAMING AGENTS

4.1` GENERAL

Mostly proprietary foaming agents have been used in the earlier studies for foamed concrete production. Imported proprietary foam concentrates are not cost-effective in several developing countries. Hence there is a need for efficient foaming agent which would make the foamed concrete production simple and economical. The foam parameters namely dilution ratio and generation pressure to be adopted for stable foam production are predefined by the manufacturer when proprietary foaming agents and foam generator are used. However such parameters have to be determined for new surfactants. A review of literature indicates that a systematic study of production parameters on the foam characteristics needs to be undertaken. Most of the investigations on foamed concrete in the past have been confined to the evaluation of foamed concrete properties alone rather than on the foam characteristics itself which is more important to attain the desired properties of foamed concrete. Selection of surfactant has an impact on the properties of foam as it affects the surface tension and gas-liquid interfacial properties. The nature of the surfactant also modifies the properties of the thin liquid film which separates the bubbles (Marze et al., 2005). When the method of foam generation is considered in comparison to air aspiration method, compressed air mode of foam generation is reported to result in a foam having uniform bubble size distribution (Magrabi et al., 2002). At low pressures (< 30 kPa), the physical properties of solutions, density, viscosity and dynamic surface tension determine the size of bubble being formed. However as the pressure and hence the flow rate of the air increases, the solution effects are negated and the bubble diameter is determined by the generation pressure (Wilde, 1996; Quebaud et al 1998; Kearsely and Visagie, 1999; Nambiar and Ramamurthy, 2006c).

Stable aqueous foams are required in many of the industrial applications. One of the important requirements of foam stability in foamed concrete is to ensure a fine and uniform texture throughout the whole hardening process. Several techniques have been used in earlier studies to evaluate the properties of foam produced with surfactants. Hence proper selection of foaming agent, foam generation method and foam production parameters are essential since the quality of foam will have a considerable bearing on final strength of foamed materials. Hence this chapter is aimed at assessing the relative characteristics of foam produced with four synthetic surfactants through a systematic experiment design based on Response surface methodology and checking their suitability for use in foamed concrete production as per ASTM C 796-97. The surfactant concentration and foam generation pressure required to produce stable foam was determined first. As a next step, the behaviour of the foam in cement slurry was studied, which established the stability of the foam in the mix.

4.2 FOAM CHARACTERISTICS

The performance evaluation of surfactants to qualify as potential foaming agents is through the following characteristics of foam produced.

(i) Foam capacity: It is a measure of expansion ratio of foaming solution. Aqueous foams used in fire fighting applications are mainly classified by their expansion ratio which is expressed as ratio of total volume of foam to the liquid volume (Magrabi et al., 2002). Foam capacity is an user friendly term for foam users since it gives a volumetric measurement of foam that could be produced per unit quantity of foam concentrate. The foam capacity can also be taken as a measure of foamability or foam generating power of surfactant solution. Foam which is over-expanded (say expansion ratio greater than 50:1) and thus of lower foam density may collapse and increase the concrete density.

(ii) Foam output rate: It is the property which decides the rate at which the foam is generated from the hose of foam generator.

(iii) Foam density: It is useful to calculate the volume of foam required to be added for achieving a desired density of foam concrete. For this purpose the initial foam density is presently being used as the basis.

(iv) Stability of foam: The stability of the foam may be affected depending on the surfactant, its concentration and foam generation pressure. One of the important requirements of foam stability is to ensure the fine and uniform texture throughout the whole hardening process of foamed concrete (Koudriashoff, 1949). There are two interacting processes which contribute to the instability of foam, viz; (i) the drainage of liquid in lamelle and (ii) the interbubble diffusion causing the expansion of larger bubbles at the expense of the smaller bubbles present in the foam called as coarsening. Apart from these, internal and external disturbances also lead to the collapse of foam. Hence it is a complex problem for both analysis and measurement (Sarma et al., 1988). Since coarsening is a difficult phenomenon to measure, drainage rate is often used to characterize the stability of foam (Magrabi et al., 2001). Life time of foam is generally defined as drain time, i.e. the time required for the foam to decompose into the original liquid and the gas phase. It is determined by measuring the amount of separation of surfactant solution at various time intervals (Magrabi et al., 2001) either as free drainage or forced drainage (Hutzler et al., 2005).

4.3 MATERIALS AND METHODOLOGY

4.3.1 Materials Used

Foam was produced by aerating four commercially available synthetic surfactants viz; Sodium Lauryl Sulfate (SLS), Sodium Lauryl Ether Sulfate (SLES), Sulfanol (SULF) (ionic surfactants) and Cocodiethanolamide (CDA) (non-ionic surfactant). Table 4.1 shows an overview of their chemical classification. All the surfactants selected are basically amphiphiles having both hydrophilic and hydrophobic group. The hydrophilic group may be charged (ionic surfactants) or uncharged (nonionic surfactants). This bifunctionality in one molecule provides the basic properties to act as foaming agent (Myers, 1998).

4.3.2 Foam Generator Used

A laboratory based model of foam generator developed earlier at IIT Madras was used in the present study with the view of generating foam for small laboratory casting. The working principle of foam generation system used is based on the compressed air method wherein the foam is generated by mixing compressed air and foaming solution in high density restrictions comprising of two important components viz;

i. A device with control devices for flow and pressure for combining the liquid phase (foaming agent solution) with the non-soluble expansion gas (compressed air) producing mono-disperse particles of this solution.
ii. An arrangement allowing for a thorough mixing of foaming agent solution with air to form foam when pressure drops. The thorough mixing is very important otherwise foam quality will be less than optimum with reduced drain time (Paul, 2007).

Fig. 4.1 show the laboratory model foam generator used with various components viz., (1) Pressure container, (2) Compressor, (3) Pressure regulator, (4) Air inlet, (5) Outlet nozzle(s), (6) Outlet hose and (7) Foam outlet.

Table 4.1 An Overview of foaming agents used for the present study

Name of foaming agent	Chemical synonyms	General Group name	Chemical Formula	Classification based on charge	Availability /cost (as on 2006-2008)
Sodium lauryl sulfate	Sodium dodecyl sulfate	Alkyl sulfates	$C_{12}H_{25}NaO_4S$	Anionic	Easily Available/ Rs.666/kg
Sodium lauryl ether sulfate	Sodium laureth sulfate	Alkyl ether sulfate	$C_{16}H_{33}NaO_6S$	Anionic	Easily Available/ Rs.520/litre
Sulfanol	Sodium dodecyl benzene sulfonate	Linear alkyl benzene sulfonate	$C_{18}H_{29}NaO_3S$	Anionic	Imported from Germany/ Rs.4910 /kg
Cocodiethanol amide	Coconut diethanolamide, Cocamide DEA	Alkanolam ides	$C_{16}H_{33}NO_2$	Non ionic	Easily Available/ Rs.460/kg

.

4.3.3 Parameters and Properties Studied

Surfactant concentration and foam generation pressure are the parameters considered. Surfactant concentration (SC) / Dilution ratio (DR) represents the concentration of surfactant in the foaming premix solution prepared. It can also be expressed in terms of dilution ratio, say 1: x which means one part of foaming agent is diluted with x parts of water.

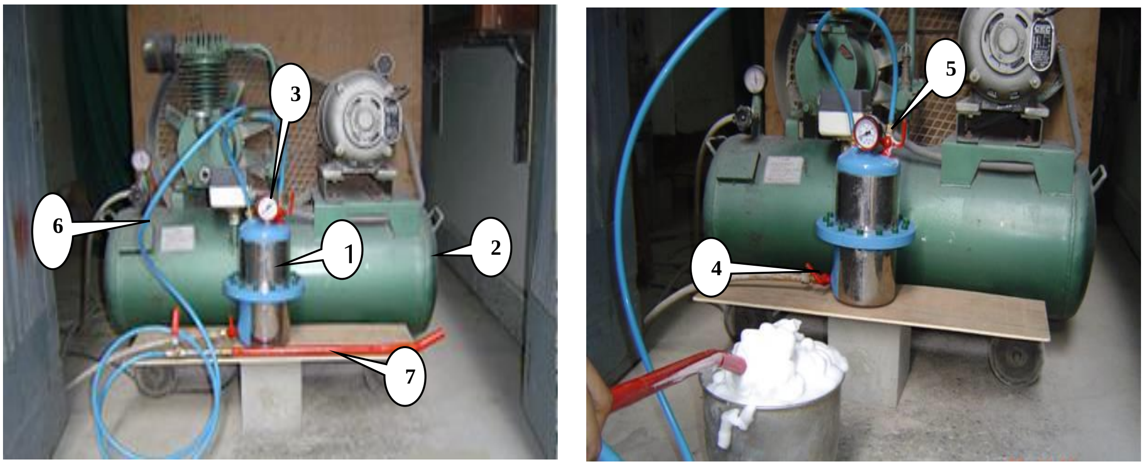

Fig 4.1 Foam Generator (Laboratory Model)

The surfactant concentration range adopted in the present study is from 0.5% (1:200) to 10 % (1:10). The required amount of surfactant was weighed to make respectively 0.5, 1, 2, 4 and 10% of surfactant in deionized water. Homogenous mixing of surfactant in water was achieved with the help of a stirrer. The surfactant solution prepared was poured through a nozzle into the pressure container of foam generator. The pressure at which the foam was generated ranged between 98 and 294 kPa with a help of pressure regulator. After thorough mixing of surfactant solution with compressed air, the foam was generated through the foam outlet. All possible mechanical vibrations were avoided and the measurement conditions were maintained identical during measurement of foam properties.

The rate of foam generation was measured by the time taken for collection of foam in a container of known volume. Foam capacity was calculated as reciprocal of Initial foam density which is the unit weight of foam measured immediately after its collection. The stability of foam was assessed by free drainage test as prescribed by Def Standard 42–40 (2002). A drainage pan of 1612 ml nominal volume with a conical base rounded to accept externally a 12.7 mm bore by 25 mm long polymethyl methacrylate tube with a 1.6mm bore brass cock at its lower end as illustrated in Fig 4.2 was used. The pan was filled with foam and the volume of the solution drained and the weight of foam was measured at various time intervals. The small variations in the height of foam with time were accounted for in the density calculation. The percentage volume drained was calculated from the measured initial foam density values.

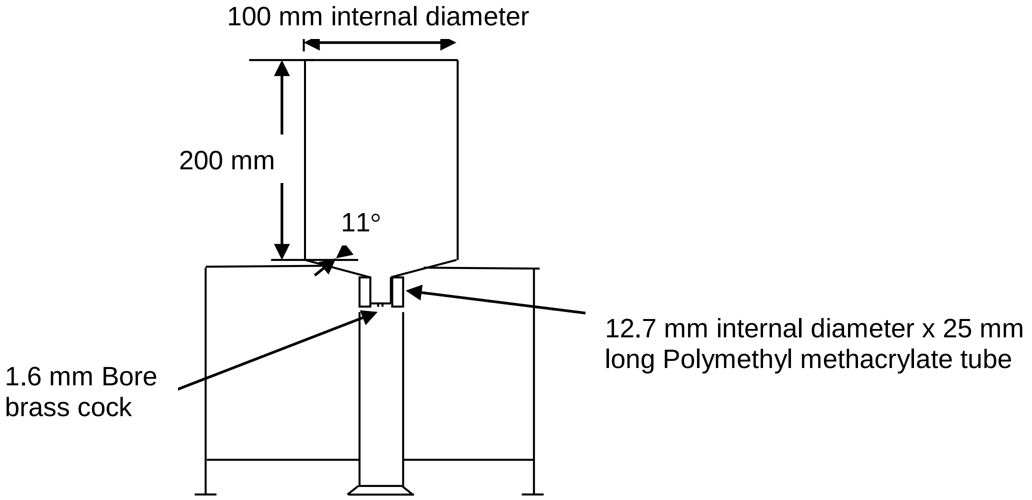

Fig. 4.2 Experimental setup for foam drainage study (Def Standard 42-40 (2002))

4.3.4 Experimental Design

Response surface methodology, a statistical method of experimental design is adopted when the response of interest is influenced by several variables and the objective is to optimize the response. Hence for the present study, a special case of factorial design based on response surface methodology (RSM) using a two factor central composite design (CCD) with rotatability or equal precision (to provide equal precision of estimates in all directions) was employed to study the effect of two independent variables x_1, surfactant concentration (SC) and x_2, foam generation pressure (FGP) on four response variables namely Foam Output Rate (FOR), Foam Capacity (FC), Initial Foam Density (IFD), Foam Stability (FS) respectively. The relationship between independent variables and response variables was fitted using second order model (to take care of curvature in the relationship) with the following objectives viz., (i) study the main and interaction effects of independent variables on response variables studied; (ii) create the possible response surface models for predicting the variation of response variables as a function of independent variables and (iii) determine an optimum level of the independent variables leading to desirable response goals (Montgomery, 2001). For each surfactant thirteen experimental treatments were assigned based on the CCD with two independent variables at five levels of each variable (Tables 4.2-4.3). The center point was repeated five times and experiments were randomized in order to minimize the effects of unexplained variability in the actual responses due to extraneous factors.

The experimental design matrix, data analysis and optimization procedure were performed using Statistical Analysis Software (SAS Release 8.02). Multiple regression coefficients were determined by employing least squares technique to predict the polynomial models for the response variables studied. The generalized polynomial model proposed for predicting the response variables is given below:

$$Yi = \beta o + \beta_1 x_1 + \beta_2 x_2 + \beta_{11} x_1^2 + \beta_{22} x_2^2 + \beta_{12} x_1 x_2 \quad (4.1)$$

Where Yi is predicted response, βo is offset term, β_1 and β_2 are regression coefficients for main variable effects, β_{11} and β_{22} are quadratic effects and β_{12} is interaction effect of independent variables.

4.4 REGRESSION ANALYSIS

The results were analysed using the Statistical Analysis Software (SAS Release 8.02) to determine the quadratic response surface models. The quadratic Response Surface Models (RSM) were used to assess the relative performance of foam produced with the four surfactants. The details of model equations for foam output rate, foam capacity, initial foam density and foam density at various time intervals, % solution drained and foam density ratio at various time intervals after foam generation are presented in Tables 4.4 to 4.8.

4.4.1 Effect of Factors and their Interaction

The significance of the estimated regression coefficients for each response variable was assessed by F-ratio at a probability (p) of 0.05 (Table 4.9). As shown in Table 4.9, the main effects of independent variables appear to have the most significant effect ($p<0.05$) as compared to quadratic and interaction effects. Though most of the regression models showed no interaction effects between surfactant concentration and foam generation pressure, to understand the variation of factors, the plots were made using models containing all the terms. From the Table 4.9 it is observed that the main effect of surfactant concentration and foam generation pressure exhibits both positive and negative effects on the response variables. Positive effect implies that any increase in the factor level is associated with a corresponding increase in response variable. Negative effect implies that an increase in factor level is associated with a decrease in response variable.

4.4.2 Model Adequacy Check

The adequacy of response models were determined using model analysis, coefficient of determination (R^2) analysis, by examining the residuals for trends in diagnostic plots and by comparing the experimental data with values predicted by response surface models (Montgomery, 2001). Validation of the second order polynomial regression models with additional experimental data were observed to be highly adequate to interpret a reliable relationship between the independent and response variables with a satisfactory coefficient R^2 (>0.9) for most of the regression models (Tables 4.9-4.11). Also the check of the normality assumption may be made by constructing a normal probability plot of the residuals, as in Figs. 4.3 to 4.11.Since the residuals plot approximately along a straight line, hence the normality assumption is satisfied. Figs. 4.3 to 4.11 present a plot of residuals versus the predicted response. The residuals randomly scatter on the display suggesting that the variance of the original observations is constant for all the values of y. As a next step, relative performance of foam produced with the four surfactants are discussed in terms of foam characteristics mentioned above by plotting graphs using these empirical models.

4.5 FOAM OUTPUT RATE

Figs. 4.12 to 4.14 show the variation in foam output rate with surfactant concentration and foam generation pressure. For ionic surfactants, the foam output rate increases with an increase in surfactant concentration up to a dosage of around 4% after which a marginal reduction is observed (Fig 4.13). This reduction is attributed to the more viscous foam produced at higher surfactant concentration (Ranjani and Ramamurthy, 2010). For non-ionic surfactant (Cocodiethanolamide) the surfactant concentration has insignificant effect on the foam output rate irrespective of the foam generation pressure. For all the four surfactants used, the variation of foam output rate with surfactant concentration is marginal when compared to that with variation in foam generation pressure. Hence the main effects of surfactant concentration are observed to be insignificant ($p>0.05$) for all surfactants with the exception of Sodium lauryl ether sulfate from regression model studies (Table 4.9).

Table 4.2 Components of central composite rotatable second order design

No of variables	Number of design points			Total run	alpha
	factorial	axial	central		
2	4	4	5	13	1.414

Table 4.3 Matrix of the Central Composite Design (CCD)

Treatment runs	Surfactant concentration (%)	Foam generation pressure (kPa)
1(C)	5.25	196
2(C)	5.25	196
3	8.61	265.3
4	0.5	196
5	5.25	196
6	5.25	294
7(C)	5.25	196
8	1.89	126.7
9(C)	1.89	265.3
10	8.61	126.7
11(C)	5.25	196
12	5.25	98
13	10	196

Table 4.4 RSM for foam output rate (FOR) for different surfactants

Surfactant	Response surface models
SLS	$\mathrm{FOR} = 0.321202 + 0.165003 * SC - 0.00681 * FGP - 1.8 * 10^{-18} * SC * FGP - 0.01631 * SC^2 + 3.54 * 10^{-5} * FGP^2$
SLES	$\mathrm{FOR} = -0.30973 + 0.045338 * SC + 0.003009 * FGP + 0.000276 * SC * FGP - 0.0069 * SC^2 + 1.5 * 10^{-7} * FGP^2$
SULF	$\mathrm{FOR} = -0.55855 + 0.075444 * SC + 0.005964 * FGP + 3.84 * 10^{-5} * SC * FGP - 0.00715 * SC^2 - 2.2 * 10^{-6} * FGP^2$
CDA	$\mathrm{FOR} = 0.330787 + 0.003542 * SC - 0.00588 * FGP + 1.46 * 10^{-5} * SC * FGP - 8.3 * 10^{-5} * SC^2 + 3.03 * 10^{-5} * FGP^2$

Table 4.5 RSM for foam capacity (FC) for different surfactants

Surfactant	Response surface models
SLS	$\mathrm{FC} = 0.050506 + 0.003232 * SC - 0.00015 * FGP + 2.85 * 10^{-6} * SC * FGP - 0.00024 * SC^2 + 2.36 * 10^{-7} * FGP^2$
SLES	$\mathrm{FC} = 0.045012 + 0.005904 * SC - 0.00023 * FGP - 9.6 * 10^{-7} * SC * FGP - 0.00043 * SC^2 + 3.74 * 10^{-7} * FGP^2$
SULF	$\mathrm{FC} = 0.064076 + 0.781 * 10^{-3} * SC - 1.3 * 10^{-4} * FGP + 8.63 * 10^{-6} * SC * FGP - 0.000161 * SC^2 - 1.1 * 10^{-7} * FGP^2$
CDA	$\mathrm{FC} = 0.016079 - 0.00161 * SC + 3.27 * 10^{-5} * FGP + 6.83 * 10^{-6} * SC * FGP + 1.66 * 10^{-5} * SC^2 - 1.4 * 10^{-7} * FGP^2$

There is no interaction effect observed between Surfactant Concentration (SC) and foam generation pressure (FGP) on foam output rate for all the surfactants taken for study with the exception of Sodium lauryl ether sulfate for which interaction effect is significant.

For a constant surfactant concentration the foam output rate increases significantly with an increase in foam generation pressure for all the four surfactants. It is observed from the Fig 4.14 that the effect of foam generation pressure on foam output rate is higher for Sulfanol and Sodium lauryl sulfate irrespective of surfactant concentration. Hence the output rate of foam produced using Sulfanol and Sodium lauryl sulfate are the highest. For all the four surfactants, foam output rate is observed to be lower at lower surfactant concentration and foam generation pressure. Based on a large number of experiments carried out it is observed that a minimum requirement of foam output rate of 0.09 m^3/hr is required to get uninterrupted foam production for the laboratory foam generator used. When the surfactant concentration less than 1% is used in combination with foam generation pressure lower than 98 kPa, the foam output rate is significantly reduced below the acceptable level for all the surfactants used. Hence it appears that there is an optimal surfactant concentration and foam generation pressure which can produce foam with a acceptable foam output rate.

Table 4.6 RSM for foam density (FD) at various time intervals for different surfactants

Foam property	Surfactant	Response surface models
IFD	SLS	$\mathrm{IFD} = 20.12124 - 2.05373 * SC + 0.08349 * FGP - 0.0038 * SC * FGP + 0.184089 * SC^2$ $- 9.7 * 10^{-5} * FGP^2$
	SLES	$\mathrm{IFD} = 40.96705 - 9.17408 * SC + 0.09647 * FGP + 0.671866 * SC^2$
	SULF	$\mathrm{IFD} = 17.5775 - 0.91786 * SC + 0.02379 * FGP - 0.00565 * SC * FGP + 0.132912 * SC^2 + 0.0002 * FGP^2$
	CDA	$\mathrm{IFD} = 68.63874 + 6.673567 * SC - 0.20224 * FGP - 0.03073 * SC * FGP - 0.00825 * SC^2 + 0.000757 * FGP^2$
FD at 5th minute	SLS	$\mathrm{FD} = 18.39425 - 1.68899 * SC + 0.066825 * FGP - 1.17893 * 10^{-3} * SC * FGP + 0.15216 * SC^2 - 1.32224 * 10^{-4} * FGP^2$
	SLES	$\mathrm{FD} = 36.70574 - 5.80818 * SC + 0.019059 * FGP + 0.41971 * SC^2$
	SULF	$\mathrm{FD} = 20.66503 + 0.65285 * SC - 0.086648 * FGP - 3.57686 * 10\wedge{-3} * SC * FGP + 7.9726 * 10^{3} * SC^2$ $+ 3.67456 * 10^{-4} * FGP^2$
	CDA	$\mathrm{FD} = 59.94294 + 10.83776 * SC - 0.24160 * FGP - 0.027712 * SC * FGP - 0.31490 * SC^2 + 7.29971 * 10^{-4} * FGP^2$
FD at 10th minute	SLS	$\mathrm{FD} = 7.51031 - 0.19505 * SC + 1.00621 * 10^{-4} * FGP - 2.64309 * 10^{-3} * SC * FGP + 0.096673 * SC^2$ $+ 3.67349 * 10^{-5} * FGP^2$
	SLES	$\mathrm{FD} = 16.60996 - 2.10015 * SC - 0.035515 * FGP + 1.25622 * 10^{-3} * SC * FGP + 0.14902 * SC^2 + 6.54138 * 10^{-5} * FGP^2$
	SULF	$\mathrm{FD} = 14.5659 + 0.55116 * SC - 0.11302 * FGP + 5.94545 * 10^{-4} * SC * FGP - 0.036546 * SC^2 + 2.83675 * 10^{-4} * FGP^2$
	CDA	$\mathrm{FD} = 14.68048 + 22.21186 * SC - 0.22063 * FGP - 0.026326 * SC * FGP - 1.03357 * SC^2 + 6.25567 * 10^{-4} * FGP^2$

Table 4.7 RSM for solution drained at various time intervals for different surfactants

Foam property	Surfactant	Response surface models
SD at 5th minute	SLS	$\mathrm{SD} = 8.573218 - 0.26454 * SC + 0.023221 * FGP - 0.0057 * SC * FGP - 0.0263 * SC^2 + 0.000161 * FGP^2$
	SLES	$\mathrm{SD} = -22.5585 - 0.62119 * SC + 0.396609 * FGP - 0.0024 * SC * FGP + 0.093638 * SC^2 - 0.00059 * FGP^2$
	SULF	$\mathrm{SD} = -18.3512 - 1.3044 * SC + 0.3521 * FGP - 0.00671 * SC * FGP + 0.10701 * SC^2 - 0.000429 * FGP^2$
	CDA	$\mathrm{SD} = 11.79883 - 5.66816 * SC + 0.074943 * FGP - 0.00976 * SC * FGP + 0.509695 * SC^2 - 4.3 * 10^{-5} * FGP^2$
SD at 10th minute	SLS	$\mathrm{SD} = 62.52708 - 2.00598 * SC + 0.088524 * FGP - 0.006969 * SC * FGP - 0.18314 * SC^2 - 0.0006969 * FGP^2$
	SLES	$\mathrm{SD} = 38.60558 + 0.73728 * SC + 0.31590 * FGP + 1.99233 * 10^{-6} * SC * FGP - 0.11764 * SC^2 - 0.00058 * FGP^2$
	SULF	$\mathrm{SD} = 29.57482 - 3.11757 * SC + 0.47401 * FGP - 0.003834 * SC * FGP + 0.21923 * SC^2 - 0.0008915 * FGP^2$
	CDA	$\mathrm{SD} = 95.50594 - 25.73125 * SC - 0.024022 * FGP - 0.007806 * SC * FGP + 1.75069 * SC^2 - 3.007 * 10^{-4} * FGP^2$

4.6 FOAM CAPACITY

The effects of surfactant concentration and foam generation pressure on the foam capacity are plotted in Figs.4.15 to 4.17. For ionic surfactants i) the maximum foam capacity or foamability is achieved when lower foam generation pressure and higher surfactant concentration is adopted and ii) the foam capacity increases with an increase in surfactant concentration of up to 4% after which there is only a marginal variation, particularly at lower foam generation pressure (Fig.4.16(a)). This is because at lower foam generation pressure and higher surfactant concentration, the foam is relatively dry and hence produces higher volume of foam. For non-ionic surfactant (Cocodiethanolamide), i) the surfactant concentration has relatively lesser effect on the foam capacity irrespective of foam generation pressure ii) the foam capacity decreases marginally with an increase in surfactant concentration at lower foam generation pressure (Fig.4.16(a)), and iii) this trend is reversed at higher foam generation pressure (Fig.4.16(b)).

For a given surfactant concentration, an increase in foam generation pressure reduces the foam capacity for all the ionic surfactants. For non-ionic surfactant (Cocodiethanolamide), i) the foam generation pressure does not have significant effect on the foam capacity particularly at lower surfactant concentration (Fig 4.17(a)) ii) at higher surfactant concentration, foam capacity increases with an increase in foam generation pressure unlike ionic surfactants (Fig 4.17(b)).

Table 4.8 RSM for foam Density Ratio (DR) at various time intervals

Foam property	Surfactant	Response surface models
DR at 5th minute	SLS	$\mathrm{DR} = 0.914268 + 0.002645 * SC - 0.00023 * FGP + 5.7 * 10^{-5} * SC * FGP + 0.000263 * SC^2 - 1.6 * 10^{-6} * FGP^2$
	SLES	$\mathrm{DR} = 1.211507 + 0.005659 * SC - 0.00382 * FGP + 2.4 * 10^{-5} * SC * FGP - 0.00088 * SC^2 - 5.53 * 10^{-6} * FGP^2$
	SULF	$\mathrm{DR} = 1.183513 + 0.013044 * SC - 0.00352 * FGP + 6.71 * 10^{-5} * SC * FGP - 0.00107 * SC^2 - 4.3 * 10^{-6} * FGP^2$
	CDA	$\mathrm{DR} = 0.846081 + 0.068741 * SC - 0.00056 * FGP + 4.88 * 10^{-5} * SC * FGP - 0.00515 * SC^2 - 5.4 * 10^{-7} * FGP^2$
DR at 10th minute	SLS	$\mathrm{DR} = 0.3906 + 0.017643 * SC - 0.0012514 * FGP - 7.606 * 10^{-5} * SC * FGP + 0.0021565 * SC^2 + 3.1149 * 10^{-6} * FGP^2$
	SLES	$\mathrm{DR} = 0.59876 - 0.002223 * SC - 0.003159 * FGP - 1.59642 * 10^{-19} * SC * FGP + 0.000748 * SC^2 + 5.8 * 10^{-6} * FGP^2$
	SULF	$\mathrm{DR} = 0.73550 + 0.026757 * SC - 0.005060 * FGP + 3.83446 * 10^{-5} * SC * FGP - 0.00107 * SC^2 + 9.774 * 10^{-6} * FGP^2$
	CDA	$\mathrm{DR} = 0.0538 + 0.25828 * SC + 0.000132 * FGP + 6.83039 * 10^{-5} * SC * FGP - 0.017341 * SC^2 - 2.6853 * 10^{-6} * FGP^2$

Table 4.9 ANOVA and regression coefficients of the response surface models fitted

Foaming agent	Variables		Main effects		Quadratic effects		Interaction effect
			x_1	x_2	x_1^2	x_2^2	$x_1 x_2$
SLS	Foam output rate	p-value	0.8826	<0.0001	0.0069	0.005	1
		F-ratio	0.023	104.19	14.28	16.18	0
SLES		p-value	0.0011	<0.0001	0.0024	0.9615	0.0168
		F-ratio	28.53	441.82	21.27	2.506×10^{-3}	9.76
SULF		p-value	0.372	<0.0001	0.0405	0.7119	0.8264
		F-ratio	0.91	172.03	6.29	0.15	0.052
CDA		p-value	0.6109	<0.0001	0.9802	0.0019	0.9401
		F-ratio	0.28	152.39	6.596×10^{-4}	23.4	6.068×10^{-3}
SLS	Foam Capacity	p-value	<0.0001	<0.0001	<0.0001	0.0052	0.1422
		F-ratio	190.18	147.31	69.87	15.98	2.73
SLES		p-value	<0.0001	<0.0001	<0.0001	0.0087	0.7626
		F-ratio	64.67	174.63	67.93	12.98	0.099
SULF		p-value	0.1258	0.0004	0.2630	0.6971	0.3046
		F-ratio	3.02	41.32	1.48	0.16	1.227
CDA		p-value	0.0351	0.0006	0.4362	0.009	0.0006
		F-ratio	6.79	35.34	0.68	12.8	34.15
SLS	Initial foam density	p-value	<0.0001	0.0004	0.0005	0.163	0.0737
		F-ratio	80.41	40.21	36.74	2.43	4.42
SLES		p-value	<0.0001	<0.0001	<0.0001	-	-
		F-ratio	48.47	45.13	45.41	-	-
SULF		p-value	0.0161	<0.0001	0.0605	0.1373	0.1519
		F-ratio	9.92	66.49	5	2.81	2.59
CDA		p-value	0.0096	0.0001	0.9186	0.0015	0.0003
		F-ratio	12.46	57.25	0.01122	25.13	46.11

Table 4.9 ANOVA and regression coefficients of the response surface models fitted (Continued)

Foaming agent	Variables		Main effects		Quadratic effects		Interaction effect
			x_1	x_2	x_1^2	x_2^2	$x_1 x_2$
SLS	Foam density at 5th minute	p-value	0.0003	0.0018	<0.0001	0.0054	0.2646
		F-ratio	44.292	23.58	87.00	15.75	0
SLES		p-value	<0.0001	0.0221	<0.0001	-	-
		F-ratio	91.22	7.62	76.71	-	-
SULF		p-value	0.4713	0.0001	0.7866	0.0003	0.07
		F-ratio	0.5796	61.81	0.079	41.74	4.56
CDA		p-value	<0.0001	<0.0001	<0.0001	<0.0001	<0.0001
		F-ratio	412.28	502.09	71.54	102.27	164.32
SLS	Foam density at 10th minute	p-value	0.0007	0.9206	0.0006	0.306	0.0297
		F-ratio	33.56	0.0107	35.22	1.219	7.411
SLES		p-value	0.001	0.1273	<0.0001	0.1269	0.2958
		F-ratio	29.59	2.99	62.71	3	1.28
SULF		p-value	0.0039	0.2036	0.1275	0.0003	0.6486
		F-ratio	17.80	1.97	2.99	44.67	0.226
CDA		p-value	<0.0001	0.0005	0.0002	0.0701	0.0199
		F-ratio	186	36.4	46.79	4.56	9.00
SLS	Percentage solution drained in 5 minutes	p-value	<0.0001	<0.0001	0.5535	0.1042	0.0579
		F-ratio	138.16	77.43	0.39	3.48	5.13
SLES		p-value	0.7684	<0.0001	0.3927	0.0252	0.7049
		F-ratio	0.094	127.96	0.83	8.05	0.16
SULF		p-value	0.0041	<0.0001	0.3574	0.0895	0.3305
		F-ratio	17.52	102.86	0.97	3.9	1.09
CDA		p-value	0.0002	0.0172	0.0009	0.818	0.113
		F-ratio	53.97	9.64	30.19	0.057	3.28

Table 4.9 ANOVA and regression coefficients of the response surface models fitted (Continued)

Foaming agent	Variables		Main effects		Quadratic effects		Interaction effect
			x_1	x_2	x_1^2	x_2^2	$x_1 x_2$
SLS	Percentage solution drained in 10 minutes	p-value	0.0001	0.0087	0.1166	0.3941	0.2906
		F-ratio	61.76	12.98	3.20	0.82	1.30
SLES		p-value	0.1177	<0.0001	0.2044	0.0109	1
		F-ratio	3.18	68.98	1.96	11.80	0
SULF		p-value	0.0002	<0.0001	0.0153	0.0003	0.3771
		F-ratio	51.08	153.95	10.16	41.62	0.89
CDA		p-value	<0.0001	0.1049	<0.0001	0.4254	0.4872
		F-ratio	235.08	3.47	91.2	0.72	0.54
SLS	Foam density ratio at 5th minute	p-value	<0.0001	<0.0001	0.5535	0.1042	0.0579
		F-ratio	138.16	77.43	0.39	3.48	5.13
SLES		p-value	0.7826	<0.0001	0.4477	0.0404	0.7226
		F-ratio	0.082	109.14	0.65	6.3	0.14
SULF		p-value	0.0041	<0.0001	0.3574	0.0895	0.3305
		F-ratio	17.52	102.86	0.97	3.88	1.09
CDA		p-value	0.0001	0.0076	0.0012	0.7861	0.4208
		F-ratio	59.48	13.75	27.5	0.079	0.73
SLS	Foam density ratio at 10th minute	p-value	<0.0001	0.0112	0.0612	0.1592	0.2289
		F-ratio	67.52	11.66	4.96	2.48	1.74
SLES		p-value	0.0787	<0.0001	0.4025	0.0109	1
		F-ratio	4.23	69.03	0.79	11.81	0
SULF		p-value	0.0002	<0.0001	0.0373	0.0002	0.3771
		F-ratio	51.08	153.95	6.58	50.03	0.889
CDA		p-value	<0.0001	0.0887	<0.0001	0.4836	
		F-ratio	229.9	3.90	85.75	0.547	0.394

Table 4.10 R^2, probability values and F values for the final models

Foaming agent	Variables	R^2	R^2 adj	Regression p value	F value
SLS	Foam output rate	0.9521	0.9179	0.0002	27.85
SLES		0.9862	0.9764	<0.0001	100.36
SULF		0.9624	0.9356	<0.0001	35.86
CDA		0.9619	0.9346	<0.0001	35.3
SLS	Foam capacity	0.9842	0.9729	<0.0001	87.29
SLES		0.9792	0.9643	<0.0001	65.92
SULF		0.8706	0.7782	0.0052	9.42
CDA		0.9284	0.8772	0.0007	18.16
SLS	Initial foam density	0.9599	0.9312	<0.0001	33.48
SLES		0.9392	0.9189	<0.0001	46.34
SULF		0.9247	0.8709	0.0008	17.19
CDA		0.9529	0.9192	0.0002	28.307
SLS	Foam density at 5th minute	0.9633	0.9371	<0.0001	36.74
SLES		0.9512	0.935	<0.0001	58.52
SULF		0.9397	0.8966	0.0004	21.8
CDA		0.9945	0.9907	<0.0001	255.64
SLS	Foam density at 10th minute	0.916	0.86	0.0012	15.26
SLES		0.9327	0.8847	0.0006	19.41
SULF		0.9109	0.8472	0.0015	14.31
CDA		0.9762	0.9592	<0.0001	57.5

Table 4.10 R^2, probability values and F values for the final models (Continued)

Foaming agent	Variables	R^2	R^2 adj	Regression p value	F value
SLS	Percentage solution drained in 5 minutes	0.9698	0.9483	<0.0001	44.99
SLES		0.9517	0.9172	0.0002	27.58
SULF		0.9477	0.9104	0.0002	25.38
CDA		0.9329	0.885	0.0006	19.46
SLS	Percentage solution drained in 10 minutes	0.9193	0.8616	0.0011	15.94
SLES		0.9238	0.8694	0.0009	16.98
SULF		0.9742	0.9557	<0.0001	52.81
CDA		0.9792	0.9644	<0.0001	66.09
SLS	Foam density ratio at 5th minute	0.9698	0.9483	<0.0001	44.99
SLES		0.9435	0.9032	0.0003	23.39
SULF		0.9477	0.9104	0.0002	25.38
CDA		0.9355	0.8895	0.0005	20.32
SLS	Foam density ratio at 10th minute	0.926	0.8731	0.0008	17.51
SLES		0.9241	0.87	0.0009	17.05
SULF		0.9746	0.9564	<0.0001	53.66
CDA		0.9786	0.9633	<0.0001	64.03

Both the main effects of surfactant concentration and foam generation pressure significantly ($p<0.05$) influence the foam capacity with the exception of Sulfanol for which only the foam generation pressure has significant effect (Table 4.9). The interaction effects of the factors are observed to be less significant for all the surfactants with the exception of Cocodiethanolamide. Foams produced with synthetic foaming agents tend to have higher expansion ratio than those produced with natural foaming agents. Very high foam capacity, say greater than 0.05 m^3, results in over-expanded foam with low densities. Such low density foams tend to have larger bubbles with thin walls, poor strength and hence are likely to collapse.

4.7 RELATION BETWEEN FOAM OUTPUT RATE AND FOAM CAPACITY

The relation between foam output rate and foam capacity is distinct for the four surfactants. From Fig.4.18 it is observed that for all the ionic surfactants the foam capacity increases with foam output rate up to 4% concentration of surfactant. Beyond this concentration, the foam capacity is higher or lower depending upon the surfactant.

For Sodium lauryl sulfate beyond 4% concentration, the foam capacity is higher even when the foam output rate is lower. Such behaviour is attributed to the relatively higher influence of SLS concentration on foam capacity than on foam output rate (which is primarily dependent on foam generation pressure) (Table 4.9). Hence at higher SLS concentration (say 10%) the foam capacity is higher irrespective of foam output rate. For Sodium lauryl ether sulfate, beyond 4% concentration the foam capacity is lower irrespective of foam output rate. This is because beyond 4% SLES concentration, up to a foam generation pressure of 137 kPa the foam capacity reduces with a decrease in foam output rate at higher surfactant concentration. Beyond foam generation pressure of 137 kPa, the foam capacity reduces even when the foam output rate is higher at concentration above 4%. This is because the ratio of total volume of foam to liquid volume is lower in very wet foam produced at higher foam generation pressures.

For Sulfanol, the foam capacity reduces with a reduction in foam output rate beyond 4% surfactant concentration up to a foam generation pressure of 137 kPa. Beyond 137 kPa, the foam capacity is higher even when the foam output rate is lower. Such a behaviour is attributed to the relatively higher influence of surfactant concentration on foam capacity than on foam output rate even at higher foam generation pressure. It is also observed from the Figs. 4.18(a) to 4.18(c) that for all ionic surfactants the foam generating power of surfactant solution reduces with an increase in foam generation pressure, i.e. ratio of total volume of foam to liquid volume is lower in very wet foam produced at higher foam generation pressures.

Table 4.11 Observed and predicted responses for confirmation of models

Surfactant	Factors		Foam Output rate (m^3/hr)		Foam Capacity (m^3)		Initial Foam Density (kg/m^3)	
	SC	FGP	Predicted	Observed	Predicted	Observed	Predicted	Observed
SLS	0.5	117	0.09	0.12	0.037	0.036	27	28
	0.5	196	0.427	0.42	0.031	0.033	31	30
	0.5	294	1.464	1.56	0.028	0.029	35	34
	2	117	0.275	0.24	0.042	0.044	25	24
	2	196	0.614	0.58	0.036	0.040	28	25
	2	294	1.65	1.69	0.033	0.035	31	29
	10	117	0.03	0.054	0.047	0.047	22	21
	10	196	0.368	0.32	0.043	0.045	23	22
	10	294	1.405	1.2	0.042	0.043	23	23
SLES	0.5	117	0.084	0.1	0.026	0.023	43	44
	0.5	196	0.334	0.32	0.017	0.017	55	58
	0.5	294	0.65	0.64	0.012	0.014	65	69
	2	117	0.175	0.20	0.033	0.03	37	38
	2	196	0.458	0.45	0.024	0.022	44	45
	2	294	0.814	0.8	0.019	0.018	54	55
	10	117	0.135	0.12	0.038	0.036	28	28
	10	196	0.59	0.58	0.028	0.027	35	37
	10	294	1.16	1.13	0.023	0.026	45	47
SULF	0.5	117	0.151	0.12	0.049	0.043	23	26
	0.5	196	0.566	0.53	0.037	0.034	29	31
	0.5	294	1.047	0.98	0.019	0.022	46	43
	2	117	0.244	0.25	0.051	0.049	22	22
	2	196	0.66	0.65	0.040	0.037	27	27
	2	294	1.15	1.14	0.024	0.027	37	37
	10	117	0.197	0.18	0.05	0.047	21	21
	10	196	0.64	0.7	0.044	0.043	23	25
	10	294	1.15	1.07	0.035	0.036	29	28
CDA	0.5	117	0.062	0.09	0.018	0.017	57	59
	0.5	196	0.35	0.3	0.017	0.016	58	63
	0.5	294	1.232	1.1	0.014	0.012	73	78
	2	117	0.07	0.1	0.016	0.017	61	58
	2	196	0.35	0.33	0.017	0.017	61	63
	2	294	1.24	1.2	0.014	0.014	70	71
	10	117	0.104	0.13	0.012	0.012	85	80
	10	196	0.401	0.35	0.016	0.016	64	63
	10	294	1.299	1.1	0.019	0.018	50	55

Table 4.11 Observed and predicted responses for confirmation of models (Continued)

Surfactant	Factors		Foam density at 5th minute (kg/m^3)		Foam density at 10th minute (kg/m^3)		Solution drained in 5 minutes (%)	
	SC	FGP	Predicted	Observed	Predicted	Observed	Predicted	Observed
SLS	0.5	117	24	23	8	8	13	17
	0.5	196	26	24	9	8	19	19
	0.5	294	26	25	10	9	28	27
	2	117	21	21	7	8	11	9
	2	196	23	21	8	8	16	15
	2	294	23	22	9	9	25	23
	10	117	21	20	13	13	2	3
	10	196	22	21	12	13	3	3
	10	294	22	22	11	12	7	8
SLES	0.5	117	36	35	12	14	16	20
	0.5	196	38	39	11	15	32	31
	0.5	294	40	42	11	12	43	39
	2	117	29	31	10	12	12	14
	2	196	31	29	9	10	31	32
	2	294	32	31	9	11	41	40
	10	117	23	24	9	10	16	18
	10	196	24	25	9	10	31	29
	10	294	26	27	9	11	40	40
SULF	0.5	117	16	20	6	6	16	20
	0.5	196	18	20	4	7	33	35
	0.5	294	27	25	6	6	46	42
	2	117	16	18	6	7	13	13
	2	196	18	19	5	6	29	30
	2	294	26	24	7	7	42	37
	10	117	19	20	8	9	7	5
	10	196	19	20	6	9	19	15
	10	294	24	23	10	10	26	20
CDA	0.5	117	45	44	7	9	18	22
	0.5	196	43	45	4	9	24	27
	0.5	294	53	50	11	11	33	36
	2	117	56	52	31	32	10	9
	2	196	50	54	25	29	15	14
	2	294	56	56	29	28	22	21
	10	117	85	80	85	80	4	0
	10	196	63	61	63	60	4	0
	10	294	47	53	45	50	4	4

Table 4.11 Observed and predicted responses for confirmation of models (Continued)

Surfactant	Factors		Solution drained in 10 minutes (%)		Foam density ratio at 5th minute		Foam density ratio at 10th minute	
	SC	FGP	Predicted	Observed	Predicted	Observed	Predicted	Observed
SLS	0.5	117	70	69	0.87	0.82	0.29	0.29
	0.5	196	72	70	0.81	0.80	0.27	0.27
	0.5	294	72	72	0.72	0.73	0.27	0.26
	2	117	67	62	0.88	0.91	0.31	0.35
	2	196	70	65	0.84	0.84	0.29	0.32
	2	294	71	67	0.75	0.76	0.29	0.31
	10	117	40	35	0.98	0.95	0.59	0.62
	10	196	48	45	0.97	0.95	0.51	0.59
	10	294	54	52	0.93	0.94	0.46	0.52
SLES	0.5	117	68	65	0.84	0.80	0.31	0.32
	0.5	196	79	73	0.68	0.67	0.2	0.26
	0.5	294	82	81	0.57	0.61	0.17	0.17
	2	117	68	65	0.85	0.82	0.31	0.32
	2	196	79	74	0.69	0.64	0.2	0.22
	2	294	82	79	0.59	0.56	0.17	0.20
	10	117	63	62	0.83	0.86	0.36	0.36
	10	196	74	72	0.69	0.68	0.25	0.27
	10	294	77	76	0.6	0.57	0.22	0.23
SULF	0.5	117	71	72	0.84	0.77	0.29	0.23
	0.5	196	86	80	0.67	0.65	0.14	0.23
	0.5	294	90	85	0.54	0.58	0.11	0.14
	2	117	67	64	0.87	0.82	0.33	0.31
	2	196	81	78	0.71	0.70	0.18	0.22
	2	294	84	80	0.58	0.65	0.16	0.19
	10	117	59	55	0.93	0.95	0.41	0.43
	10	196	71	68	0.81	0.86	0.3	0.36
	10	294	71	68	0.74	0.82	0.3	0.36
CDA	0.5	117	84	82	0.81	0.75	0.16	0.15
	0.5	196	89	86	0.75	0.71	0.15	0.14
	0.5	294	95	88	0.68	0.64	0.15	0.14
	2	117	51	43	0.9	0.90	0.5	0.55
	2	196	55	52	0.85	0.85	0.45	0.46
	2	294	65	62	0.78	0.79	0.35	0.39
	10	117	5	0	1	1	0.96	1
	10	196	5	5	0.98	0.97	0.96	0.95
	10	294	9	7	0.95	0.96	0.91	0.91

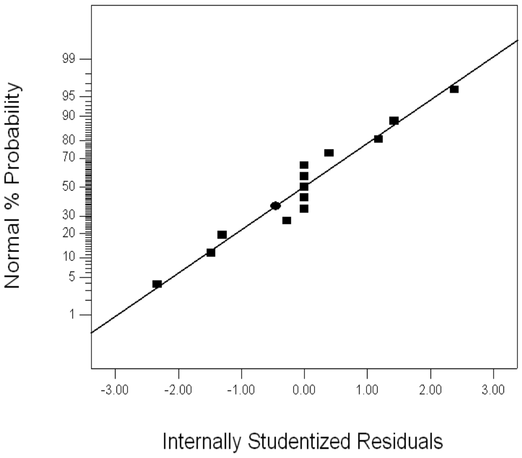

Fig. 4.3(a) Normal probability plot (SLS)

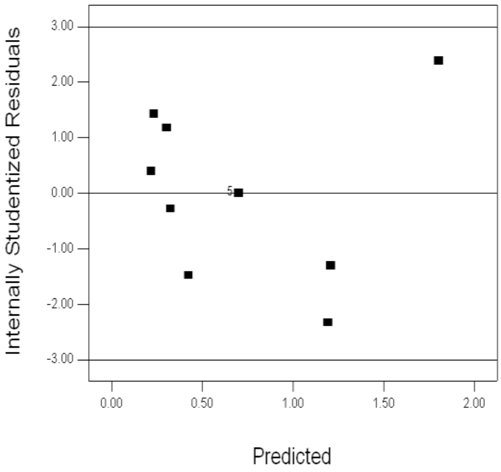

Fig. 4.3(b) Residual plot (SLS)

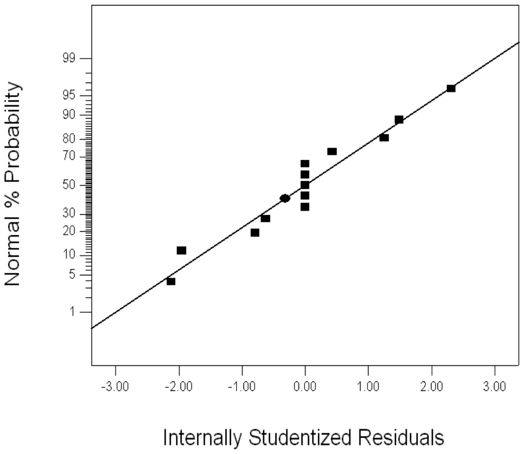

Fig.4.3(c) Normal probability plot (SLES)

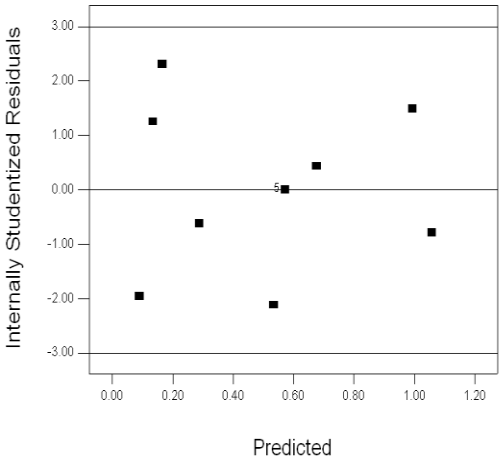

Fig. 4.3(d) Residual plot (SLES)

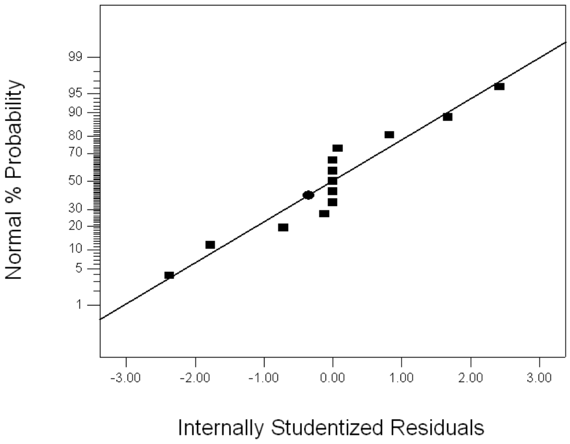

Fig. 4.3 (e) Normal probability plot (SULF)

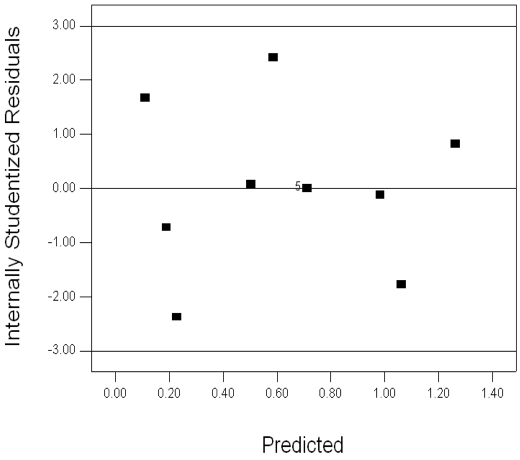

Fig. 4.3 (f) Residual plot (SULF)

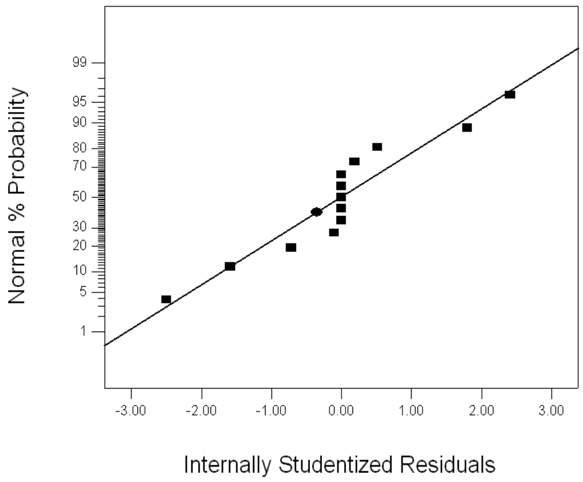

Fig. 4.3(g) Normal probability plot (CDA)

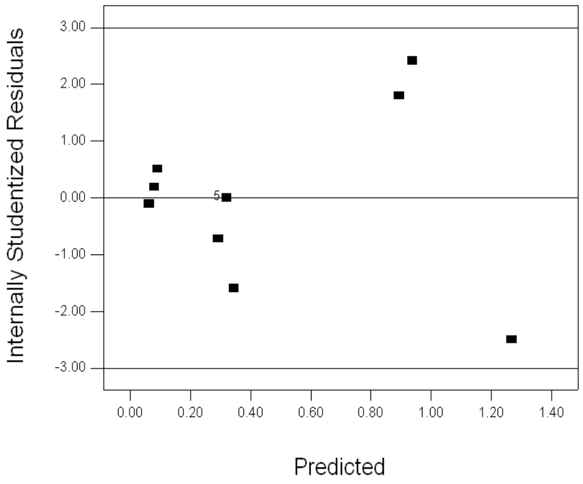

Fig. 4.3(h) Residual plot (CDA)

Fig 4.3 Diagnostic plots for foam output rate

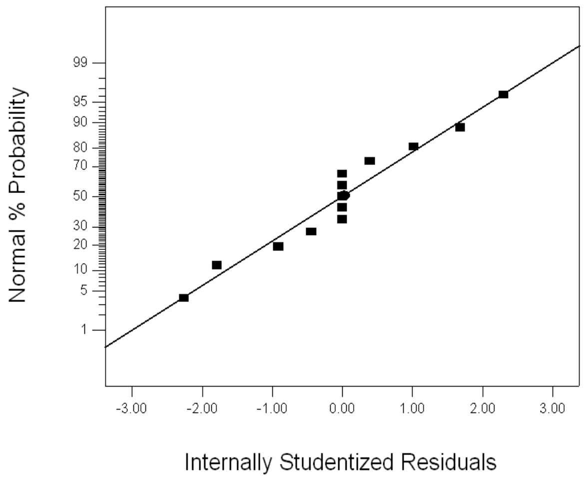

Fig. 4.4(a) Normal probability plot (SLS)

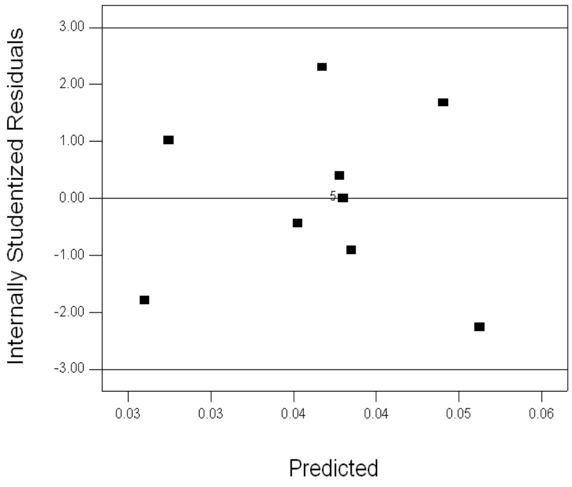

Fig. 4.4(b) Residual plot (SLS)

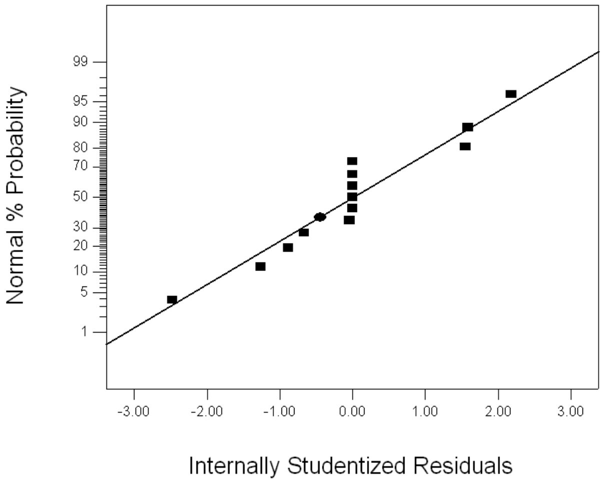

Fig. 4.4(c) Normal probability plot (SLES)

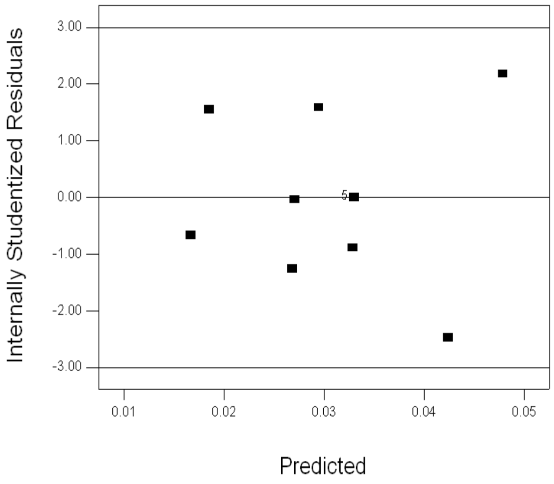

Fig. 4.4(d) Residual plot (SLES)

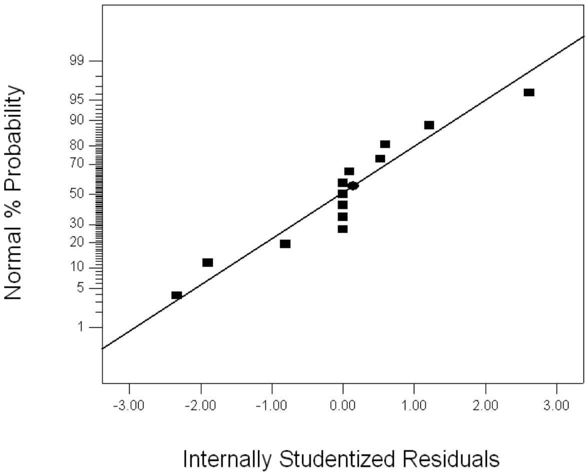

Fig. 4.4(e) Normal probability plot (SULF)

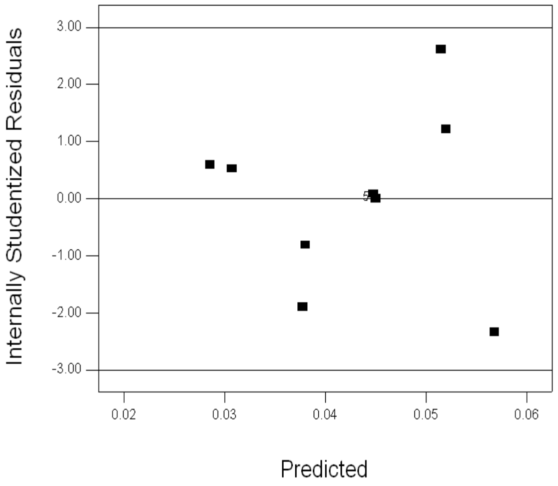

Fig. 4.4 (f) Residual plot (SULF)

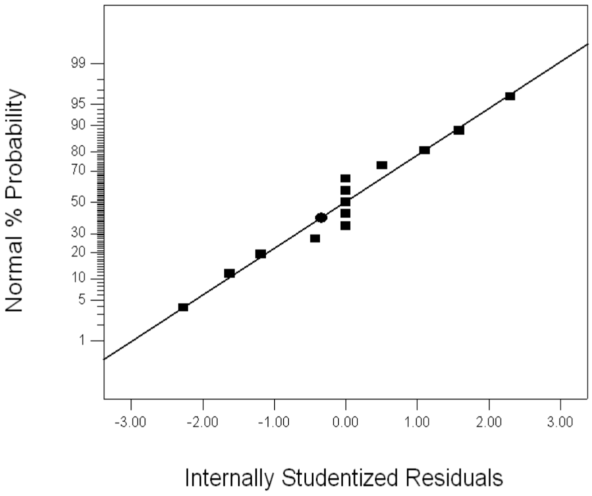

Fig. 4.4 (g) Normal probability plot (CDA)

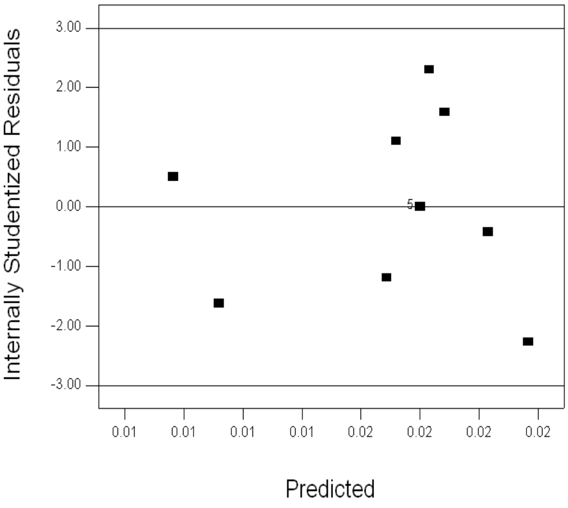

Fig. 4.4 (h) Residual plot (CDA)

Fig. 4.4 Diagnostic plots for foam capacity

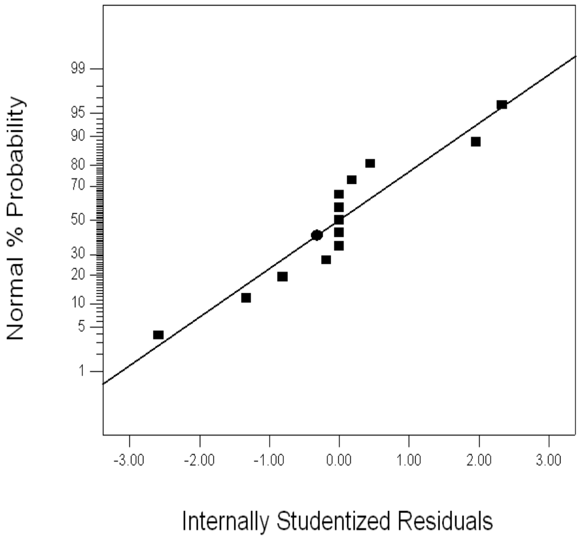

Fig. 4.5 (a) Normal probability plot (SLS)

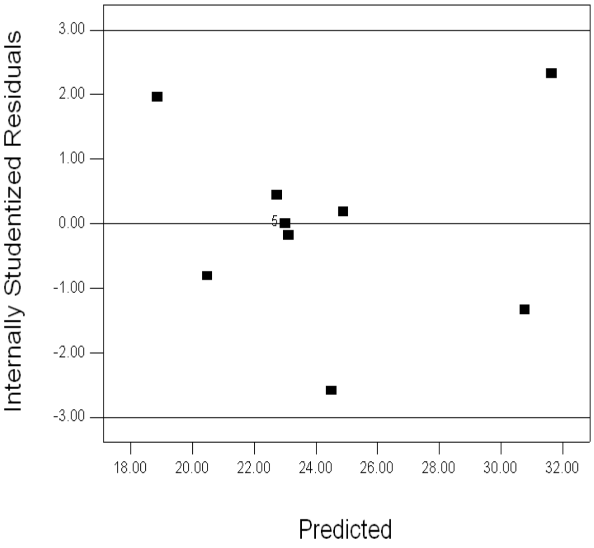

Fig. 4.5(b) Residual plot (SLS)

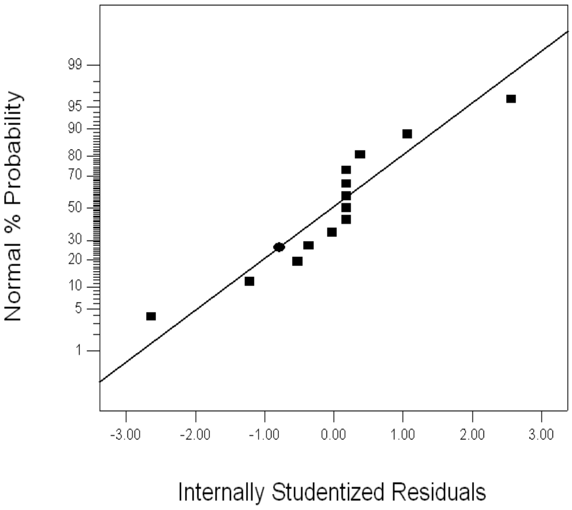

Fig. 4.5(c) Normal probability plot (SLES)

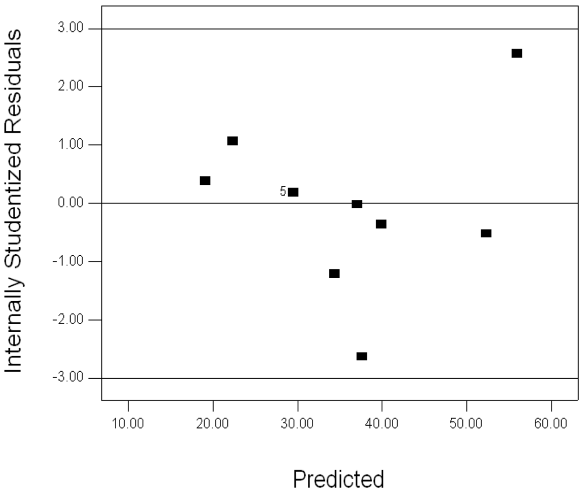

Fig. 4.5(d) Residual plot (SLES)

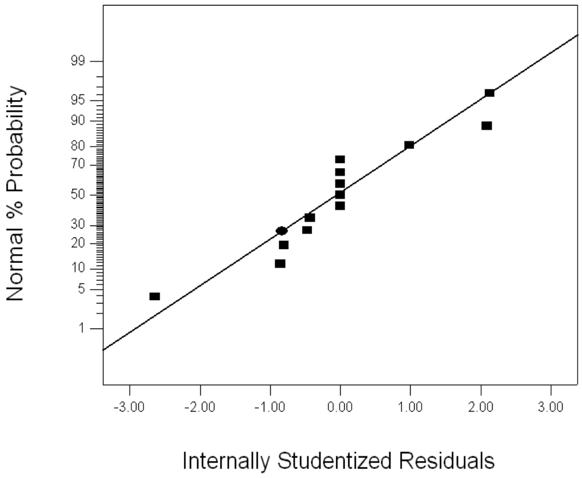

Fig. 4.5(e) Normal probability plot (SULF)

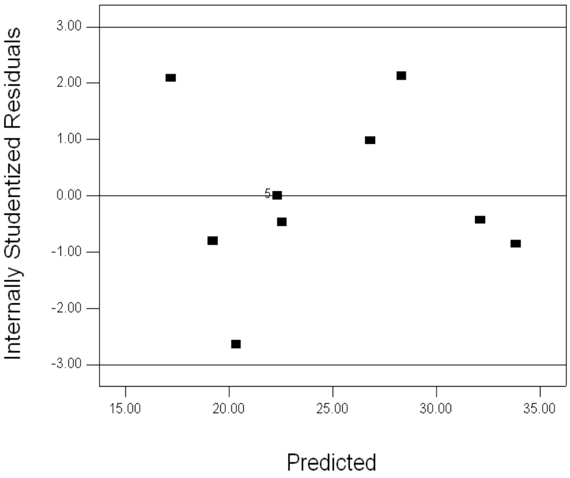

Fig. 4.5(f) Residual plot (SULF)

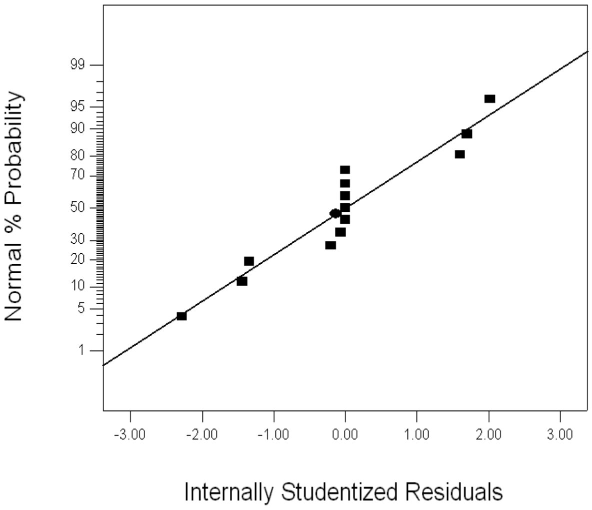

Fig. 4.5(g) Normal probability plot (CDA)

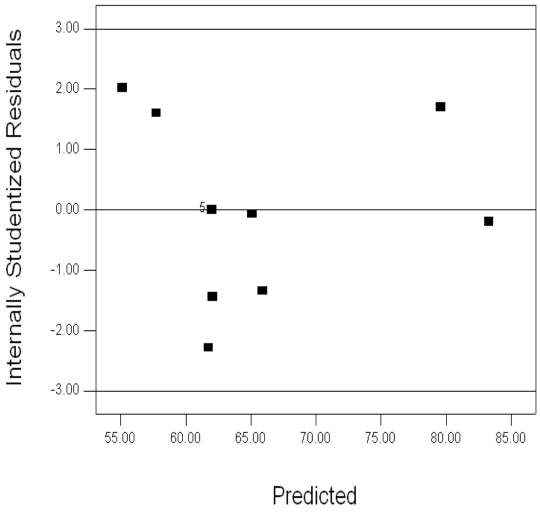

Fig. 4.5(h) Residual plot (CDA)

Fig. 4.5 Diagnostic plots for initial foam density

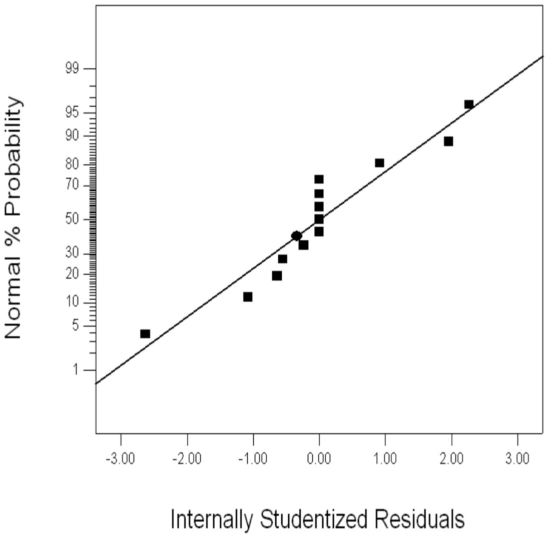

Fig. 4.6 (a) Normal probability plot (SLS)

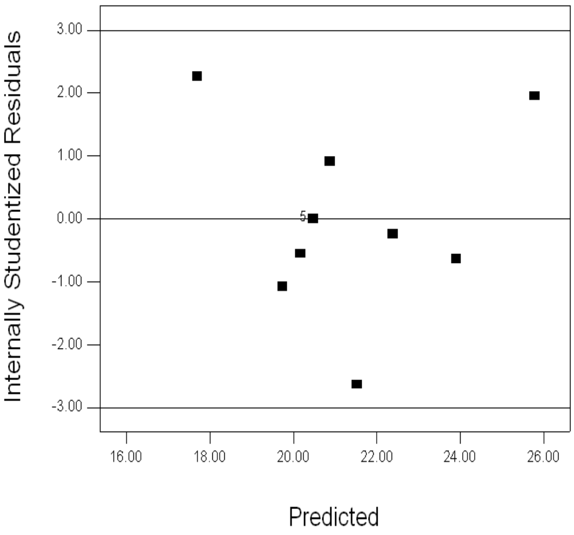

Fig. 4.6(b) Residual plot (SLS)

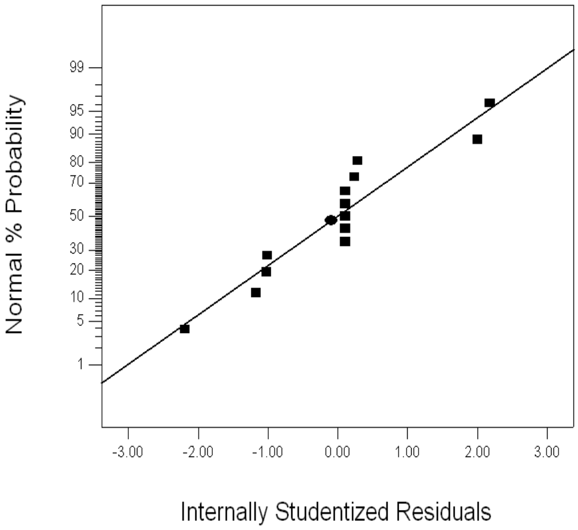

Fig. 4.6(c) Normal probability plot (SLES)

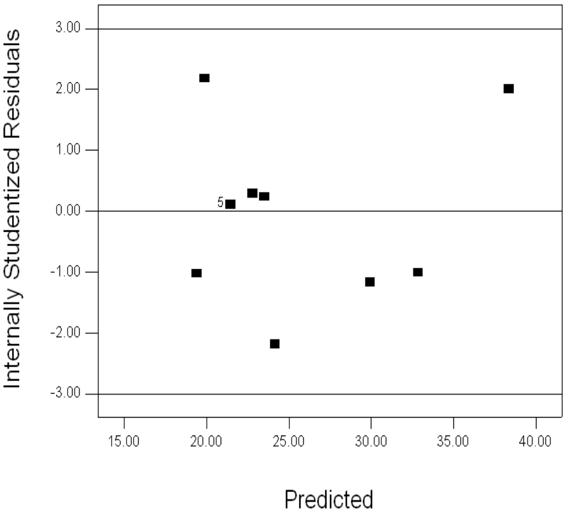

Fig. 4.6(d) Residual plot (SLES)

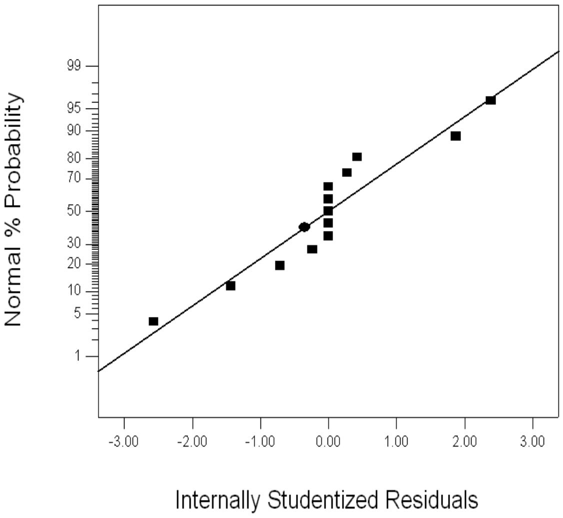

Fig. 4.6 (e) Normal probability plot (SULF)

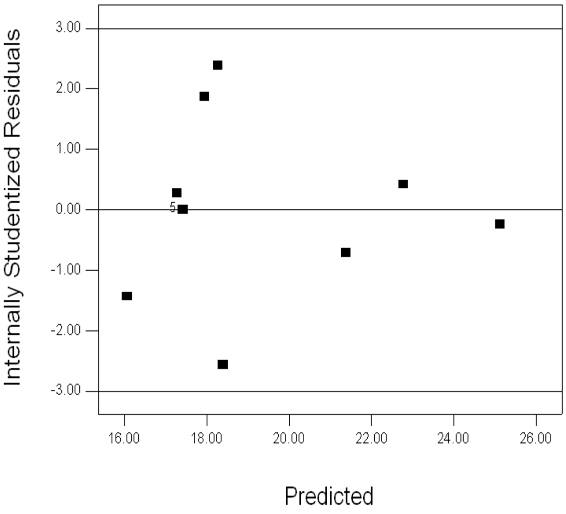

Fig. 4.6 (f) Residual plot (SULF)

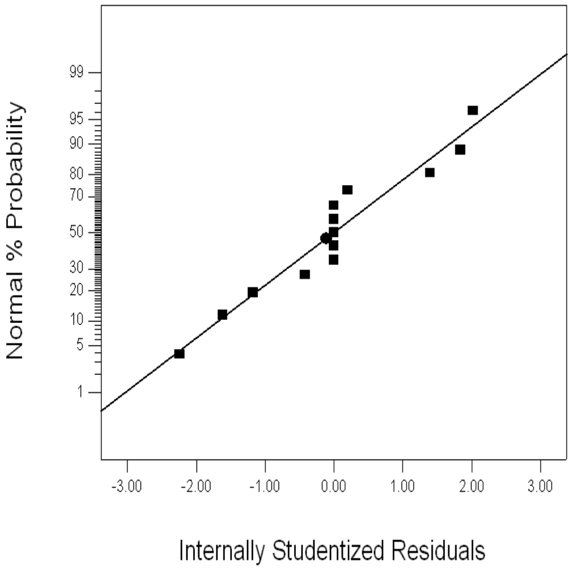

Fig. 4.6 (g) Normal probability plot (CDA)

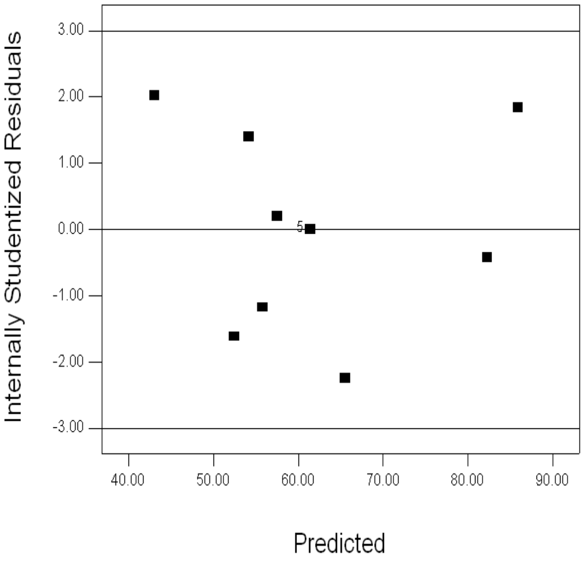

Fig. 4.6 (h) Residual plot (CDA)

Fig. 4.6 Diagnostic plots for foam density at fifth minute

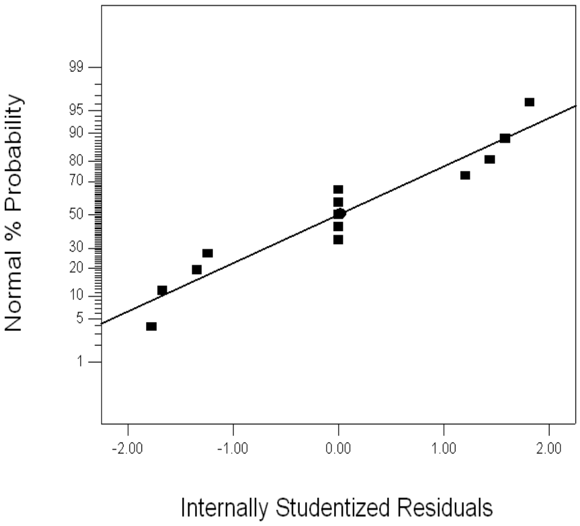

Fig. 4.7(a) Normal probability plot (SLS)

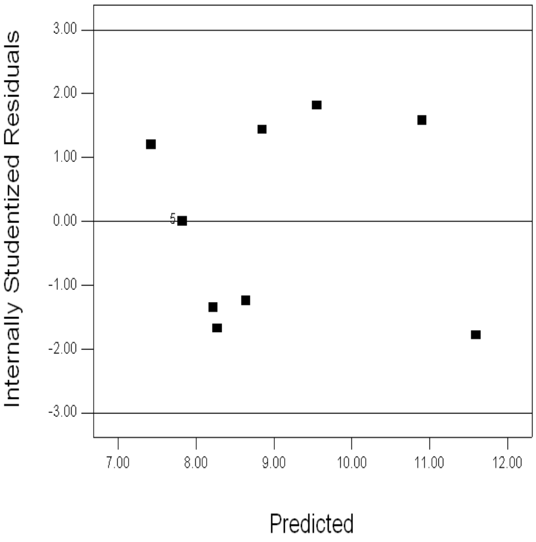

Fig. 4.7(b) Residual plot (SLS)

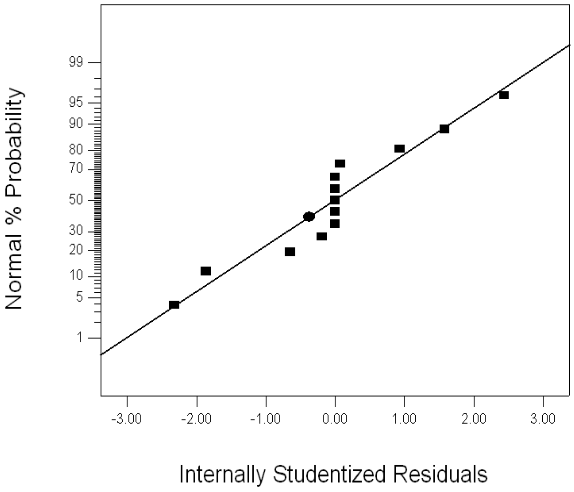

Fig. 4.7(c) Normal probability plot (SLES)

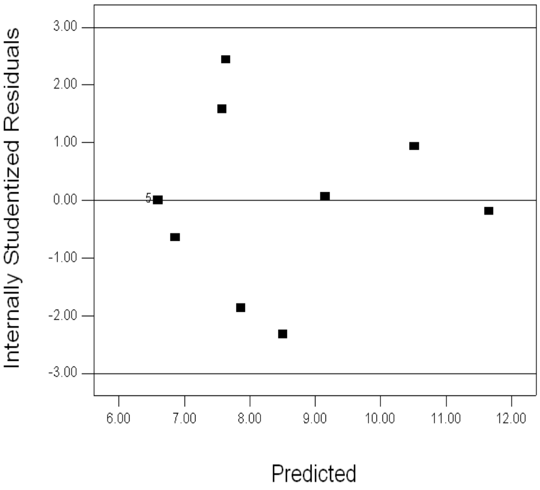

Fig. 4.7(d) Residual plot (SLES)

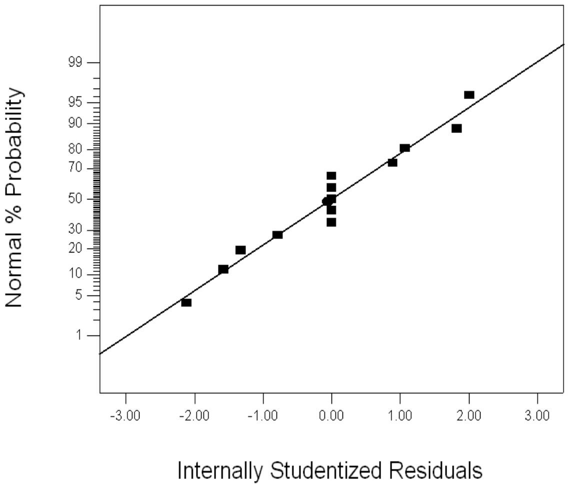

Fig. 4.7 (e) Normal probability plot (SULF)

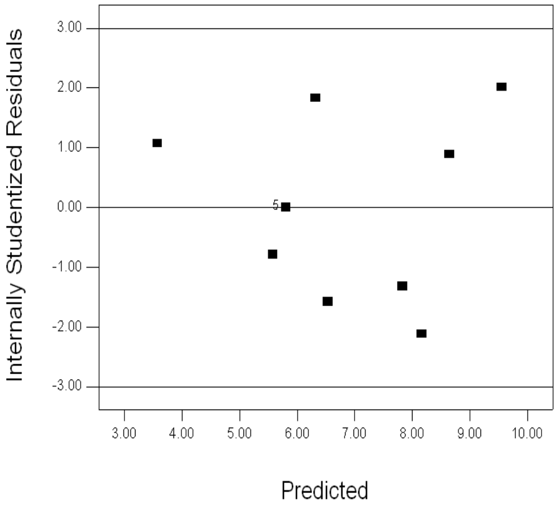

Fig. 4.7 (f) Residual plot (SULF)

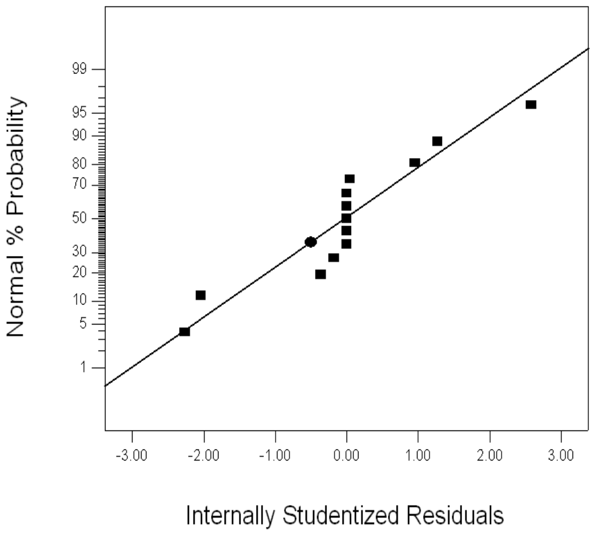

Fig. 4.7(g) Normal probability plot (CDA)

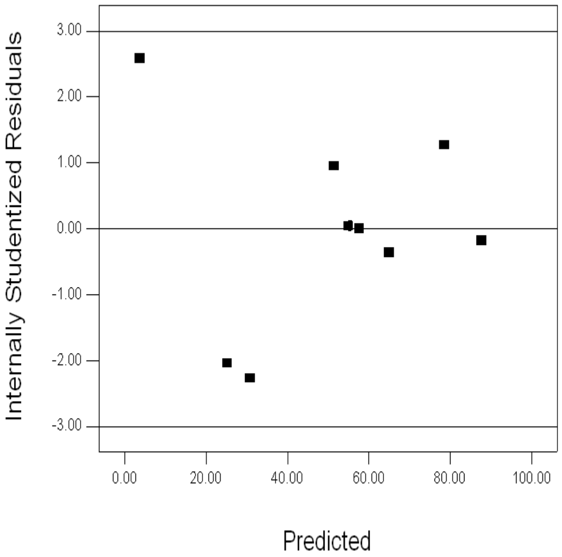

Fig. 4.7 (h) Residual plot (CDA)

Fig. 4.7 Diagnostic plots for foam density at tenth minute

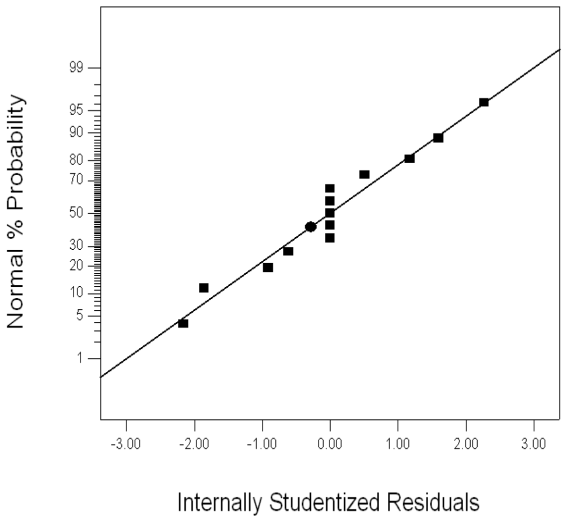

Fig. 4.8 (a) Normal probability plot (SLS)

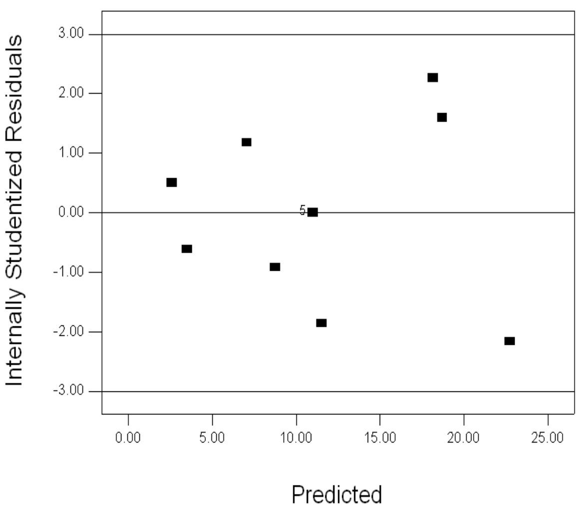

Fig. 4.8(b) Residual plot (SLS)

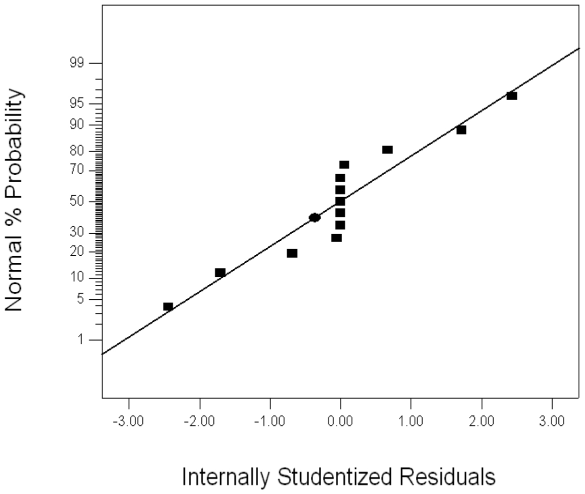

Fig. 4.8 (c) Normal probability plot (SLES)

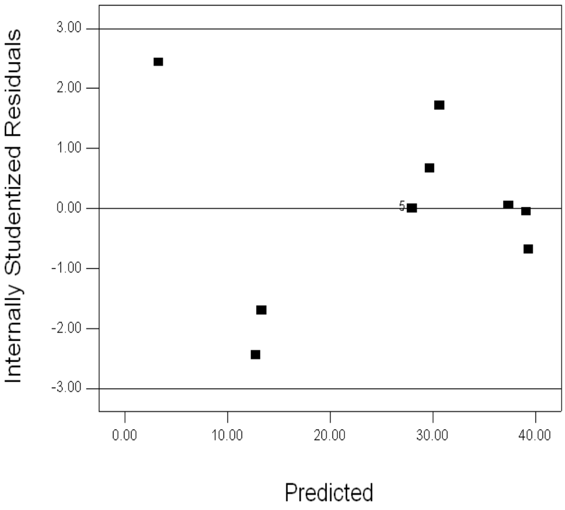

Fig. 4.8 (d) Residual plot (SLES)

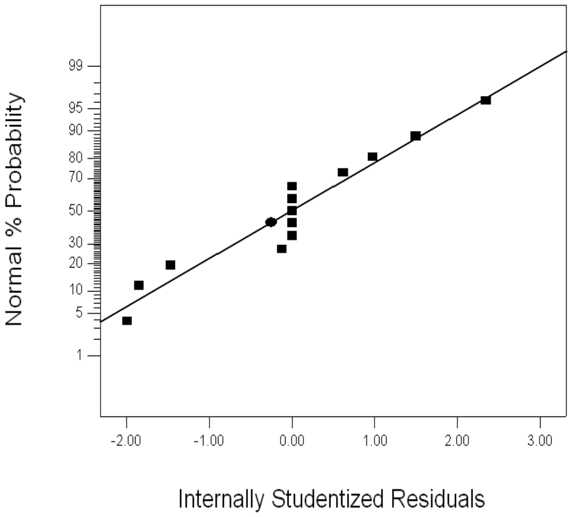

Fig. 4.8(e) Normal probability plot (SULF)

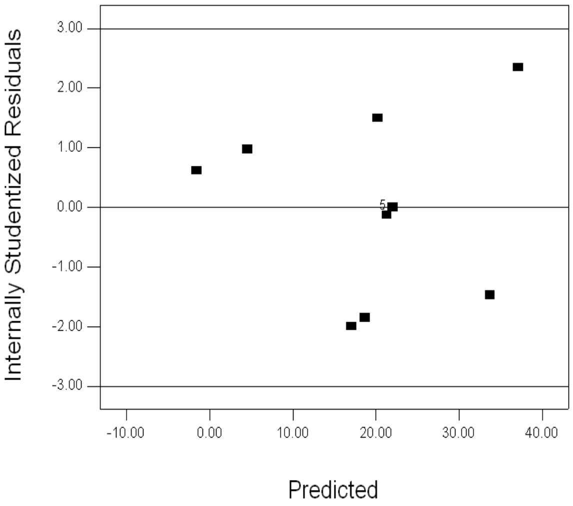

Fig. 4.8(f) Residual plot (SULF)

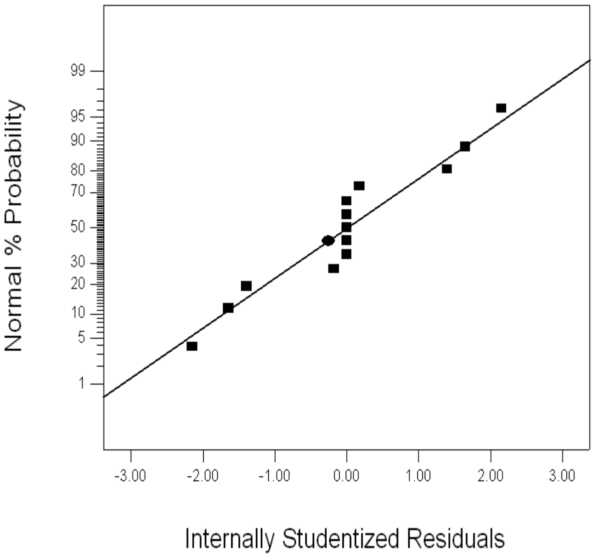

Fig. 4.8(g) Normal probability plot (CDA)

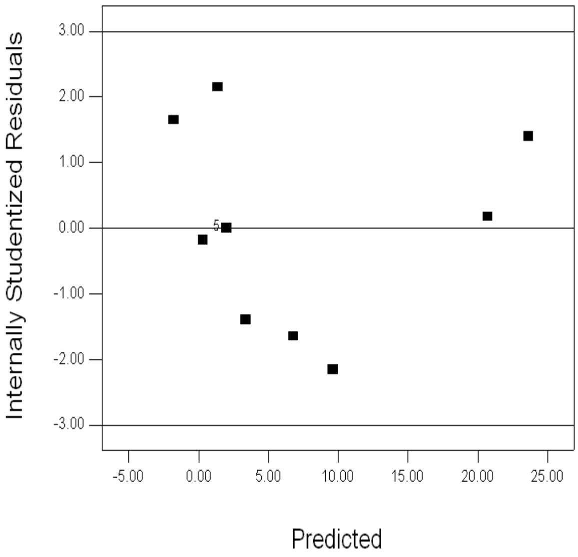

Fig. 4.8(h) Residual plot (CDA)

Fig. 4.8 Diagnostic plots for percentage solution drained in five minutes

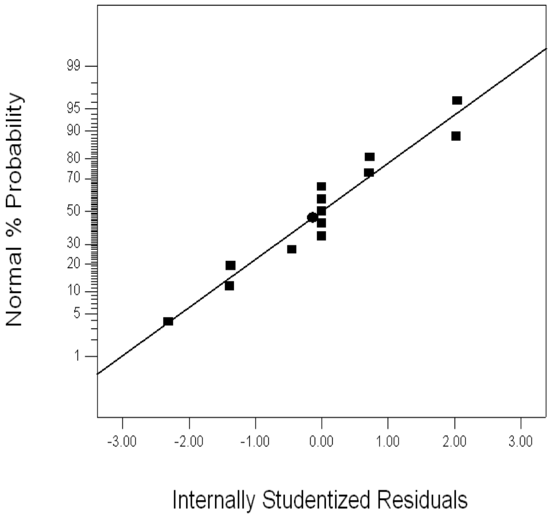

Fig. 4.9 (a) Normal probability plot (SLS)

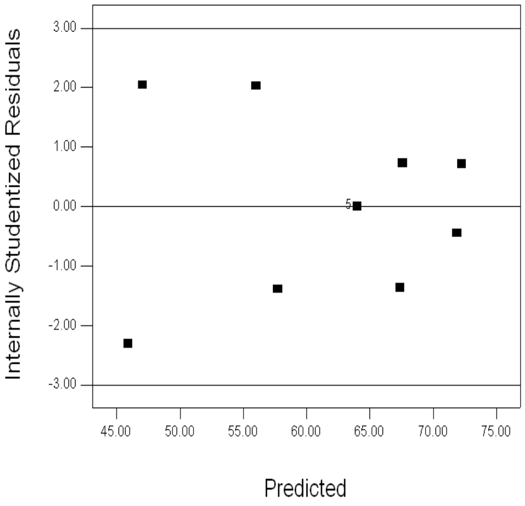

Fig. 4.9(b) Residual plot (SLS)

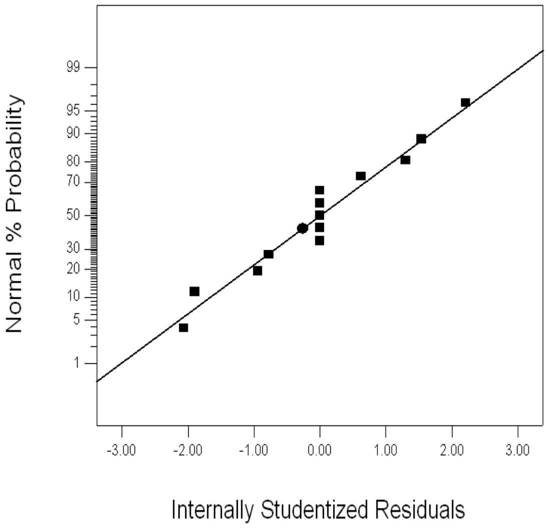

Fig. 4.9(c) Normal probability plot (SLES)

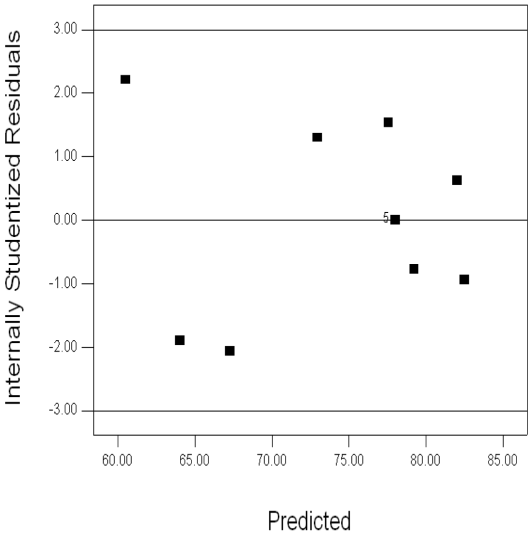

Fig. 4.9(d) Residual plot (SLES)

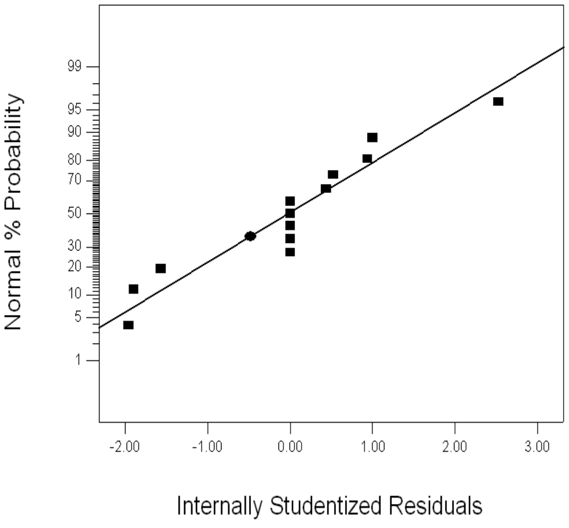

Fig. 4.9 (e) Normal probability plot (SULF)

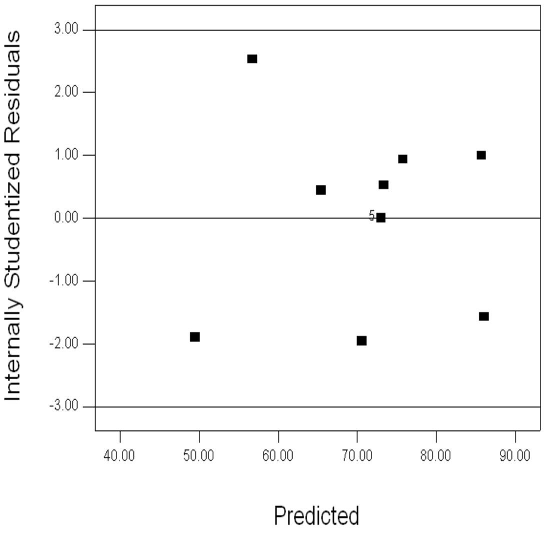

Fig. 4.9 (f) Residual plot (SULF)

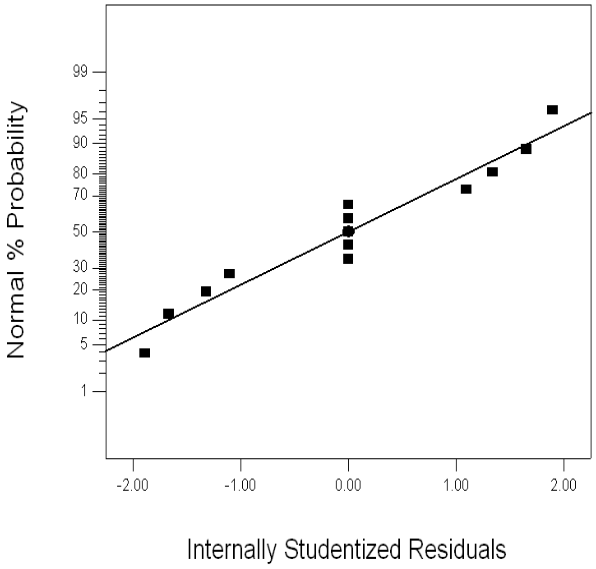

Fig. 4.9 (g) Normal probability plot (CDA)

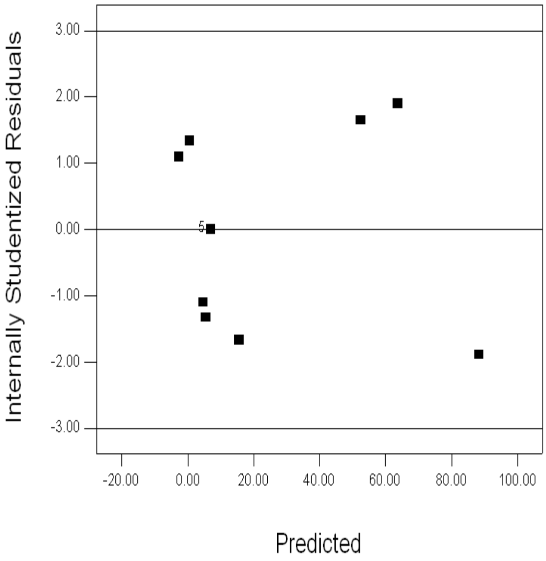

Fig. 4.9 (h) Residual plot (CDA)

Fig. 4.9 Diagnostic plots for percentage solution drained in ten minutes

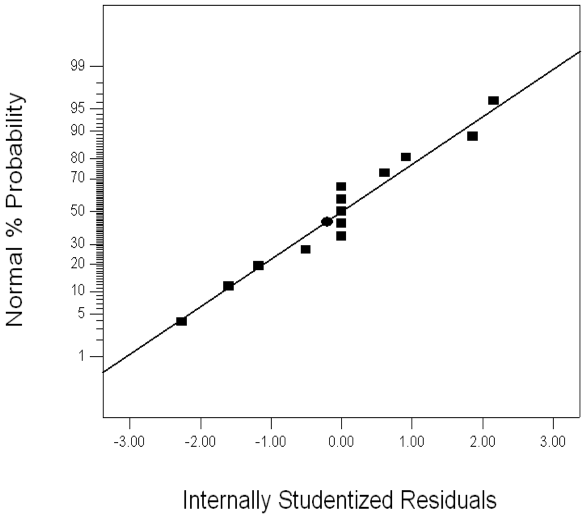

Fig. 4.10 (a) Normal probability plot (SLS)

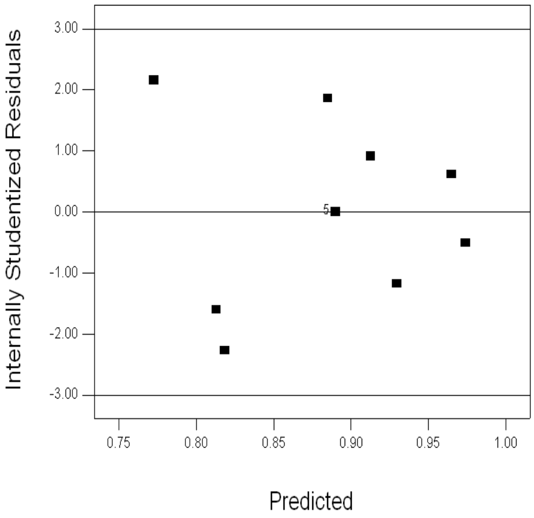

Fig. 4.10 (b) Residual plot (SLS)

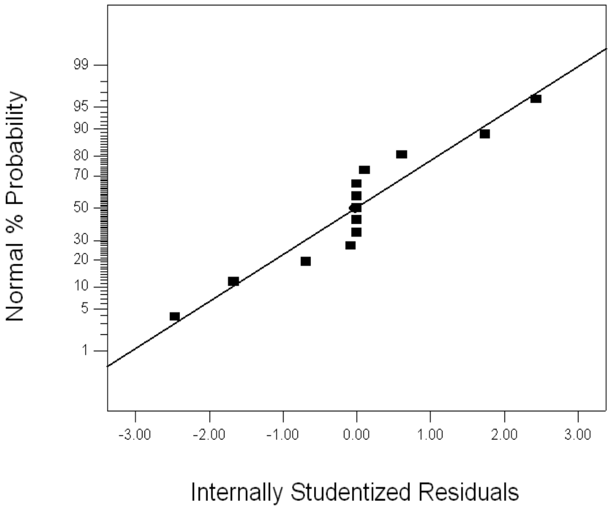

Fig. 4.10(c) Normal probability plot (SLES)

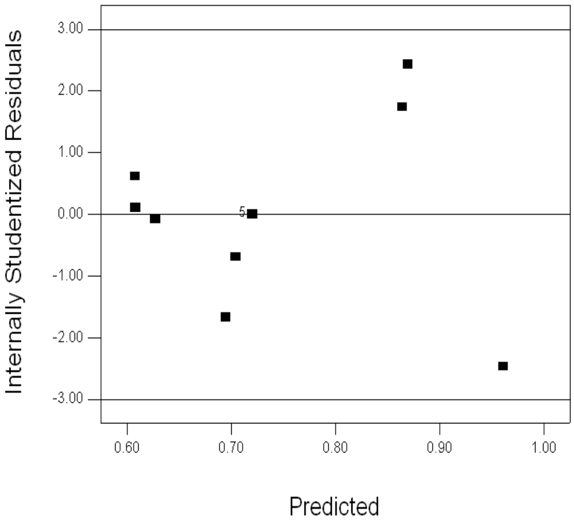

Fig. 4.10 (d) Residual plot (SLES)

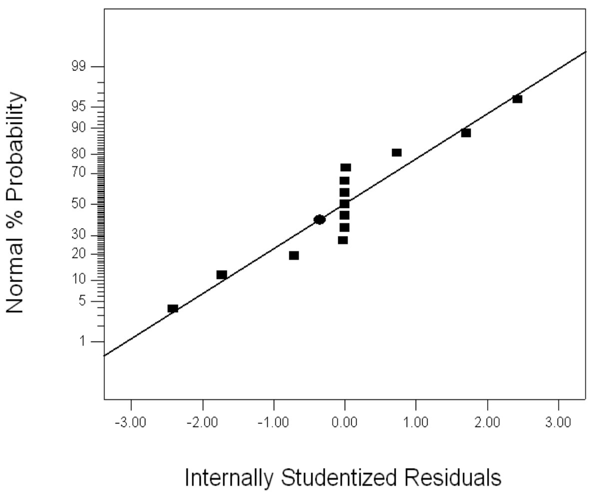

Fig. 4.10(e) Normal probability plot (SULF)

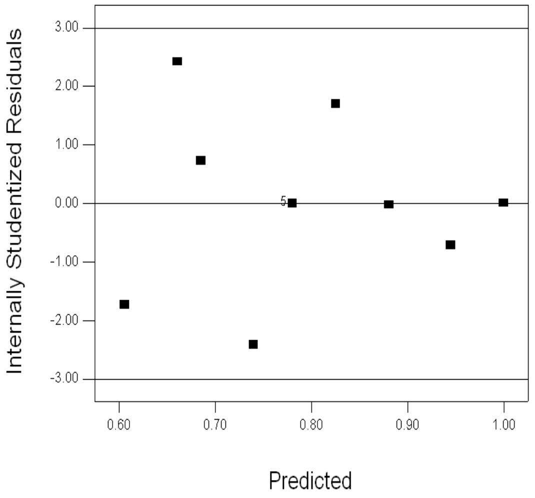

Fig. 4.10(f) Residual plot (SULF)

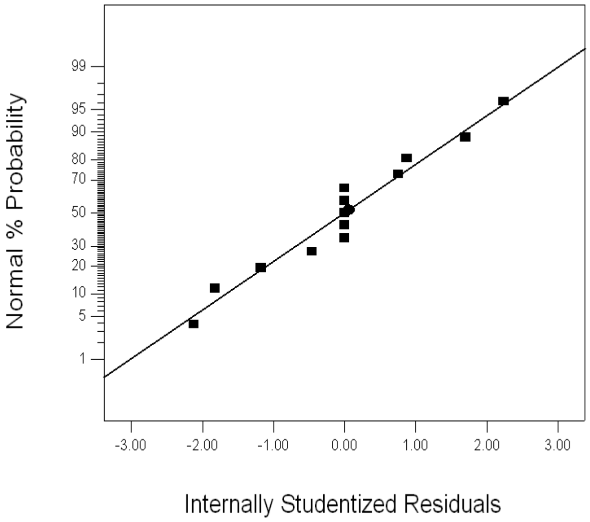

Fig. 4.10(g) Normal probability plot (CDA)

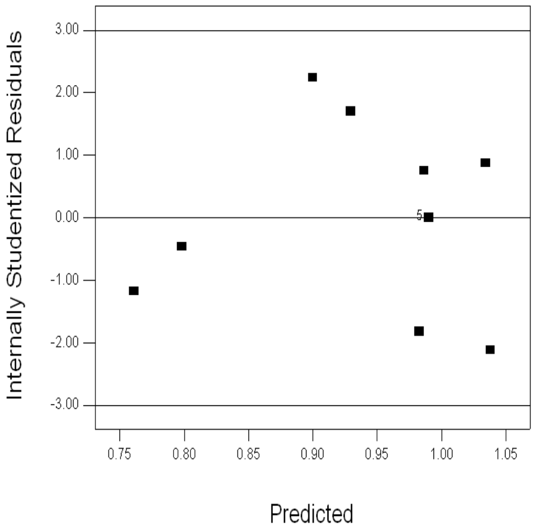

Fig. 4.10(h) Residual plot (CDA)

Fig. 4.10 Diagnostic plots for foam density ratio at fifth minute

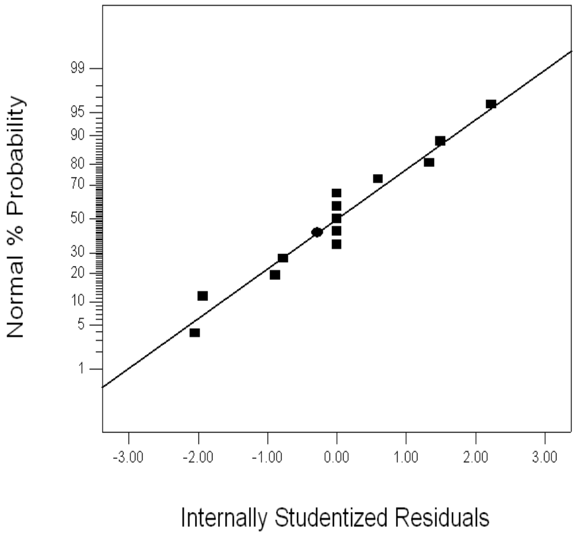

Fig. 4.11(a) Normal probability plot (SLS)

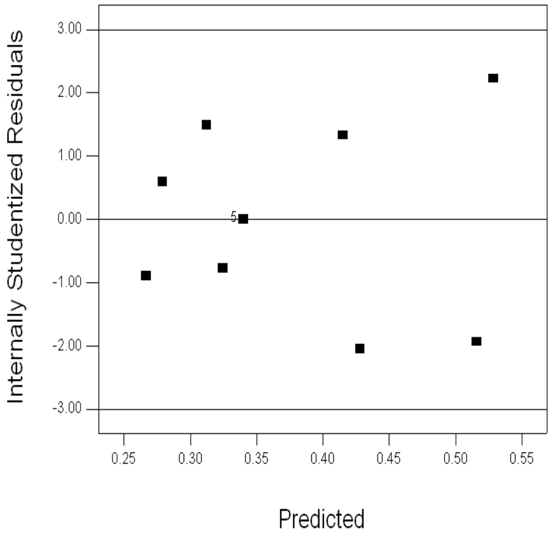

Fig. 4.11(b) Residual plot (SLS)

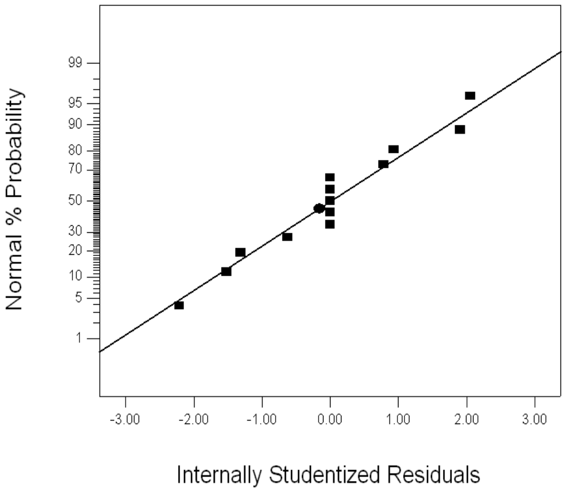

Fig. 4.11(c) Normal probability plot (SLES)

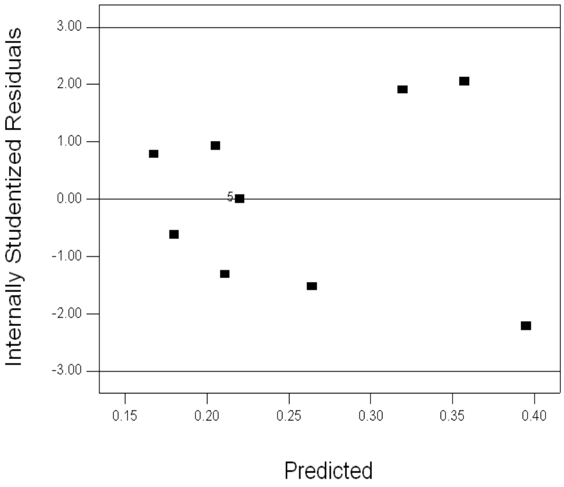

Fig. 4.11(d) Residual plot (SLES)

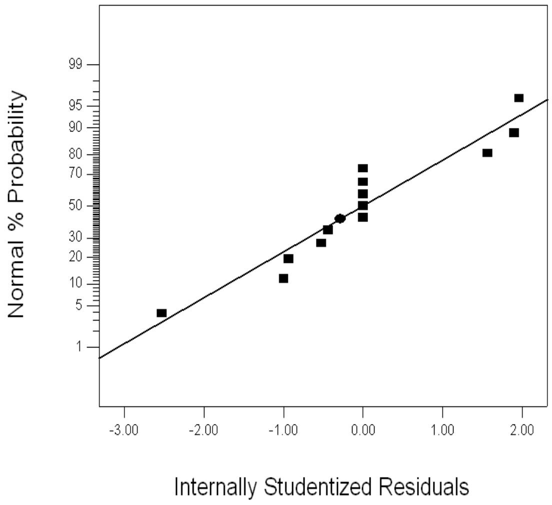

Fig. 4.11(e) Normal probability plot (SULF)

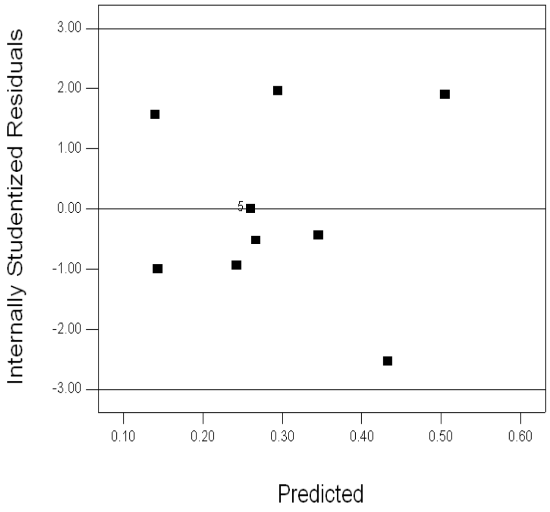

Fig. 4.11(f) Residual plot (SULF)

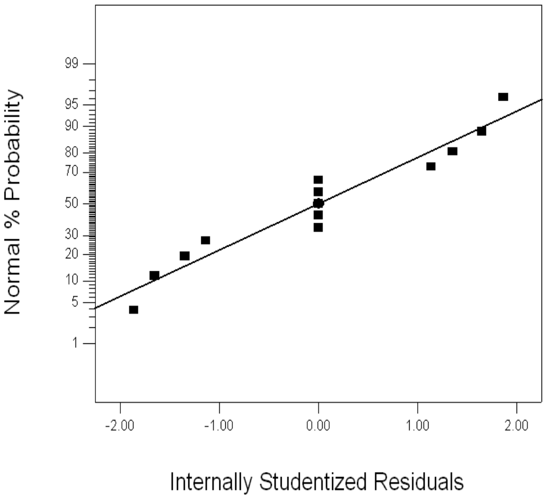

Fig. 4.11(g) Normal probability plot (CDA)

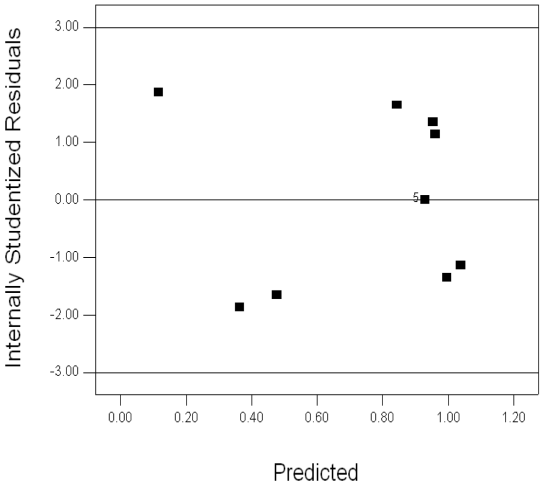

Fig. 4.11(h) Residual plot (CDA)

Fig. 4.11 Diagnostic plots for foam density ratio at tenth minute

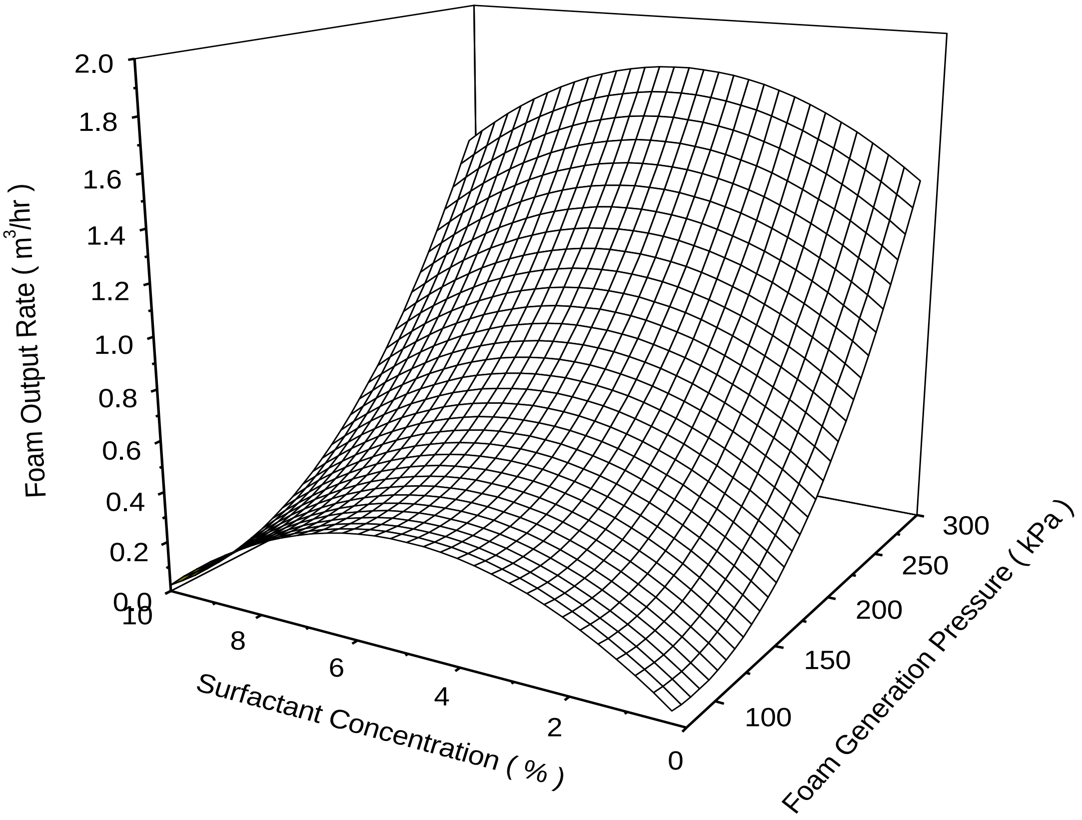

(a) Sodium lauryl sulfate

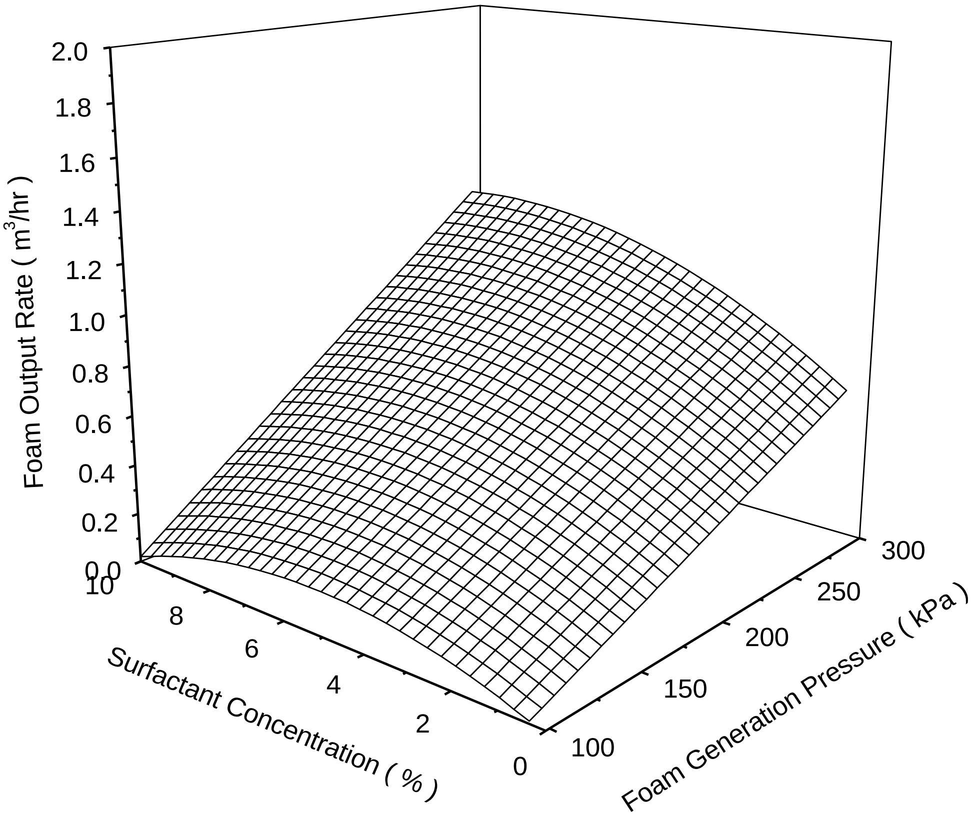

(b) Sodium lauryl ether sulfate

Fig 4.12 Response surface plots for foam output rate

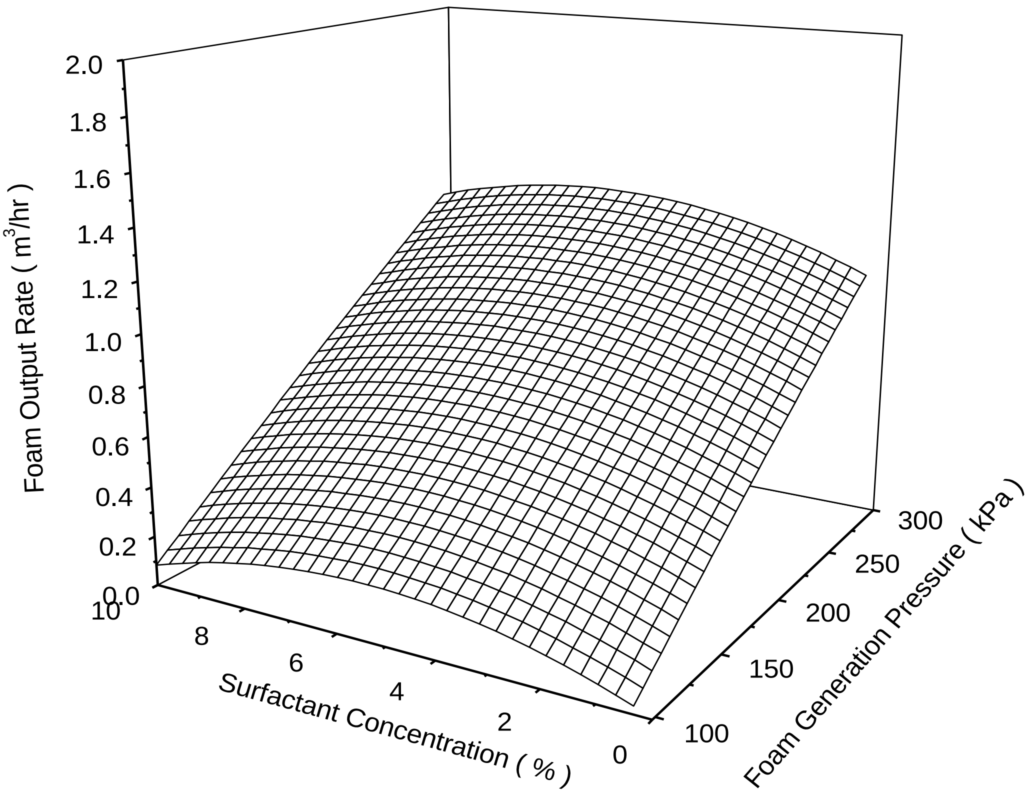

(c) Sulfanol

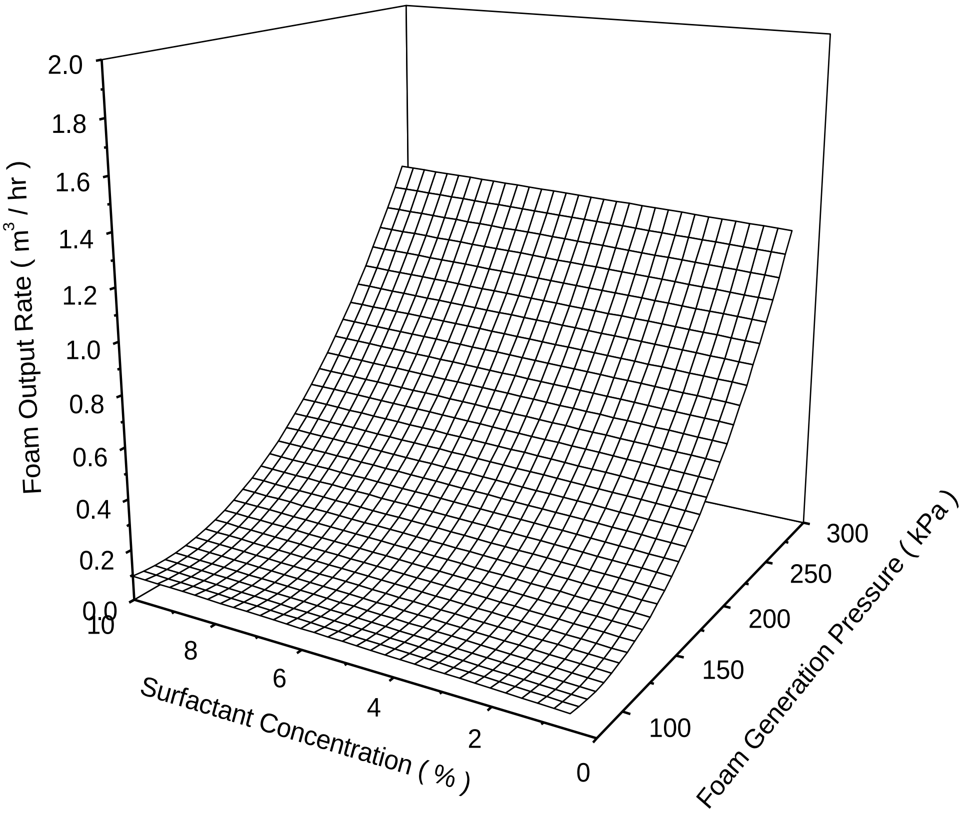

(d) Cocodiethanolamide

Fig 4.12 Response surface plots for foam output rate

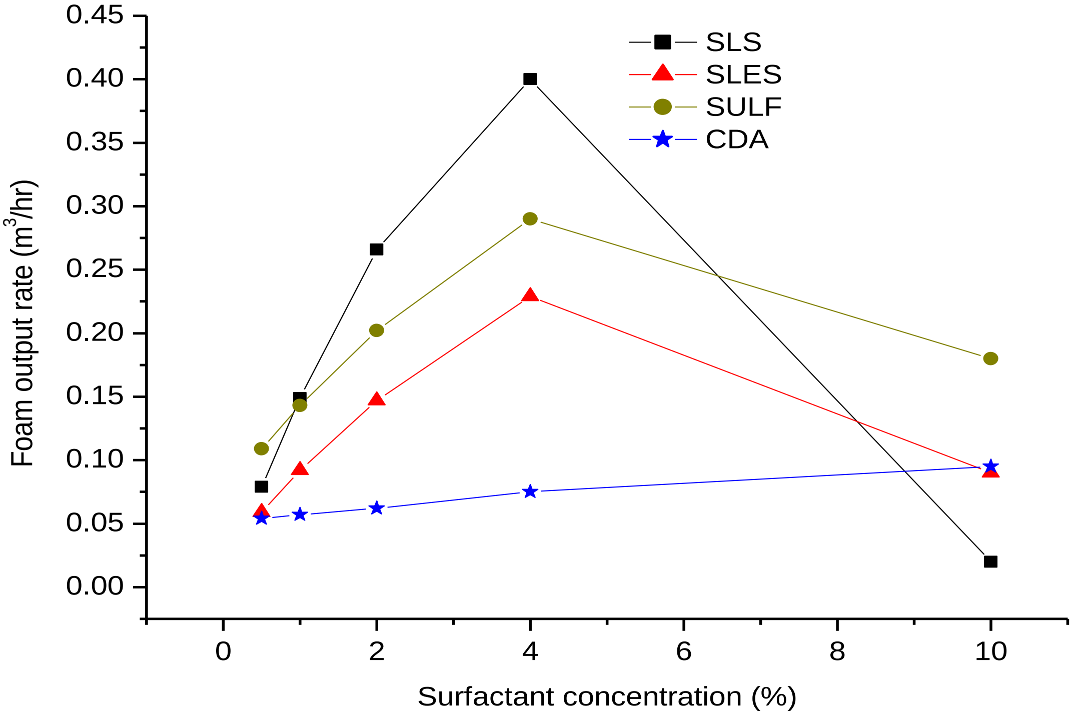

(a) FGP 110 kPa

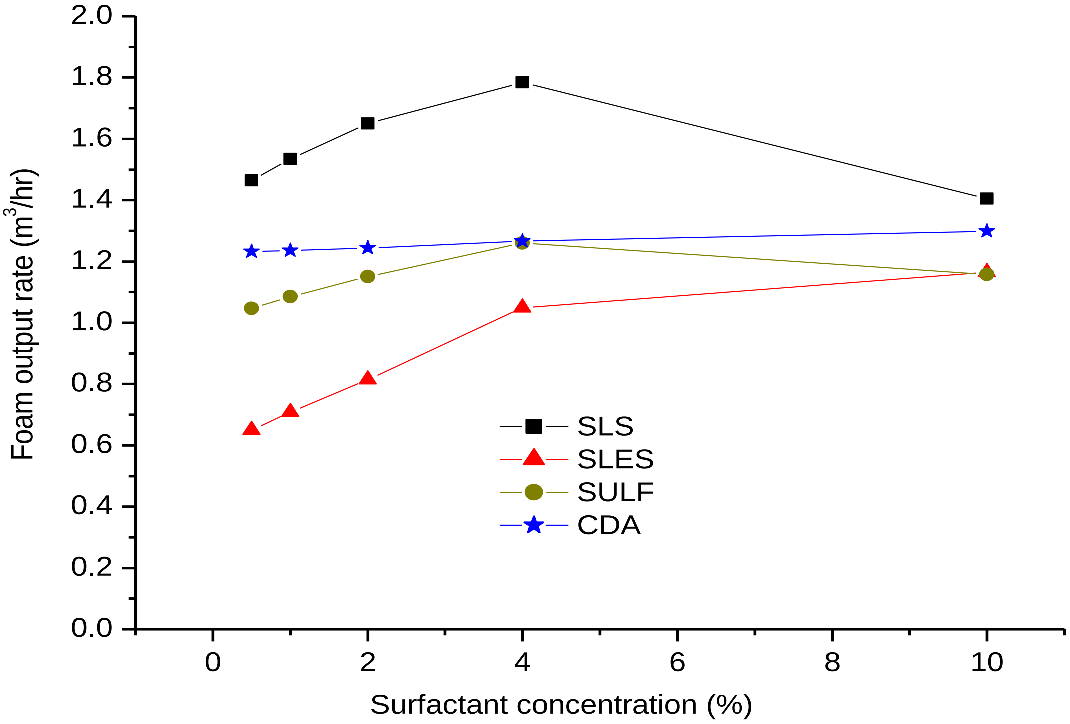

(b) FGP 294 kPa

Figure 4.13 Variation in foam output rate with surfactant concentration

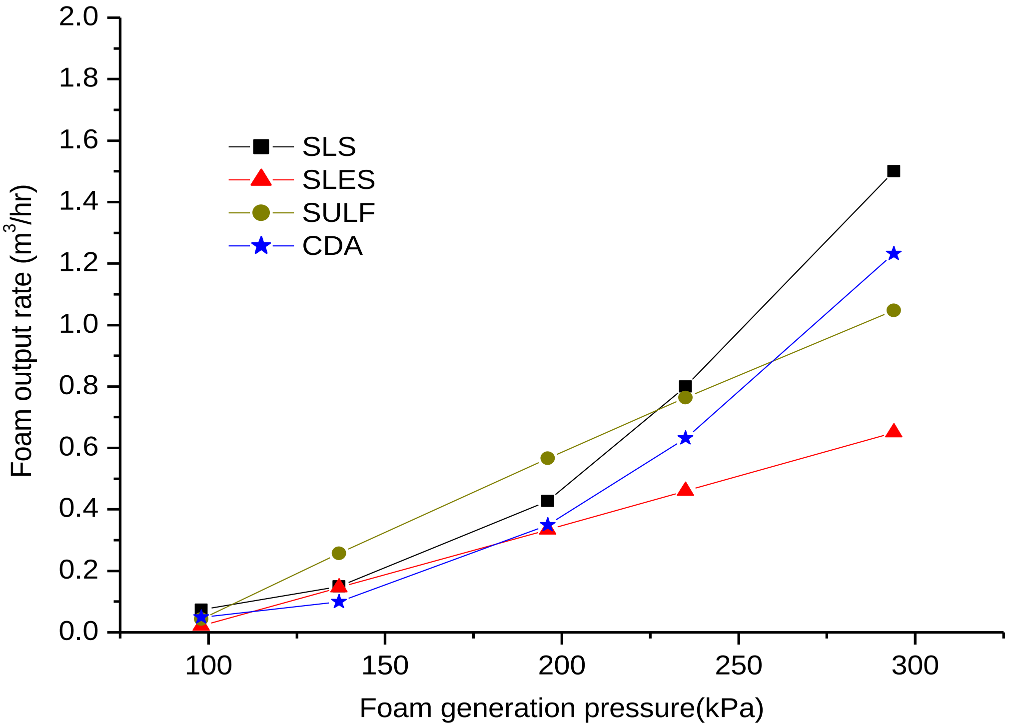

(a) SC 0.5%

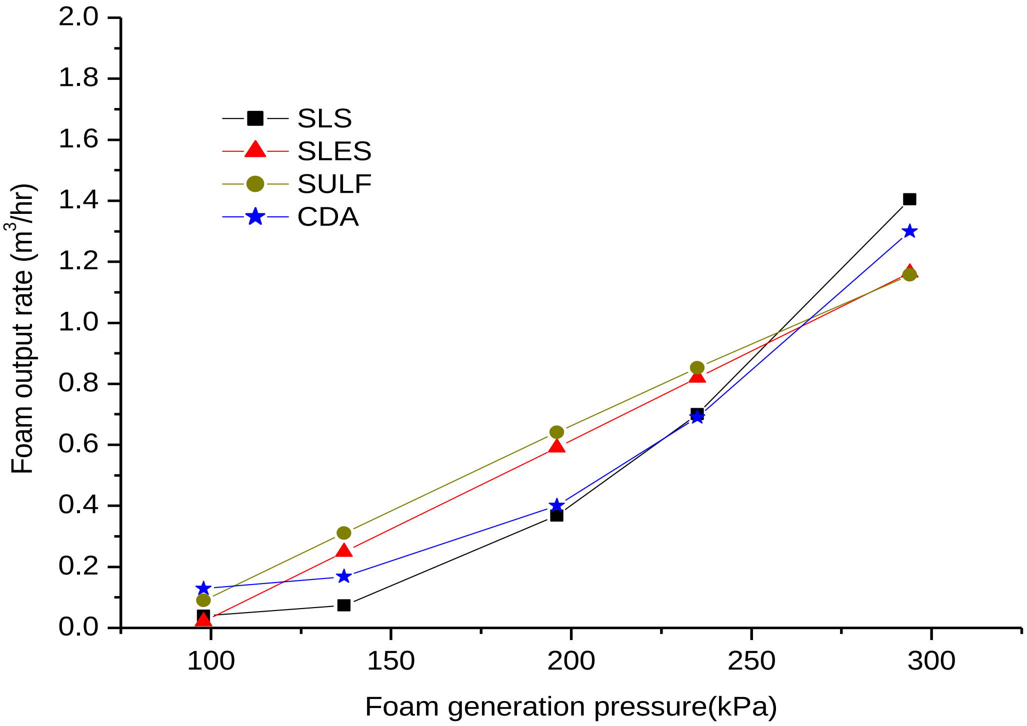

(b) SC 10%

Figure 4.14 Variation in foam output rate with foam generation pressure

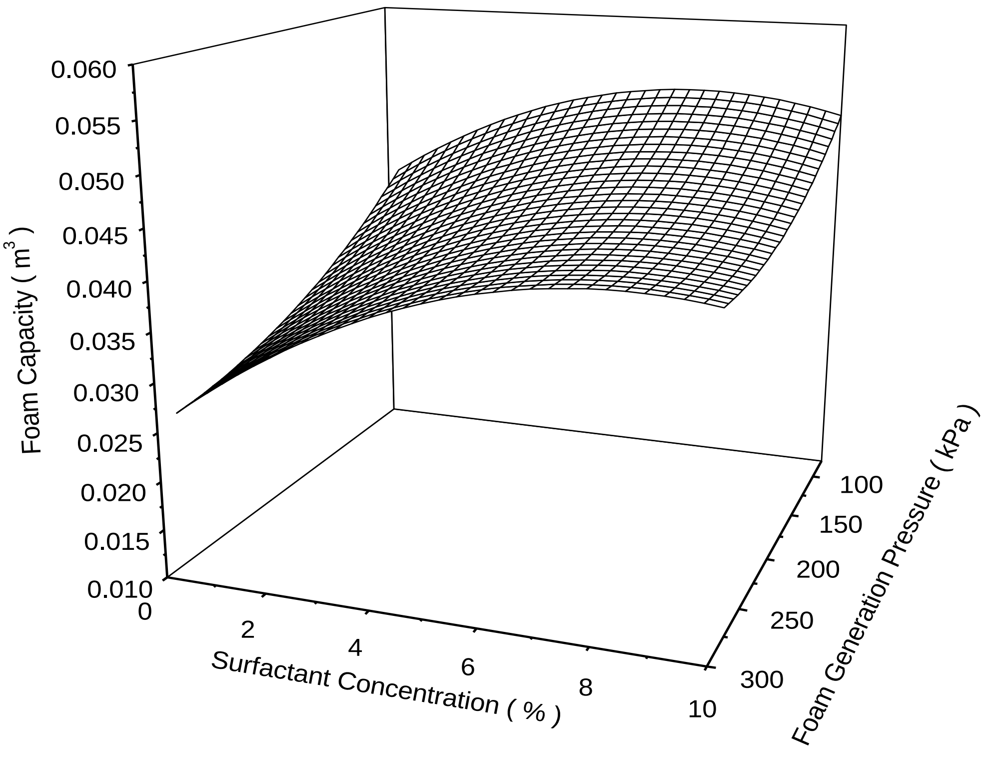

(a) Sodium lauryl sulfate

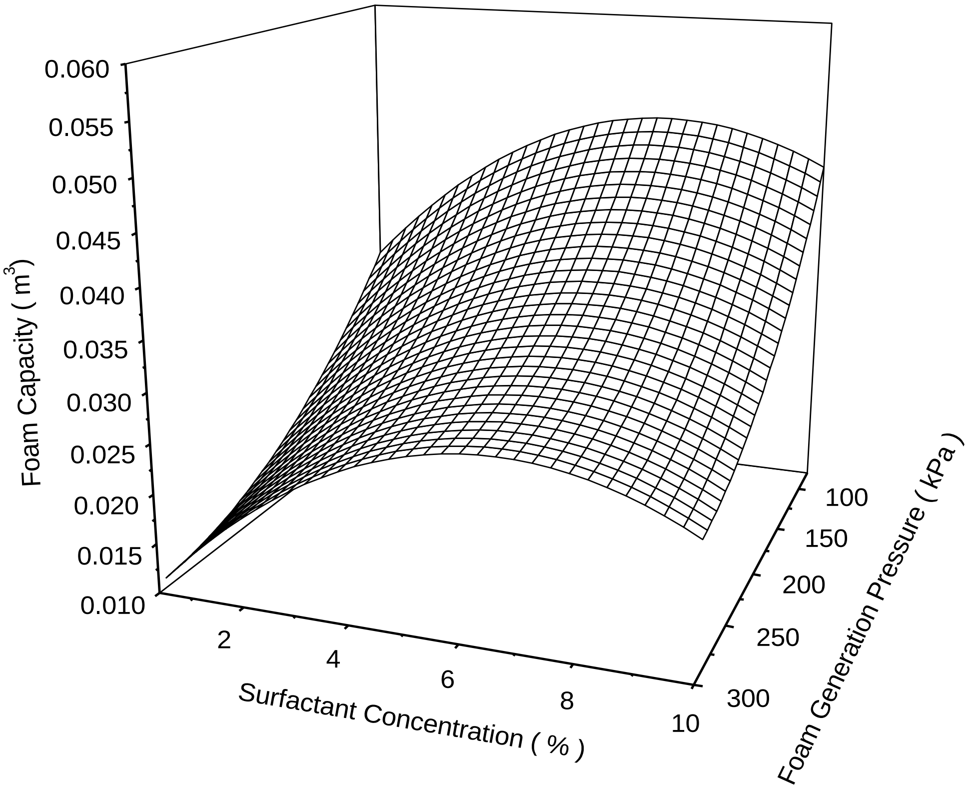

(b) Sodium lauryl ether sulfate

Fig 4.15 Response surface plots for foam capacity

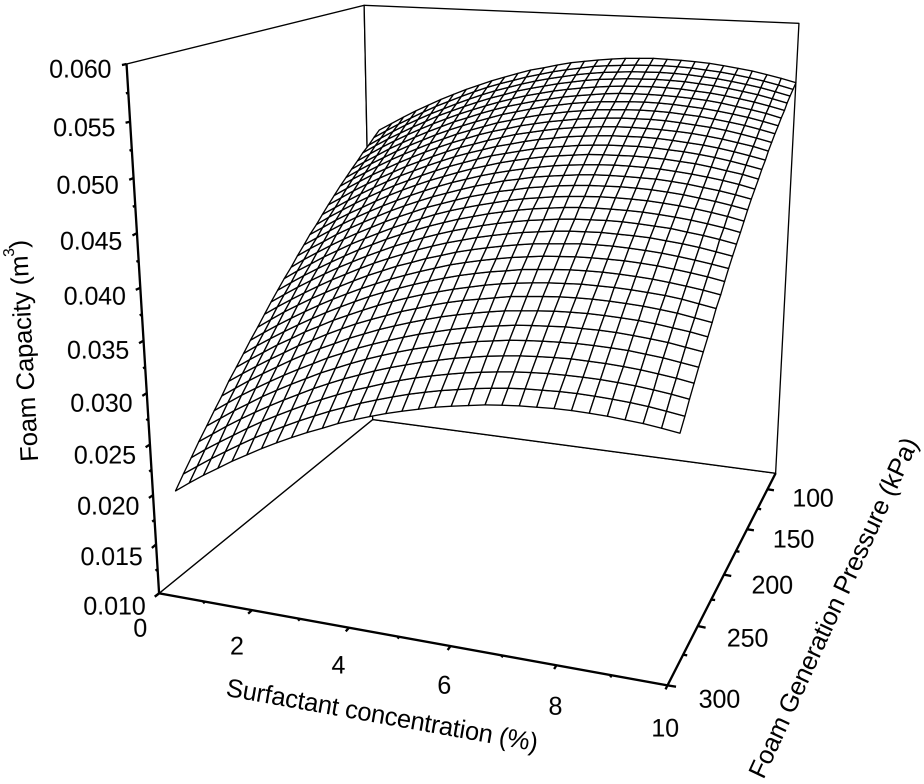

(c) Sulfanol

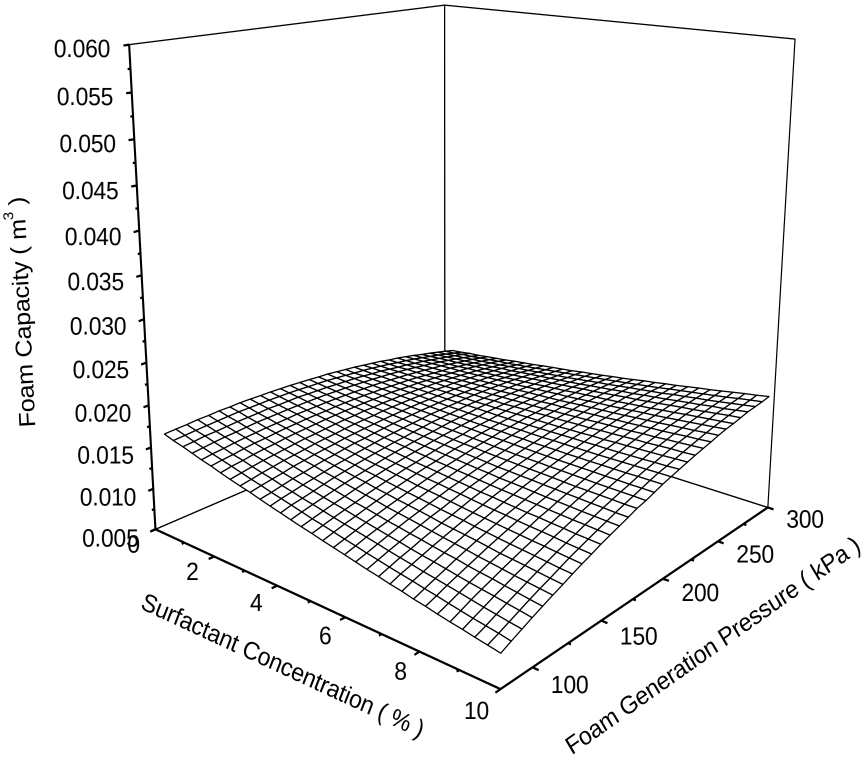

(d) Cocodiethanolamide

Fig 4.15 Response surface plots for foam capacity

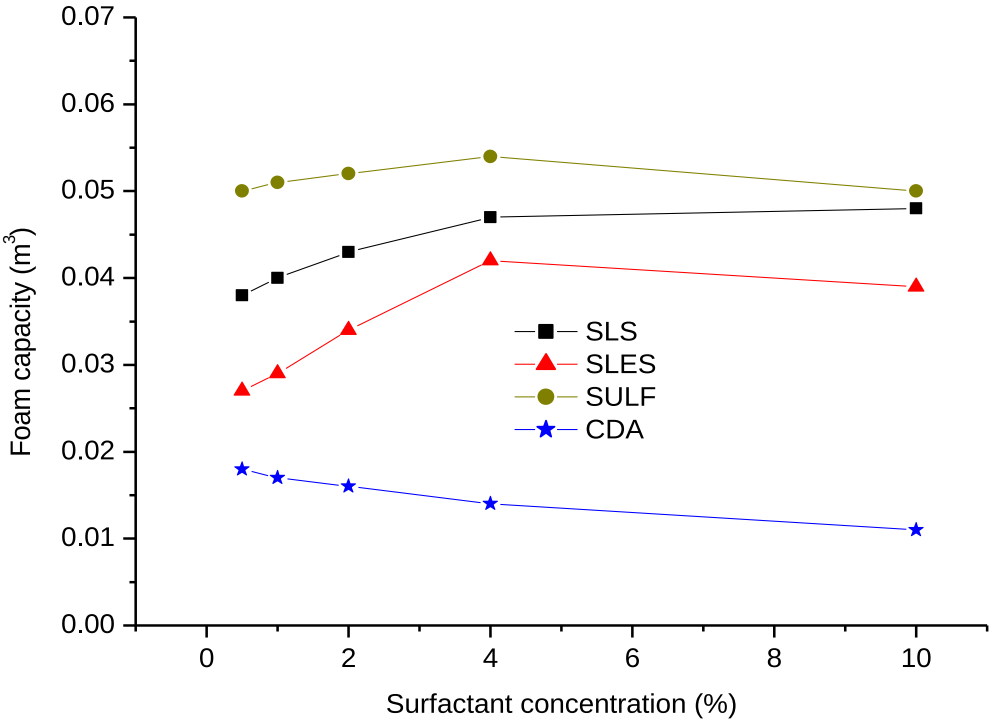

(a) FGP 110 kPa

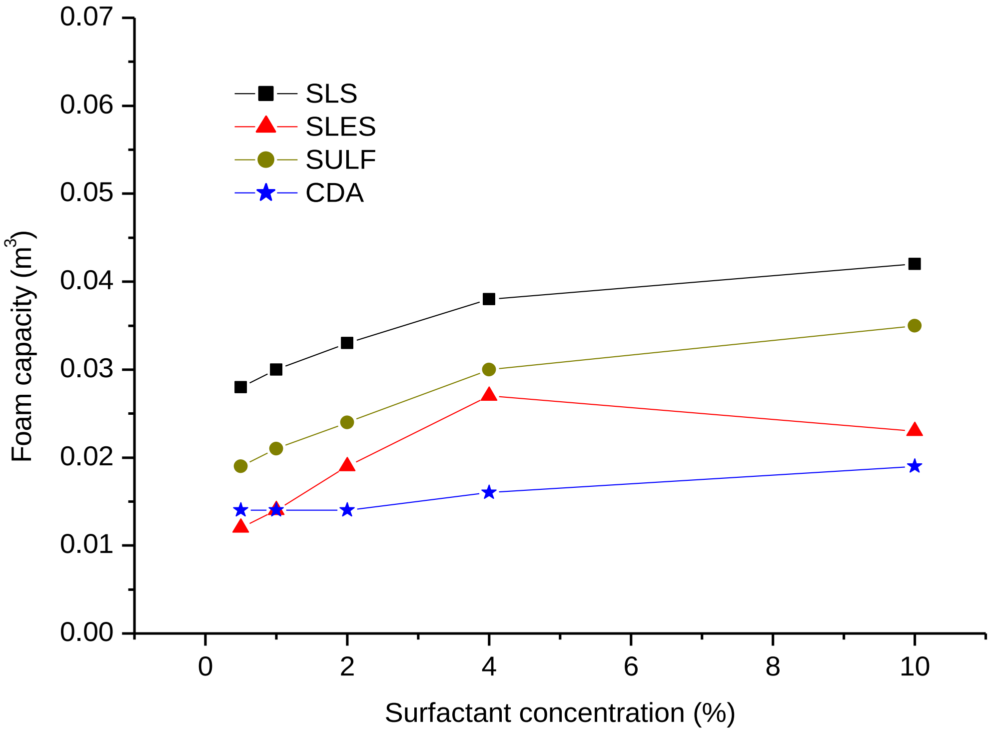

(b) FGP 294 kPa

Figure 4.16 Variation in foam capacity with surfactant concentration

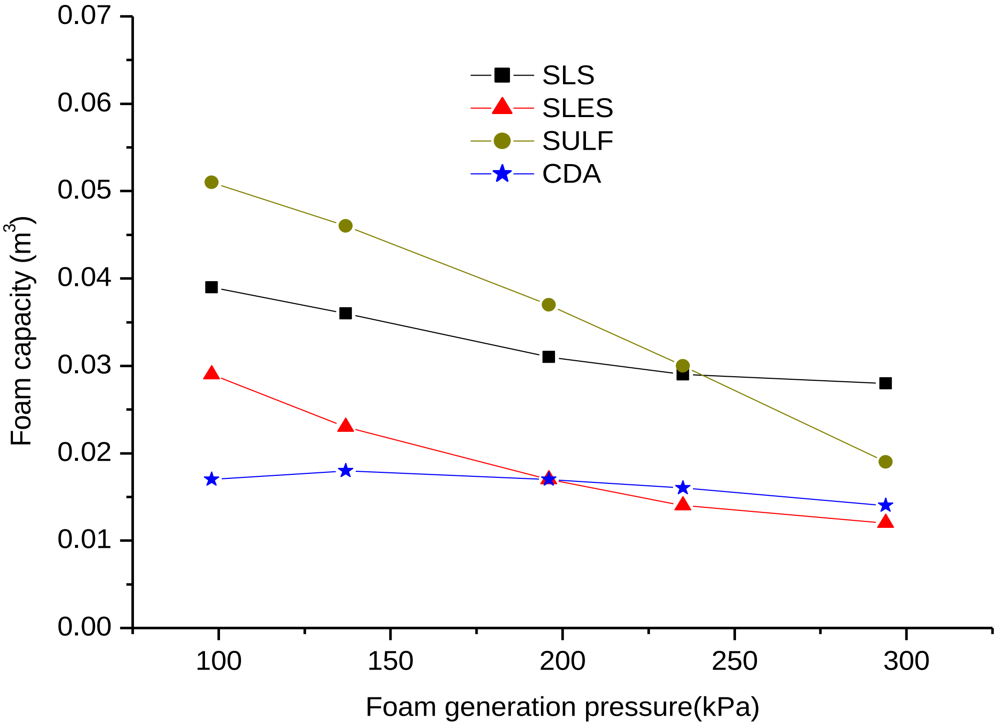

(a) SC 0.5%

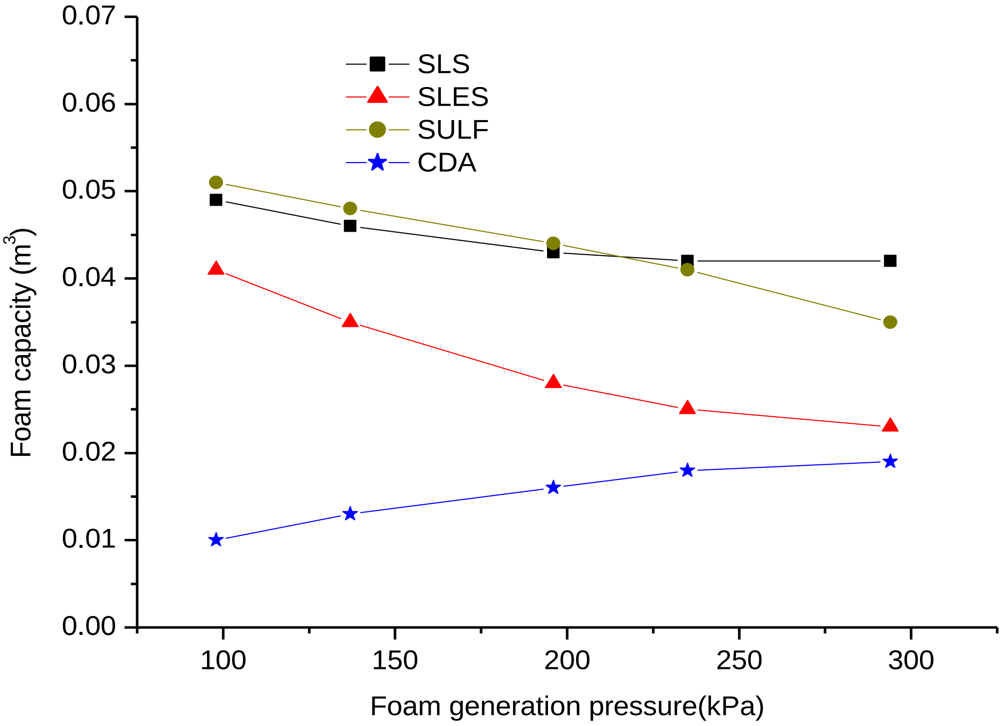

(b) SC 10%

Figure 4.17 Variation in foam capacity with foam generation pressure

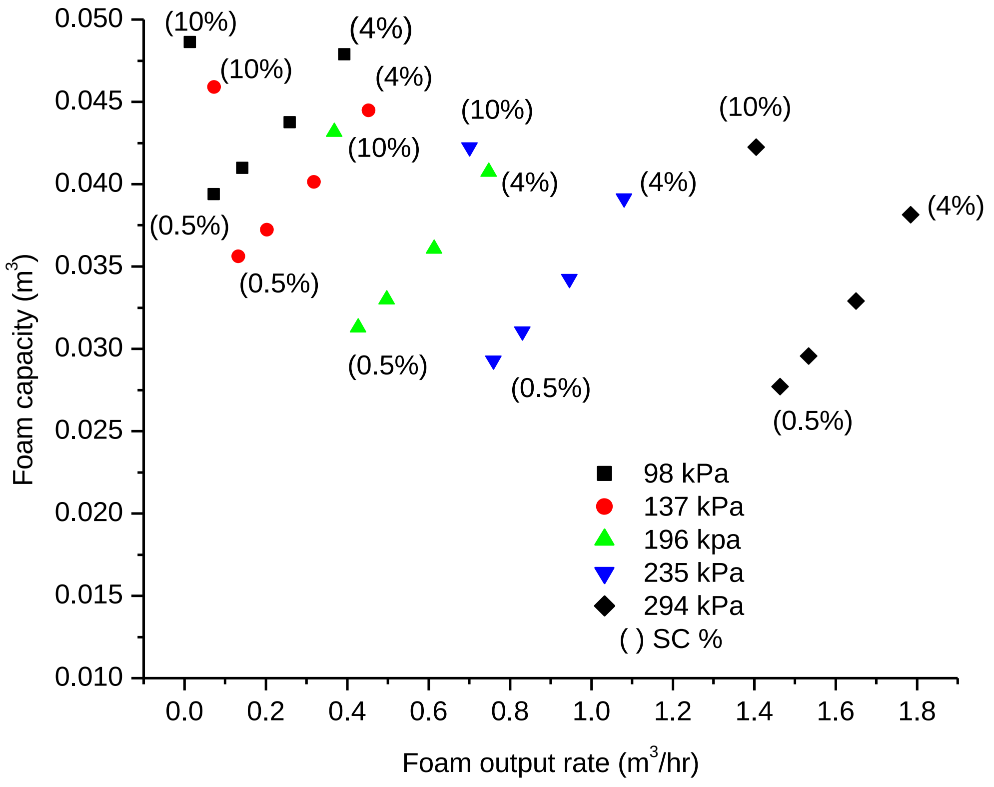

(a) Sodium lauryl sulfate

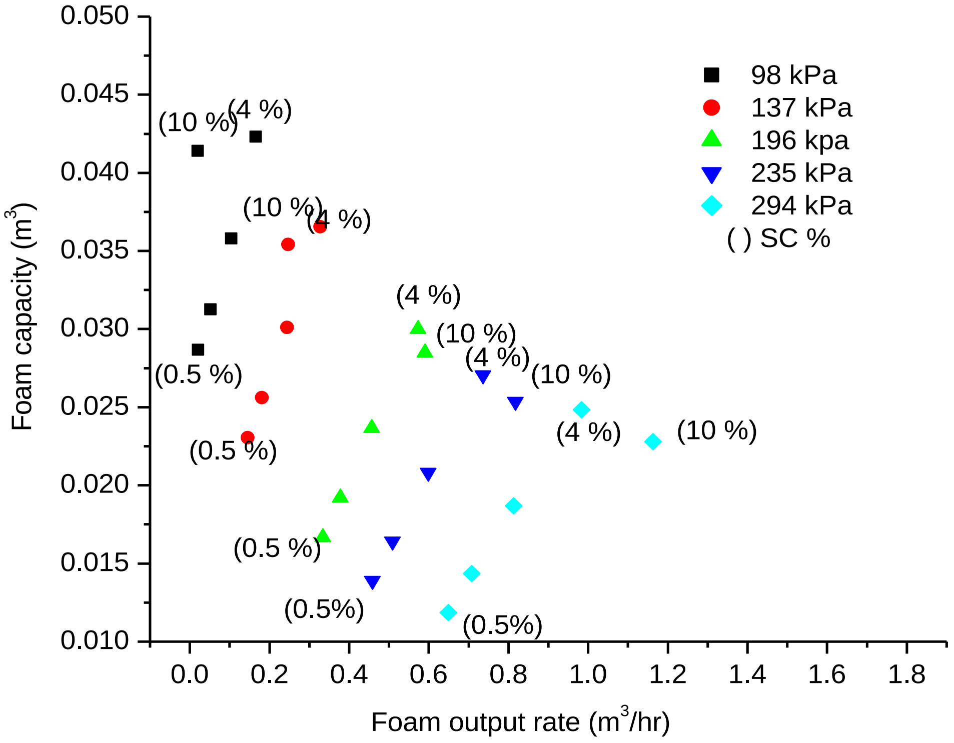

(b) Sodium lauryl ether sulfate

Fig 4.18 Variation of foam output rate with foam capacity

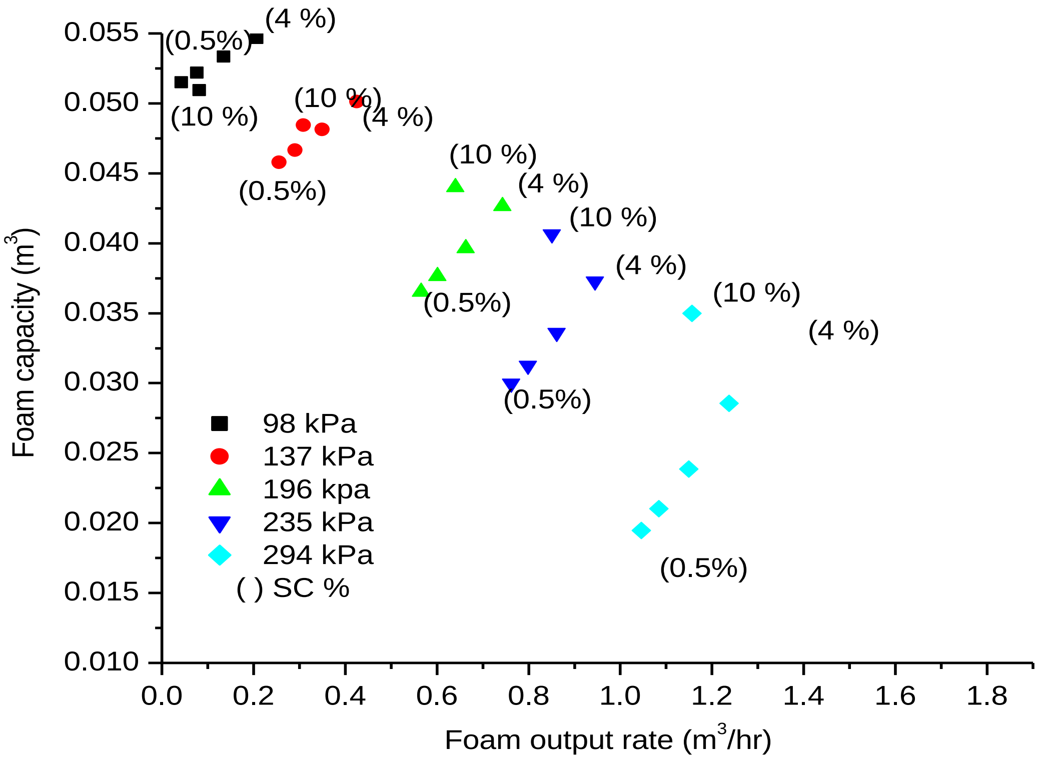

(c) Sulfanol

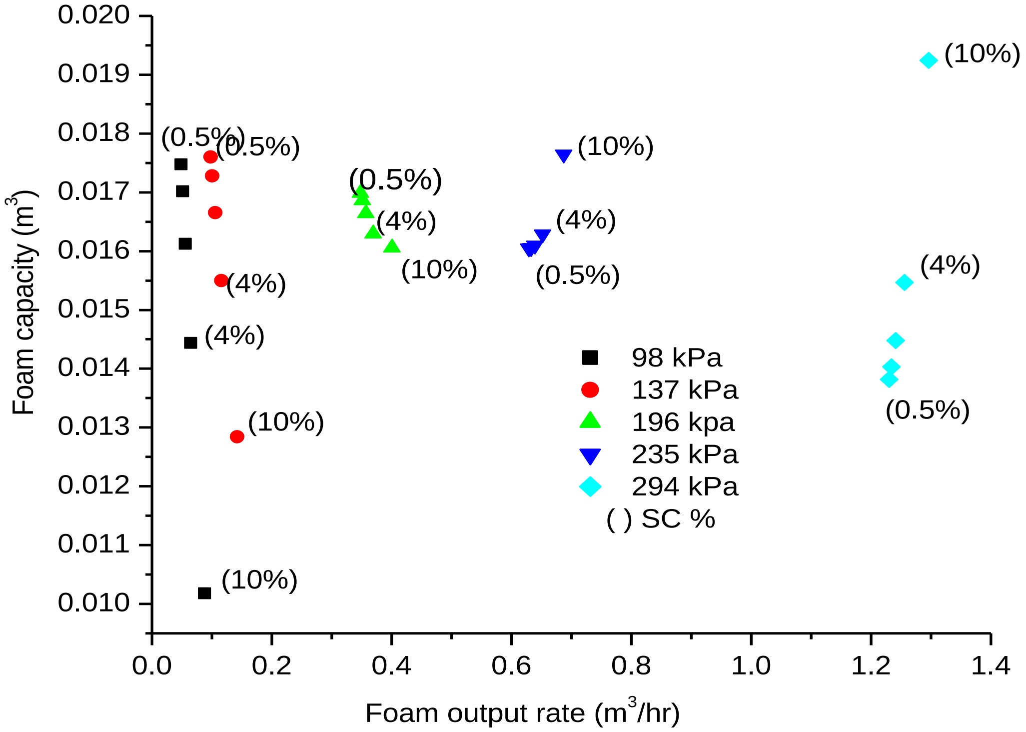

(d) Cocodiethanolamide

Fig 4.18 Variation of foam output rate with foam capacity

For Cocodiethanolamide (non ionic surfactant), even for the narrow variation of foam output rate with surfactant concentration there is greater variation of foam capacity (Fig 4.18(d)). Up to foam generation pressure of 196 kPa, the foam capacity reduces with even smaller increase in foam output rate. Beyond foam generation pressure of 196 kPa, the trend is reversed.

4.8 INITIAL FOAM DENSITY

The effects of surfactant concentration and foam generation pressure on the initial foam density are plotted in Figs.4.19 to 4.21. For ionic surfactants i) the foam density is maximized when the surfactant concentration and foam generation pressures are at lower and higher levels respectively, and ii) the initial foam density decreases with an increase in surfactant concentration of up to 4% after which there is only a marginal increase (Fig.4.20 (a)).

This is because at higher foam generation pressure and lower surfactant concentration, foam is observed to have more liquid and less air resulting in higher foam density which is confirmed by higher drainage values obtained (as discussed in the next section). For non-ionic surfactant (Cocodiethanolamide), i) the initial foam density increases with an increase in surfactant concentration at lower foam generation pressure (Fig 4.20(a)), and ii) this trend is reversed at higher foam generation pressure (Fig. 4.20(b)). This is attributed to the entry of more foaming solution into foam due to turbulence at lower surfactant concentration, which is not significant at lower foam generation pressure unlike ionic surfactants.

For foam concrete, ASTM C 796 specifies the foam unit weight range of 32 to 64 kg/m^3 with a remark that this range could be adjusted to manufacturer's recommendation based on foam chemical and generator used. For the surfactant concentrations and foam generation pressures adopted, the range of initial foam density produced with Sodium lauryl sulfate, Sodium lauryl ether sulfate, Sulfanol and Cocodiethanolamide respectively are 20-35 kg/m^3, 20-65 kg/m^3, 20-40 kg/m^3 and 40-100 kg/m^3. For all the four surfactants, the initial foam density obtained is satisfying the ASTM requirements at lower surfactant concentration and higher foam generation pressure.

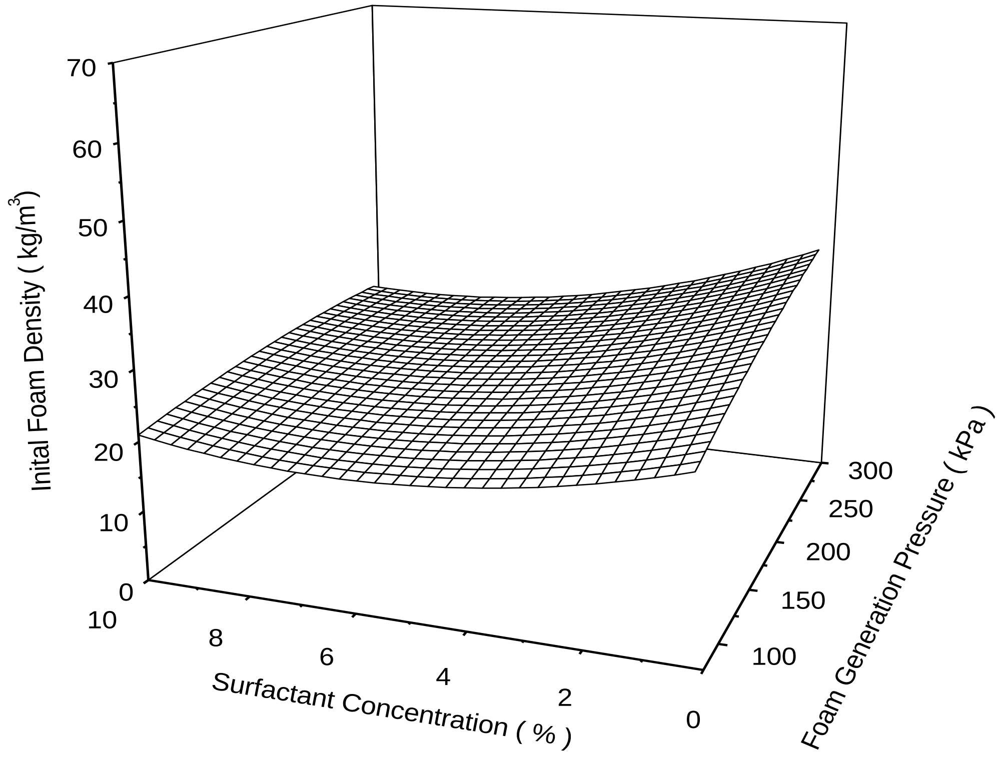

(a) Sodium lauryl sulfate

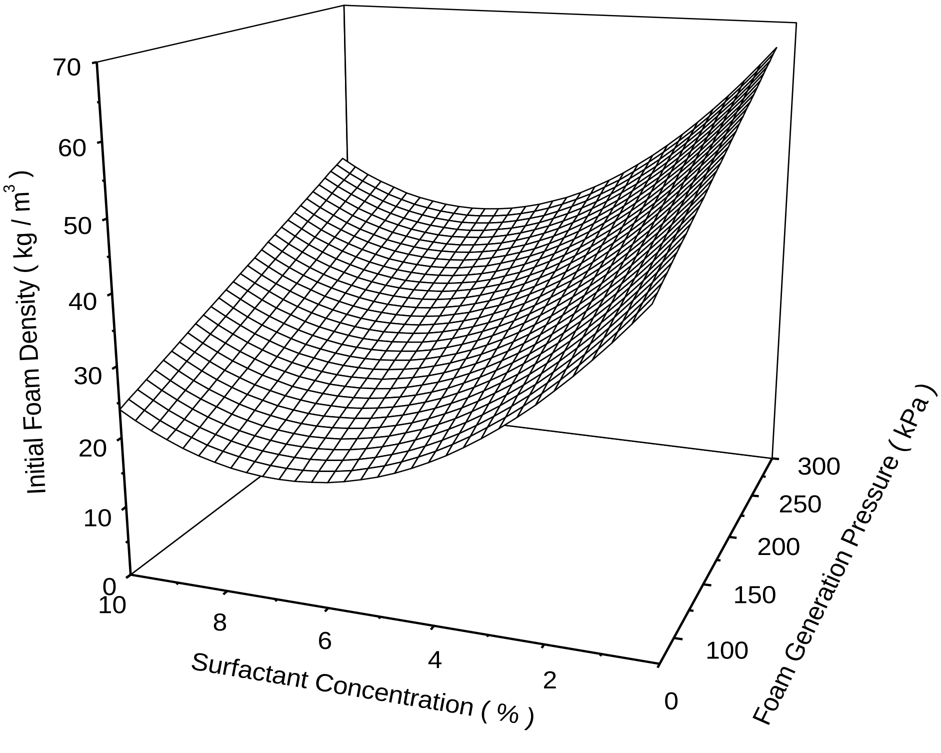

(b) Sodium lauryl ether sulfate

Fig 4.19 Response surface plots for initial foam density

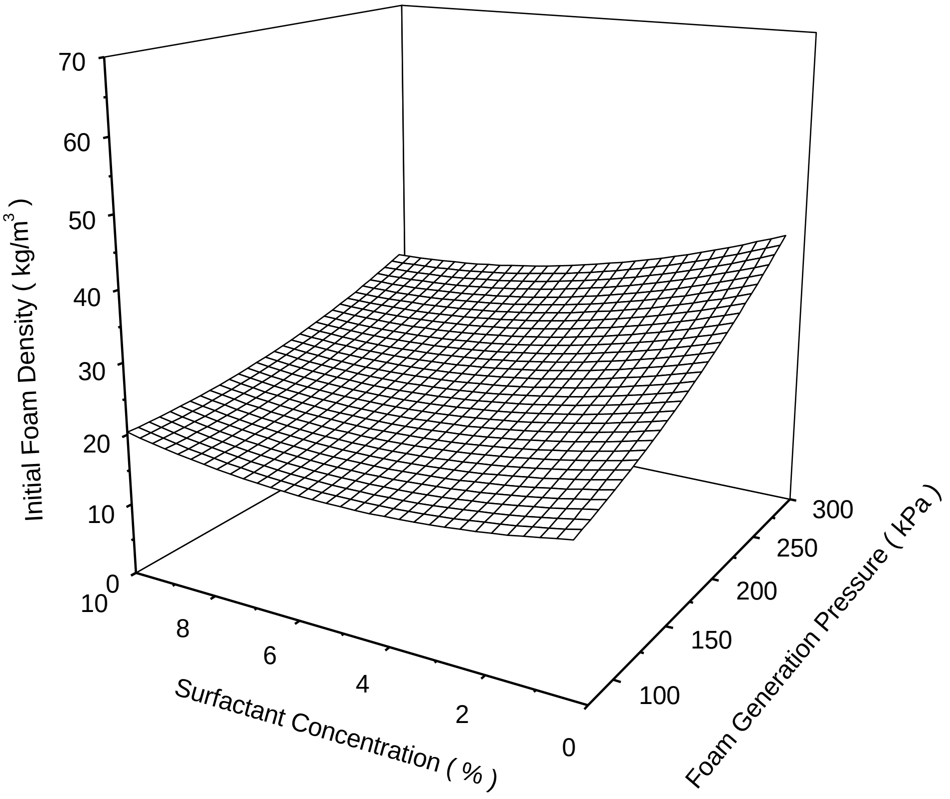

(c) Sulfanol

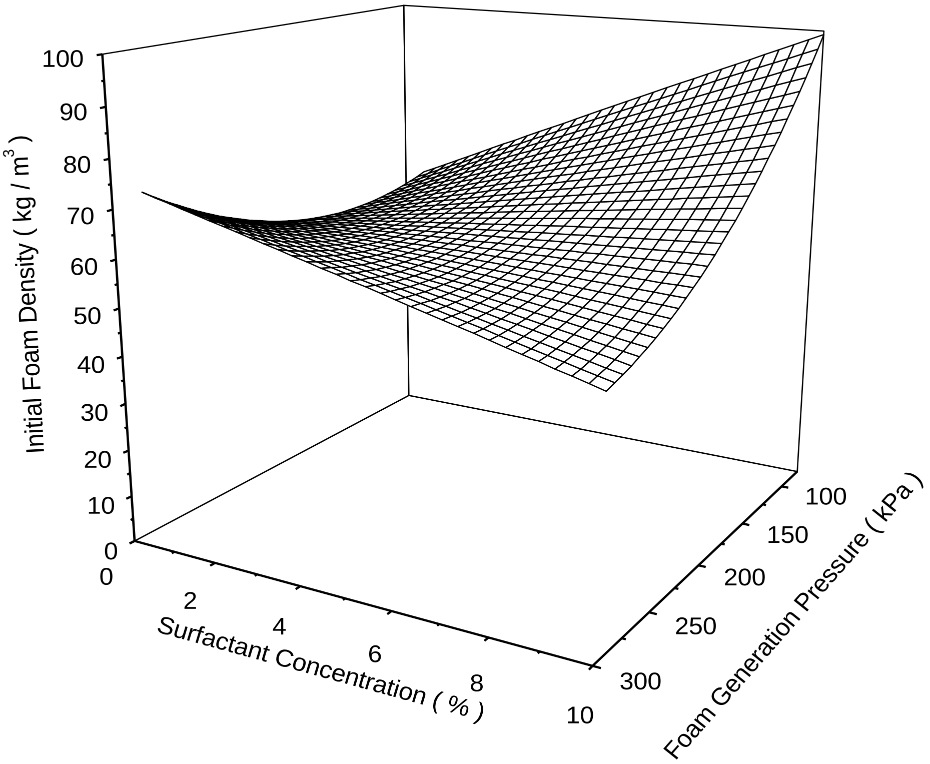

(d) Cocodiethanoamide

Fig 4.19 Response surface plots for initial foam density

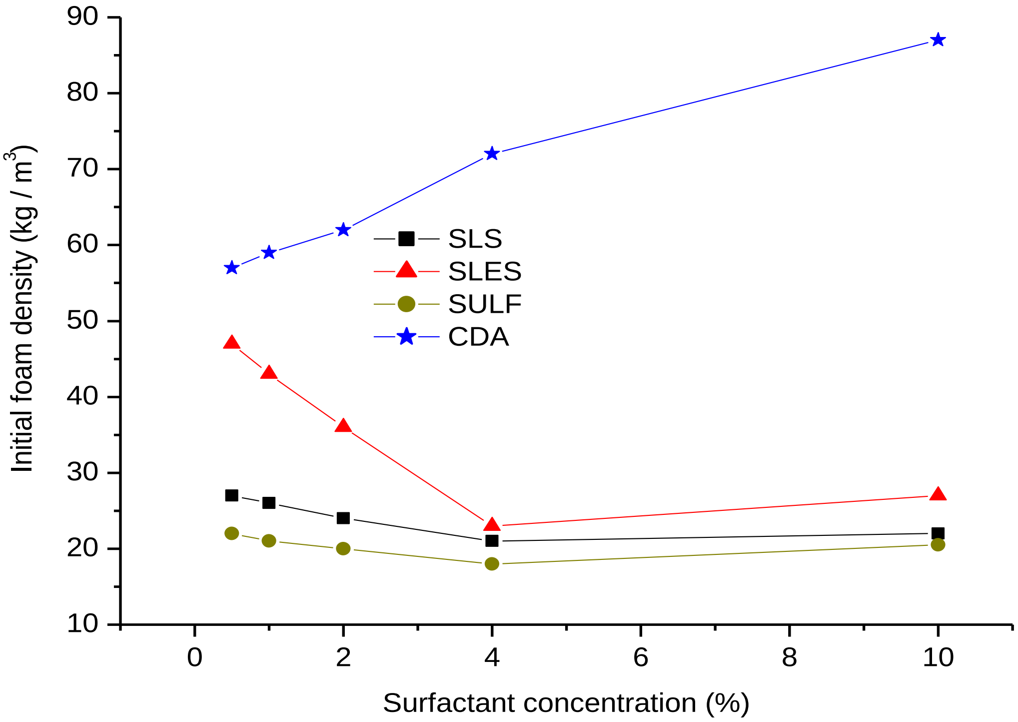

(a) FGP 110 kPa

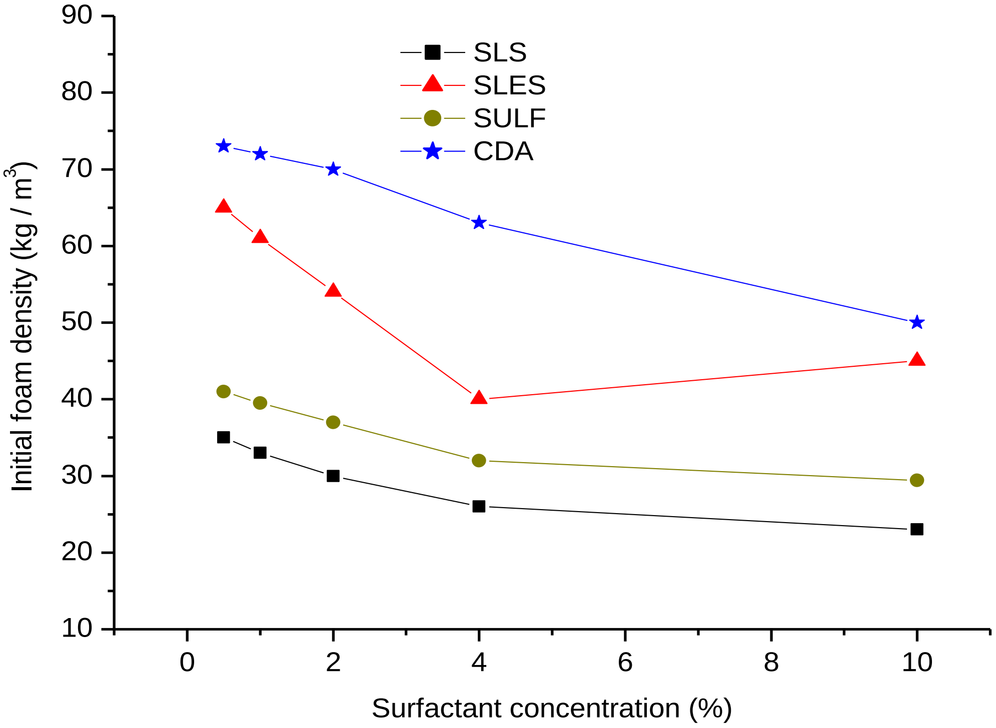

(b) FGP 294 kPa

Fig. 4.20 Variation in initial foam density with surfactant concentration

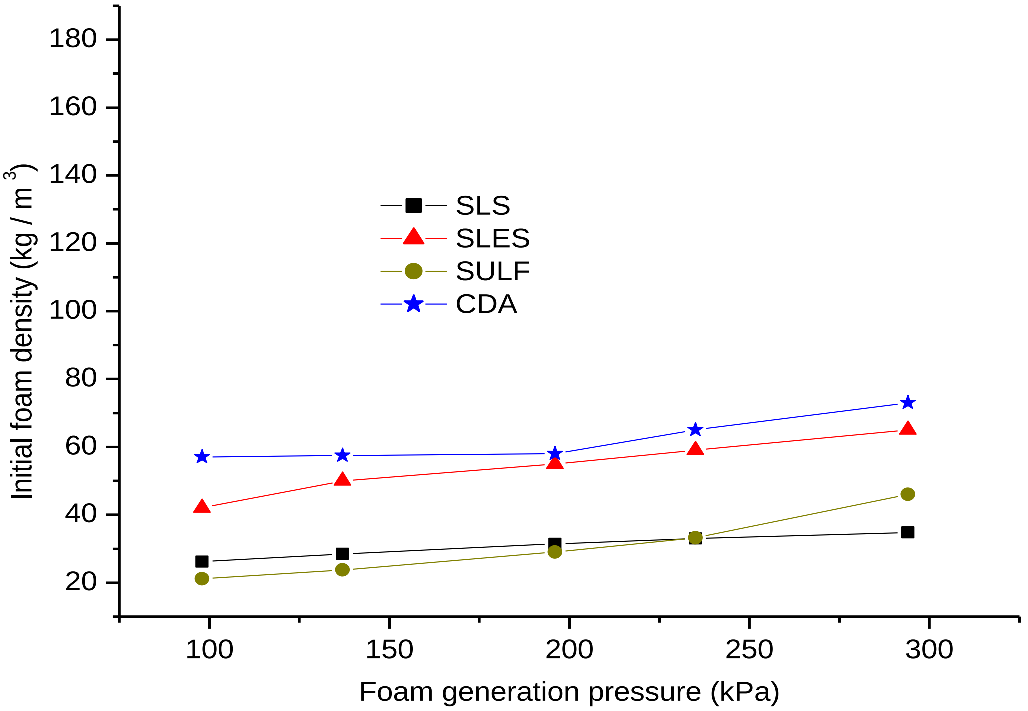

(a) SC 0.5%

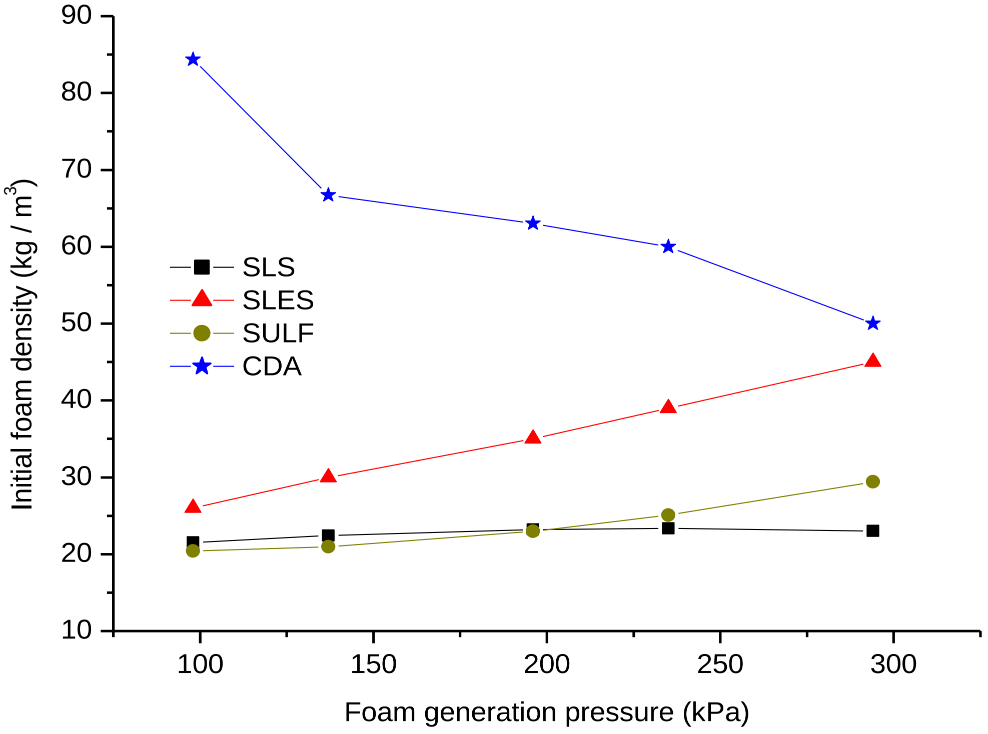

(b) SC 10%

Fig. 4.21 Variation in initial foam density with foam generation pressure

But such foam with higher initial foam density was observed to contain foaming solution entrapped with the foam due to turbulence resulting in foams with lower stability. This aspect is confirmed by higher drop in density with time as discussed in the next section.

The foam generation pressure controls the mixing of air with foaming liquid and hence the foam density varies with foam generation pressure. For a given surfactant concentration the initial foam density increases with an increase in foam generation pressure for all surfactants except in the case of Cocodiethanolamide. It is observed from Fig. 4.21 that the effect of foam generation pressure on the initial foam density is lower for Sodium lauryl sulfate and Sulfanol irrespective of the surfactant concentration. Hence the densities of the foam produced using Sulfanol and Sodium lauryl sulfate are the lowest.

The ASTM specified range of initial foam density is not achieved when foam is produced at lower foam generation pressure for surfactants Sodium lauryl sulfate and Sulfanol. In the case of Sodium lauryl ether sulfate at higher surfactant concentration the effect of foam generation pressure is significant. Cocodiethanolamide produces foam with highest initial foam density irrespective of the foam generation pressure. For Cocodiethanolamide, the foam generation pressure has significant effect on initial foam density i.e., at higher surfactant concentration an increase in foam generation pressure results in a reduction in initial foam density and vice versa at lower surfactant concentration. For all the four surfactants the main effects viz., surfactant concentration and foam generation pressure ($p<0.05$) influence the initial foam density with no interaction between them with the exception of Cocodiethanolamide for which interaction term is significant (Table 4.9).

4.9 FOAM STABILITY

The foam stability is assessed through the variation in foam density with time which is caused predominantly by the drainage of diluted foaming agent entrapped along the walls of the bubbles and to a minor extent due to breakage of foam bubbles. Response surface plots for variation of foam density with time for the four surfactants are shown in Fig. 4.22. Fig.4.23 shows the variation in foam density with time for the effect of surfactant concentration at lower and higher foam generation pressures. For all the four surfactants, the drainage increases with an increase in foam generation pressure resulting in unstable foam. For the three ionic surfactants within the range of surfactant concentration studied, the drainage is proportional to the initial foam density at different foam generation pressures. For the ionic surfactants the rate of drainage is significantly higher after five minutes which is evident from the higher drop in foam density (Fig 4.22). For the three ionic surfactants, within ten minutes more than 40% of foam density is reduced. In the case of Cocodiethanolamide, a concentration of 4% and above has resulted in retention of stability. The foam produced with Cocodiethanolamide is more stable when compared to that produced with ionic surfactants, exhibiting substantially lower drainage at high surfactant concentration.

This retardation in drainage is attributed to the high viscosity enhancing and foam stabilizing property of Cocodiethanolamide. Also the surfactant concentration has opposite effect at lower and higher levels of foam generation pressure for this non-ionic surfactant. This is because at lower foam generation pressure, the effect of lower surfactant concentration on foam stability is not significant unlike ionic surfactants as explained earlier. This is confirmed by lesser drop in foam density with time up to 5 minutes at lower foam generation pressure when compared to higher pressure for the non-ionic surfactant.

Foam stability is also assessed by measurement of percentage solution drained at various time intervals. The effects of surfactant concentration and foam generation pressure on the percentage solution drained at 5th and 10th minute after generation of foam are plotted in Figs.4.24-4.26. The main effects ($p<0.05$) influenced the percentage solution drained in 5 and 10 minutes with no interaction between them with the exception of Sodium lauryl ether sulfate and Cocodiethanolamaide for which the main effects of surfactant concentration and foam generation pressure are not significant in 5 minutes and 10 minutes respectively (Table 4.9). The main effects of surfactant concentration and foam generation pressure have negative and positive effects respectively on percentage solution drained. Hence for a constant surfactant concentration, the percentage solution drained increases with an increase in foam generation pressure resulting in poor stability foam. This effect is more significant when the surfactant concentration is lower. At higher foam generation pressure an increase in surfactant concentration reduces the percentage solution drained. The variation of percentage solution drained with surfactant concentration is less pronounced at lower foam generation pressure as compared to higher foam generation pressure. The percentage solution drained decreases with surfactant concentration up to a dosage of 4% after which there is no significant reduction particularly at lower foam generation pressure (Fig 4.25(a)). For surfactants Sodium lauryl ether sulfate and Cocodiethaolamide, after 4% dosage the surfactant concentration has no effect on percentage solution drained in five minutes irrespective of foam generation pressure (Fig. 4.25). The effect of foam generation pressure on foam stability (percentage solution drained in five and ten minutes) is less significant for surfactants Sodium lauryl sulfate and Cocodiethaolamide particularly at higher surfactant concentration (Fig 4.26(b)). For given foam generation pressure, Sodium lauryl sulfate and Cocodiethanolamide have the minimum % solution drained in five minutes at lower and higher surfactant concentration respectively. The percentage solution drained becomes significantly higher after five minutes for all surfactants. For any combination of surfactant concentration and foam generation pressure, the time taken for 25% foam drainage volume is observed to be more than 210 seconds as prescribed by Def Standard 42–40 (2002) for synthetic aqueous film forming foam fire extinguishant. Also solution drained in five minutes is lesser than 25% irrespective of surfactant concentration used for foam generation pressure less than 200 kPa.

Foam stability can also be expressed in terms of foam density ratio. The foam density ratio, the ratio of foam density at different time interval to the initial foam density is the inverse function of percentage solution drained. The main effects of surfactant concentration and foam generation pressure have positive and negative effect respectively on foam density ratio which is opposite to that of percentage solution drained. Figs.4.27 to 4.29 show the variation in foam density ratio with variation in surfactant concentration and foam generation pressures. For a constant surfactant concentration, the density ratio decreases with an increase in foam generation pressure resulting in production of poor stability foam. This effect is more significant when surfactant concentration is lower. At higher foam generation pressure an increase in surfactant concentration increases the density ratio. The variation of density ratio with surfactant concentration is less pronounced at lower foam generation pressure as compared to higher foam generation pressure.

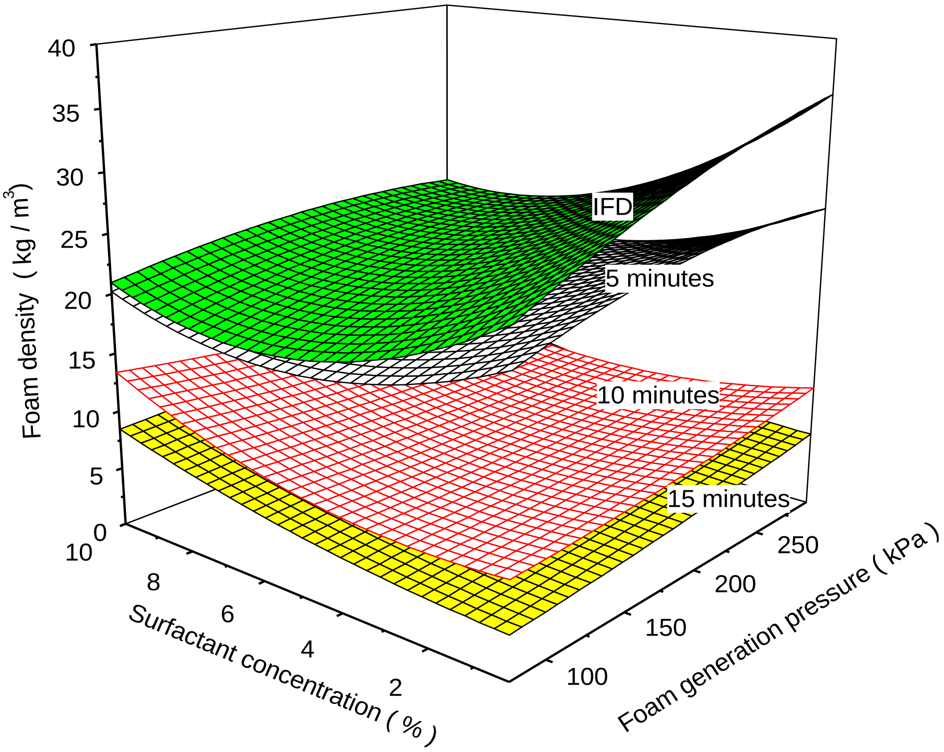

(a) Sodium lauryl sulfate

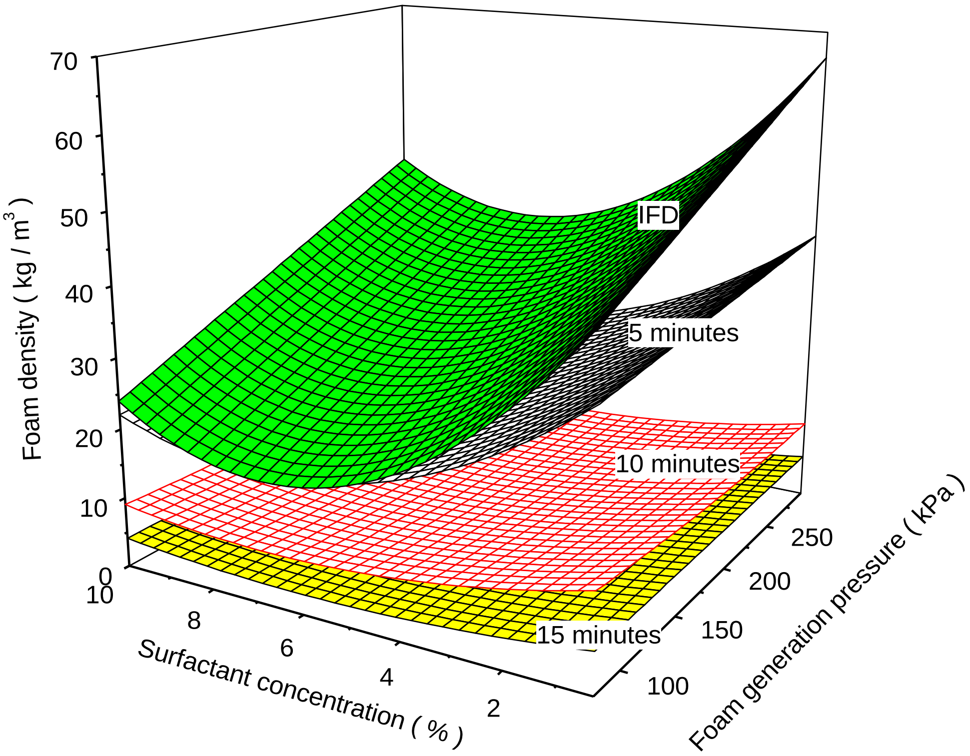

(b) Sodium lauryl ether sulfate

Fig 4.22 Response surface plot for variation in foam density with time

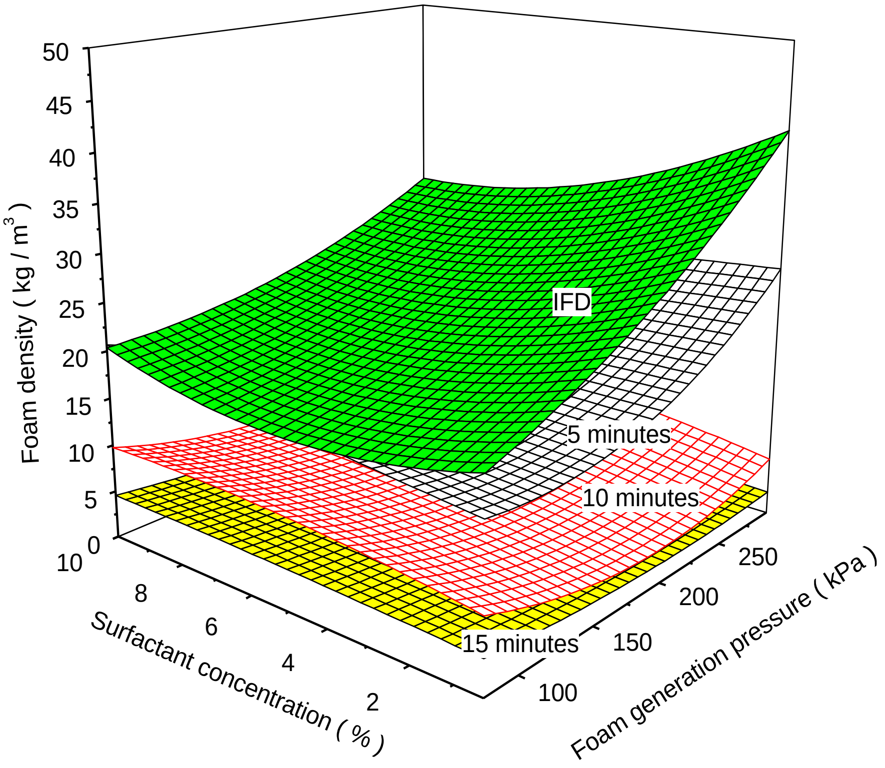

(c) Sulfanol

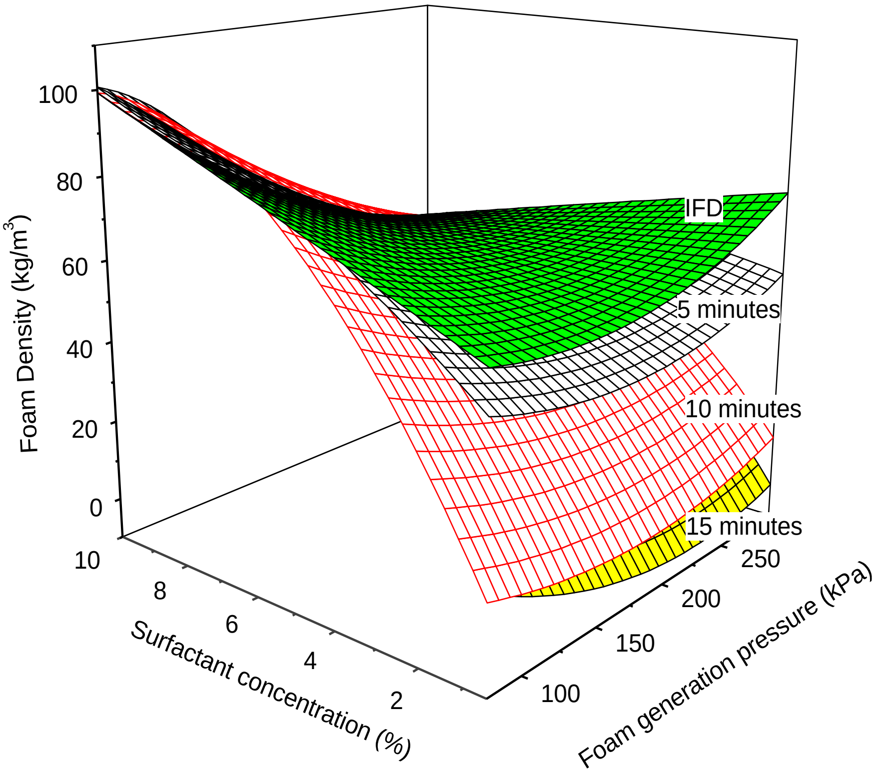

(d) Cocodiethanolamide

Fig 4.22 Response surface plot for variation in foam density with time

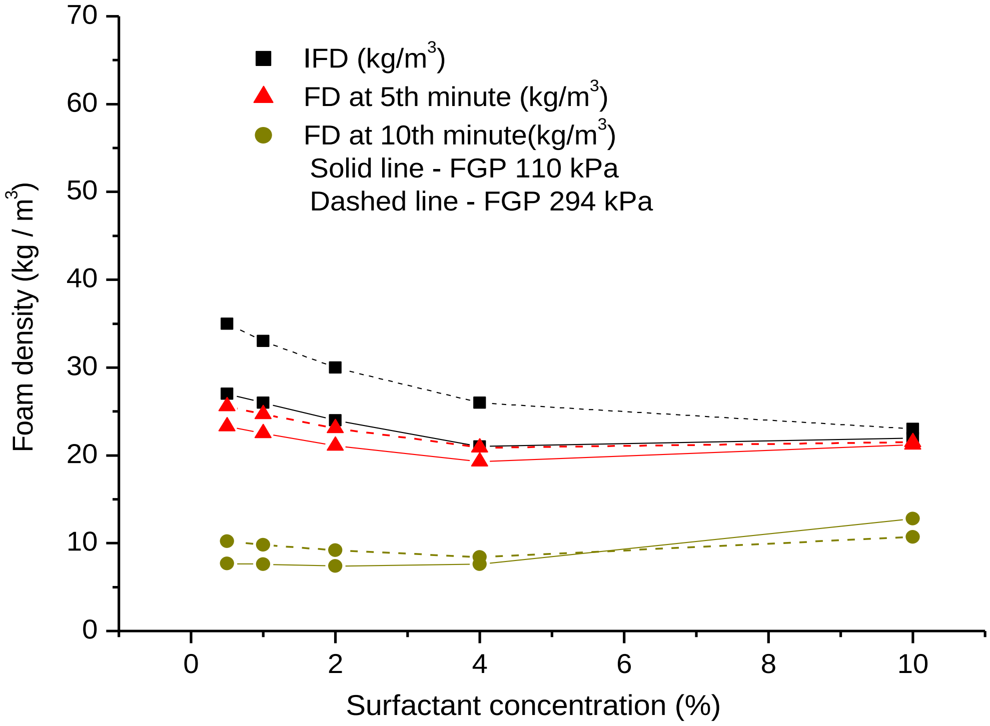

(a) Sodium lauryl sulfate

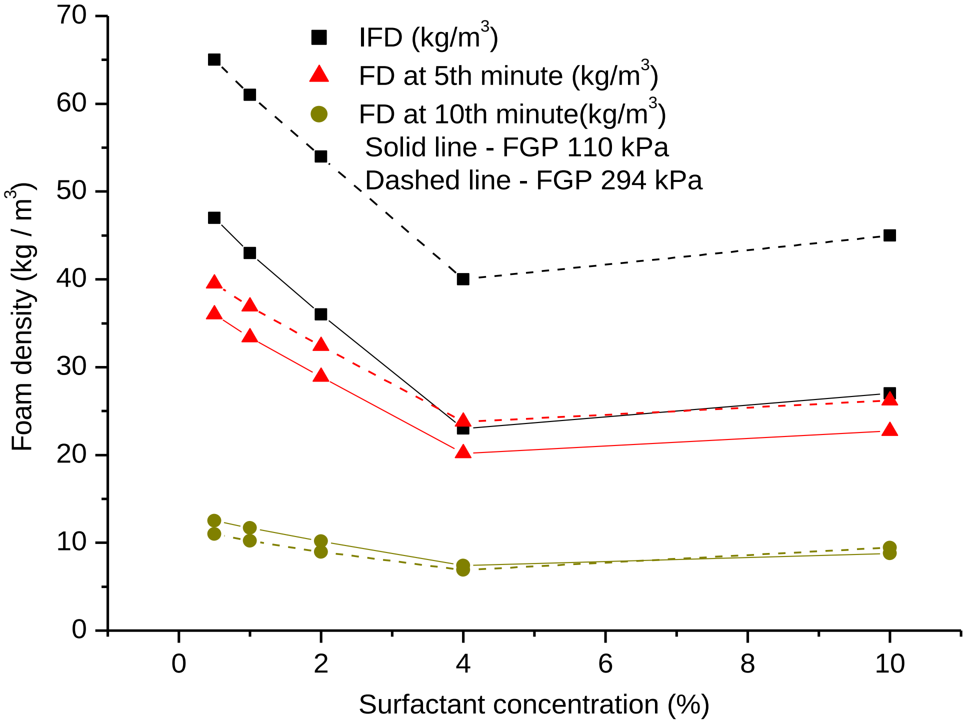

(b) Sodium lauryl ether sulfate

Figure 4.23 Effect of SC and FGP on foam density with time for various surfactants

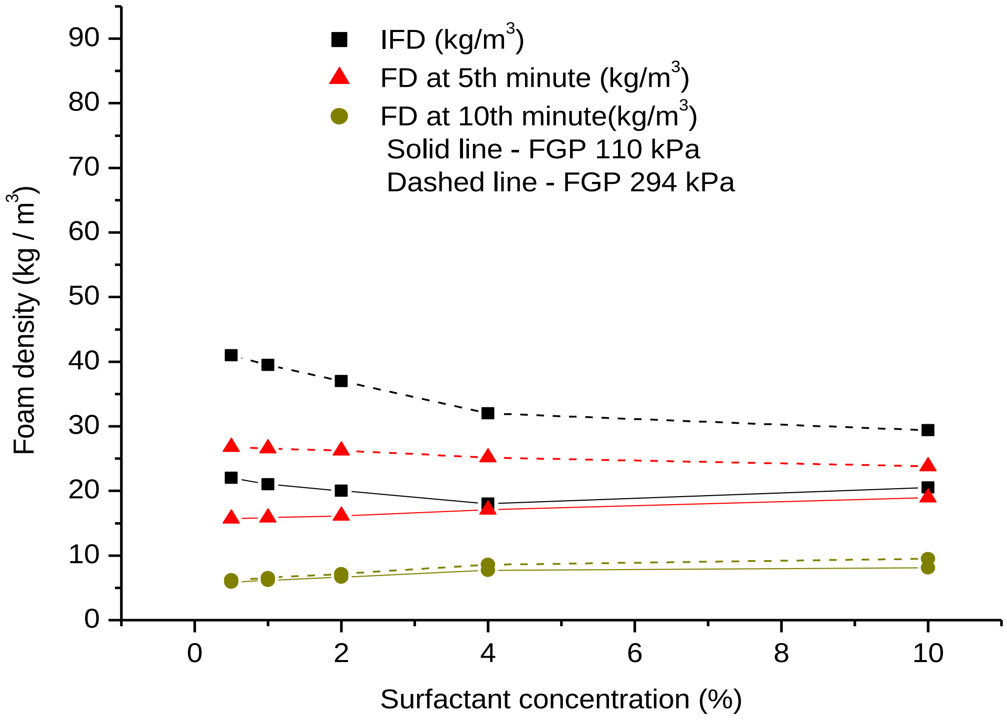

(c) Sulfanol

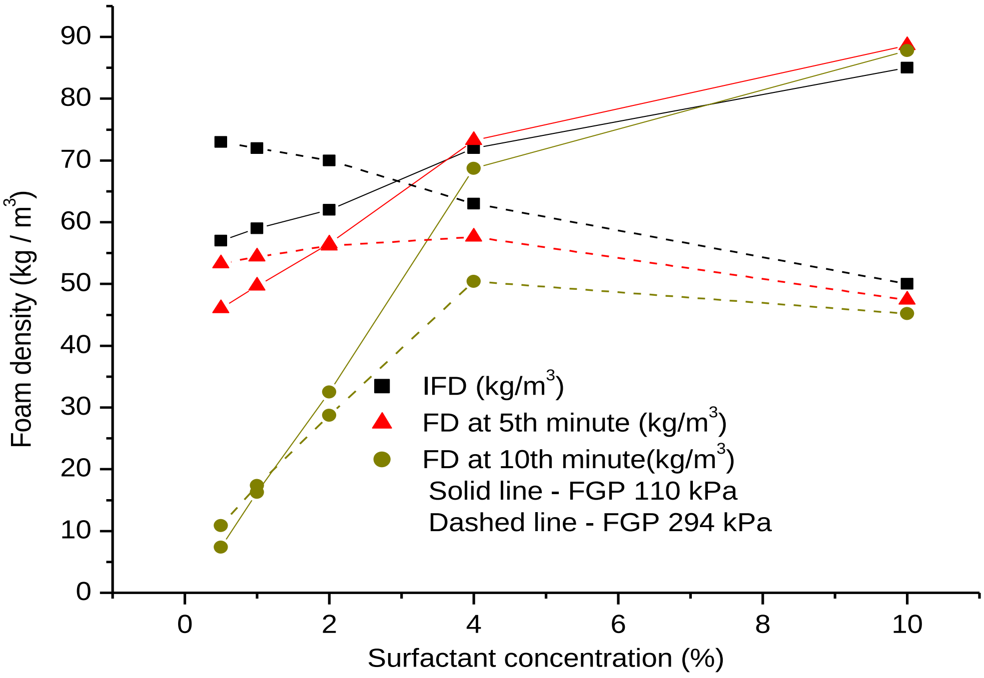

(d) Cocodiethanolamide

Figure 4.23 Effect of SC and FGP on foam density with time for various surfactants

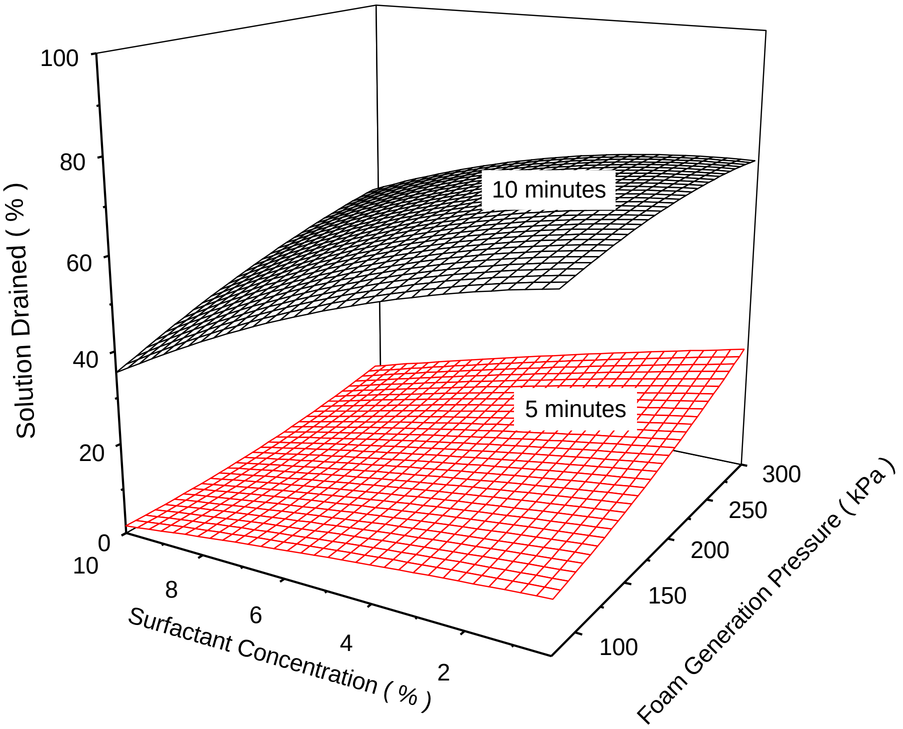

(a) Sodium lauryl sulfate

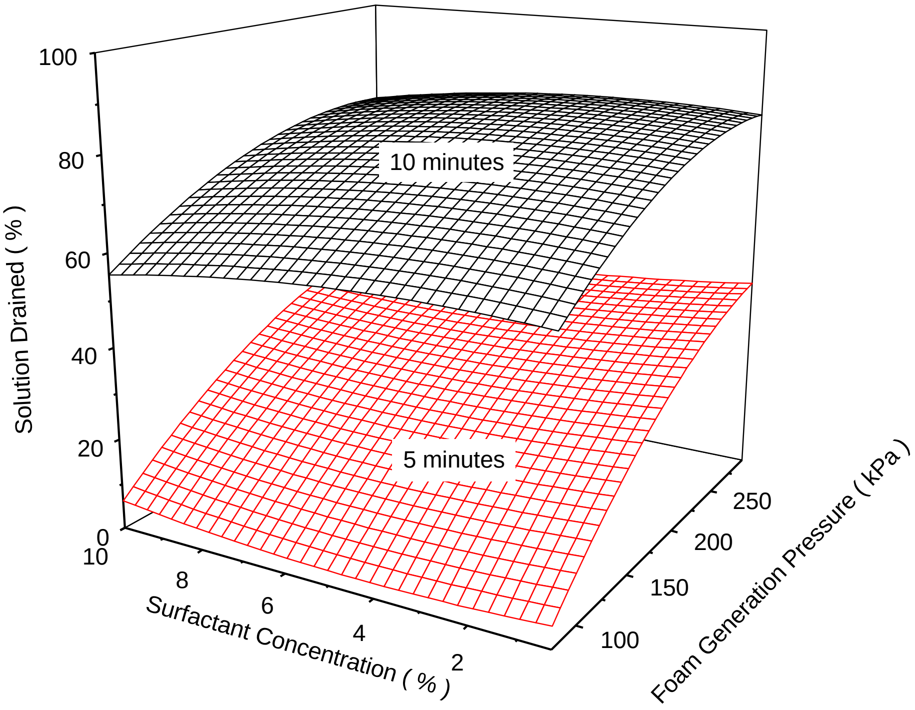

(b) Sodium lauryl ether sulfate

Fig 4.24 Response surface plots for variation of percentage solution drained with time

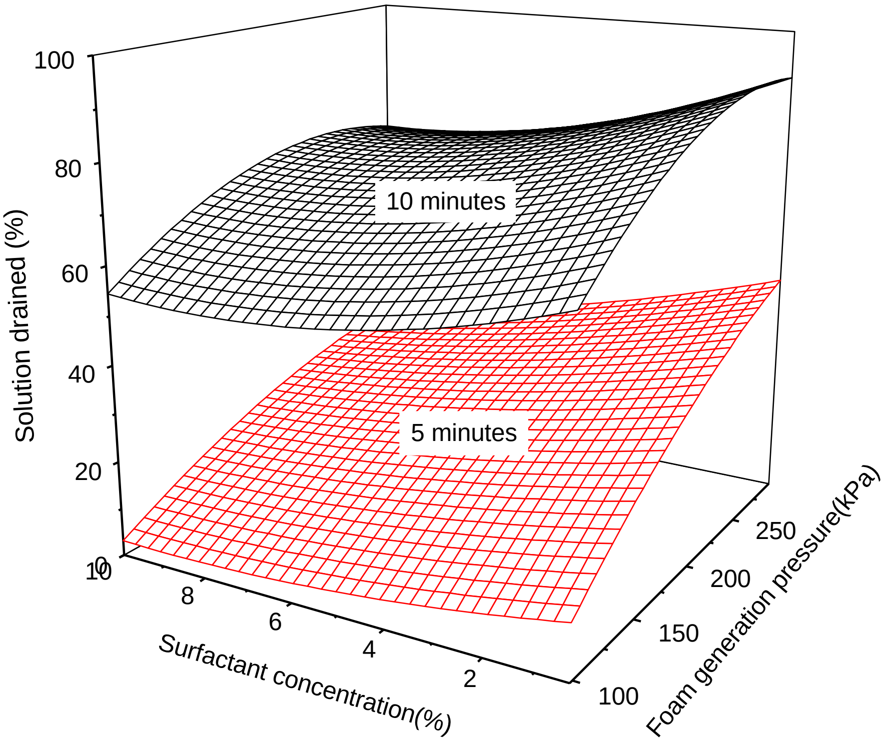

(c) Sulfanol

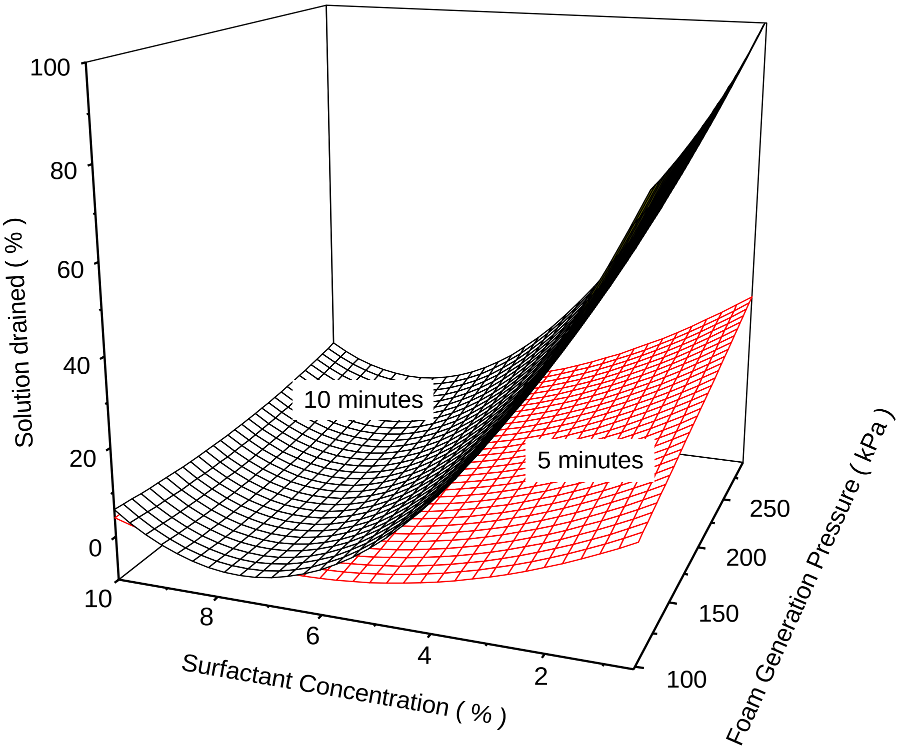

(d) Cocodiethanolamide

Fig 4.24 Response surface plots for variation of percentage solution drained with time

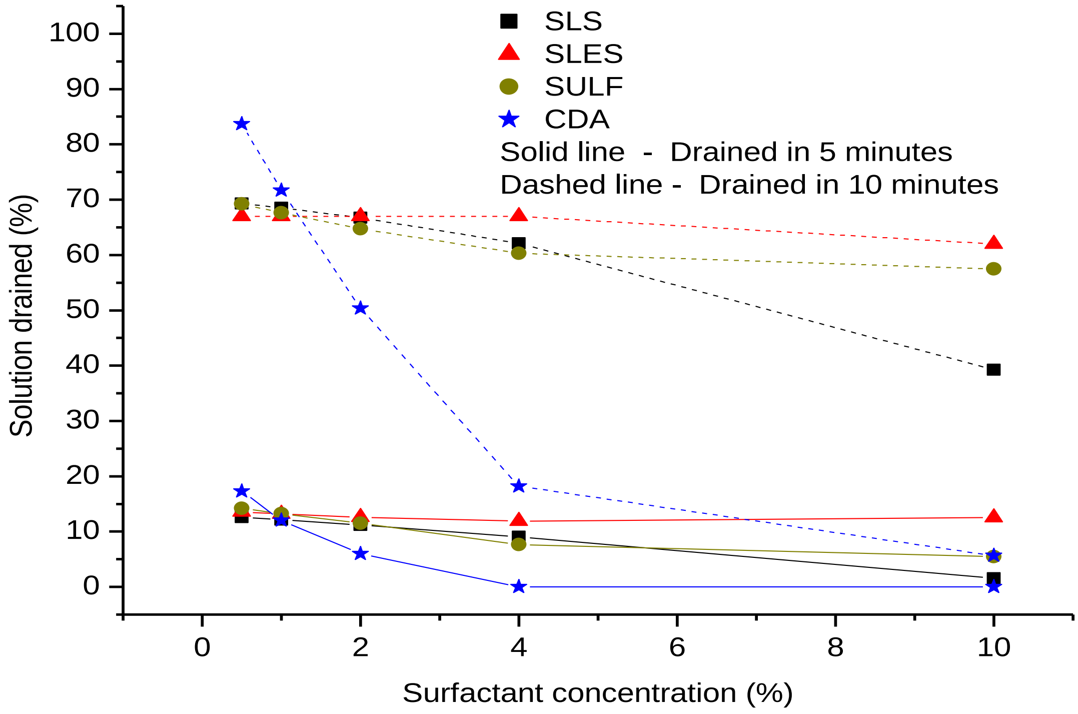

(a) FGP 110 kPa

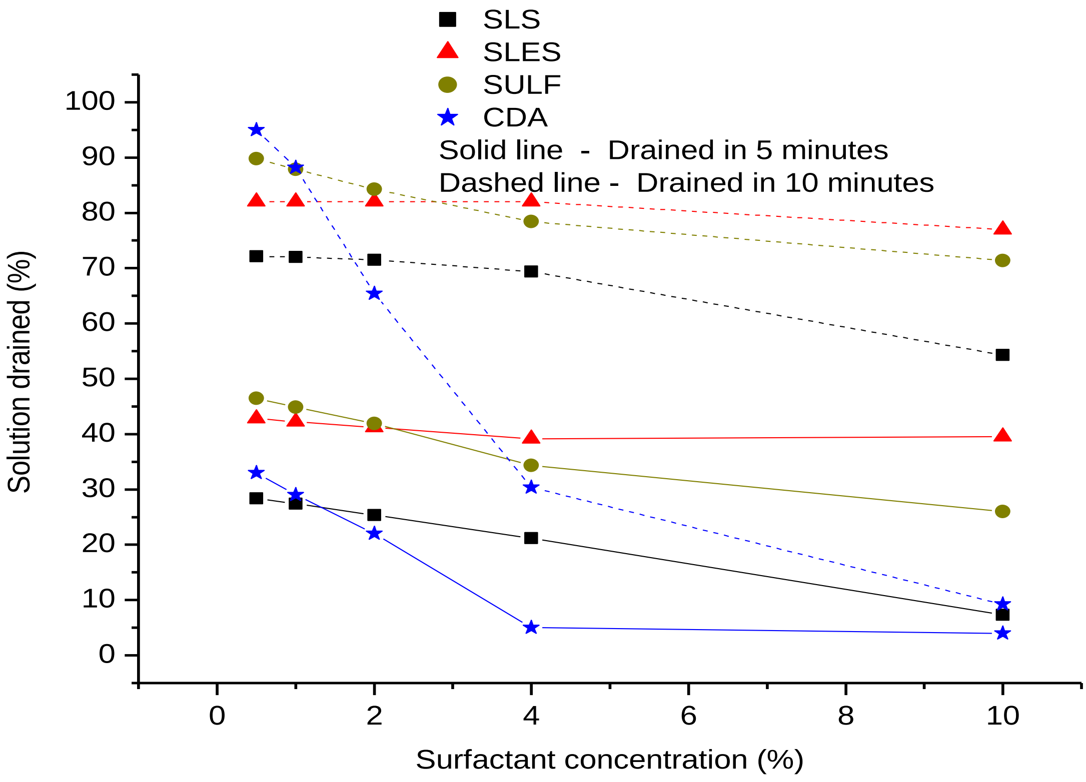

(b) FGP 294 kPa

Figure 4.25 Variation in percentage solution drained with surfactant concentration

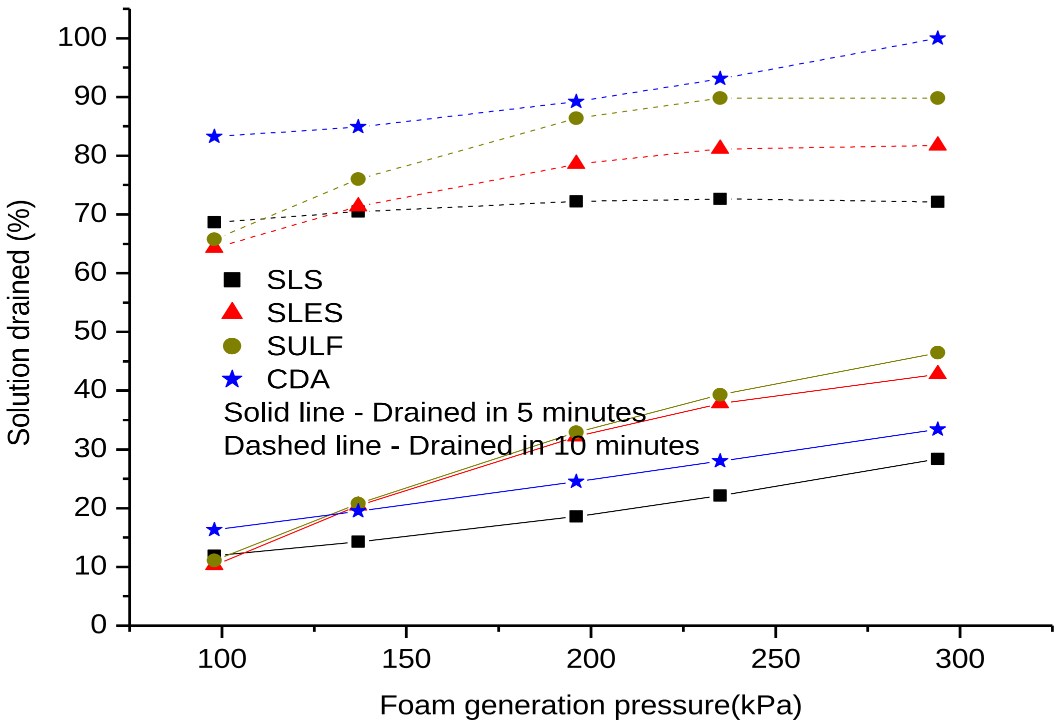

(a) SC 0.5%

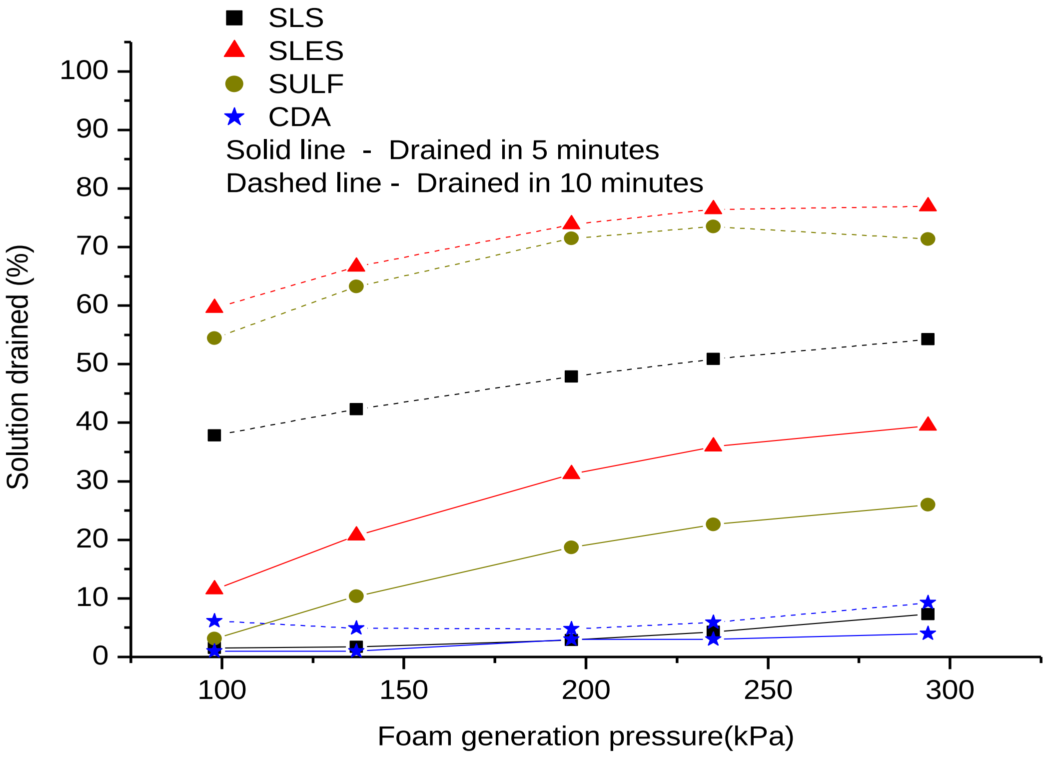

(b) SC 10%

Figure 4.26 Variation in percentage solution drained with foam generation pressure

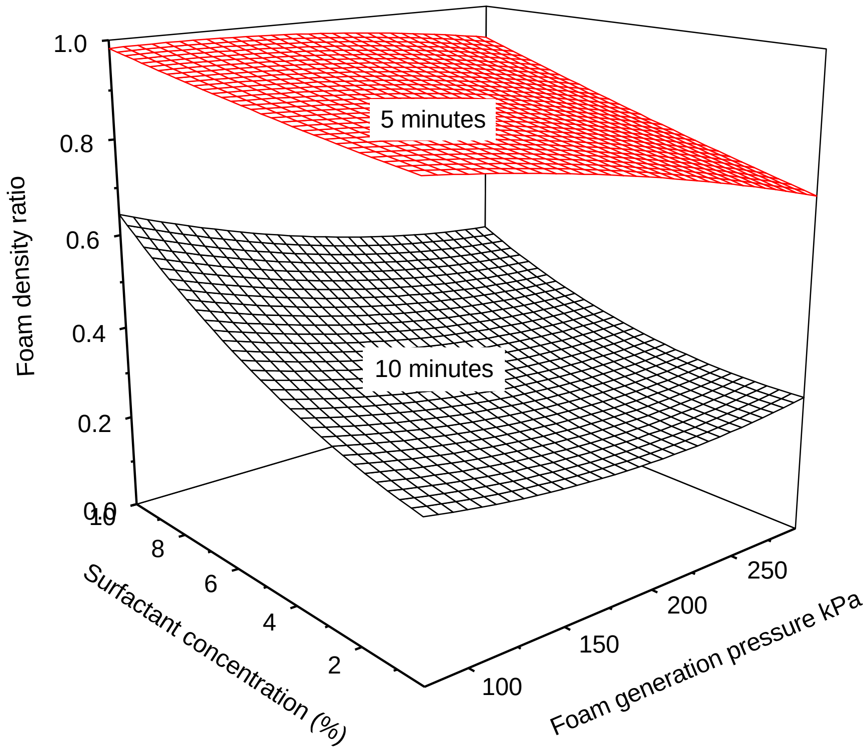

(a) Sodium lauryl sulfate

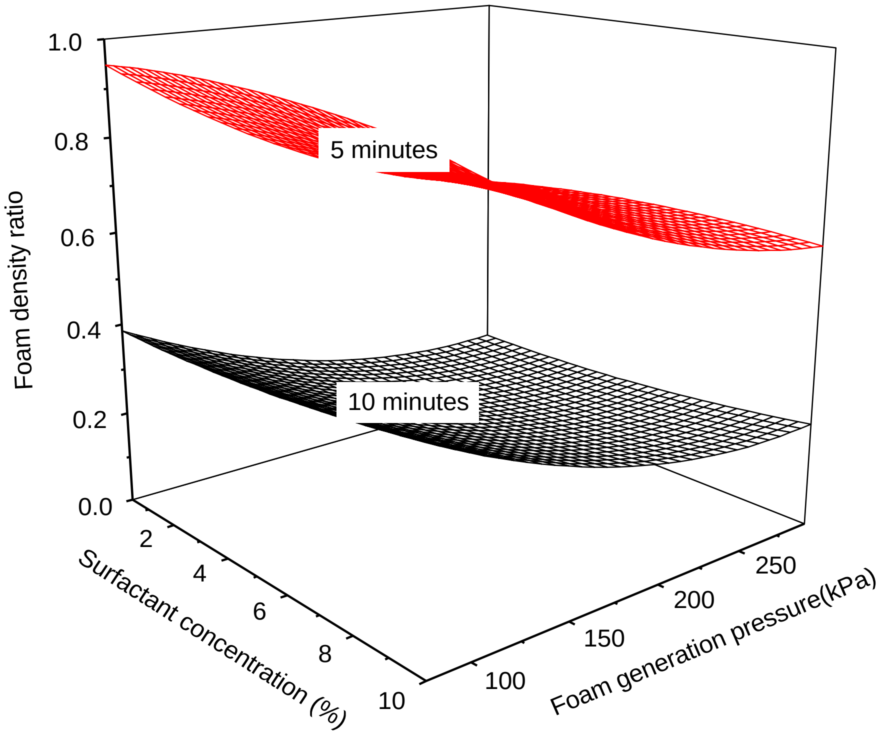

(b) Sodium lauryl ether sulfate

Fig 4.27 Response surface plots for variation of foam density ratio with time

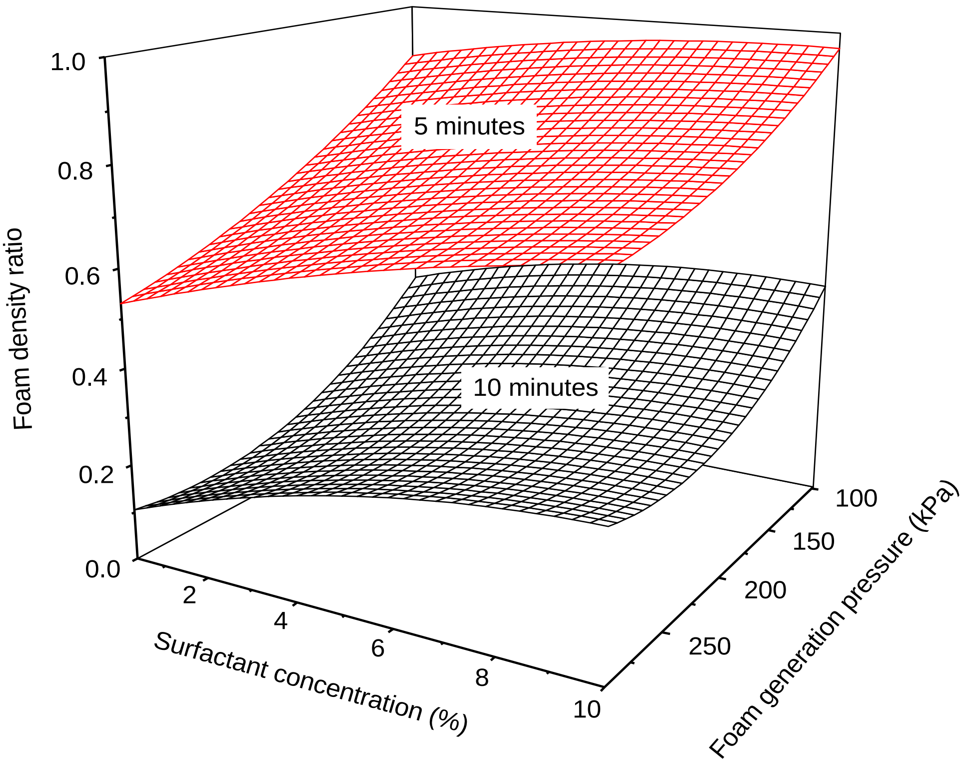

(c) Sulfanol

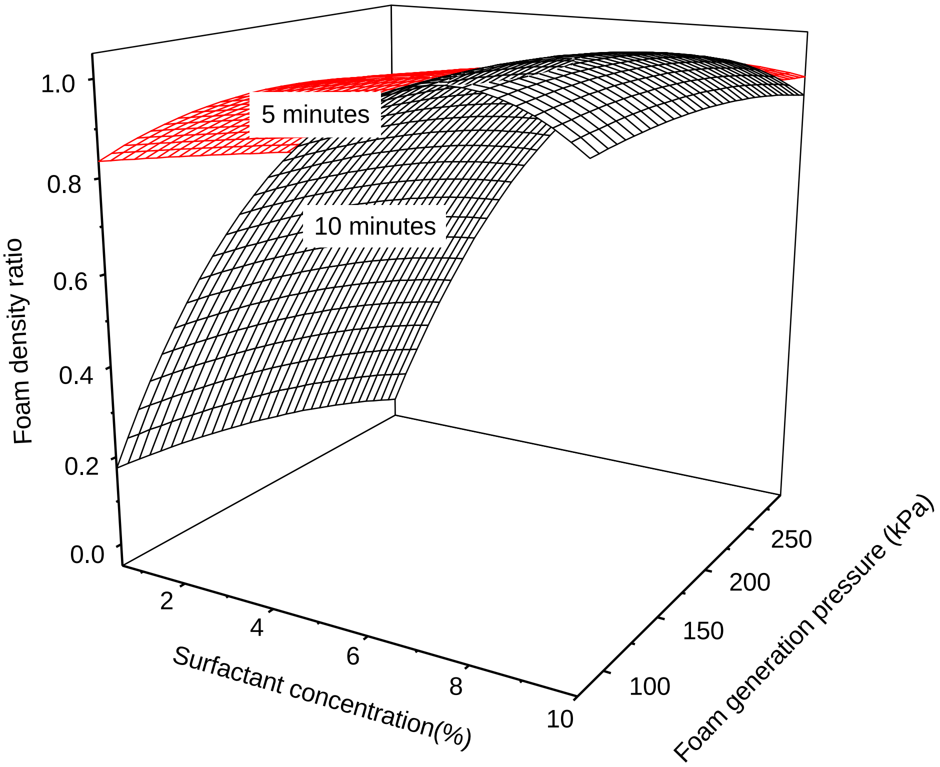

(d) Cocodiethanolamide

Fig 4.27 Response surface plots for variation of foam density ratio with time

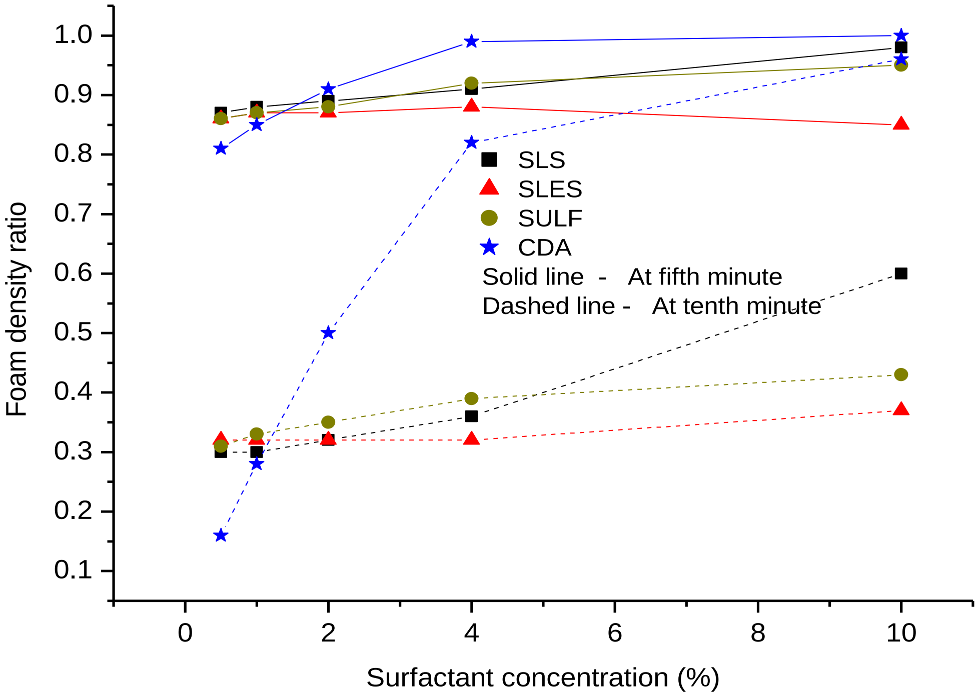

(a) FGP 110 kPa

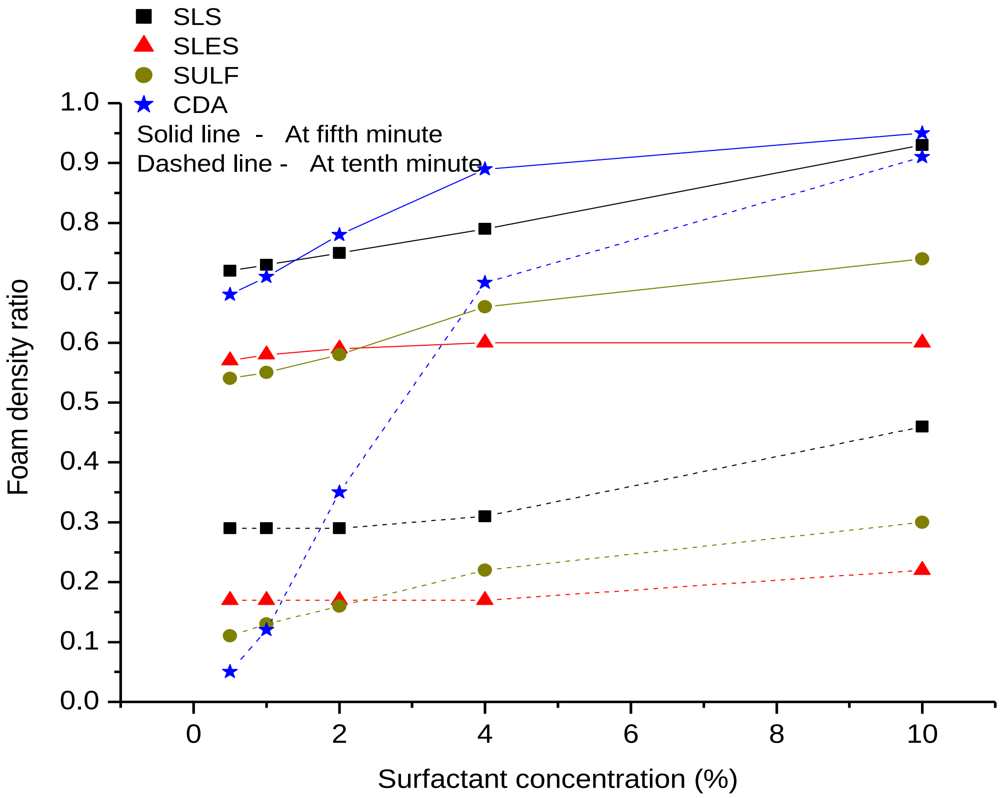

(b) FGP 294 kPa

Figure 4.28 Variation in foam density ratio with surfactant concentration

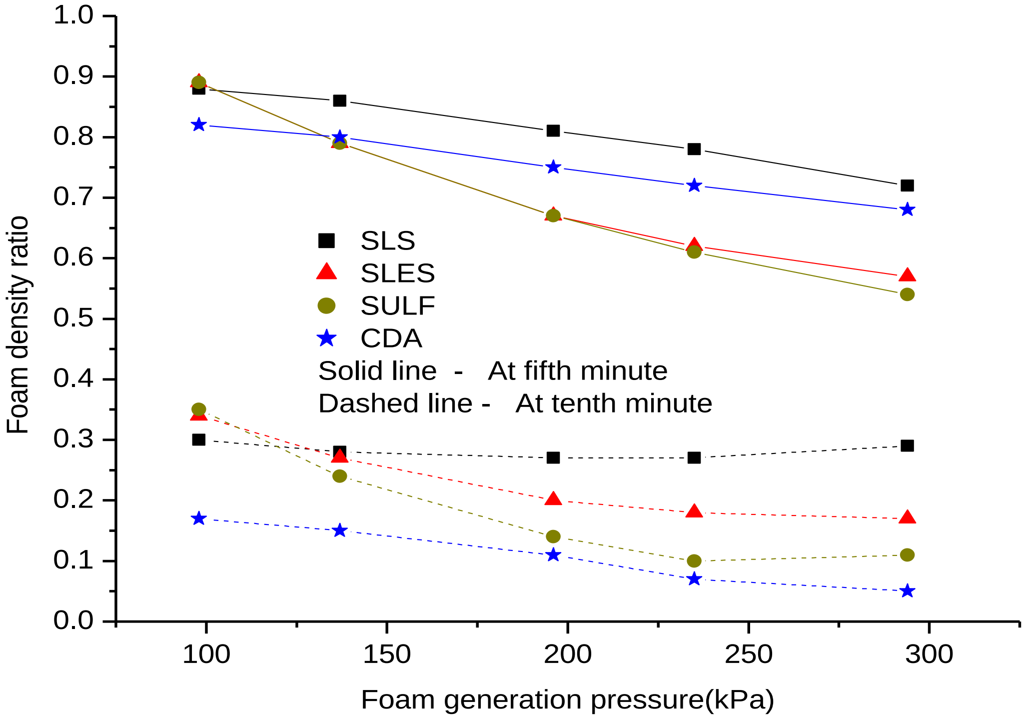

(a) SC 0.5%

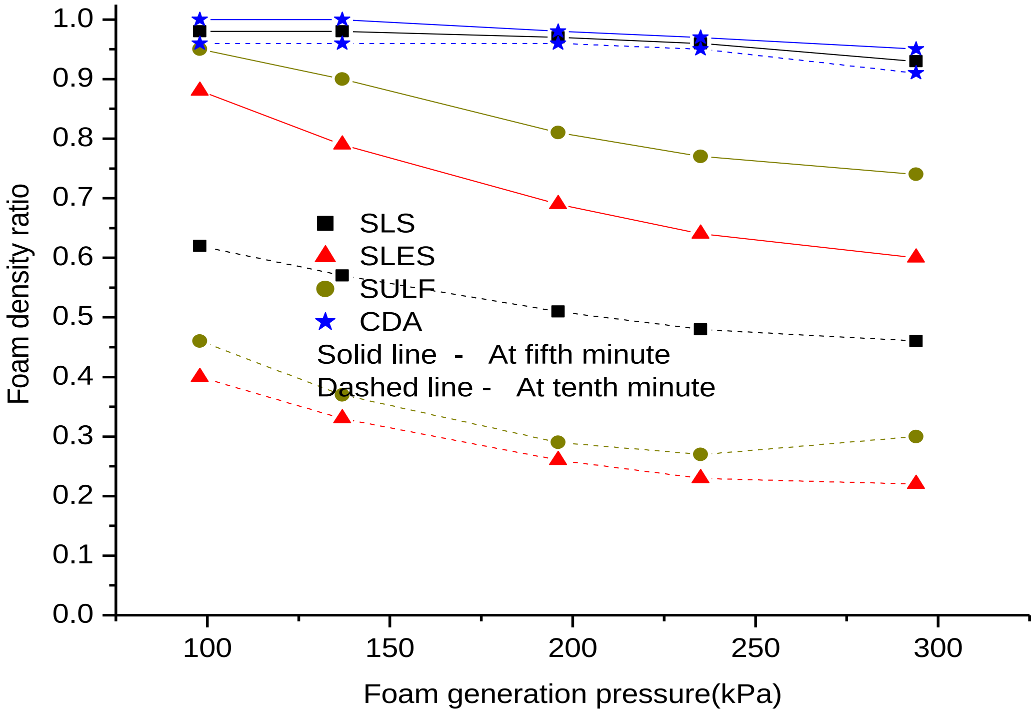

(b) SC 10%

Figure 4.29 Variation in foam density ratio with foam generation pressure

From Fig 4.27 it is observed that the rate of drainage increases after five minutes which is evident from the higher drop in foam density ratio. As the usage of higher surfactant concentration is not economical, the selection of lower concentration is preferable for use in foam concrete production. But at very low surfactant concentration and higher foam generation pressure, though the foam produced has high initial density, the stability is poor. Hence it appears that there is an optimal surfactant concentration and foam generation pressure which can produce stable foam. The selection of surfactant concentration and foam generation pressure should not only be based on achieving higher foam density (to satisfy the ASTM specified range of density) but should be based on stability also.

4.10 OPTIMIZATION OF RESPONSE SURFACE MODELS

Having identified that the foam stability is an important factor, a multiple optimization was carried out by numerical optimization method using SAS Release 8.02 to predict the optimum levels of surfactant concentration and foam generation pressure for the following criteria; minimize percentage solution drained, maximize foam density ratio (ratio of foam density to initial foam density) at fifth minute after generation of foam (to increase foam stability), minimize surfactant concentration (to reduce cost), and to achieve a target foam output rate of at least 0.09 m^3/hr which was observed to be the minimum requirement to get uninterrupted foam production. Each response has been assigned an importance value (weightage) relative to the other responses. Percentage solution drained and foam density ratio was assigned an importance of 4 while the other responses were assigned of 3 out of 5 scale. Hence higher weightage was assigned to foam stability. From this study, the optimum surfactant concentration values are 2% and 5% when economy is considered as one of the factors for ionic and non ionic surfactants respectively. However for all the four surfactants the optimum foam generation pressure ranges between 110 to 120 kPa under which a stable foam with drainage less than 13% in 300 seconds (by considering economy as a factor) is achieved (Table 4.12). This drainage value is very low when compared to the value of 25% drainage obtained in time not less than 210 seconds as prescribed by Def Standard 42-40 (2002) for synthetic aqueous film forming foam for fire extinguishing. However by assigning higher importance to foam stability (without considering economy) the solution drained can be reduced further for ionic surfactants when higher surfactant concentration say 4% is used.

4.11 STABILITY OF FOAM IN THE MIX

With the establishment of optimal surfactant concentration and foam generation pressure, as a next step, the suitability of these four surfactants for the production of foam concrete i.e., whether the requirements of ASTM C 869 with respect to fresh density, strength and water absorption of foamed cement paste are fulfilled need to be verified. This especially is essential as the initial foam densities of foam produced by two ionic surfactants are marginally lower than the ASTM specified range. ASTM C 796-97 furnished a way of measuring in the laboratory, the performance of a foaming chemical to be used in producing foam for making cellular concrete through the following equations for arriving at the foam volume required for achieving a cement paste of known design density 641 kg/m^3 and water-cement ratio of 0.58.

$$V_f = 1000\, V_a / (1000 - W_{uf}) \text{ (per m}^3 \text{ of cement paste)} \quad (4.2)$$

$$V_a = (0.359 * W_{tw} + 0.7965\, W_c) / 641 \text{ m}^3 \quad (4.3)$$

Where V_f = volume of foam; V_a = volume of air; Wuf = unit weight of foam; W_{tw} = total weight of water; and W_c = weight of cement.

Foam concrete was made by mixing the cement slurry with a water-cement ratio 0.58 and preformed foam produced from the surfactants at the optimized economical surfactant concentration and foam generation pressure. The stability of test mixes was assessed by comparing the calculated (cal) and actual (Act) quantities of foam required to achieve a plastic density within ±50 kg/m^3 of the design value and are summarized in Table 4.13 along with ASTM specifications. The foamed concrete made with the foam produced with all the four surfactants, at the optimized surfactant concentration and foam generation pressure, met the physical requirements of ASTM, which confirmed the foam stability. Though the foam density of Sodium lauryl sulfate and Sulfanol did not meet the minimum criteria of 32 kg/m^3 as specified by ASTM Standards, the actual quantity of foam required to attain the plastic density of 641 kg/m^3 within ±50 kg/m^3 of the design value was the same as the calculated quantity which again confirmed the stability of the mix.

Table 4.12 Optimized parameters and corresponding response goals

Foaming agent	SC %	FGP kPa	Foam Output Rate m^3/hr	Initial Foam Density kg/m^3	Foam Capacity m^3	Solution Drained in 5 minutes %	Foam Density Ratio in 5 minutes
SLS	2	117	0.274	25	0.04	11	0.88
SLES	2	117	0.175	38	0.03	12	0.86
SULF	2	117	0.24	21	0.05	13	0.87
CDA	5	122	0.09	70	0.014	0	1

Table 4.13 Comparison of test results with ASTM Specifications

SI No	Surfactant	SC (%)	FGP kPa	Foam density kg/m^3	Fresh density kg/m^3	Dry density kg/m^3	Compressive strength, MPa	Water absorption % by volume	Act/cal foam ratio
1	SLS	2	117	25	642	516	2.01	15	1
2	SLES	2	117	38	674	522	2.32	25	1
3	SULF	2	117	21	681	535	2.8	18	1
4	CDA	5	122	70	676	527	1.4	22	1
ASTM C 869-91 Requirements				32 to 70	641±48	487±40	1.40 (min)	25% (max)	1

From the Table 4.12 and Table 4.13 it is observed that among the four surfactants used, Sodium lauryl sulfate had higher foam output rate, better foam capacity and lower water absorption when used in foam cement paste. Among the ionic surfactants, Sodium lauryl ether sulfate had better foam density and good strength when used in foam cement paste but the water absorption of foam cement paste is relatively higher. Sulfanol is not a locally available chemical and hence its cost is high. Though the nonionic surfactant Cocodiethanolamide has good stability, its output rate is very low due to high viscous nature of solution. Also its performance in foam cement paste is poor in terms of strength and water absorption. Hence the further studies are carried out with more easily available and better performing surfactants Sodium lauryl sulfate and Sodium lauryl ether sulfate.

4.12 SUMMARY

The surfactants which could be used for foam concrete production have been identified. The essential characteristics of foam which are to be evaluated to qualify a surfactant as a potential foaming agent are sorted out. Also the relative characteristics of the foam produced with four different synthetic surfactants have been assessed through a systematic experiment design based on Response surface methodology. The possible response surface models have been developed for predicting the variation of foam characteristics as the function of foam production parameters. The validity of empirical models developed is verified experimentally. Optimization has been carried out to determine the optimal level of foam production parameters that could be used to produce the foam with desirable characteristics. The foam thus produced has been tested for suitability for making preformed foam concrete as per ASTM recommendations. From the four surfactants, Sodium lauryl sulfate and Sodium lauryl ether sulfate have been selected based on its relatively better performance for further studies on foam concrete.

CHAPTER 5

FRESH AND HARDENED PROPERTIES OF FOAM CONCRETE

5.1 GENERAL

The chapter 4 comprised of studies on evaluation of relative performance of foam produced with four commercially available synthetic surfactants viz; Sodium lauryl sulfate, Sodium lauryl ether sulfate, Sulfanol (ionic surfactants) and Cocodiethanolamide (non-ionic surfactant). Their suitability in foamed concrete have been assessed with foamed cement paste as per ASTM C 796-97. Out of these, Sodium lauryl sulfate and Sodium lauryl ether sulfate yielded relatively better foam capacity, higher foam output rate than other surfactants and lower drainage among ionic surfactants. These were also observed to possess relatively better strength and lower water absorption among the four surfactants when used in foamed cement paste. Having identified their potential as foaming agents, as a next step, the relative workability and strength behavior of foam concrete produced using these two surfactants are discussed in this chapter.

This chapter deals with the experimental investigation conducted to ascertain the influence of foam volume on the fresh and hardened state properties of foam concrete. The water-solids ratio required to produce stable and workable foam concrete of desired density was determined. The relationship between fresh density and dry density was established and the influence of variation in density of foam concrete on its mechanical properties namely compressive strength, split tensile strength and flexural strength of foam concrete were discussed.

5.2 MATERIALS AND METHODOLOGY

5.2.1 Materials

Foam was produced by aerating Sodium lauryl sulfate and Sodium lauryl ether sulfate to a density of around 25 kg/m^3 and 38 kg/m^3 respectively using the foam generator. The optimal values of foam generation pressure and surfactant concentration, 118 kPa and 2% respectively arrived through optimization studies described in Chapter 4 were adopted. Ordinary Portland cement of 53 grade conforming to IS 12269-1987 was used. For a given density Nambiar and Ramamurthy (2006a) reported that the compressive strength increased with an increase in fineness of sand and sand passing through 300 µm sieve yielded maximum strength. Hence the river sand was pulverized and sand finer than 300µm (Specific gravity 2.52) was used. From the grain size distribution shown in Fig 5.1 it was observed that 100% of the sand passes through 300µm sieve. A commercially available polycarboxylate ether based superplasticiser was used for studying the influence of reduction in water content. A cement - sand ratio of 1:1 by weight was adopted throughout the study.

5.2.2 Mixture Composition and Mixing

Three design densities of foam concrete viz., 1000, 1250 and 1500 kg/m^3 and control cement paste of density 641 kg/m^3 were designed. ASTM C 796-97 has prescribed the following equation 5.1 to calculate the foam volume for a cement paste of design density 641 kg/m^3 and w/c ratio of 0.58.

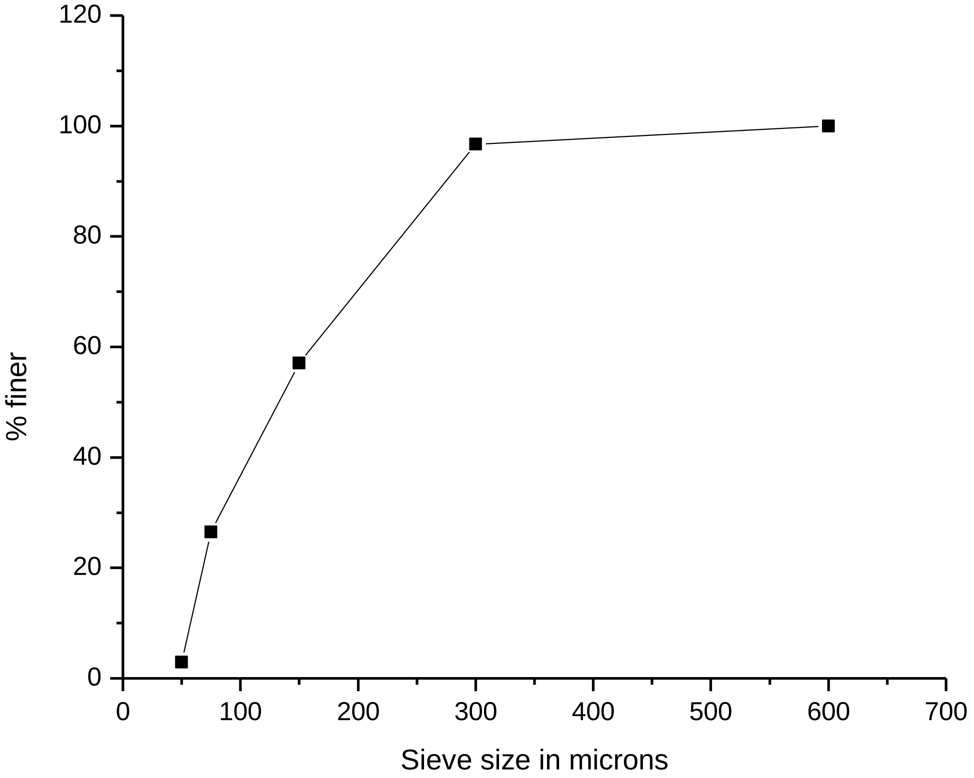

Fig 5.1 Grain size distribution of sand used

Wet density, 641 kg/m^3 = $(W_{tw} + Wc) / [(W_{tw}/1000) + (Wc / (3.15*1000)) + Va)]$ (5.1)

Where W_{tw} = weight of total water including the water present in the foam;

Wc = weight of cement; Va = Volume of air

After solving for the volume of air, the volume of foam (V_f) can be determined from the equation 5.2, arrived at by treating the diluted foam chemical as water;

$V_f = Va + (W_f /1000)$ (5.2)

Where $W_f = W_{uf} * V_f$ (5.3)

W_f = weight of foam ; Wuf = unit weight of foam;

As cement mortar was used in the present study for making foam concrete, the equation 5.1 was modified by including the sand component (Ws is the weight of sand) to calculate the foam volume for mortar of known design density, water-cement (w/c) ratio and cement-sand (c/s)ratio.

$Wc + Wtw + Ws = 1250$ (5.4)

$Wc+ 0.8\, Wc + Wc = 1250$ (5.5)

$Wc = 446$ kg / m^3

Having arrived at the cement content, the foam volume for mortar was determined in a way similar to that described for cement paste as follows;

Wet density, 1250 kg /m^3 = $(W_{tw} + Wc +Ws) / [(W_{tw}/1000) + (Wc /(3.15*1000)) + (Ws / (2.52*1000)) + Va)$ (5.6)

The details of mix proportions determined for various densities of foamed concrete are presented in Table 5.1. Hand mixing was done for all the mixes to maintain uniformity. The mixing sequence consisted of first preparation of homogenous base mix of cement and sand slurry, followed by the addition of calculated weight of foam to the base mix. The mixing was done till the foam was uniformly blended into the slurry.

Table 5.1 Mix proportions for Portland cement and cement-sand foam concrete mixes

		Foam concrete			Mortar		
					Base mix-1	Base mix-2	Base mix-3
Fresh density (kg/m^3)		1000	1250	1500	1813	1832	1884
Cement (kg/m^3)		344.8	438.6	545.4	632.4	646.9	687.4
Fine aggregate (pulverized sand) (kg/m^3)		344.8	438.6	545.4	632.4	646.9	687.4
Air volume equation V_a		$(0.683 W_c + 0.6032 W_s) / 1000$	$(0.603 W_c + 0.504 W_s - 0.25 W_{tw}) / 1250$	$(0.524 W_c + 0.405 W_s - 0.5 W_{tw}) / 1500$	NA	NA	NA
w/s	SLS	0.45	0.425	0.375	0.434	0.416	0.37
	SLES	0.45	0.425	0.4			
Foam volume (%)	SLS	45.49	32.19	20.66	NA	NA	NA
	SLES	46.1	32.62	20.94			

Where Vf = volume of foam; Va = volume of air; Wtw = total weight of water; Wc = weight of cement; Ws = weight of sand.

5.2.3 Test Procedure

The ratio of measured fresh density to the design density is represented as the density ratio. The objective of this study is to identify the water-solids ratio required to produce stable and workable foam concrete of desired density. To achieve this, as a first step, the water-solids ratio required to produce foam concrete within ± 50 kg/m^3 of the design density was determined. This would be achieved within a narrow range of water-solids ratio. As a next step the workability of the mixes within the above range of water-solids ratio was evaluated through measurement of (i) spread in a flow table (ASTM C 230-98) and (ii) flow in modified marsh cone (Jones et al., 2003). The details of specimens used for different tests on hardened mechanical properties are presented in Table 5.2. Specimens were demoulded after 24 hours and moist curing was adopted. For measuring the dry density, the cubes after subjecting to 28 days moist-curing were placed in the oven at 110^{o}C till the cubes attained constant weight.

For strength tests as per ASTM C 796-97, the specimens were removed from curing after 25 days and placed in the oven at 60°C for 3 days prior to testing.

Table 5.2 Foam concrete specimens for tests on mechanical properties

Test	Specimen	Specimen dimension	No of specimens	Test code provision
Compressive strength	Cube	50 mm	6	ASTM C 495 (1991)
Split Tensile strength	Cylinder	100 mm dia, 200 mm high	6	ASTM C 496 (1996)
Flexural strength	Prism	40 X 40 X 160 mm	6	(BS 1881: Part 118:1983)
Modulus of Elasticity	Cylinder	150 mm dia, 300 mm high	3	ASTM C 469 (1994)

5.3 FRESH STATE PROPERTIES OF FOAM CONCRETE

The important fresh state properties of foam concrete are flowability and self-compactability. Foam concrete is normally designed for a particular design density. First, the foam volume required to achieve the design density was calculated and then the minimum water solids ratio required to achieve the design density was determined. The water demand was determined by gradually increasing the water-solids ratio to the point where design fresh density is achieved with no signs of segregation or bleeding. The range of water-solids ratio (w-s) to be adopted for study has been determined based on trial and error. Hence in this case the water solids ratio is decided based on the stability of the mix unlike the conventional (normal weight) concrete wherein the water solids ratio is decided based on strength. This section actually deals with the study of influence of water-solids ratio on the stability of the foam concrete with a range of foam volume (18 to 46%).

5.3.1 Water-solids Ratio Vs Density Ratio

The water-solids ratio required to produce a mix of desired design density was determined for mixes with different foam volumes. Superplasticiser (sp) was used to study whether its use can result in a consistent, stable and workable mix along with a reduction in water content in the mix. Figs. 5.2 to 5.4 show that, for a given foam volume in the mix, the addition of superplasticiser reduces the water-solids ratio required to achieve the desired design density. For each of 18%, 32% and 46% foam volume used there exists corresponding optimal superplasticiser dosage viz., 0.3%, 0.2% and 0.1%, which result in a mix of desired density (± 50 kg/m^3) along with a reduction in water-solids ratio. When the dosage of superplasticiser was lower than the optimum, appreciable reduction in water-solids ratio was not observed, while with a dosage higher than the optimum, either the design density was not achieved or bleeding/segregation was observed which can be attributed to collapse of foam in the mix. Having identified the optimal superplasticiser dosage, as a next step, the variation in density ratio with water-solids ratio for different foam volumes at the optimum dosages of superplasticiser and without superplasticiser is presented in Fig 5.5. As the foam volume increases, the mix becomes unstable at higher dosages of superplasticiser used and hence the optimum dosage of superplasticiser and the amount of reduction in water-solids ratio caused by the addition of superplasticiser reduces with an increase in foam volume. At optimum dosages of superplasticiser, the reduction in water demand achieved for surfactant Sodium lauryl sulfate and Sodium lauryl ether sulfate are 13.3%, 5.9%, 2.7% and 19%, 11.8% and 5% respectively for foam volumes 18% 32% and 46% in the mix. The reduction in water demand achieved by the addition of superplasticiser is relatively higher for surfactant Sodium lauryl ether sulfate. For foam concrete mixes with higher foam volume (32 to 46%) with surfactant Sodium lauryl ether sulfate are resistant to segregation and bleeding when certain higher dosages of superplasticiser (0.4% for foam volume 32% and 0.3% for foam volume 46%) are adopted. The corresponding mixes produced with surfactant Sodium lauryl sulfate segregated which can be observed from the Figs. 5.3 and 5.4 through a shift of density curve below the stable zone. This indicates that the surfactant Sodium lauryl ether sulfate is relatively more compatible with the superplasticiser used and which would have resulted in greater reduction in water demand for superplasticised mixes produced with Sodium lauryl ether sulfate. Fig 5.5 shows that as the foam volume increases, the water-solids ratio required to achieve the desired design density (density ratio of 1) increases indicating that the workability of foam concrete is significantly influenced by the foam content. The behaviour of foam concrete at foam volume of 18% is similar for both the surfactants. But at higher foam volume (beyond 32%), the behaviour is different between foam concrete with the two surfactants. This is because the degree of compatability of the superplasticiser with the surfactant is observed only when higher foam volume is used.

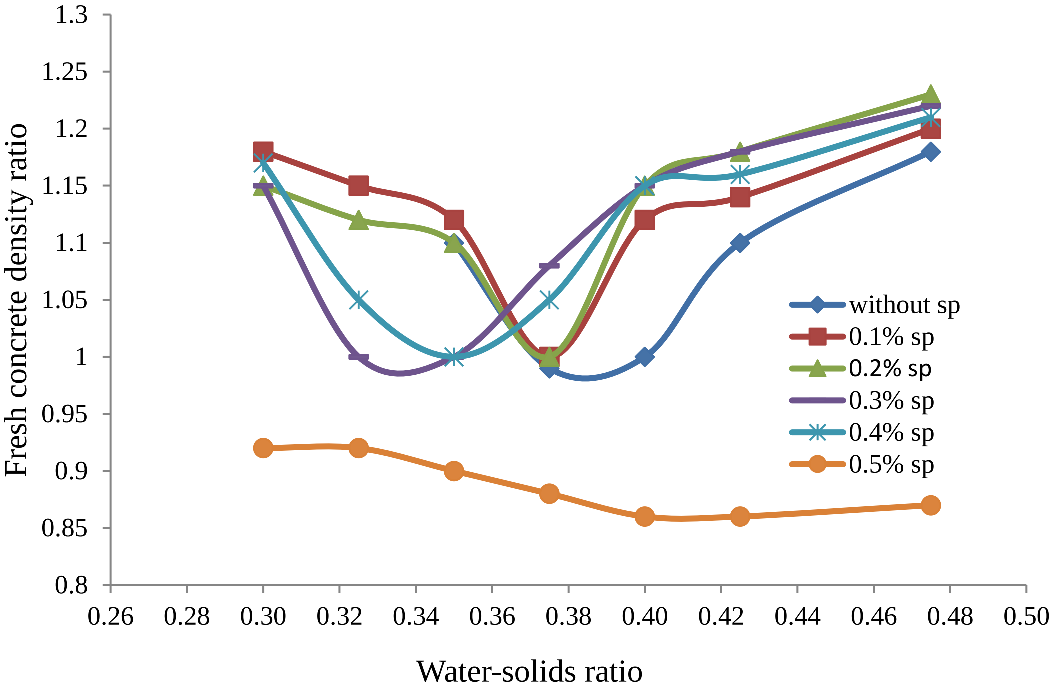

(a) Sodium lauryl sulfate

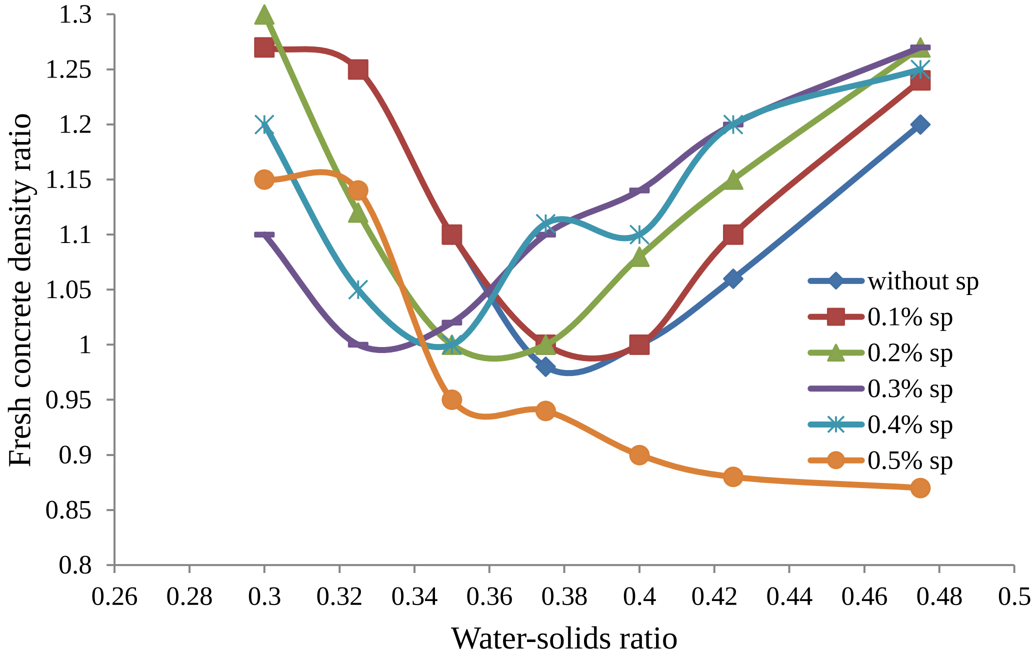

(b) Sodium lauryl ether sulfate

Fig. 5.2 Variation of density ratio with water-solids ratio for foam volume 18%

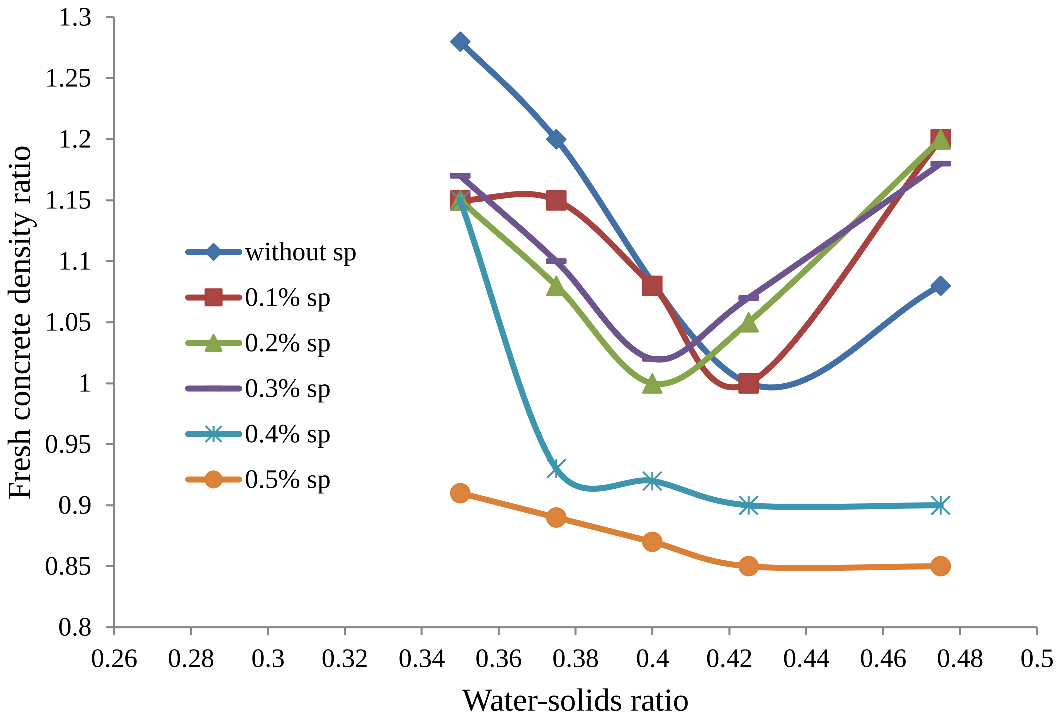

(a) Sodium lauryl sulfate

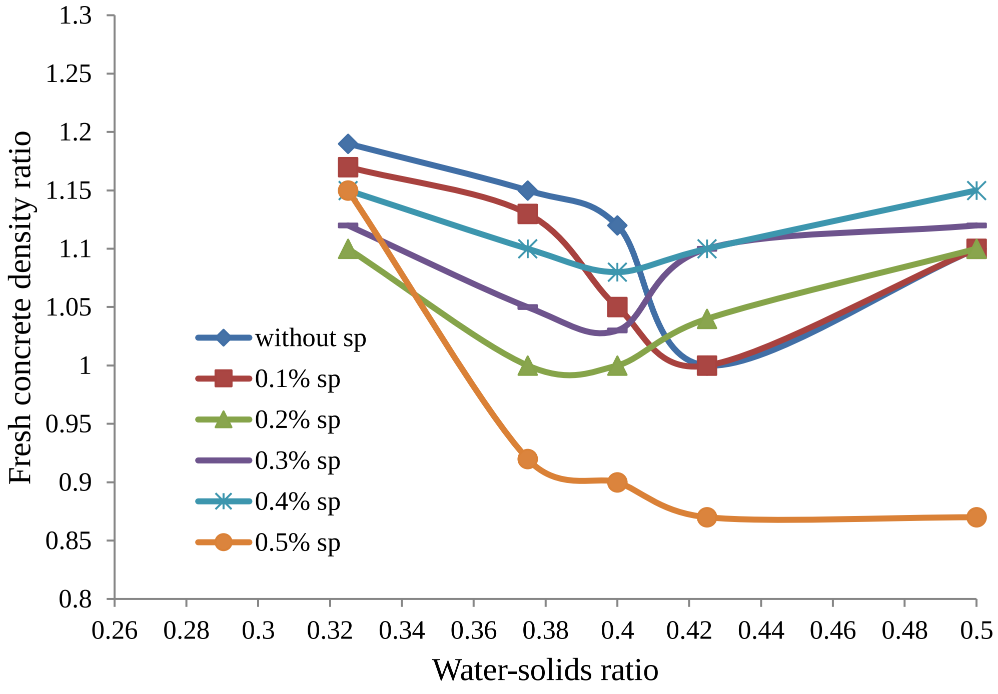

(b) Sodium lauryl ether sulfate

Fig. 5.3 Variation of density ratio with water-solids ratio for foam volume 32%

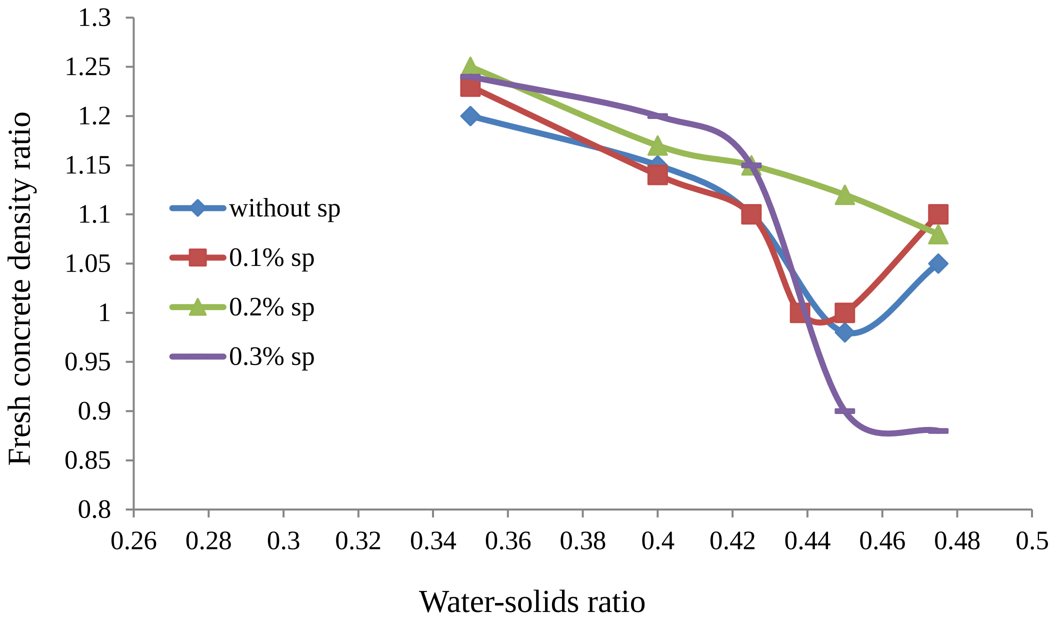

(a) Sodium lauryl sulfate

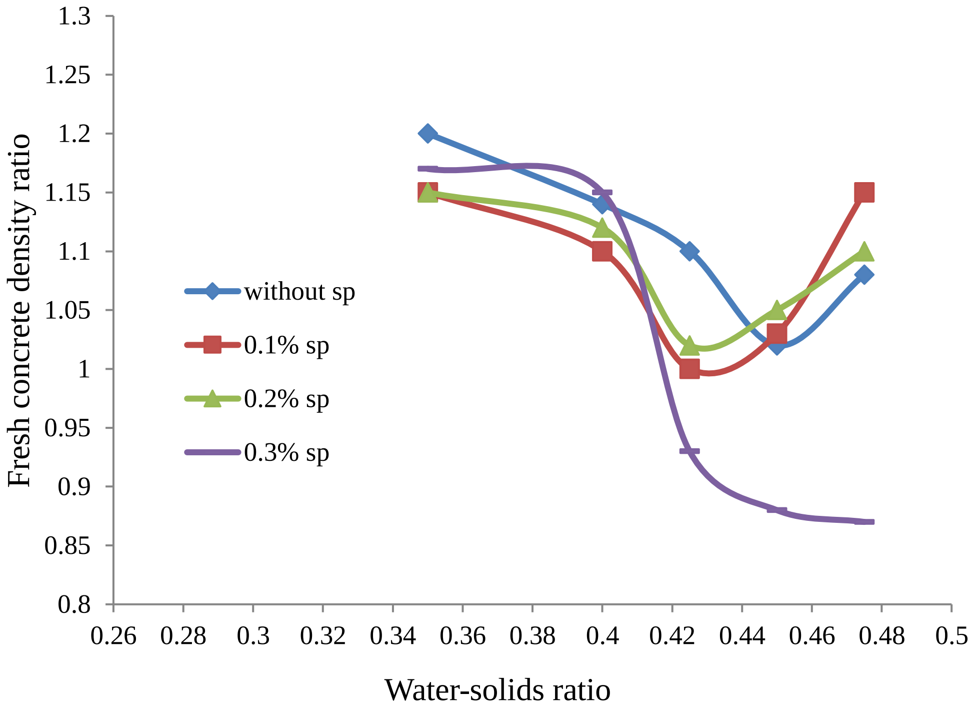

(b) Sodium lauryl ether sulfate

Fig. 5.4 Variation of density ratio with water-solids ratio for foam volume 46%

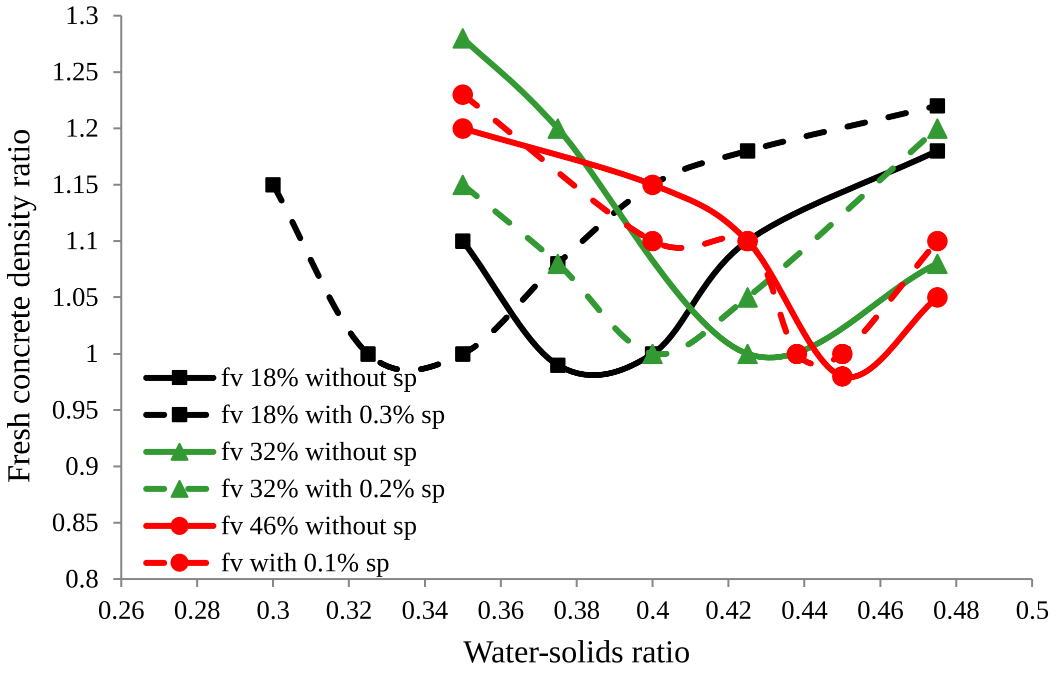

(a) Sodium lauryl sulfate

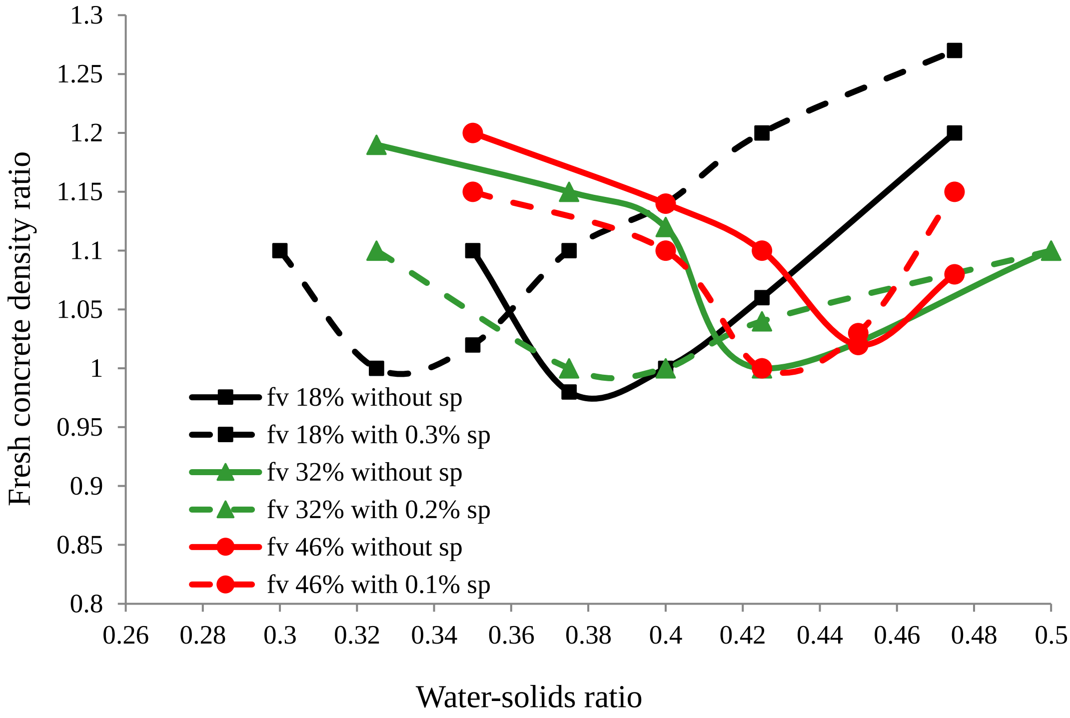

(b) Sodium lauryl ether sulfate

Fig. 5.5 Variation of density ratio with water-solids ratio at optimum dosages of superplasticiser

5.3.2 Consistency of Foam Concrete Mixes

As the foam is added to wet concrete mix, the consistency of the mix is very important to achieve the desired design density. Having identified the narrow range of water solids ratio and optimum superplasticiser dosage required to produce stable mix, as a next step the workability of these mixes with the range of water solids ratio as mentioned in Table 5.3 are to be studied. For this purpose two workability measurement techniques viz., spreadability and marsh cone flow were evaluated.

5.3.2.1 Flow spread test

The spreadability was measured using ASTM standard flow cone (ASTM C 230-98) without any shocking motion of the flow table as it would affect the entrained air bubbles. After filling the cone with foam concrete, the cone was lifted and the spread of concrete was measured at four locations for each trial and the average spread was expressed as a percentage of base diameter of the cone (Fig 5.6). For the foam concrete produced with both the surfactants Fig 5.7 shows that for a constant water-solids ratio, the spread reduces with an increase in foam volume. Alternatively to achieve a particular workability, an increase in foam volume in the mix demands a higher water-solids ratio. Hence the foam volume has considerable influence on the flow behaviour of foam concrete. The reduction in consistency of the mix in the presence of foam has been attributed to the reduced self-weight and greater cohesion of foam bubbles resulting from higher air content (Nambiar and Ramamurthy, 2008a). The spreadability requirement for mixes without superplasticiser to attain the desired design density ranges between 47 and 88% for Sodium lauryl sulfate and between 44 and 75% for Sodium lauryl ether sulfate. The addition of optimum dosages of superplasticiser has resulted in a reduction in water-solids ratio required for achieving the desired density. It also has resulted in higher workability requirement with spreadability in the range of 98 to 138% and 90 to 125% for surfactants Sodium lauryl sulfate and Sodium lauryl ether sulfate respectively. Hence the workability requirement to produce stable mixes with superplasticiser is relatively higher as compared to mixes without superplasticiser. The mixes with above mentioned spread % are observed to be workable as there was no difficulty in handling of the concrete. The variation of spread % with foam volume and water-solids ratio is similar for both the surfactants.

Table 5.3 Fresh Density ratio and water-solids ratio requirement for stable mixes

Fresh density, kg/m^3		Corresponding fresh density ratio range	Range of water-solids ratio for stable mixes			
Design fresh density	Permitted range as per ASTM C 869-91		Without superplasticiser		With superplasticiser	
			SLS	SLES	SLS	SLES
1000	1000 ± 50	0.95 to 1.05	0.435 to 0.47	0.44 to 0.47	0.435 to 0.46	0.42 to 0.46
1250	1250 ±50	0.96 to 1.04	0.41 to 0.455	0.412 to 0.46	0.382 to 0.42	0.35 to 0.42
1500	1500 ± 50	0.97 to 1.03	0.36 to 0.415	0.36 to 0.42	0.317 to 0.36	0.315 to 0.36

Fig 5.6 Flow cone test

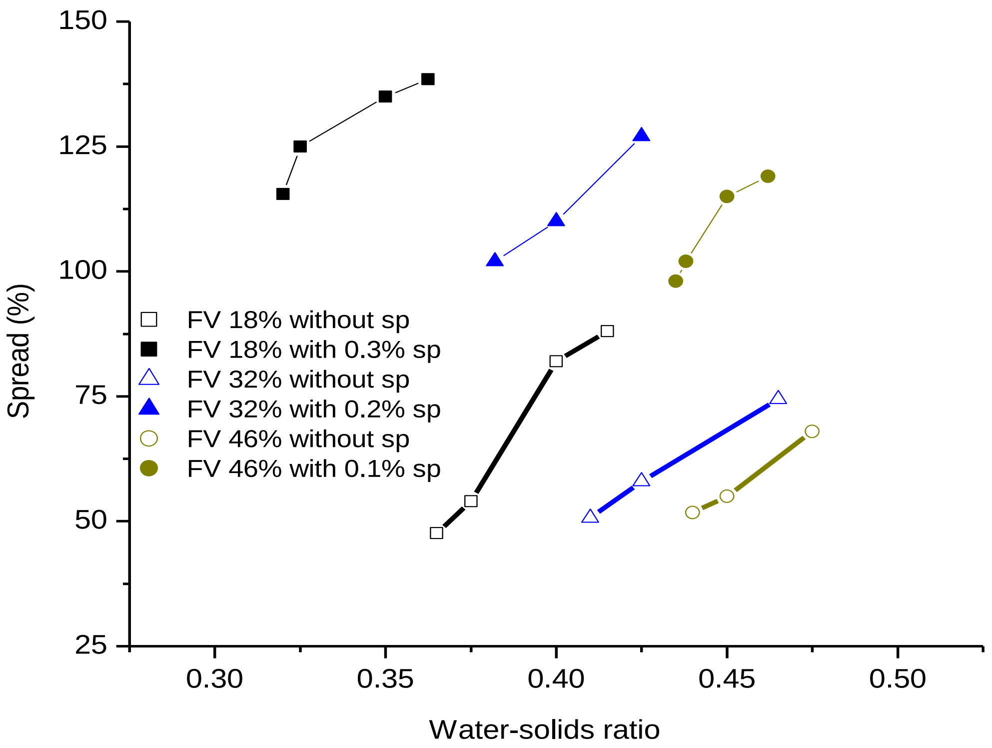

(a) Sodium lauryl sulfate

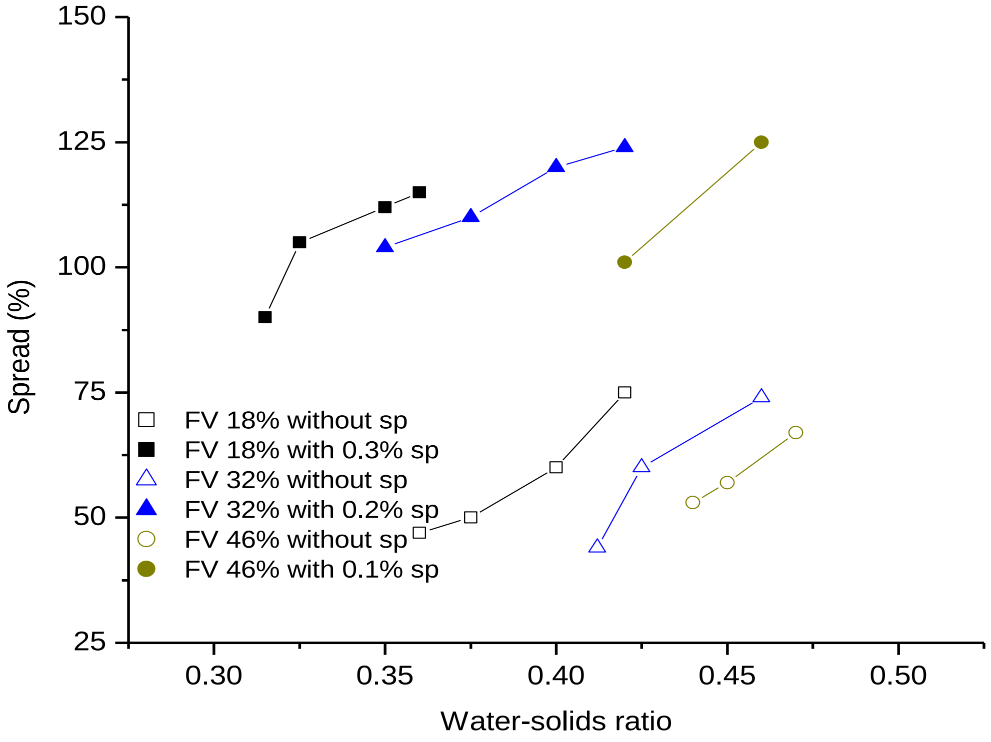

(b) Sodium lauryl ether sulfate

Fig 5.7 Effect of water-solids ratio on spread (%) of foam concrete in stable density ratio range

5.3.2.2 Marsh cone flow test

The flowability, which depends on the fluidity of the mix, was determined using the Marsh cone. This test was modified by Jones et al. (2003) in terms of orifice diameter (increased from 8 mm to 12.5 mm) and volume of efflux (1 litre instead of 200 ml) to take into account of the fine aggregate particles. The cone was filled with 1.5 litre of sample. The time taken for 1.0 litre of foam concrete to flow through the constricted orifice was measured (Fig 5.8). The Marsh cone efflux time is an indication of the plastic viscosity, i.e., as the fluidity of the mix increases the flow time decrease. Fig 5.9 shows the variation of flowability of stable foam concrete mixes having density ratio range as in Table 5.3. For a constant water-solids ratio, the flow time increases with an increase in foam volume. The variation of flow time with foam volume and water-solids ratio is similar for both the surfactants. The flow time requirement to produce stable mix varies from 9 to 20 seconds. However the addition of superplasticiser reduces the water-solids ratio required to produce a workable mix. It also results in narrowing the flow time variation i.e., between 9 and 12 seconds for a range of water-solids ratio. As expected, for the range of design plastic densities considered, greater spread values (hence lower yield stresses) corresponds to shorter flow times (hence reduced plastic viscosity), thereby indicating a relationship between these two properties of foam concrete (Fig 5.10).

5.3.2.3 Water–solids ratio requirement for stable and workable mix

The water-solids ratios required to achieve a stable (corresponding to density ratio of 1) and workable mix for a range of design densities (as obtained from Figs 5.2 to 5.4) and the corresponding foam volume are presented in Fig 5.11. Fig 5.11 would serve as a typical design aid to arrive at the foam volume and water-solids ratio required to achieve a foam concrete of desired density and consistence. Fig 5.11 indicates that the water-solids ratio requirement reduces marginally with an increase in density. Also the water-solids ratio requirement (for mixes without superplasticiser) is observed to be almost similar for both the surfactants till the density of 1250 kg/m^3. While the water-solids ratio requirement of foam concrete produced with surfactant Sodium lauryl ether sulfate is higher above this density.

Fig 5.8 Modified Marsh cone test

5.4 HARDENED PROPERTIES OF FOAM CONCRETE

The variation of hardened density with fresh density was studied first and then the volumetric stability was assessed in the hardened state. This section also reports the results of a systematic study on the influence of variation in density of foam concrete on its mechanical properties namely compressive strength, split tensile strength and flexural strength of foam concrete.

5.4.1 Relationship between Fresh Density and Dry Density

Density of foam concrete is referred to both in the fresh and hardened states. For designing the mix, the fresh density is to be considered while designers choose foam concrete based on dry density and compressive strength. As both types of densities are useful at different stages there is a need to establish the relationship between them. Fig 5.12 exhibits a linear relationship between dry density and fresh density with an R^2 value of 0.996.

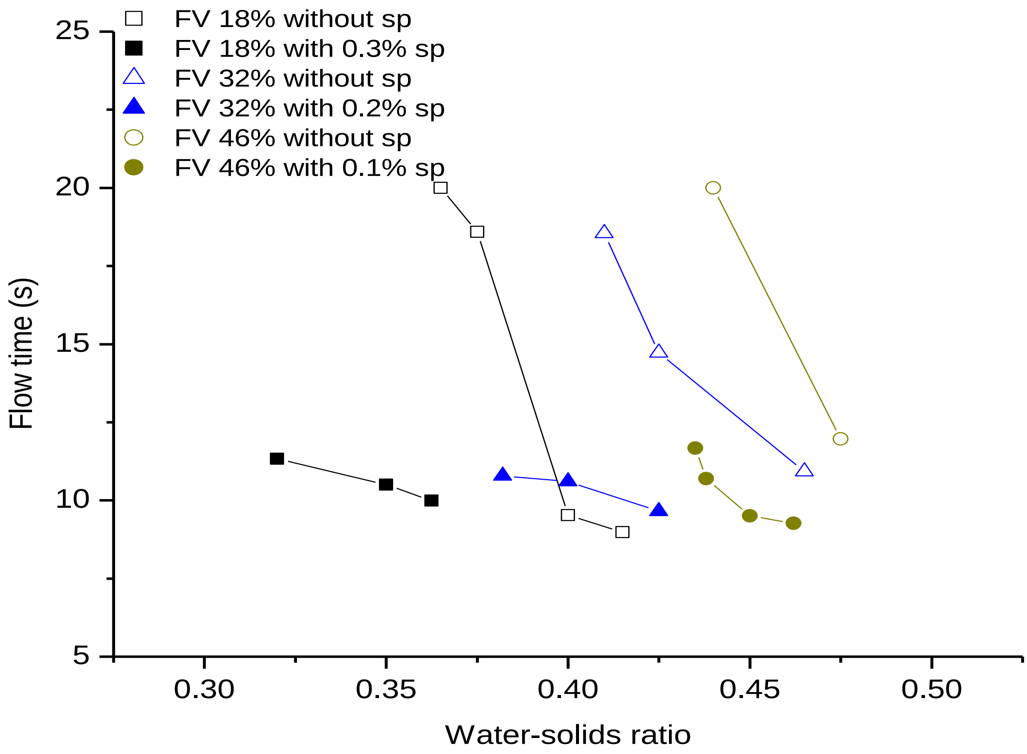

(a) Sodium lauryl sulfate

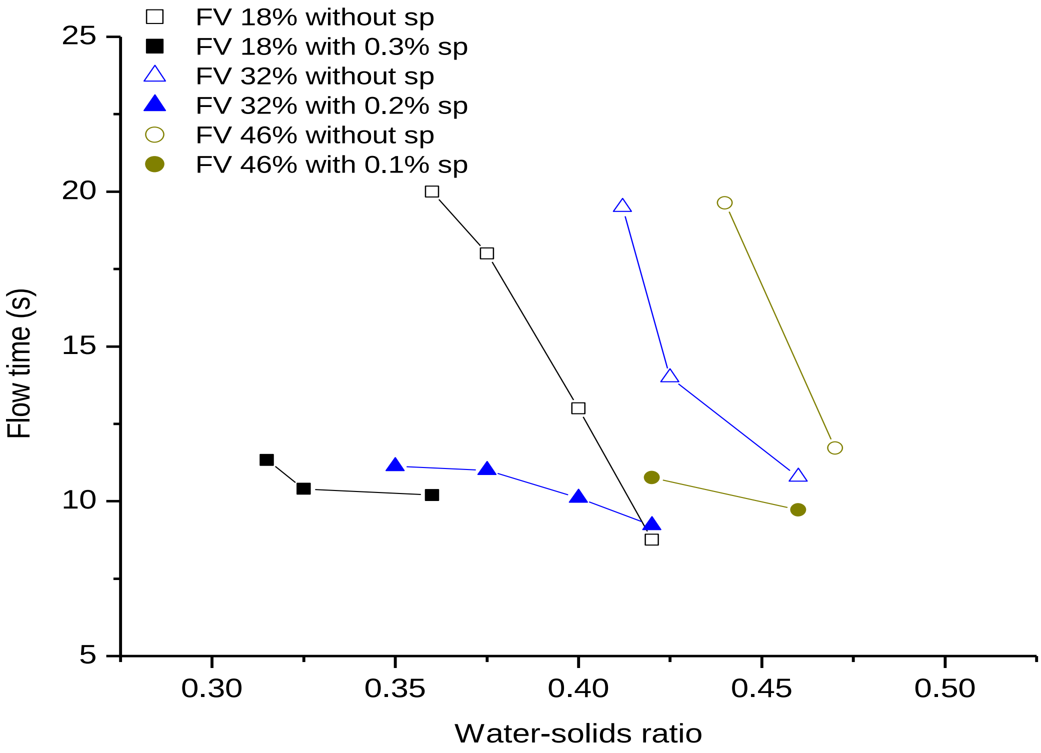

(b) Sodium lauryl ether sulfate

Fig. 5.9 Effect of water-solids ratio on flow time of foam concrete in stable density ratio range

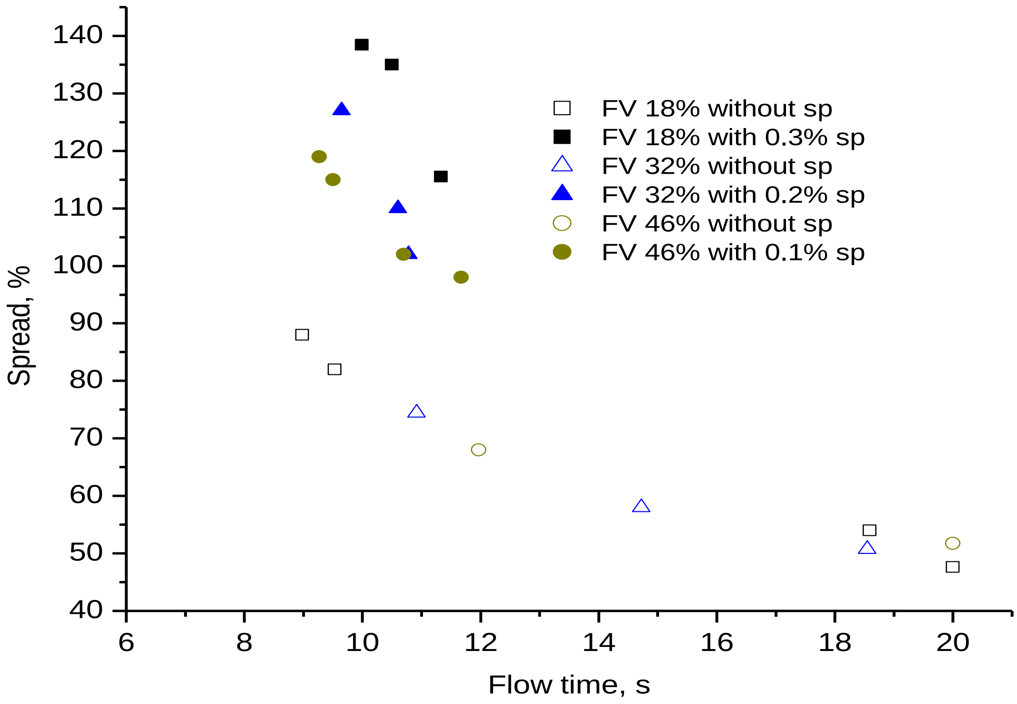

(a) Sodium lauryl sulfate

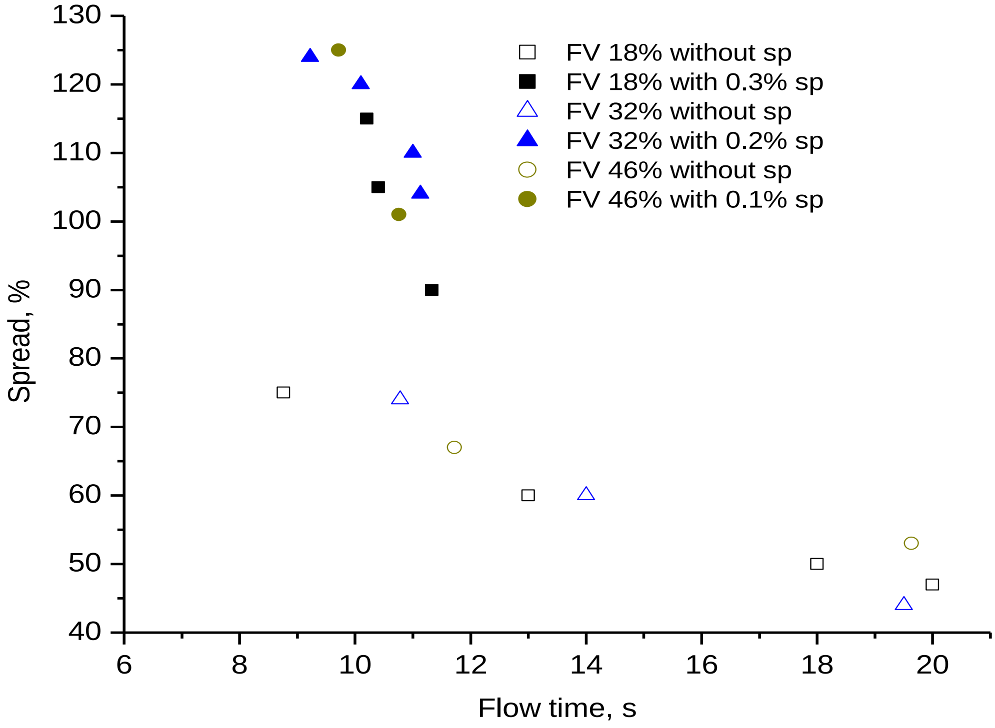

(b) Sodium lauryl ether sulfate

Fig. 5.10 Variation of flow time with spread

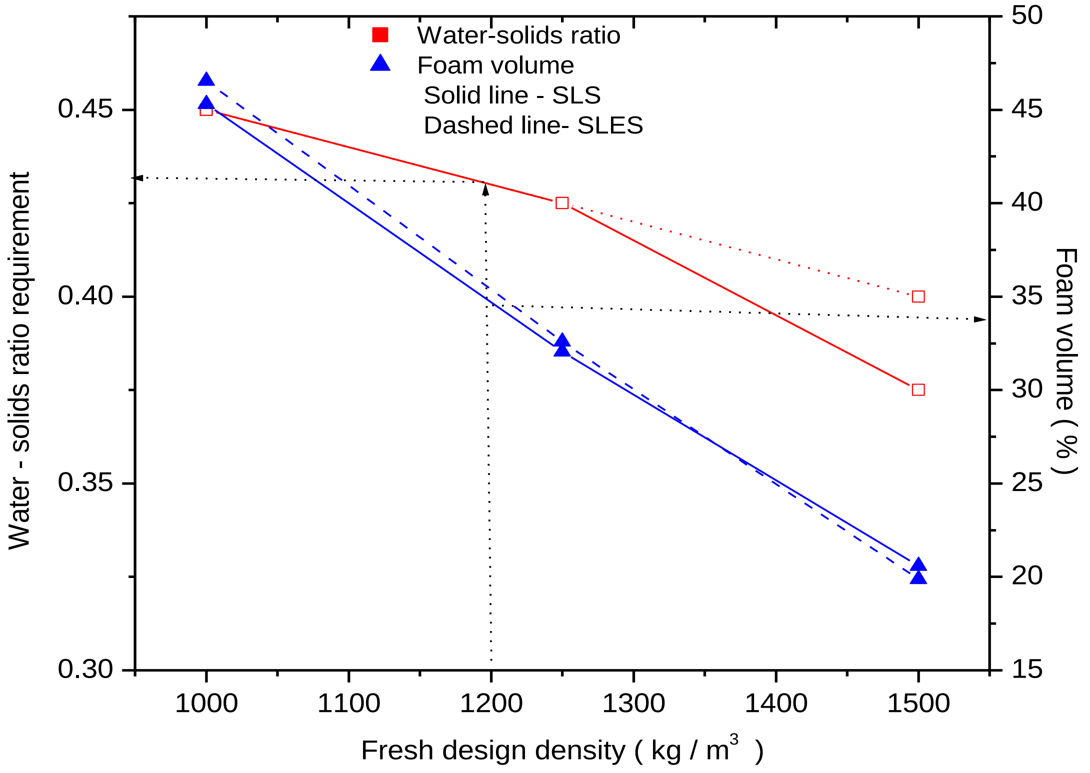

(a) Without superplasticiser

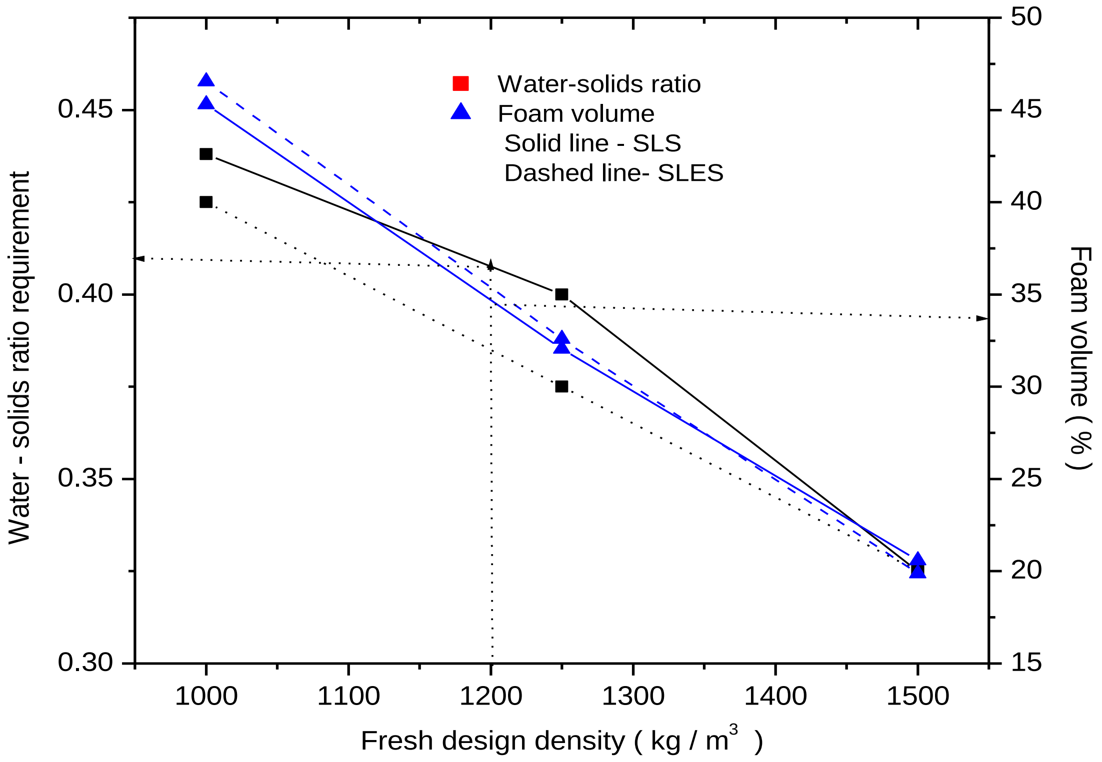

(b) With superplasticiser

Fig. 5.11 Consistency in terms of w-s ratio for different densities for two surfactants

5.4.2 Assessment of Volumetric Stability in Hardened State

The segregation of foam concrete can occur due to one of the following (i) improper mixing of foam, (ii) bleeding, (iii) mix constituents namely quantity of water and fines, (iv) use of incompatable or overdosage of chemical admixtures and (v) settling down of heavier particles at higher water-solids ratio. Hence the volumetric stability of the mix was assessed by the degree of uniformity in density across the depth of the hardened foam concrete (Jones and Mc Carthy, 2005c). Two specimens of 25mm thickness were cut from top and bottom of each of the three cylinders of size 150 x 300 mm at 28 days and were marked and kept in oven at 105 ^{o}C for 24 hrs and then their oven dry densities the mean value of slices taken at different depth of cylinder for all the densities of foam were determined. Table 5.4 shows that the dry density of cylinder did not vary more than ± 50 kg/m^3 compared to concrete used for the study. Hence, as long as the workability is maintained, an increase in foam volume does not result in breaking of bubbles at lower depths even though the foam density was lower and thus the mixes were observed to be stable at hardened state.

5.4.3 Compressive Strength and Modulus of Elasticity

The effect of dry density on 28 day compressive strength (fc) and modulus of elasticity (E) under compression of foam concrete produced with surfactants Sodium lauryl sulfate and Sodium lauryl ether sulfate for a cement-sand ratio of 1 is presented in Table 5.5. The water-solids ratio corresponding to density ratio of one from Fig 5.11 was adopted for mixes and the workability was obtained in the range of 50 to 60% and 100 to 125% for mixes without and with superplasticiser respectively. The corresponding base mixes which are defined as mortar mixes obtained by combining the cement and sand with water (by eliminating the foam in the mix) were also cast for a comparison (as it is not logical to compare foam concrete with normal weight concrete). A comparison of strengths of foam concrete with and without superplasticiser was also made. Though the addition of superplasticiser resulted in considerable reduction in water-solids ratio, it did not result in proportionate enhancement in strength (Fig 5.13). This behaviour indicate that even though the superplasticiser increases workability with lower water-solids ratio, the strength of foam concrete appear to be mainly influenced by the entrained air voids.

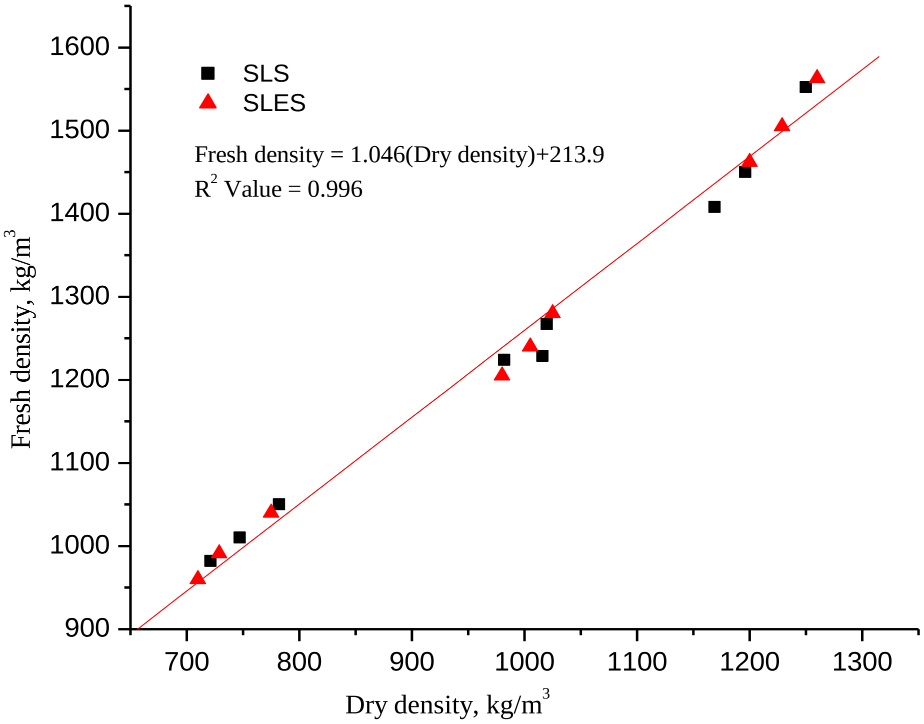

Fig. 5.12 Relation between fresh and dry density of foam concrete

Table 5.4 Assessment of volumetric stability in hardened state

Design dry density (kg/m^3)	Oven dry density of cylinder (kg/m^3)		Oven dry density of top slice (kg/m^3)		Oven dry density of bottom slice (kg/m^3)		Mean value (kg/m^3)	
	SLS	SLES	SLS	SLES	SLS	SLES	SLS	SLES
790-870	850	820	820	802	905	855	862	828
	890	857	844	802	951	868	898	835
	860	840	870	850	900	870	885	860
942-1022	990	980	970	922	1020	990	995	956
	1010	1005	975	987	1030	1030	1002	1008
	1024	1031	1000	1000	1052	1068	1026	1034
1160-1240	1180	1200	1127	1180	1218	1240	1173	1210
	1208	1229	1200	1160	1201	1230	1200	1195
	1220	1260	1195	1220	1263	1280	1229	1250

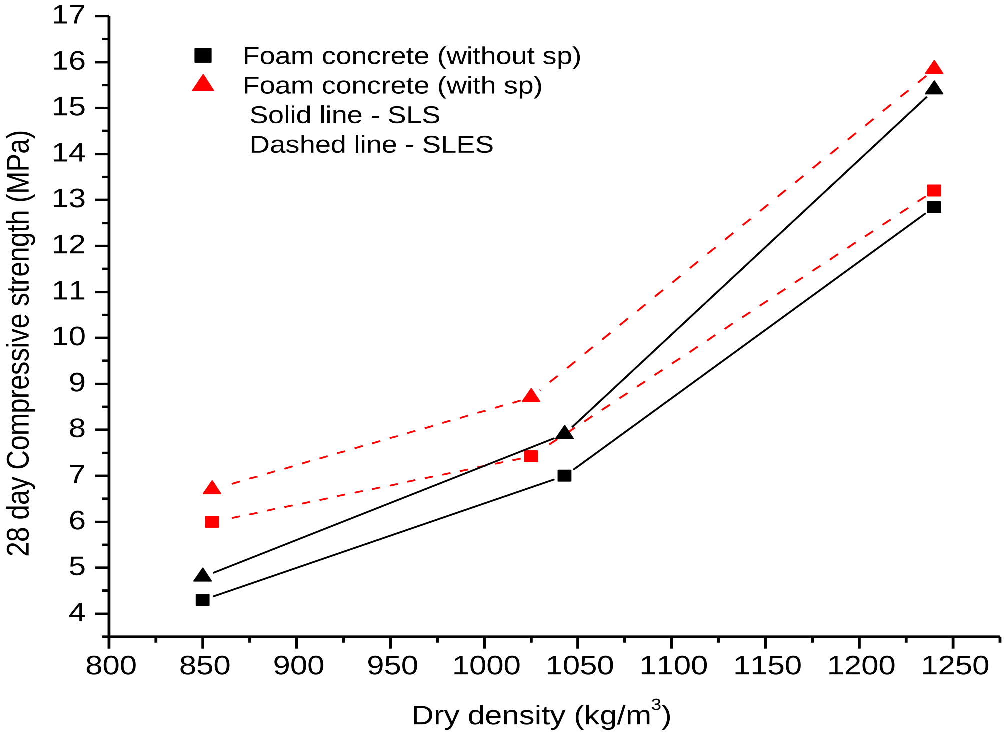

Fig. 5.13 Variation of strength with dry density

Similar observations with respect to water-solids ratio on strength of aerated concrete was observed by Narayanan and Ramamurthy (2000). From Fig 5.13 it is observed that 12 to 20% enhancement in strength is achieved for dry density ranging from 850 to 1240 kg/m^3 because of reduction in water demand obtained by usage of optimum dosages of superplasticiser for the foam concrete produced with both the surfactants. The compressive strength values achieved are observed to be comparable to those results reported in literature (20% higher and 10% lower than the values reported for corresponding mixes by Nambiar and Ramamurthy (2006a) and Jones (2001) respectively.

The static modulus of elasticity of foam concrete was determined under compression and the relationship with corresponding 28-day compressive strength was determined. Though the modulus of elasticity of foam concrete is lower than the base mix with values typically ranging from 2.5 to 7.25 kN/mm^2 for dry densities between 850 to 1215 kg/m^3, the specific strength of foam concrete is higher.

Table 5.5 Splitting Tensile strength (f_t), Static Modulus of Elasticity (E) and Flexural strength of foam concrete

Type of mix	Dry density kg/m^3	f_c N/mm^2		f_t N/mm^2		f_t / f_c		Flexural strength N/mm^2		E N/mm^2		E/ f_c	
		SLS	SLES	SLS	SLES	SLS	SLES	SLS	SLES	SLS	SLES	SLS	SLES
Foam concrete	800	4.3	6	0.29	0.33	0.067	0.055	0.3	0.35	2348.2	3047	546	508
	1042	7	7.42	0.5	0.6	0.07	0.081	0.911	1.2	3481.5	3500	580	472
	1215	12.5	13.2	1.096	1.13	0.088	0.086	1.316	1.721	7113.6	7250	647	549
Base mix-1	1430	22		1.2		0.054		2.35		8160		371	
Base mix-2	1464	22.9		1.28		0.056		2.4		8250		360	
Base mix-3	1517	24		1.34		0.06		2.58		8499.5		354	

SLS = Sodium lauryl sulfate ; SLES = Sodium lauryl ether sulfate

This indicates that the increase in modulus of elasticity with strength is proportional for foam concrete than that of the base mix. The specific strength is marginally higher for foam concrete produced with Sodium lauryl sulfate than those using Sodium lauryl ether sulfate as foaming agent (Table 5.5).

5.4.4 Split Cylinder and Flexural Tensile Strength

Split cylinder and flexural tensile strength tests were undertaken in accordance with ASTM C 496-96 and BS 1881. 28-day split cylinder and flexural tensile strength of foam concrete produced with surfactant Sodium lauryl ether sulfate is higher than those using Sodium lauryl sulfate as foaming agent. Tensile strength values of foam concrete of dry densities from 850 to 1215 kg/m^3 range between 6 to 9% (split cylinder) and 6 to 13% (flexural) of compressive strength. When compared to base mix, the flexural strength is around 11 to 65% of that of base mix (Table 5.5). The tensile/compressive strength ratio (ft/fc) ranges from 0.067 to 0.088 and 0.055 to 0.086 for dry densities from 850 to 1215 kg/m^3 for surfactants Sodium lauryl sulfate and Sodium lauryl ether sulfate respectively (Table 5.5). The lower tensile/compressive strength ratio (ft/fc) for foam concrete relates to the fact that it is a mortar made with very fine sand and hence the interlocking effect of sand particles with cement paste is lower which resulted in lesser strength.

5.5 SUMMARY

The relative workability and strength behavior of foam concrete produced with two synthetic surfactants have been studied. The water-solids ratio which would satisfy both the stability and consistence requirement of the mix for different design densities has been determined. The optimum superplasticizer dosage which would result in a stable mix along with a reduction in water demand is determined for different foam volumes. This optimum dosage of superplasticiser reduces with increase in foam volume as the mixes become unstable at higher dosages of superplasticiser. It is observed that the workability requirement to produce stable mixes with superplasticiser is relatively higher as compared to mixes without superplasticiser and as long as the workability is maintained, the mixes are observed to be stable at hardened state. Resistance to segregation and bleeding has been confirmed both visually in fresh state and by testing of hardened concrete for different foam volumes.

The influence of dry density on mechanical properties has been verified experimentally. Though the addition of superplasticiser results in considerable reduction in water-solids ratio, it did not result in proportionate enhancement in strength because the strength of foam concrete is mainly influenced by the entrained air voids. In order to understand this behaviour a detailed study of air-void parameters has been undertaken and presented in the next chapter.

CHAPTER 6

ANALYSIS OF AIR-VOID SYSTEM IN FOAM CONCRETE USING IMAGE ANALYSIS TECHNIQUE

6.1 GENERAL

The pore system of autoclaved aerated concrete has been classified into micro-capillaries (< 50 nm) and macro capillaries (> 50 nm to 50 µm) and artificial air pores (> 50 µm) (Tada and Nakano, 1983). In a similar fashion the structure of foam concrete consists of water filled voids (gel and capillary pores) as well as air voids (air entrained and entrapped pores) (Visagie and Kearsely, 2002). The influence of shape and orientation of the pores on the mechanical properties of aerated concrete have been studied by Cabrillac et al., (2000, 2006). Narayanan and Ramamurthy (2000) investigated the paste–void interface of aerated concrete in relation to paste aggregate interface in normal concrete and observed that larger pores in aerated concrete can be treated as aggregates of zero density. Several researchers made attempts to characterize the spacing of air-voids in air-entrained concrete by developing spacing equations (Philleo, 1983; Attiogbe, 1993). Some of these equations estimated the proximity of the paste to voids and others estimated the proximity of voids to one another (Snyder, 1998).

Usually techniques such as mercury intrusion porosimetry or Brunauer Emmett Teller (BET) surface area are used to characterize the pore structure. The major limitation of such techniques is that interpretation of results involves approximate assumption about pore shape. Direct observation of pore structure by capturing images through optical and electron microscopes provide the pore shape directly (Lange 1994). Computer based image processing has been successfully used for pore characterization of cement based materials (Chatterji and Gudmundsson, 1977; Lange et al., 1994; Petrov and Schlegel, 1994; Pleau et al., 2001; Visagie and Kearsely, 2002). The key step in image processing is to select features of interest from background by a large number of iterations. The quantitative evaluation of the air void system in terms of size distribution and shape of voids can yield valuable input for establishing correlation to mechanical and durability properties. Mathematical distribution function like modified Rossin-Rammler distribution has been used to characterize the size distribution of the powders and cementitious materials (Ramakrishnan, 2000). It has been reported by Laundess et al., (2009) and Visagie and Kearsely (2002) that the air void size and bubble size distribution of foam can be fitted to modified Rosin-Rammler distribution function. This chapter discusses the investigations made to characterize the void system of foam concrete of three different design densities viz., 1000, 1250 and 1500 kg/m^3 produced with two synthetic surfactants by processing and analyzing the images of the prepared surfaces of specimens captured by an optical microscope in terms of volume, size distribution, shape and spacing.

6.2 EXPERIMENTAL INVESTIGATIONS

6.2.1 Specimen and Surface Preparation

The materials and their properties and mix proportioning have been described in the earlier section 5.2. Foam concrete mixes of fresh densities viz., 1000, 1250 and 1500 kg/m^3 were made by varying foam volume from 46% to 18%. For each density, 4 cubes of size 50 mm were cast and moist-cured for 28 days. The cubes were then sliced using a diamond rotary saw into 25 mm thickness, parallel and perpendicular to the cast surface and at different depths of specimen. Such slicing yielded the following 6 specimens (cut surfaces) of size 50 x 50 x 25 mm, for each mix, as shown in Table 6.1.

The cut surface of each specimen was very carefully lapped by abrasive paper of fineness grade 1000 using a polishing machine to obtain a plane surface on which the boundaries of the air-voids and matrix are sharp and easily discernible. Then the specimens were cleaned with compressed air to remove all dust and then dried in the oven at 50^{o}C for 3 days. Two coats of black ink were applied on the surface using permanent marker pen and was allowed to dry. The white powder was spread over the surface and worked into the air voids by means of finger tip. Finally the excess powder was removed with the edge of razor blade and with a lightly oiled finger tip. All voids thus appear white and remaining area is black in colour and is ready for measurement.

Table 6.1 Details of preparation of specimens for image analysis

Cut surface	Cube number	Method of slicing
1	1	Cut in the middle parallel to cast surface
2	2	Cut in the middle perpendicular to cast surface
3 and 4	3	25 mm slice is taken at depth of 12.5 mm parallel to cast surface
5 and 6	4	25 mm slice is taken at a depth of 12.5 mm perpendicular to the cast surface.

6.2.2 Image Analysis Test Setup

As the objective was to investigate the structure of macropores of foam concrete, voids with diameter greater than 50 µm were analysed using an optical microscope and a computer with image analysis software (Image J, 2006). A magnification of 20 X was selected with a pixel representing 12 microns which was determined through calibration. The optical microscope was adjusted until the prepared surface was clearly seen on the computer monitor. A total of 36 images were captured at random locations from the six prepared surfaces for each foam concrete mix. Each image was digitized, converted into binary form and few morphological operations were carried out to refine the form of objects. Standard image processing protocols such as dilation, erosion, opening closing and hole fill operations were carried out iteratively depending on the quality of the image. Dilation was used to add pixels to the edges of black objects so that small holes can be filled. Erosion was used to remove pixels from the edges of black objects and thus provided opportunity to eliminate noise but it has the disadvantage that all the remaining objects shrink in size. In order to overcome this problem erosion and dilation operations may be used together. Opening operation performs an erosion operation followed by dilation which smoothes the objects and remove isolated pixels. Closing and hole fill options are used to perform dilation operation followed by erosion which smoothes objects and fills in small holes (Soroushian and Elzafraney, 2005). Simple operations were only needed for this study as the air-voids of white colour contrast sharply with the surrounding matrix of black colour, producing almost similar to a binary image prior to the microscopic examination. Typical binary images are presented in Figs.6.1 and 6.2.

6.3. DETERMINATION OF CHARACTERISTICS OF AIR VOID SYSTEM

After the above processes the main characteristics of the air void system viz., (i) percentage of air-voids, (ii) air-void size distribution, (iii) shape of pores in terms of circularity and (iv) spacing factor were computed and analysed using the image analysis software. Air void volume which represents the number of voids per unit volume is the most important parameter and it depends on the volume of foam added. It is also helpful to check for foam stability by computation of difference in amount of foam added and the volume of air entrained in concrete. The shape of air voids are characterized based on its circularity and has been reported that the mix with circular air voids yields better strength than those with irregular air- voids (Kearsely and Visagie, 1999). The assumption that all the air voids are spherical will not hold good for mixes with higher foam volume where irregular voids are observed due to merging of bubbles (Figs 6.1 and 6.2). Hence the feret diameter which is the longest distance between any two points along the selection boundary (also known as caliper length) was determined to define the air void size (Image J, 2006). The size distribution of voids has been reported to influence the mechanical properties of foam concrete (Luping, 1986). Void-void spacing represents the thickness of paste phase surrounding the voids, which has been correlated to the strength, shrinkage and sorption (Nambiar and Ramamurthy, 2006c).

6.3.1 Calibration of Image Analysis Results through Volume of Air Voids

With the Image J, using the threshold option, the whole image was segmented into features of interest and background. The volume of air voids was determined for different densities of foam concrete by using the analyse particle command over the thresholded images of different cut surfaces. The percentage volume of voids was also calculated based on measured fresh density.

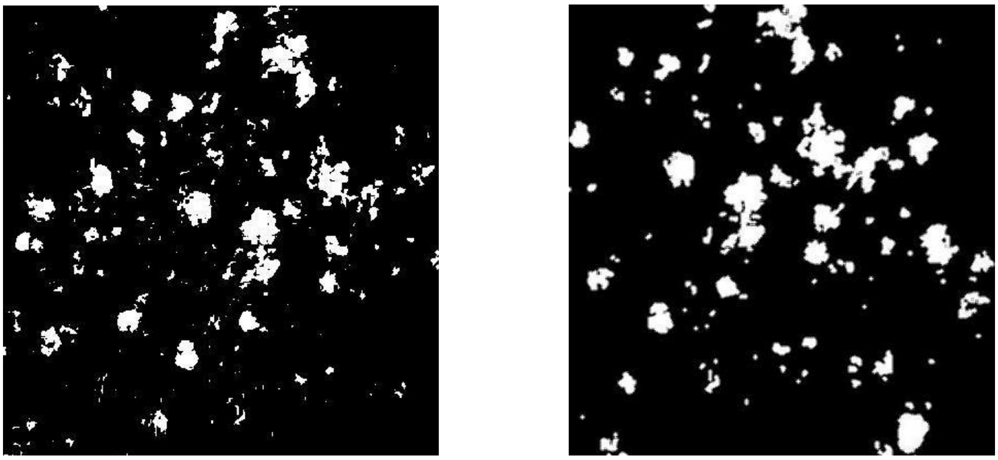

(a) Foam concrete with a fresh density 1500

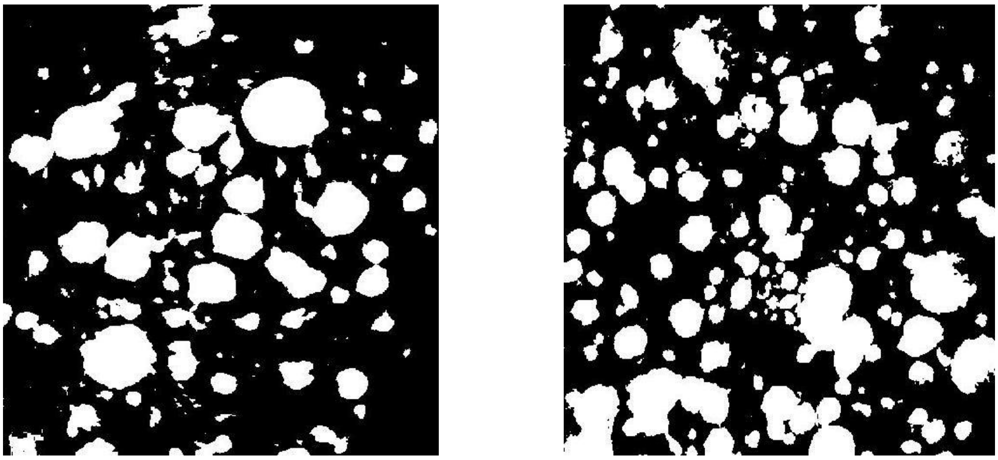

(b) Foam concrete with a fresh density 1250 kg/m3

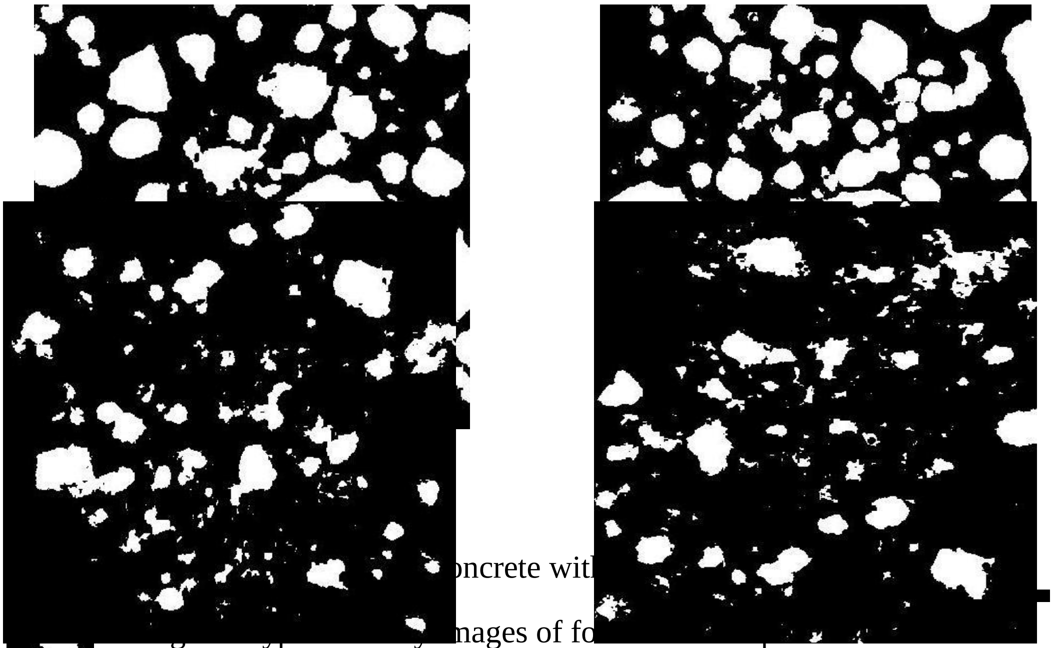

oncrete wit

mages of fo

(a)Foam concrete with a fresh density 1500 kg/m^3

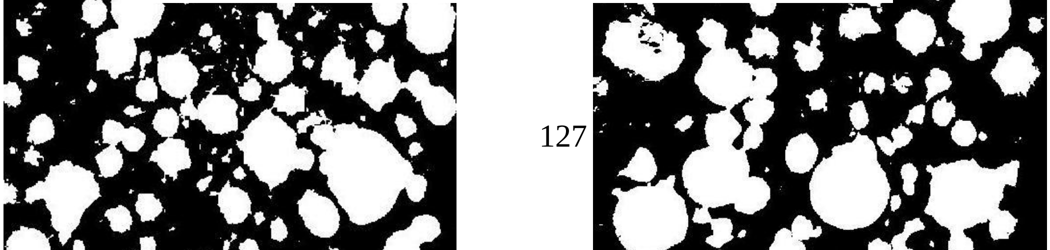

(b)Foam concrete with a fresh density 1250 kg/m^3

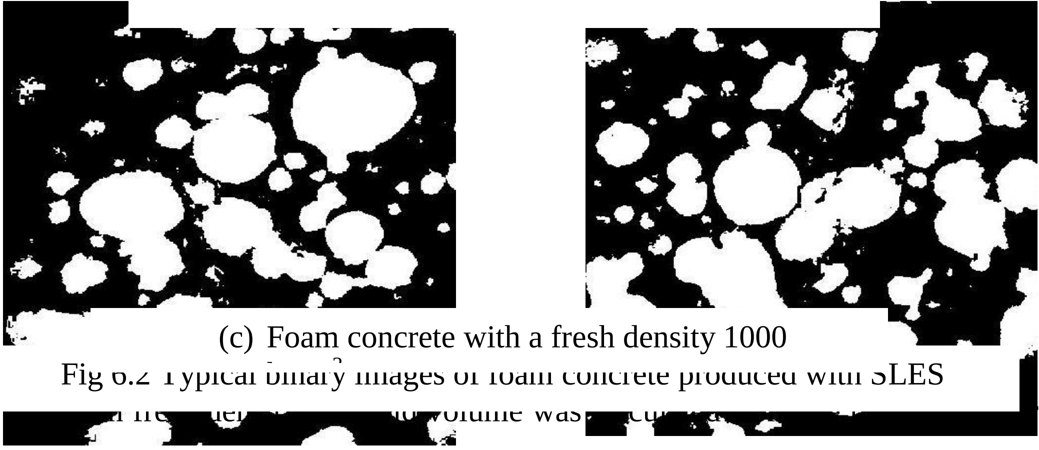

(c) Foam concrete with a fresh density 1000

Fig 6.2 Typical binary images of foam concrete produced with SLES

[illegible] volume was [illegible] iation of measured fresh density (experimental density (Dexp)) with reference to absolute density (theoretical density) calculated excluding the volume of air voids.

$$Dth = (Ww + Wc + Wf) / [(Ww/1000) + (Wc/ 3.15*1000) + (Wf / 1000)] \quad (6.1)$$

$$\text{Air content (\%)} = 100 [1- (Dexp /Dth)] \quad (6.2)$$

Ww, Wc, Wf are the weights of water, cement and foam respectively. The marginal difference between the results computed using hardened foam concrete and fresh density measurements in Table 6.2 may be attributed to collapse of a small percentage of bubbles and also error in interpretation likely to occur when the air voids overlap each other which is quite common in mixes with higher foam volume and when they touch the boundaries of image. Also during slicing all the voids are not cut exactly through its centre of cross-section, which in such cases result in a size distribution smaller than that of actual air-void sizes.

Table 6.2 Variation of percentage volume of air-voids with foam volume

Foam volume in the mix (%)	Percentage volume of air-voids in the mix based on		
	Measured fresh density of foam concrete	Image analysis of hardened concrete	
		SLS	SLES
18	17	15	14
32	32	31	30
46	43	43	42

6.3.2 Air- void Circularity

The outer contour (perimeter) and surface area for each of the identified voids was used to determine the void circularity using the relationship

$$\text{Circularity} = 4 * \text{pi} * (\text{area} / \text{perimeter}^2) \qquad (6.3)$$

A value of 1.0 indicates a perfect circle. Collapsed or merged bubbles can reduce the circularity value and this will have effect on strength of foam concrete. It is evident from the circularity frequency histogram in Fig 6.3 that the shape of the voids is similar for both the surfactants. For foam concrete with design density 1500 kg/m^3, the circularity of most of the voids are of the order of 0.8 and above indicating regular air voids. As the density reduces, the volume of paste content reduces (with increase in foam volume), the circularity deviates. The cumulative % oversize which represents the percentage of air voids having circularity greater than the values plotted are determined by plotting the value (100-y) where y is the value of the cumulative distribution. C90 represents the air void circularity, 90% of which are having circularity greater than this value and hence represents irregular voids with lower circularity values. C50 represents the circularity, 50% of which are having circularity above this value and hence it represents median circularity value of observed circularity of voids. The cumulative % oversize circularity parameters, C50 and C90 can be read from the exponential cumulative % oversize plot (Fig 6.3).

The median circularity varies from 0.65 to 0.9 indicating that practically most of the air-voids are nearly spherical unlike the aerated concrete where the expansion of concrete during gas formation results in development of ellipsoidal oriented pores (Cabrillac et al., 2006). However, a few lower values of 0.2 to 0.3 represent irregular pores produced due to merging of bubbles at higher foam volume. Figs.6.4(a) and 6.4(b) represent correlation between circularity parameters and density and strength of foam concrete produced with both the surfactants. With a reduction in strength and density, the circularity parameters C50 and C90 reduces.

6.3.3 Bubble Size of Foam Vs Air-void Size in Foam Concrete

6.3.3.1 Bubble size distribution in foam

The histograms representing the frequency of bubble size distribution determined through Feret diameter and cumulative oversize bubble size distribution for foam before addition in to concrete is shown in Fig 6.5. The bubble size distribution in foam is similar for both the surfactants. The bubble size varies mostly between 100 to 400 microns with a median value at 280 microns when optimum foam production parameters are adopted.

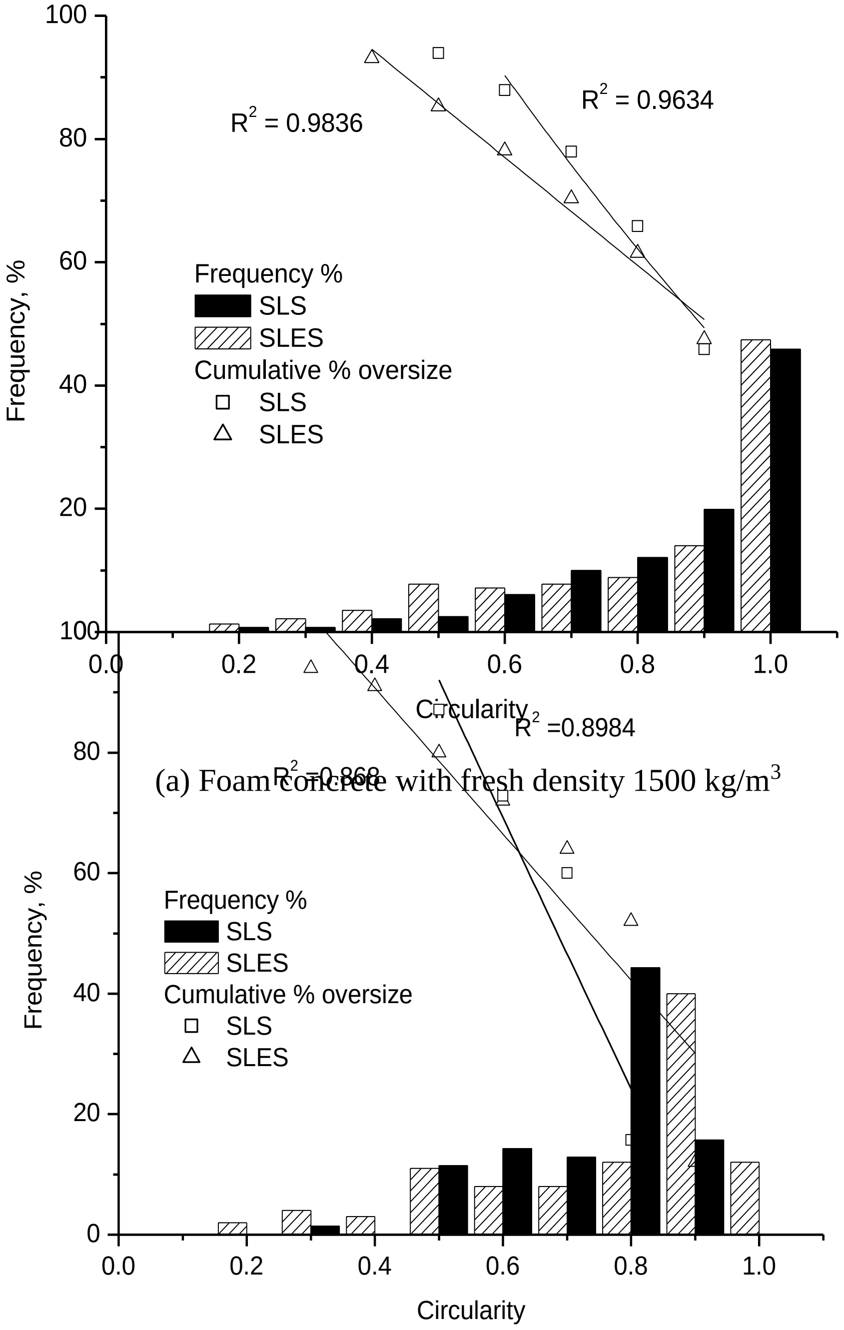

(a) Foam concrete with fresh density 1500 kg/m^3

(b)Foam concrete with fresh density 1250 kg/m^3

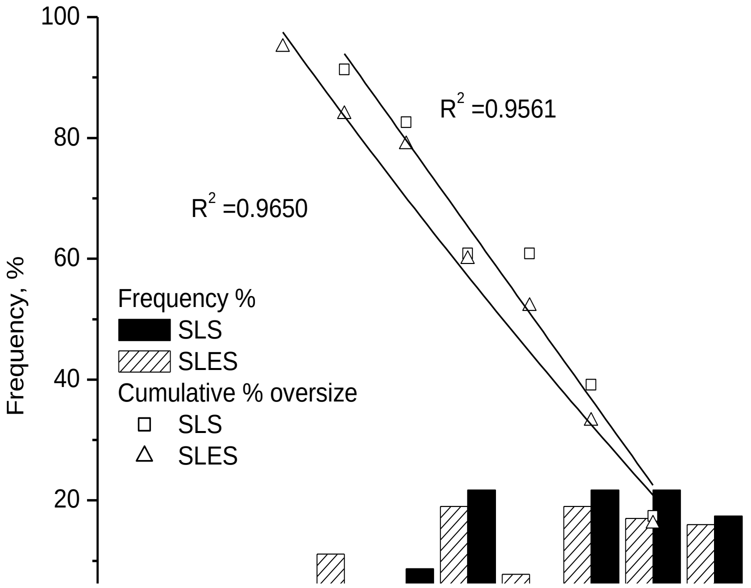

(c) Foam concrete with fresh density 1000 kg/m^3

Fig 6.3 Variation of air void shape distribution in foam concrete with density

Since the statistical R^2 value of the exponential cumulative oversize plot is around 0.99, the exponent [illegible] ive % oversize. The suitability of modified Rosin Rammler distribution function to fit the data of bubble size distribution was then verified. The modified Rosin- Rammler distribution was applied to bubble size distribution of foam in the form of $\ln\ln(\frac{1}{RR}) = n(\ln x - \ln x_0)$, where RR = cumulative % oversize, x = bubble size (µm), x_o = the position parameter, n = slope (Visagie and Kearsely, 2002).

The cumulative % oversize distribution values obtained from the exponential plots in Fig 6.5 were used to plot the modified Rosin-Rammler distribution graph lnln(1/RR) versus lnx (Fig 6.6).The modified Rossin-Rammler distribution is found to fit the data of bubble size distribution with higher statistical R^2 value.

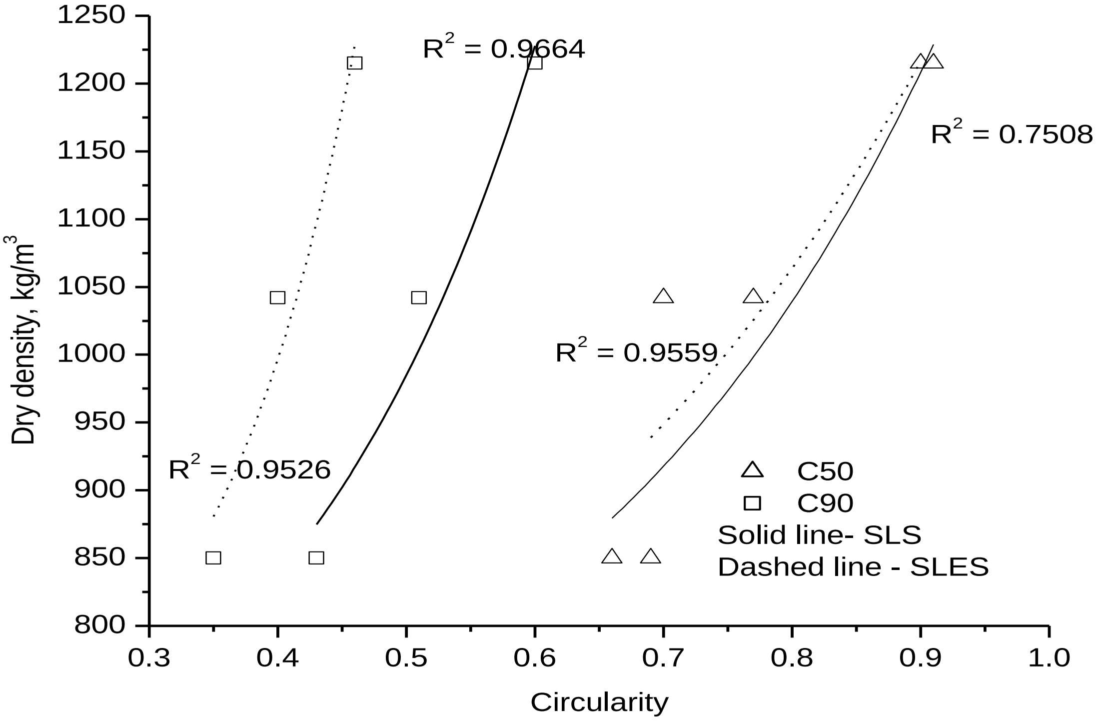

Fig 6.4 (a) Density Vs air void shape distribution parameters

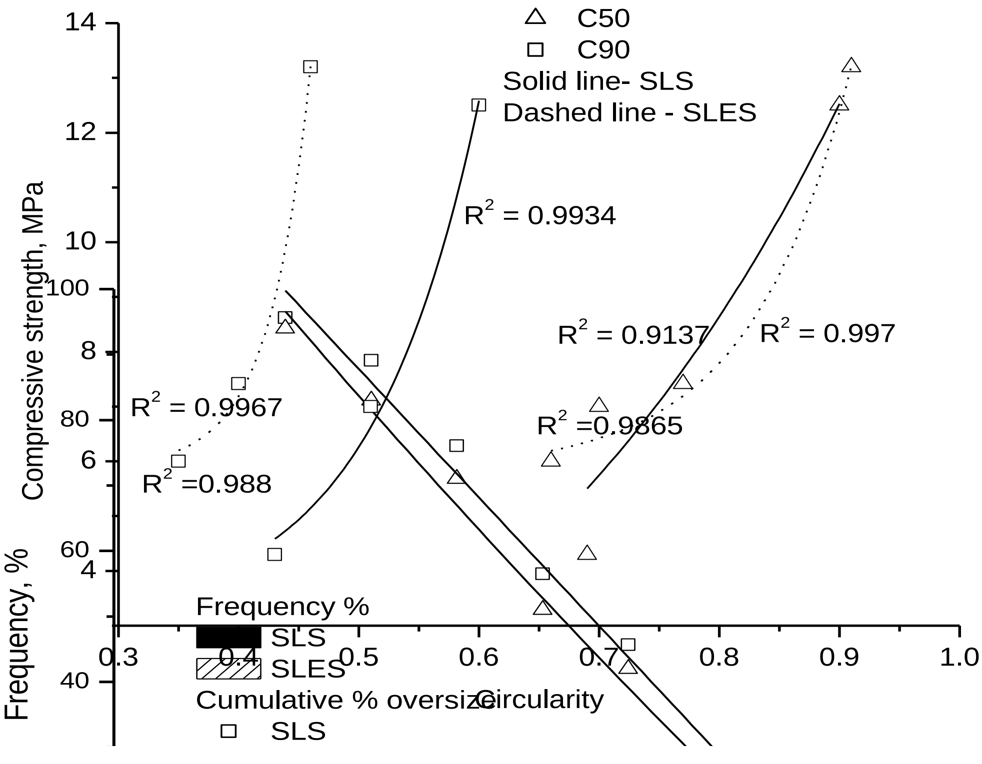

Fig 6.4(b) Strength Vs air void shape distribution parameters

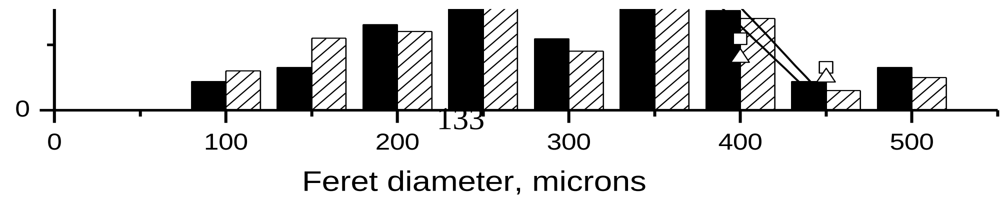

The two important parameters of the above distribution are ‘n’ the slope of straight line describes the range of bubble diameter distribution and ‘xo’, the intercept of straight line on horizontal axis (position parameter) indicates the bubble diameter (µm) which 36.8% of the bubble diameters are greater and indicates the bubble size. The bubble size when calculated based on modified Rosin Rammler distribution is 298 and 314 microns for surfactants Sodium lauryl ether sulfate and Sodium lauryl sulfate respectively.

6.3.3.2 Air-void size distribution in foam concrete

After establishing the bubble size distribution in foam, the air void size distribution in hardened concrete was determined by measurement of feret diameter and presented in Fig 6.7. The frequency distribution of air void sizes is observed to be similar for both the surfactants. The frequency distribution showed that the majority of air voids are of uniform size. At lower density the size distribution became wider with a few large sized pores which is due to the merging and overlapping of voids at higher foam volume (Nambiar and Ramamurthy 2006c; Pleau et al. 1990). The air void diameter can also be plotted as cumulative % oversize which represents the percentage of air voids which are bigger than the values plotted. The cumulative % oversize parameters D50 and D10 were determined by the same method followed for cumulative % oversize circularity parameters. These two parameters can be read from the exponential fit graph (Fig 6.7). The median diameter D50 varies between 100 to 315 microns and is similar for concrete produced with both the surfactants but D10, the number of larger size air voids is relatively higher in foam concrete produced with surfactant Sodium lauryl ether sulfate. Both D50 and D10 increases with a reduction in density of concrete , but the size of larger voids increases sharply with reduction in density. The modified Rossin-Rammler distribution function graphs are plotted (Fig 6.8) with cumulative % oversize data in order to check whether the air void size distribution data can also be fitted to this distribution function. Fig 6.8 clearly indicates that the air void diameter (or position parameter – xo value) decreases with increase in density of concrete.

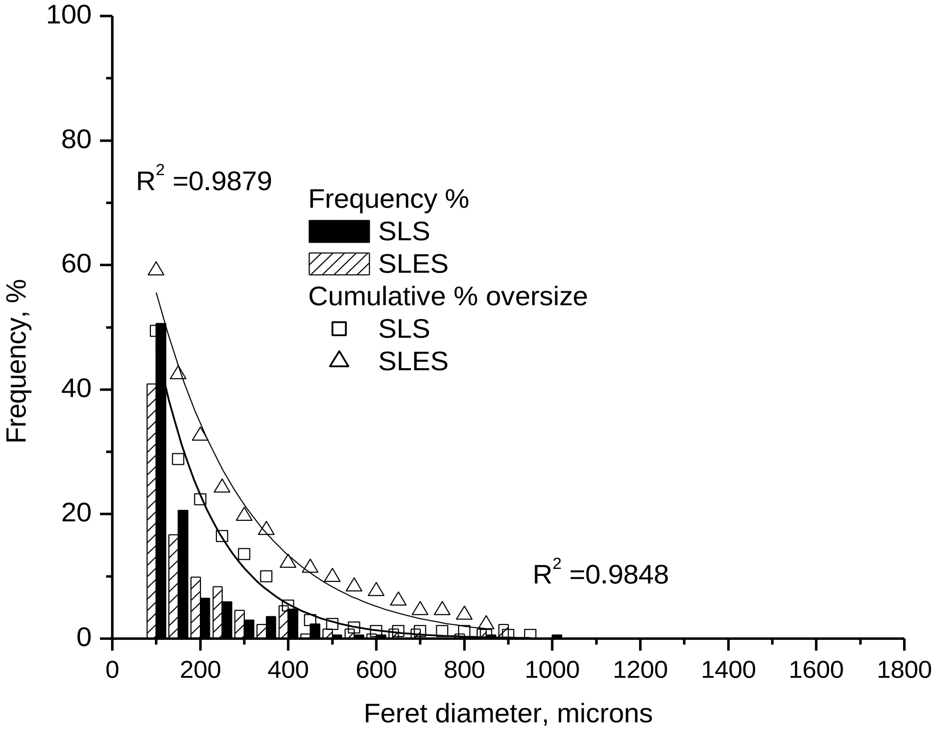

(a) Foam concrete with fresh density 1500 kg/m^3

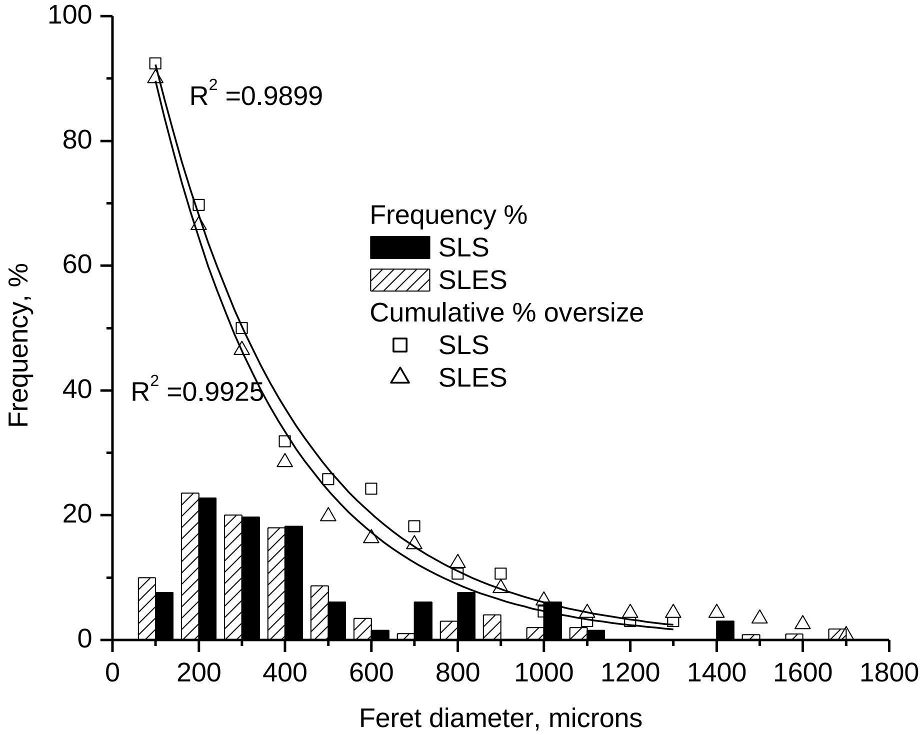

(b) Foam concrete with fresh density 1250 kg/m^3

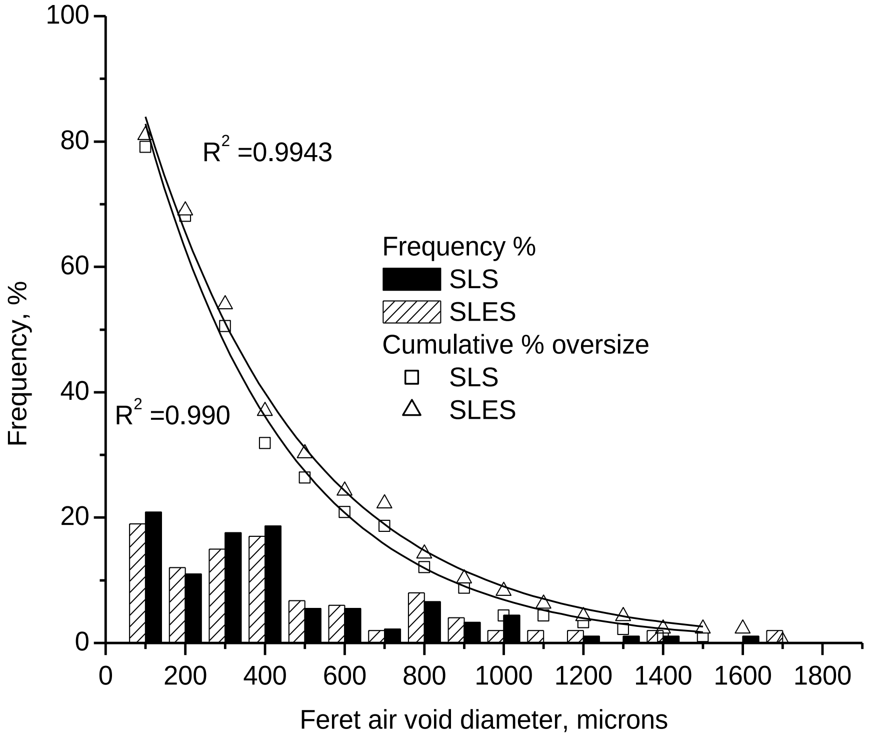

(c) Foam concrete with fresh density 1000 kg/m^3

Fig 6.7 Variation of air void size distribution with density of foam concrete

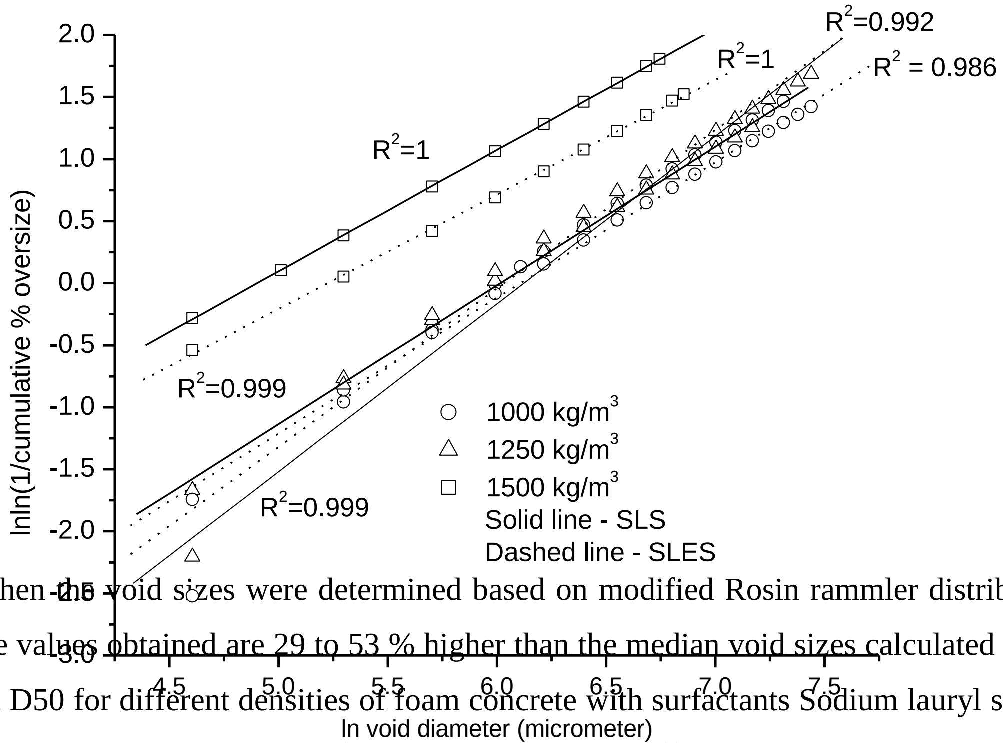

Fig 6.8 Air void diameter with density of concrete (Modified Rosin – Rammler distribution)

When the void sizes were determined based on modified Rosin rammler distribution the values obtained are 29 to 53 % higher than the median void sizes calculated based on D50 for different densities of foam concrete with surfactants Sodium lauryl sulfate and Sodium lauryl ether sulfate respectively. The difference is attributed to the fact void size distribution. While modified Rosin-Rammler distribution indicates the air void diameter above which only 36.8% of the air voids are greater in the size distribution analysis. From the cumulative % oversize plot (Fig 6.7), it is observed that the air void diameter increases with reduction in cumulative % oversize and this supports the above observation. Hence the modified Rossin-Rammler can be used as a method to describe the size distribution of voids in concrete in a simpler and easier form. When compared to bubble size distribution in foam the void size distribution in foam concrete does not deviate much. A marginally higher value of void sizes observed in foam concrete with lower density is attributed to merging of bubbles. This implies that there was not much error in measurement of air voids and also the foam was observed to be stable in concrete even though its density is lesser than ASTM requirements.

Figs.6.9(a) and 6.9(b) represent density and strength as a function of the air-void size parameters for foam concrete produced with both the surfactants. As the density increases the median void diameters become smaller. At higher densities, D10 also become smaller. It is also to be noted that the distribution curves D50 and D10 converge at higher densities (with low foam volumes) indicating that voids become smaller and more uniform in size in this range. An increase in cumulative oversize parameters leads to reduction in strength and thus the diameter and strength are inversely proportional (Fig 6.9(b)). Even smaller variation in median diameter results in steeper reduction in strength when compared to that of D90.

6.3.4 Void-void Spacing

The micro and macro capillary pores present in the pore wall surrounding the entrained air-voids is responsible for the moisture transport mechanisms (sorption and water absorption).

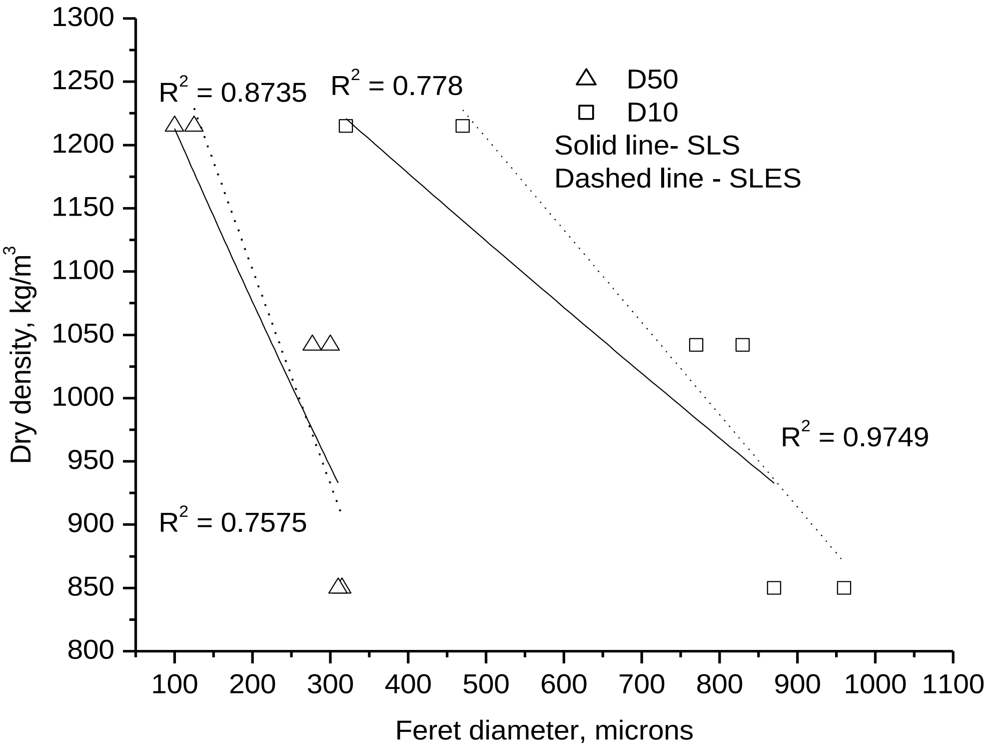

Fig 6.9(a) Density Vs air void size distribution parameters

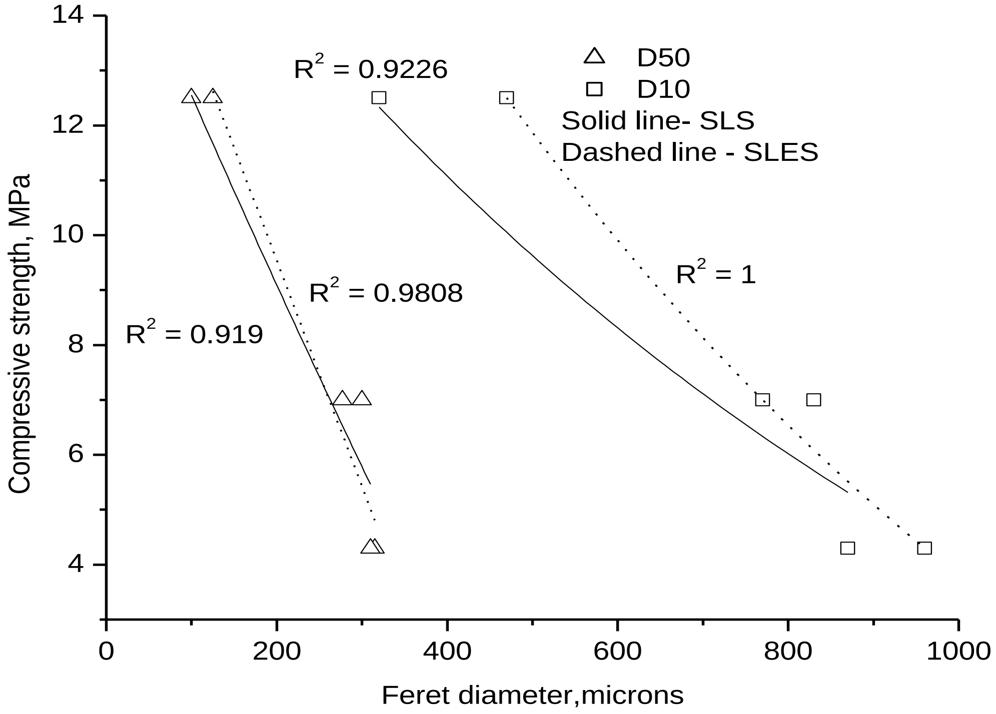

Fig 6.9(b) Strength Vs air void size distribution parameters

The thickness of this pore wall can be quantified by measuring the void-void distance which is measured as the smallest distance through the matrix between two air-voids in the vicinity on the images using the manual measurement option of the analysis software. The frequency histograms of air void spacing for foam concrete produced with two surfactants are shown in Fig. 6.10. Similar to other air-void parameters, spacing parameters are also represented by SP 50 and SP90 obtained from cumulative distribution curve (Fig 6.10). The median distance between voids varies from 150 to 450 microns for fresh density ranging from 1000 to 1500 kg/m^3. The relationship between these spacing factors and strength and density are shown in Fig 6.11 (a) and 6.11(b).

The spacing factors SP 50 and SP 90 reduces linearly with a reduction in density. This reduction in spacing can be attributed to the reduction in paste phase due to increase in foam volume. Thus the permeability related properties namely water absorption and sorption reduces with density of concrete due to reduction in amount of capillary pores with reduced volume of paste phase surrounding the voids (Nambiar and Ramamurthy, 2006c). When the relation of spacing factors with strength is considered, a steeper reduction in strength is observed for even smaller reduction in median spacing SP 50. But the variation of strength with SP 90 is relatively lower. The spacing between voids is similar for foam concrete produced with both the surfactants.

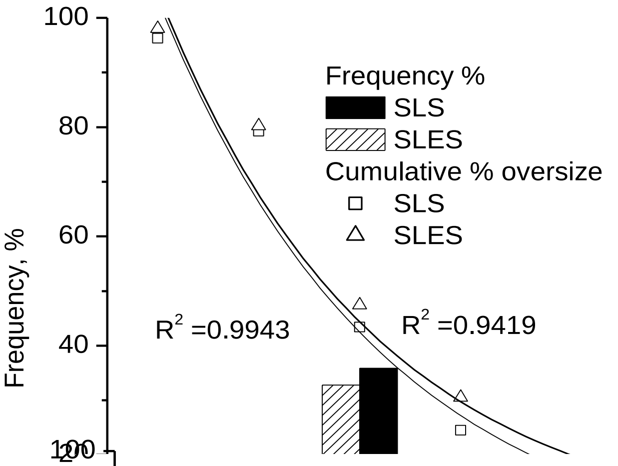

(a) Foam concrete with fresh density 1500 kg/m^3

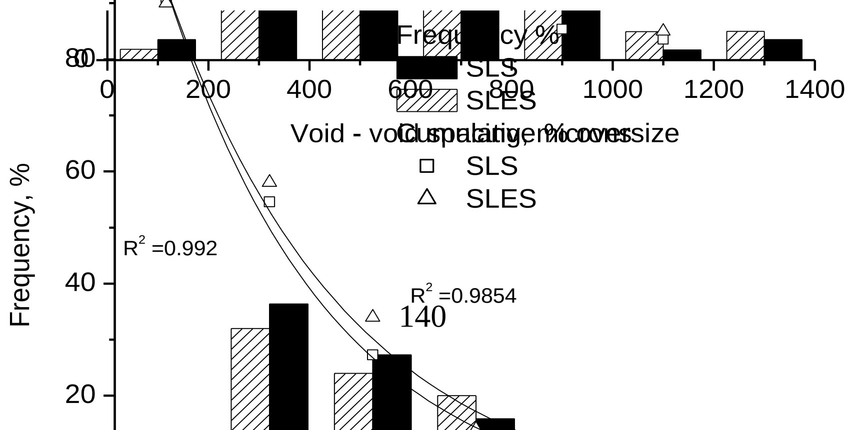

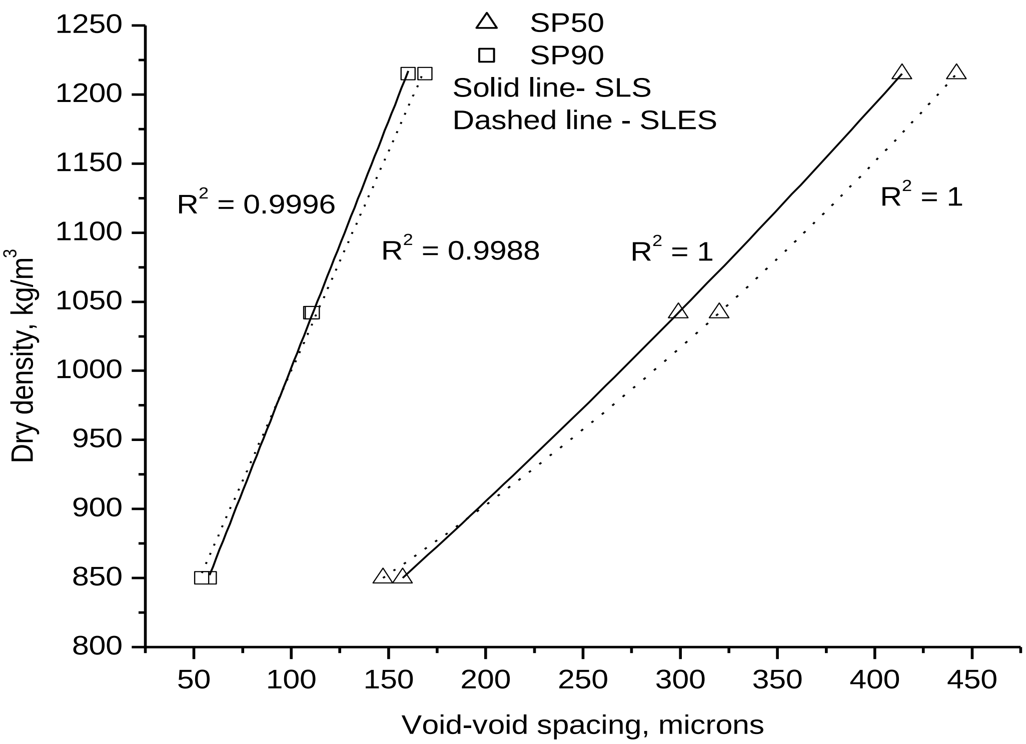

Fig 6.11 (a) Density Vs air void spacing distribution parameters

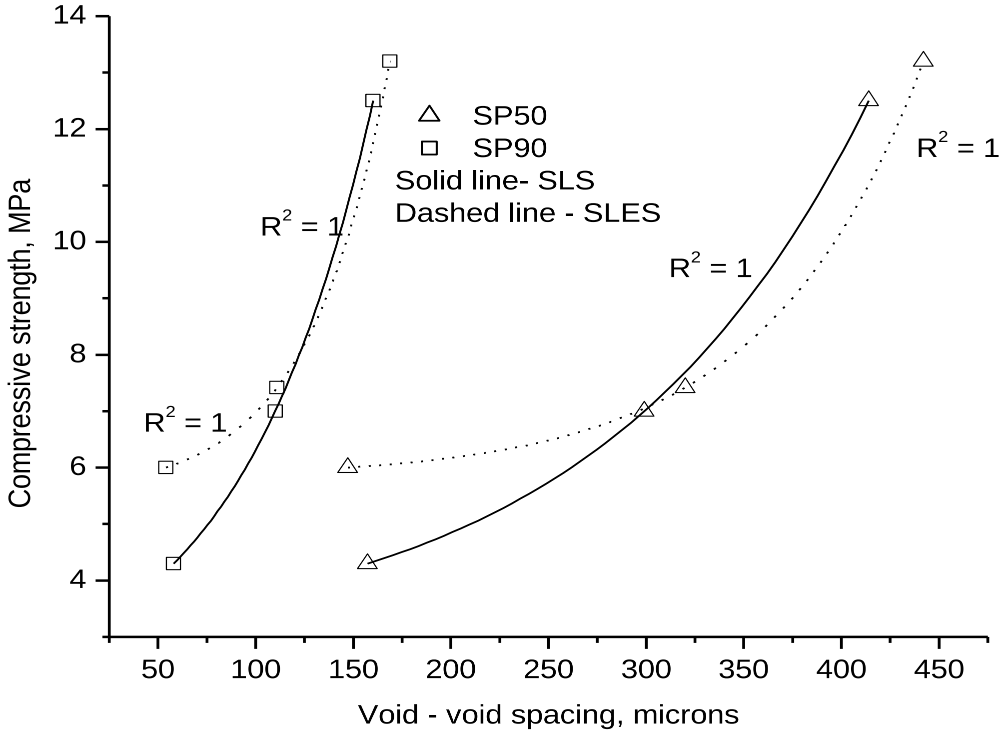

Fig 6.11(b) Strength Vs air void spacing distribution parameters

6.4 SUMMARY

The air voids in foam concrete are characterized on the basis of volume, size distribution, shape and spacing and the influence of these parameters on density and strength of foam concrete are studied. The shape of the air voids as characterized based on its circularity are found to be the order of 0.8 indicating that practically most of the air-voids are nearly spherical. However a few lower values of 0.2 to 0.3 represent irregular pores produced due to merging of bubbles at higher foam volume. The median air-void size in foam concrete varies between 106 to 345 microns for foam concrete with fresh density ranging from 1500 to 1000 kg/m^3 and this does not deviate much from the median bubble diameter in foam of 280 microns. This implies that there was not much error in measurement of air voids and also the foam was stable in concrete. For foam concrete with low density the merging of bubbles seem to produce larger air voids resulting in wider distribution of air void sizes and hence resulted in lower strength. The median diameter is found to be similar for concrete produced with both the surfactants but the number of larger size air voids is relatively higher in foam concrete produced with surfactant Sodium lauryl ether sulfate. Modified Rosin-Rammler distribution can be evaluated as a method providing easy means of describing the size distribution of air void and bubble in foam concrete and foam. The void sizes when determined based on modified Rosin rammler distribution are higher than the median void sizes calculated based on D50 derived from the plot of cumulative % oversize. The smallest distance through the matrix between two air-voids in the vicinity was measured as spacing of air-voids and this reduces with reduction in density due to the increase in foam volume. All the air void parameters studied viz., size factors, shape factors and spacing factors are found to correlate well with strength and density. It is observed that the smaller, circular and larger the spacing between voids, the greater is the strength of foam concrete.

CHAPTER 7

MOISTURE MOVEMENT BEHAVIOUR OF FOAM CONCRETE

7.1 GENERAL

The movement of moisture through any porous building material has an important bearing on its durability. As the durability is a function of porosity and permeability of concrete, foam concrete being a lightweight porous material is perceived as less durable (Kearsley and Mostert, 2005b). The transport of aggressive liquids into concrete depends on its permeation characteristics like permeability, water absorption and sorption. Sorptivity has been recognized as an important index of concrete durability because the test method reflects the way that most concrete will be penetrated by water and other agents (Dias, 2000). While sorptivity is the index of moisture movement into unsaturated concrete, the drying shrinkage represents the volume change of concrete due to removal of moisture from the surface of gel pores of unrestrained hydrated cement paste in concrete. Both these means of moisture movement affects the durability of concrete. This chapter focusses on the influence of type of surfactant and density of foam concrete on the sorption and shrinkage behavior of moist-cured preformed foam concrete.

7.2 SORPTION CHARACTERISTICS

Sorptivity and water absorption have emerged as the most useful parameters for understanding the moisture dynamics of concrete. The water absorption mainly depends on the total volume of pores. Absorption is usually measured by drying the specimen to constant mass, immersing it in water and measuring the increase in mass as a percentage of dry mass. Various procedures used are 24 h immersion in water (ASTM C 796), immersion till constant mass (ASTM C 642) and vacuum saturation method (ASTM C 1202) resulting in widely different results. Measurement of sorptivity is a short term approach of testing the durability where the material property is determined and then correlated with durability. However one of the biggest obstacles to the standardization of sorptivity testing is the fact that it is influenced by the moisture condition of concrete. Hence the sorptivity testing involves drying of some sort as preconditioning, and different drying regimes will give rise to different sorptivity values. Several researchers have investigated the sorptivity behaviour of normal weight concrete for the variations in strength of concrete, size of specimen, type of preconditioning and curing methods (Khatri et al., 1977; Hall, 1989; Dias, 2004; McCarter et al., 1992; Chan and Ji, 1998; Tasdemir, 2003). Experimental investigations have shown that the capillary permeability is substantially affected by the curing condition (Khatri et al., 1977) and its effect is reported to be higher in low strength concrete (Tasdemir , 2003). Also the longer the water curing period, the lower is the sorptivity, indicating that the additional curing reduces the pore size due to formation of more hydration products. Limited sorptivity studies have been made on foam concrete for the influences of foam volume (Giannakou and Jones, 2002, Madjoudj et al., 2002, Nambiar and Ramamurthy, 2007), filler type and fly ash replacement for fine aggregate (Jones and McCarthy, 2005c). The effect of curing on the sorption behavior has been investigated and the sorptivity coefficient is reported to have higher influence on capillary permeability of concrete (Tasdemir C, 2003). A summary of limited studies on cellular concrete have been presented in Table 7.1. The aim of this investigation is to study the influence of type of surfactant, density, strength and type of curing on sorption characteristics of foam concrete produced with two different surfactants.

7.3 MATERIALS USED

The experimental investigations comprise of single factor experiments to ascertain the influence of density and type of surfactant by keeping the cement-sand ratio at 1. The materials and their properties and mix proportioning have been described in the earlier Section 5.2.

7.4 WATER ABSORPTION BEHAVIOUR

7.4.1 Method of Measurement

For each mix, six cube specimens of size 50 mm were moist-cured for 28 days. The water absorption of mortar (base mix without foam) was also determined. Absorption was measured by the increase in weight of oven-dried specimens (to a constant mass) after immersion in water for 24 hours. As there existed significant variation in the density of foam concrete the water absorption was also expressed as percentage of volume of foam concrete.

7.4.2 Representation of Absorption by Weight and Volume

The variation in water absorption with dry density of foam concrete and base mix (mortar) are presented in Fig 7.1. The water absorption of the base mix (mortar) reduces with an increase in density when represented as percentage by mass or by volume. The percentage absorption of foam concrete reduces with density when represented as a percentage by mass while it increases with density when represented as a percentage of its volume. For a given volume of foam concrete with a reduction in density, the water absorption is lower which is caused by the reduction in the volume of paste and also that the pores are not interconnected (Kearsley and Wainwright, 2001b, Prim and Wittmann, 1983). Hence it would be appropriate to express water absorption by volume i.e kg/m^3 of foam concrete. For a constant density of foam concrete, the foam concrete made with surfactant Sodium lauryl ether sulfate exhibits marginally lower water absorption by volume than that with Sodium lauryl sulfate.

7.5 SORPTIVITY BEHAVIOUR

7.5.1 Measurement of Sorptivity

Water sorptivity was measured according to the method proposed by Hall (1989) for two extreme curing conditions viz., 28-day water curing and 28-day air curing. The study was carried out at ambient temperature and humidity (30-33°C, 70 -75% RH). Six cube specimens of size 70.7 mm after appropriate method of curing for 28 days (for each design density with each surfactant) were oven-dried and placed in a container filled with water to a height of 5 mm above the base of the specimen. The change in weight of the specimens was measured at designated time intervals for a period of 29 hours i.e till a constant mass was attained.

Table 7.1 Salient literature on sorption characteristics of aerated and foam concrete

Author (s)	Mix details	Properties studied	Salient observations
Prim and Wittmann (1983)	Aerated concrete	Sorptivity	Sorption characteristics are related to pore structure. Capillary coefficient decreases with increase in artificial air pores
Tada and Nakano (1983)	Aerated concrete	Water absorption	Classification of pore space of AAC. Influence of moisture content on water absorption. Lowering density by introduction of larger air pore exhibit low water absorption
Narayanan and Ramamurthy (2000)	Aerated concrete (non-autoclaved and autoclaved)	Sorptivity	Effect of composition and curing has been brought out. Sorptivity of NAAC is more than AAC.
Goual et al. (2000)	Aerated concrete made of clay, cement and water	Sorptivity	Investigations on average capillary transport coefficient as a function of water content for different porosities. Macropores dampen the diffusion phenomenon
Kearsely and Wainright (2001b)	Foam concrete (cement paste with and without fly ash replacement)	Water absorption	Volume of water absorbed was independent of volume of air entrainment.
M.R.Jones (2001)	Foam concrete	Sorptivity	Effects of w/c, surfactant type and fly ash replacement on sorption characteristics were studied.
Madjoudj et al (2002)	Foam concrete made of clay, cement and water	Sorptivity	Sorptivity of lightened material is less than that of denser material
Ginnakou and Jones (2002)	Foam concrete	Sorptivity	Sorptivity increases with density
Jones and McCarthy (2005c)	Foam concrete	Sorptivity	Effects of plastic density and fines content on sorptivity and the relationship between sorptivity and strength were studied. Concrete with coarse fly ash as filler exhibited slightly higher sorptivity than those of equivalent sand concrete.
Nambiar and Ramamurthy (2007)	Foam concrete	Sorptivity and water absorption	Water absorption and sorptivity decrease with an increase in foam content. Effect of use of mineral and chemical admixtures on sorptivity was also studied.

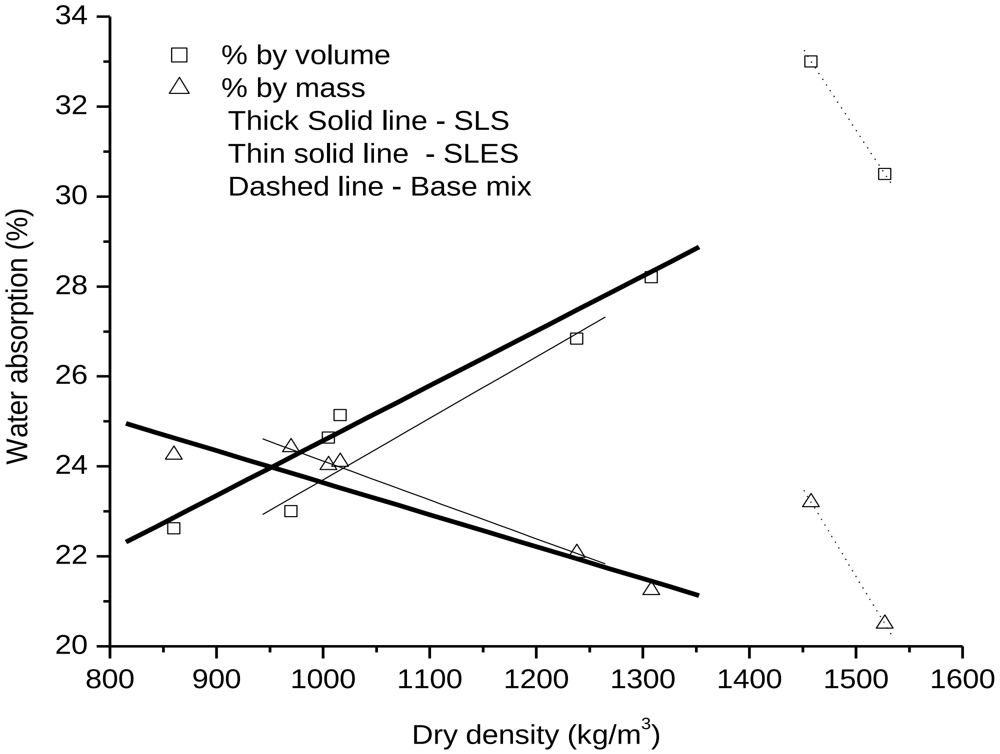

Fig 7.1 Variation of water absorption with dry density

Sorptivity(S) was obtained as the slope of the linear portion of the line of graph of cumulative water absorption per unit area of the inflow surface (i measured in mm) against square root of time (t measured in minutes) where i was calculated from $i = \Delta w / A \times \rho$, where Δw = increase in weight with time (g), A = cross sectional area (mm^2), and ρ = density of water (1000 kg/m^3).

As the depth of water penetration is also an important factor for assessing the durability of concrete, the depth of penetration of water front was measured after by splitting of samples and dusting the surface of the split sample with moisture sensitive dye. The depth of penetration'd' has also been observed to have a square root time relationship $d= do + St^{½}$ where 'do' is a constant and 'S' is the water sorptivity (McCarter et al., 1992).

7.5.2 Effect of Curing

Figs. 7.2 to 7.4 show the influence of method of curing on the sorption characteristics (mean cumulative volume absorbed at each time interval) of foam concrete for each of the design densities and their corresponding base mix (mortar without foam). Table 7.2 and Figs.7.2 to 7.4 indicate that the sorptivity coefficient of air-cured foam concrete is 2.5 times higher than that of water-cured specimens. Such higher capillary sorption of air-cured specimen is attributed (i) to lower degree of cement hydration and (ii) due to possible micro cracks on the surface of concrete resulting from the early dissipation of moisture from the concrete. The cumulative sorption of water-cured specimen increases gradually while it is steeper for air-cured foam concrete and also reaches a steady-state faster. The cumulative volume of water absorbed per unit area is lower for foam concrete as compared to base mix (Fig 7.2).

The variation of sorptivity with compressive strength at 28 days is presented in Table 7.3. The air- cured specimens gain strength of around 50% of water-cured specimens due to lower degree of cement hydration. But the sorption of air-cured specimens is 65% higher than that of water- cured specimens. Hence the method of curing has relatively higher influence on sorptivity than on strength of foam concrete.

7.5.3 Effect of Density

Cumulative sorption: Having established the effect of curing on sorptivity, further studies were confined to foam concrete subjected to water-curing. The effect of density on sorption characteristics (based on quantity of water absorbed) of foam concrete and base mixes for the period of 29 hours is presented in Fig 7.5. Table 7.4(a) shows the sorptivity and intercepts data obtained from the sorptivity equations representing the linear portion of plots in Fig 7.5. Foam concrete exhibits lower sorptivity than the corresponding base mixes (mortar without foam). The sorptivity of foam concrete reduces with the density.

The foam volume increases with a reduction in density of foam concrete and hence for a constant cement-sand ratio, the cement content in the mix decreases resulting in lower volume of sorbing paste (Table 5.1). As the sorptivity is characterized by the capillary suction and since the entrained air voids do not contribute to this transport mechanism, the sorptivity essentially depends on the number of pores which participate in the capillary suction process. Hence the decrease in sorptivity is due to the reduction in capillary pores (due to lower paste volume) caused by reduction in density (Table 7.4(a)). This behaviour conforms to those of other researchers (Giannakou and Jones, 2002; Madjoudj et al., 2002; Jones and McCarthy, 2005; Nambiar and Ramamurthy, 2007). Foam concrete produced with surfactant SLES exhibits 8 to 18% higher sorptivity than that using SLS (Fig 7.6, Table 7.4(a)).

Table 7.2 Effect of curing on sorptivity (based of 81 minutes data)

Foam volume %	Fresh density kg/m^3	Surfactant	Type of curing	Sorptivity mm/(min) $^{1/2}$	Intercept	Correlation Coefficient r
46	1000	SLS	Air	1.316	2.481	0.976
			Water	0.521	0.934	0.991
		SLES	Air	1.360	2.018	0.985
			Water	0.456	0.707	0.975
32	1250	SLS	Air	1.464	2.703	0.990
			Water	0.618	0.968	0.994
		SLES	Air	1.443	2.681	0.985
			Water	0.552	0.971	0.983
18	1500	SLS	Air	1.513	3.092	0.993
			Water	0.642	0.977	0.997
		SLES	Air	1.498	3.567	0.985
			Water	0.593	1.339	0.984
Base mix- 1	1813	NIL	Air	2.428	0.080	0.994
			Water	0.995	0.226	0.966
Base mix - 2	1832	NIL	Air	2.109	-0.537	0.991
			Water	0.994	0.023	0.969
Base mix - 3	1884	NIL	Air	1.920	-0.280	0.989
			Water	0.965	-0.352	0.971

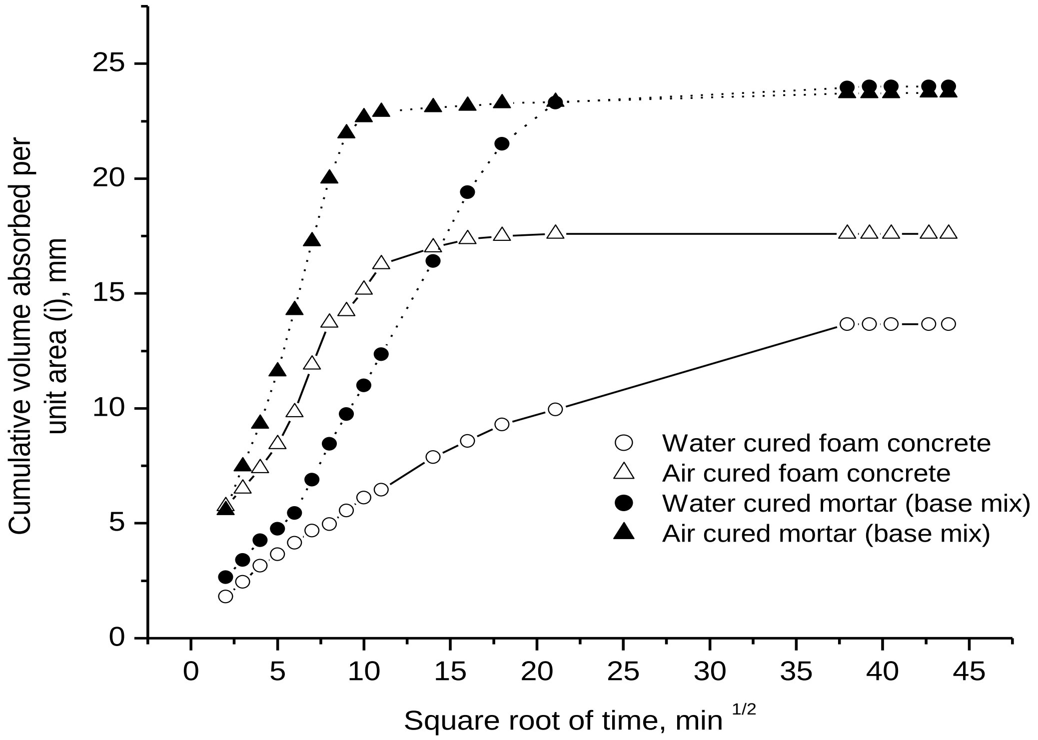

(a) SLS

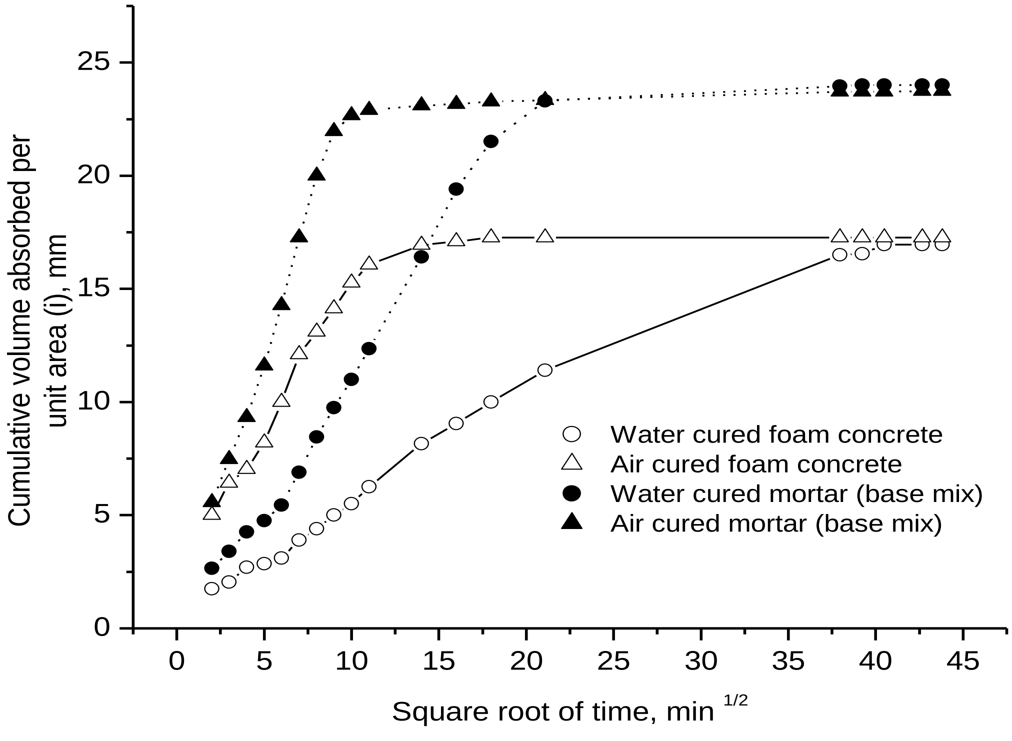

(b) SLES

Fig 7.2 Effect of curing on cumulative sorption of foam concrete of fresh density 1000 kg/m^3

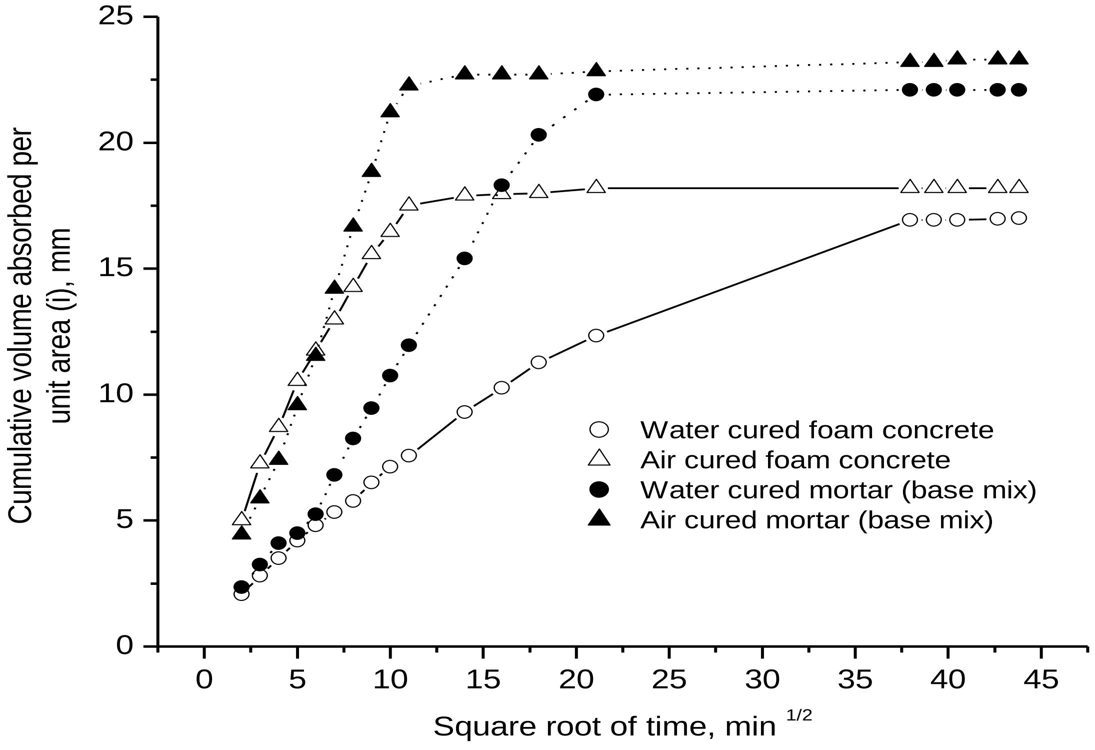

(a) SLS

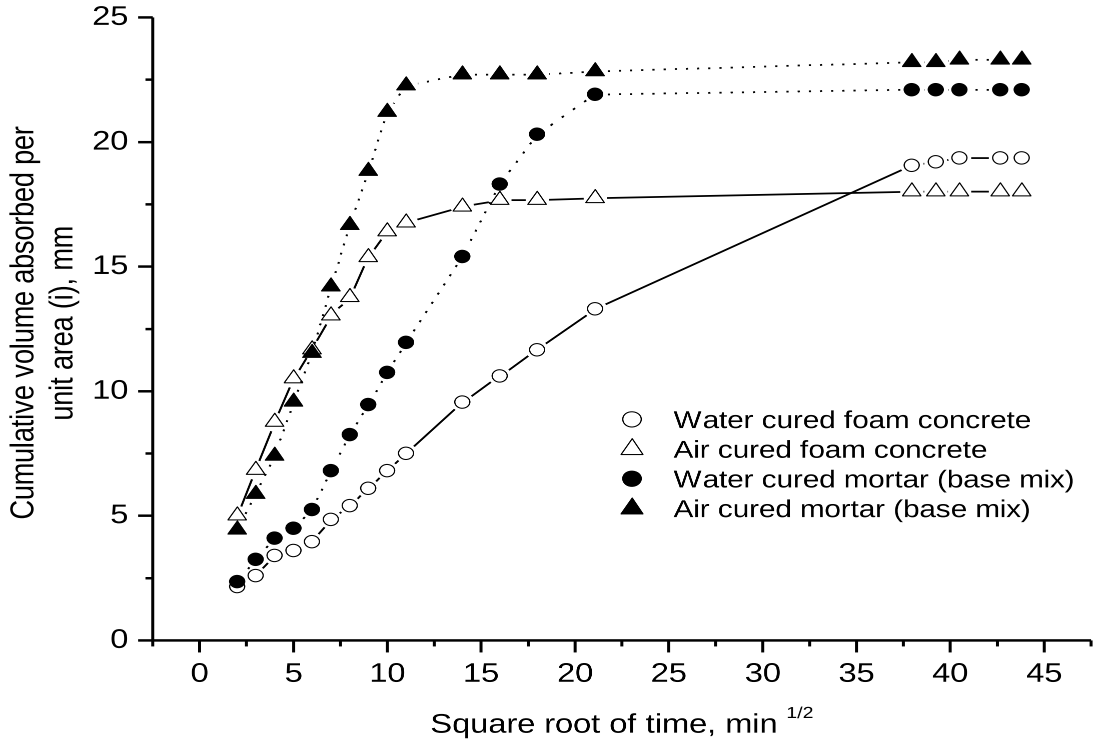

(b) SLES

Fig 7.3 Effect of curing on cumulative sorption of foam concrete of fresh density 1250 kg/m^3

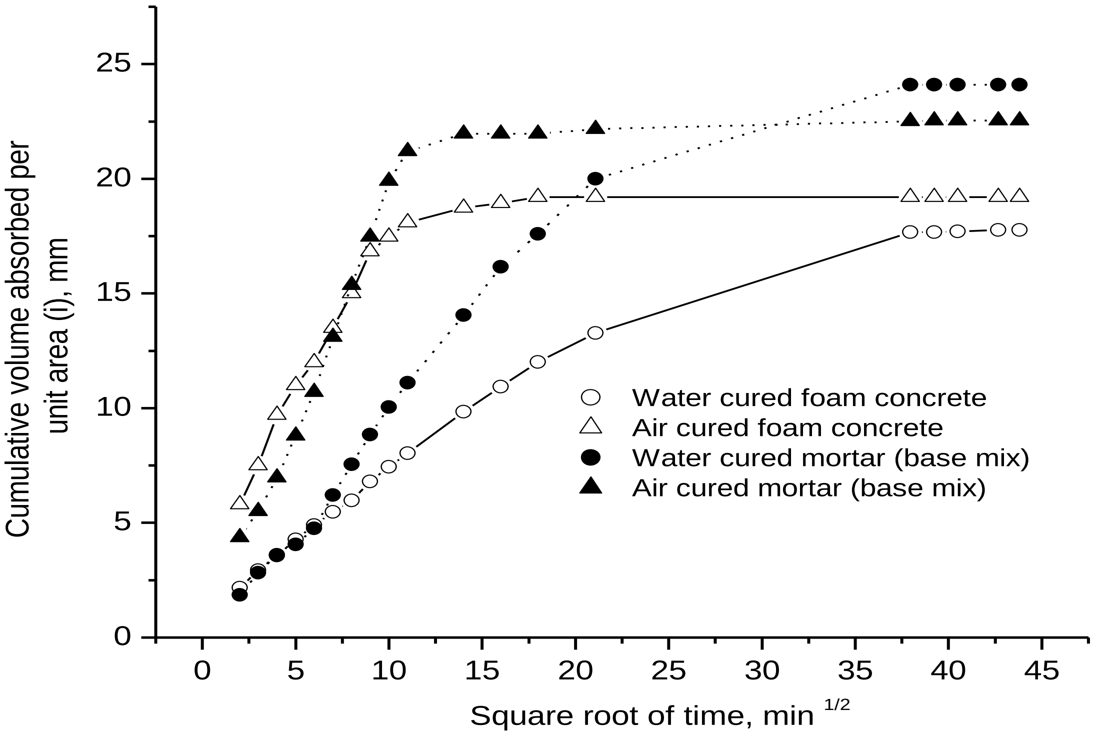

(a) SLS

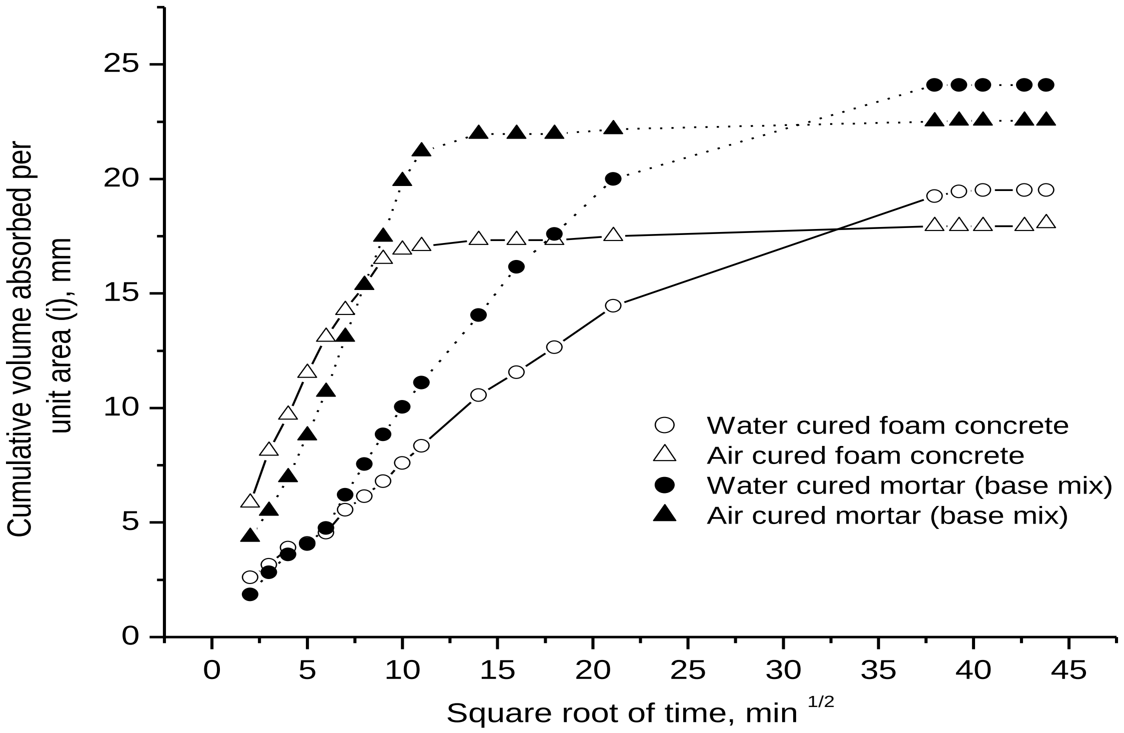

(b) SLES

Fig 7.4 Effect of curing on cumulative sorption of foam concrete of fresh density 1500 kg/m^3

Table 7.3 Variation of sorptivity with paste content and compressive strength (based on 81 minutes data)

Fresh density, kg/m^3	Foam volume, %	Paste content, m^3/m^3	Sorptivity of foam concrete mm/(min) $^{1/2}$				Compressive strength, N/mm^2			
			Foaming agent SLS		Foaming agent SLES		SLS		SLES	
			Water cured	Air-cured	Water cured	Air-cured	Water cured	Air-cured	Water cured	Air-cured
1000	46	0.556	0.521	1.316	0.456	1.360	4.3	2.08	6	2.88
1250	32	0.686	0.618	1.464	0.552	1.443	7	3.43	7.42	3.64
1500	18	0.798	0.642	1.513	0.593	1.498	12.84	6.54	13.2	6.73
Base mix -1	1813	1	0.995	2.428	0.995	2.428	18	9	18	9
Base mix- 2	1832	1	0.994	2.109	0.994	2.109	22	11.44	22	11.44
Base mix- 3	1884	1	0.965	1.92	0.965	1.92	24	12.24	24	12.24

Table 7.4(a) Sorptivity of foam concrete based on quantity of water absorbed (based on 444 minutes data)

Foam volume %	Fresh density kg/m^3	Surfactant	Sorptivity mm/(min) $^{1/2}$	Intercept	Correlation Coefficient r
46	1000	SLS	0.436	1.445	0.986
		SLES	0.532	0.335	0.994
32	1250	SLS	0.546	1.398	0.993
		SLES	0.606	0.725	0.996
18	1500	SLS	0.593	1.284	0.996
		SLES	0.643	1.126	0.996
Base mix- 1	1813	NIL	1.188	-0.699	0.989
Base mix- 2	1832	NIL	1.116	-0.512	0.991
Base mix- 3	1884	NIL	1.004	-0.429	0.993

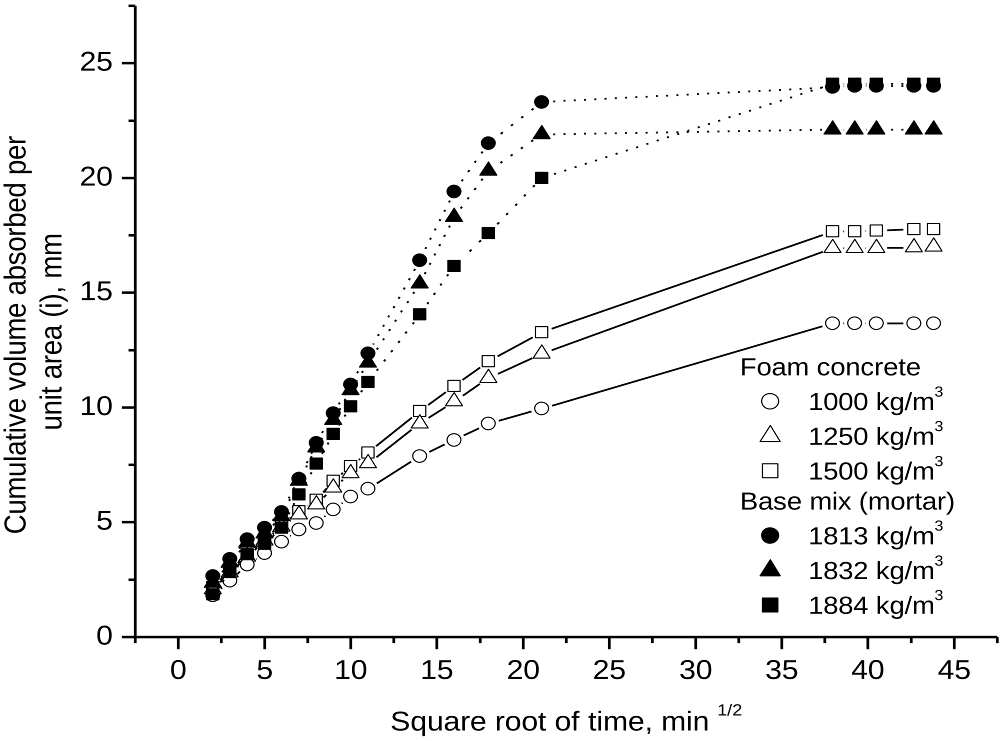

(a) SLS

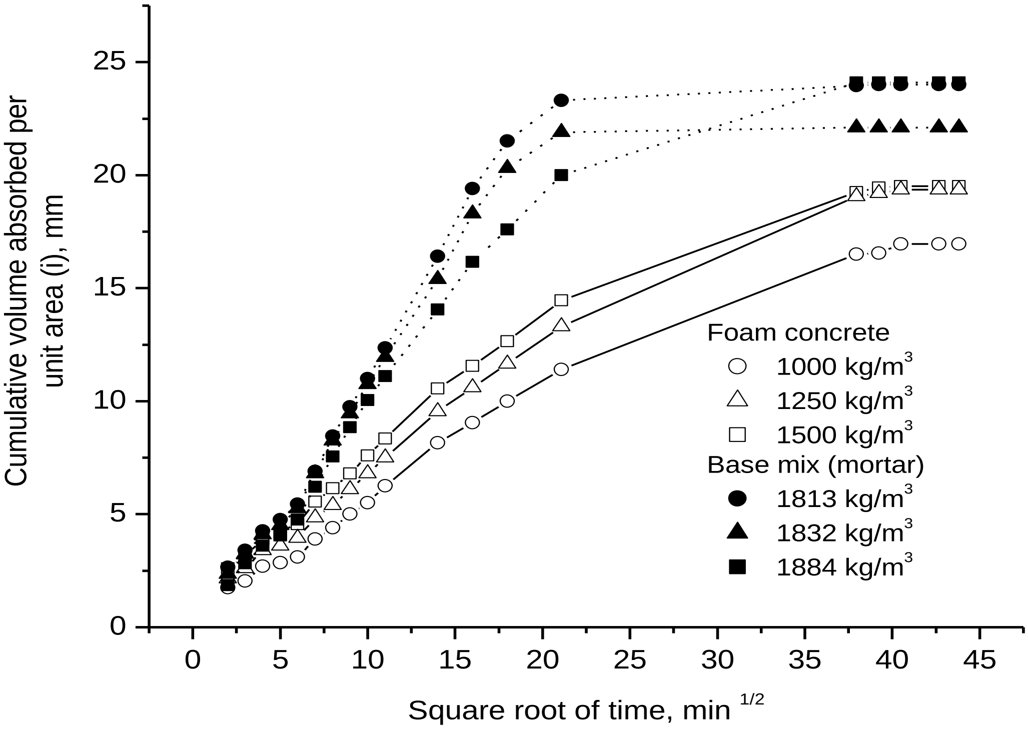

(b) SLES

Fig 7.5 Effect of density on cumulative sorption of foam concrete

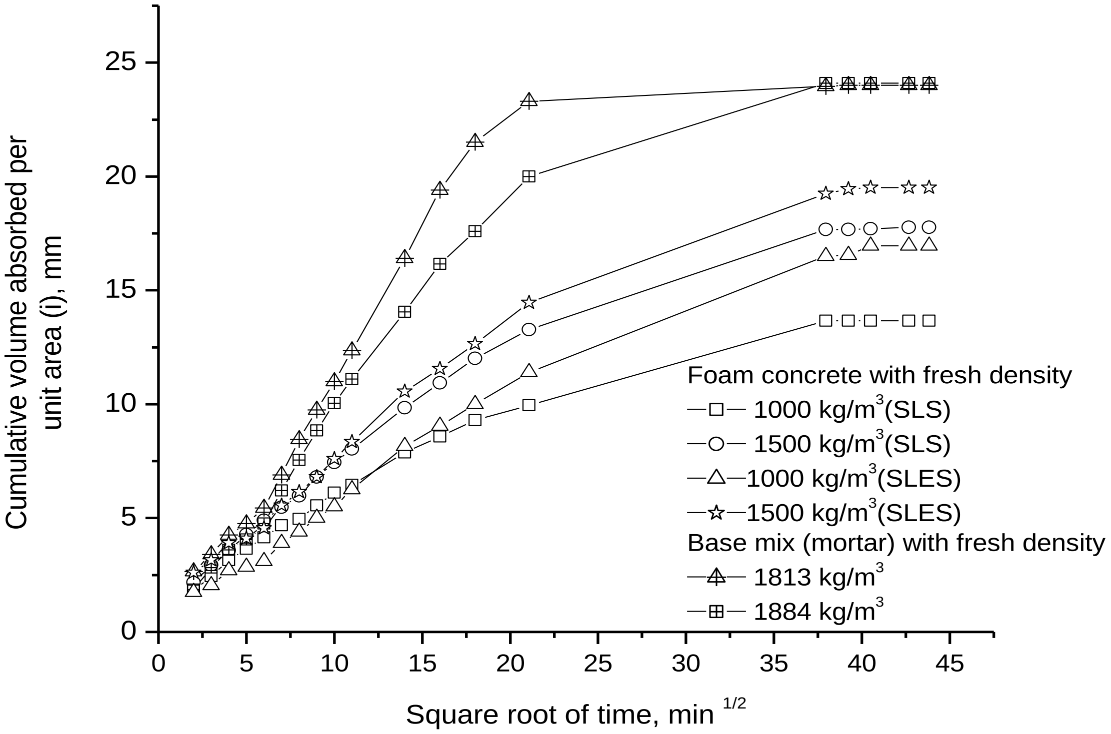

Fig 7.6 Comparison of cumulative sorption of foam concrete for two surfactants

Depth of penetration: Fig 7.7 presents the variation in the depth of penetration with square root of time over a period of 10.3 hours for foam concrete and base mix (mortar). Table 7.4(b) indicates that the depth of penetration obeys the square root of time relationship with good correlation. The greatest depth of penetration occurs in base mixes (mortar) with the water front advancing almost 70 mm (i.e., to the top surface of cube) which occurred in 8.3 hours period. A reduction in depth of penetration with density of foam concrete is attributed to the increased tortuous path of water migration due to an increase in the volume of entrained air voids (Prim and Wittmann, 1983).

7.6 SHRINKAGE BEHAVIOUR

In general, when compared to normal weight concrete the shrinkage of foam concrete is reported to be ten times higher, because of higher amount of cement content, less restraining effect of finer sand used and due to absence of coarse aggregates in the mix composition (Valore, 1954b; Jones et al., 2003).

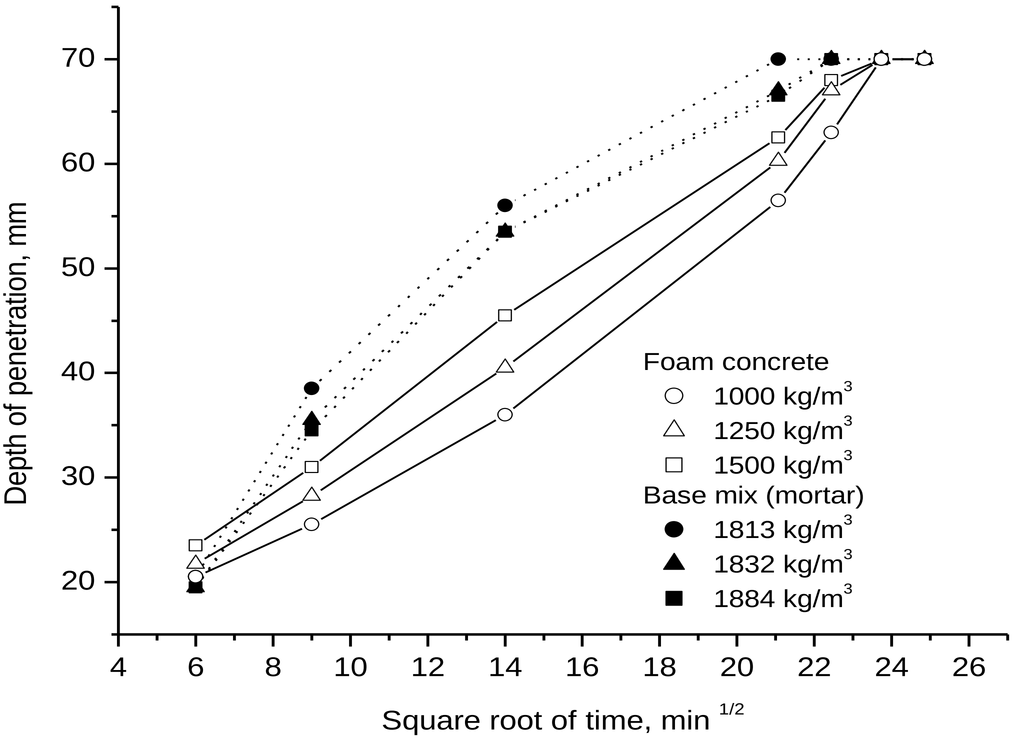

(a) SLS

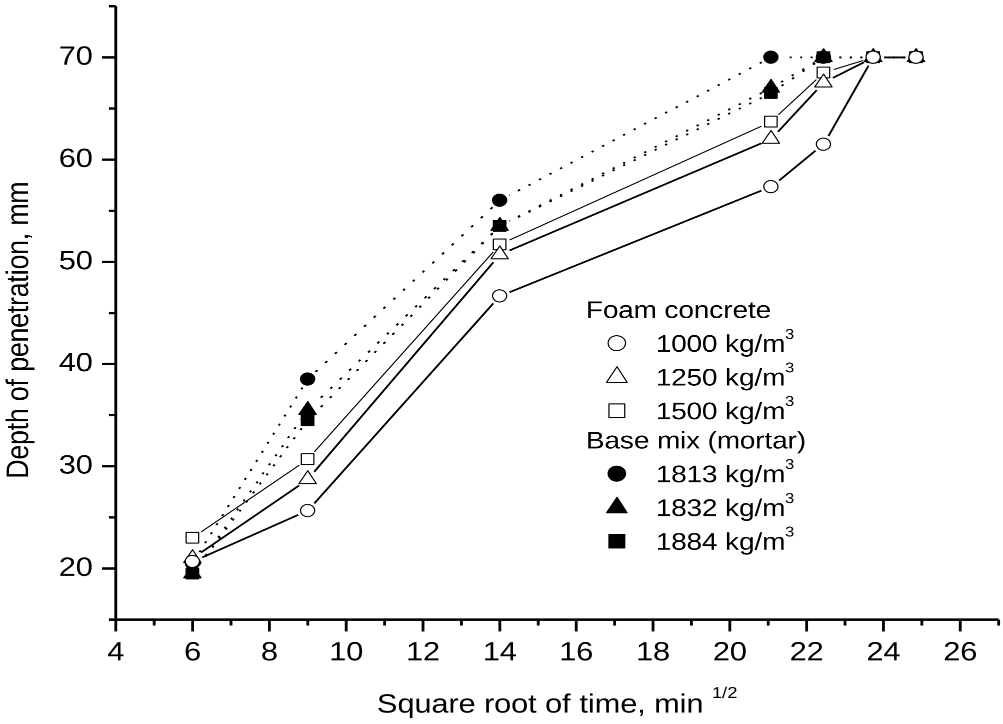

(b) SLES

Fig 7.7 Capillary absorption rate of foam concrete through depth of penetration

Table 7.4(b) Sorptivity of foam concrete based on depth of penetration

(based on 444 minutes data)

Foam volume %	Fresh density kg/m^3	Surfactant	Sorptivity mm/(min) $^{1/2}$	Intercept	Correlation Coefficient r
46	1000	SLS	2.406	4.504	0.987
		SLES	2.569	5.418	0.954
32	1250	SLS	2.567	5.555	0.997
		SLES	2.79	7.317	0.963
18	1500	SLS	2.609	7.956	0.998
		SLES	2.824	5.234	0.956
Base mix- 1	1813	NIL	3.169	6.574	0.946
Base mix- 2	1832	NIL	3.075	5.381	0.953
Base mix- 3	1884	NIL	3.069	5.079	0.953

Cement and pulverized sand being finer presents higher surface area for the adsorbed water to escape thus increasing the shrinkage.Autoclaving is reported to reduce the drying shrinkage of aerated concrete by 12-50% of that of moist-cured aerated concrete (due to a change in mineralogical composition) (Valore, 1954b, Schubert, 1983). Studies on drying shrinkage of aerated concrete identified the relative influence of the following parameters viz., volume and specific surface of finer pores (Ziembicka, 1977), pore distribution and moisture content (Schubert, 1983). A study on the shrinkage behavior of foam concrete with sand and fly ash as fillers concluded that the mixes with sand exhibited relatively smaller drying shrinkage, which has been attributed to the higher shrinkage restraining capacity of sand as compared to that of fly ash (Jones et al., 2003, Nambiar and Ramamurthy, 2009). It has also been reported that light weight aggregates could be used to reduce the shrinkage of foam concrete (Regan and Arasteh, 1990). The above discussions and a review on shrinkage behaviour of foam concrete given in Section 2.4.2.1 show that most of the earlier researches on drying shrinkage are on aerated concrete, while limited studies have been reported on foam concrete. This section reports the detailed investigations conducted to ascertain the influence of type of surfactant, density, moisture content and pore structure on the drying shrinkage of moist-cured preformed foam concrete.

7.6.1 Shrinkage Measurement

The drying shrinkage was measured on prisms of size 40 x 40 x 160 mm in accordance with ASTM C 596 (2009). For each parameter, six specimens were tested and the mean value was reported. Following demoulding, stainless steel ball bearings were secured at top and bottom of the specimens with epoxy resin and hardener and were immersed in water for ten days. The specimens were then placed in controlled environment within the temperature range of 27 ± 2 ^{0}C and relative humidity range of 50 ± 4 %. First length measurement (l_1) was made after 3 days of immersion in water and subsequent measurements were made at proper time intervals for a duration of 100 days. The shrinkage % was calculated as $((l_2 - l_1)/L_d)$ x 100 where l_1 is the first reading of length, l_2 is the final reading after 100 days and L_d is the original length of the specimen. Mechanism of drying shrinkage, which involves moisture diffusion from the interior of concrete, is closely related to the moisture content of concrete. Hence along with length changes measurement, the moisture content starting from maximum water saturation (29% by volume) to desorption moisture content (less than 1% by volume) was also measured.

7.6.2 Moisture Content Vs Drying Shrinkage

The variation in shrinkage of foam concrete and corresponding base mixes (mortar) with moisture content for a range of fresh densities are presented in Figs. 7.8 and 7.9. The water lost in the early stages of drying caused little shrinkage since this water mainly comes from large capillary pores (Tada and Nakano, 1983). The rate of increase in shrinkage is very rapid when the moisture content fell below 1% and 2.5% for foam concrete with density up to 1250 kg/m^3 and 1000 kg/m^3 respectively. At this level of moisture content the removal of water from very small pores and adsorbed water from gel surface can be attributed as a reason for such a steep increase in shrinkage without any appreciable variation in moisture content. Fig 7.9 shows that at any moisture content, the shrinkage of foam concrete is lower than that of base mix.

7.6.3 Effect of Density

The variation of drying shrinkage of foam concrete with time for a range of design densities are presented in Figs. 7.10 and 7.11. At the end of test period the shrinkage of base mix (mortar) is 27% higher than that of foam concrete with a density of 1000 kg/m^3. At early ages, (less than 14 days) (Fig. 7.10), the shrinkage achieved is 50 to 60% of the final shrinkage (reported at 100 days) and beyond 60 days the rate of shrinkage slowed down (Fig. 7.11). It is seen from Fig 7.11 that higher the density, higher is the final shrinkage. Shrinkage being a cement paste related phenomenon, the paste volume is a dominant feature (Fig 7.12). The drying shrinkage varies linearly with the paste content. Thus the higher volume of shrinkable paste in the mix with higher density is the cause for increase in shrinkage. This is consistent with the observations of earlier researchers with respect to cellular concrete (Schubert, 1983; Nambiar and Ramamurthy, 2009). The binary images representing the void system of foam concrete produced with two synthetic surfactants by processing and analysis of images of the prepared surfaces of specimens captured by an optical microscope at a magnification level of 20 X are shown in Figs. 6.1 and 6.2 for foam concrete with three densities. The analysis of binary images using the Image J analysis software showed that the median distance between voids varies from 150 to 450 microns and the median size varies from 315 to 100 microns for fresh density ranging from 1000 to 1500 kg/m^3. The reduction in pore wall thickness and thus reduced volume of micropores in the pore wall (with reduction in void-void spacing) in mixes with higher foam volume can be attributed to reduced shrinkage at lower density of foam concrete (Tada and Nakano, 1983). The difference in percentage shrinkage between foam concrete made with two surfactants is less than 6% (Fig 7.13). A comparison of 28 day drying shrinkage of foam concrete with a design density 1250 kg/m^3 produced with natural protein based foaming agent indicated that the variation is within 10% (Nambiar and Ramamurthy, 2009).

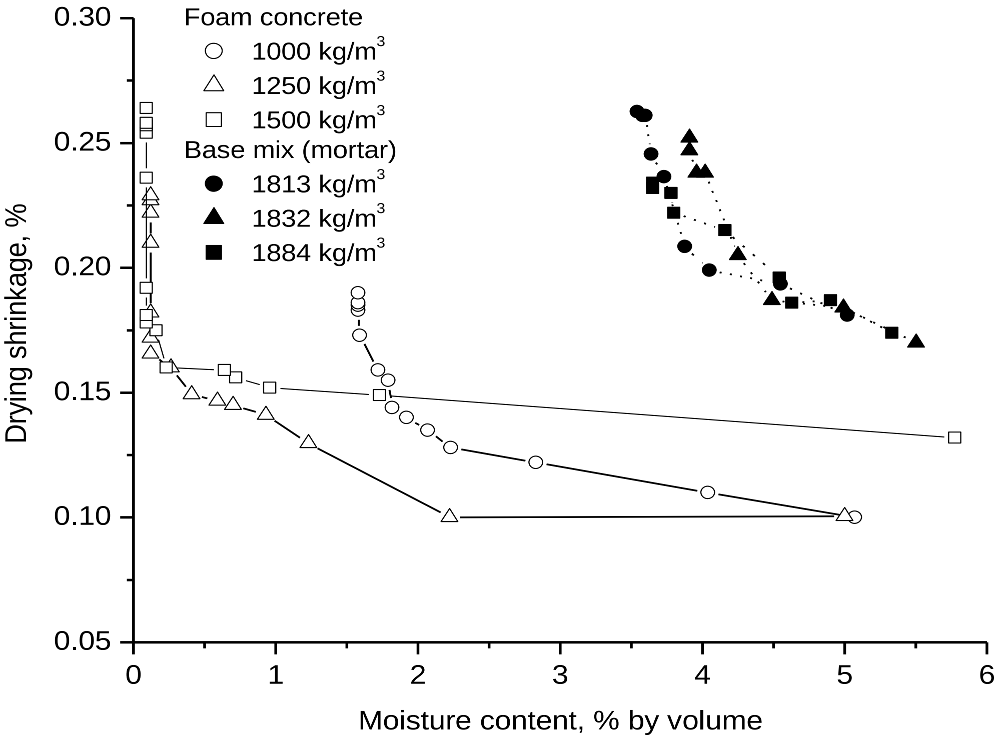

(a) SLS

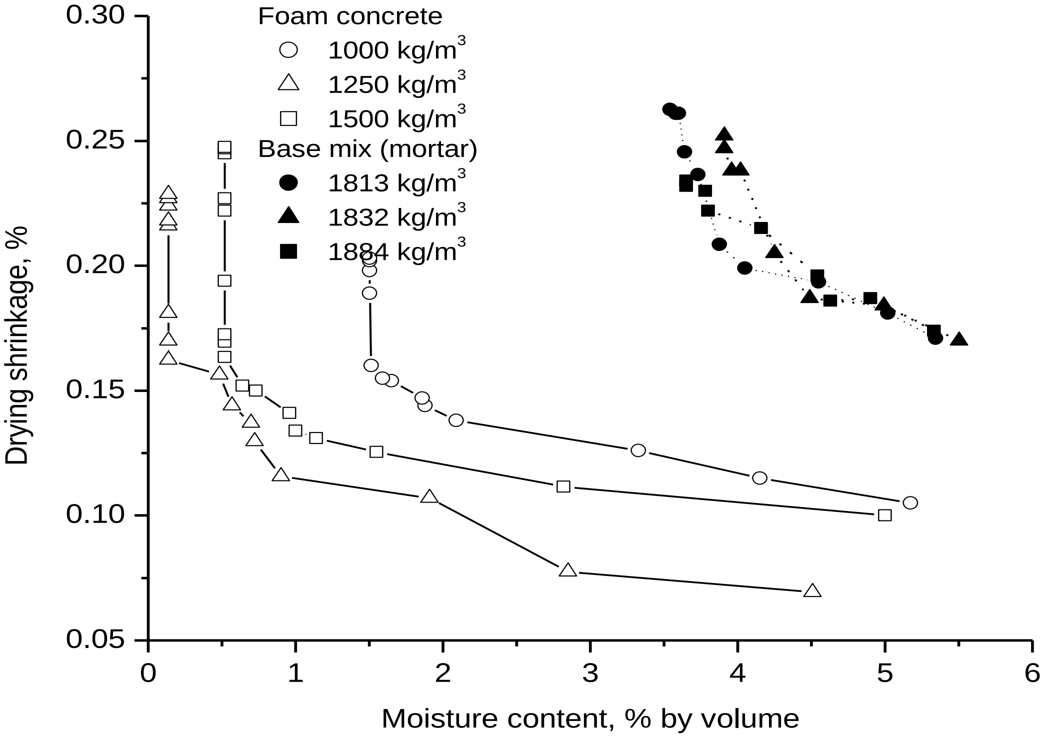

(b) SLES

Fig 7.8 Variation of shrinkage with moisture content for different design densities

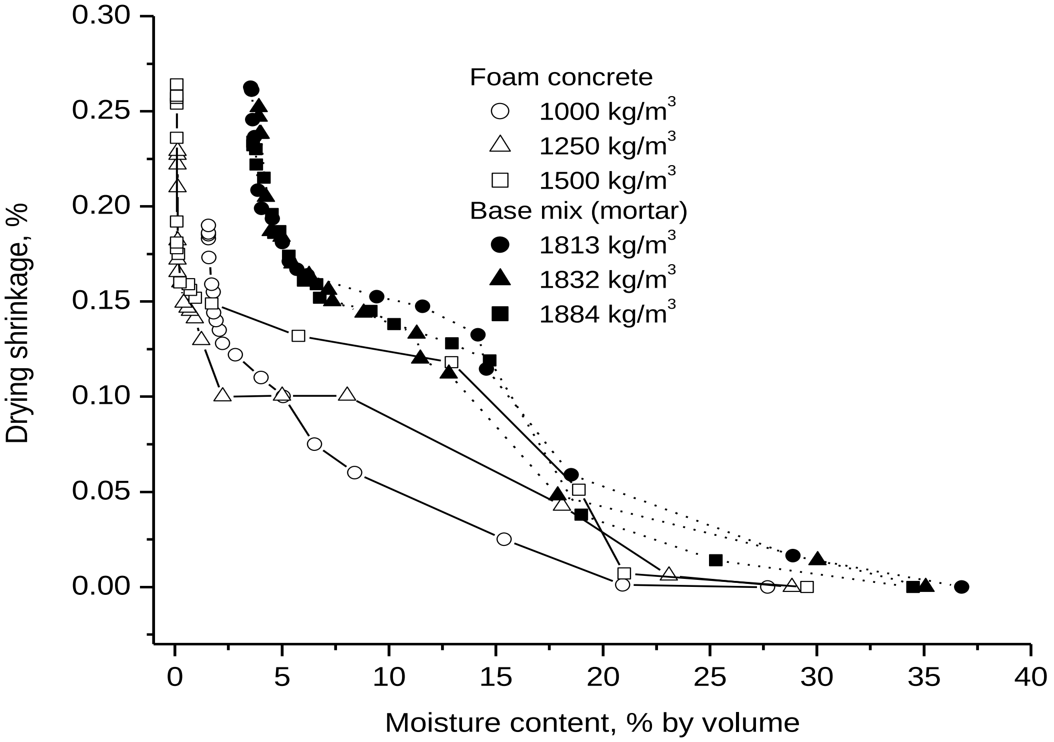

(a) SLS

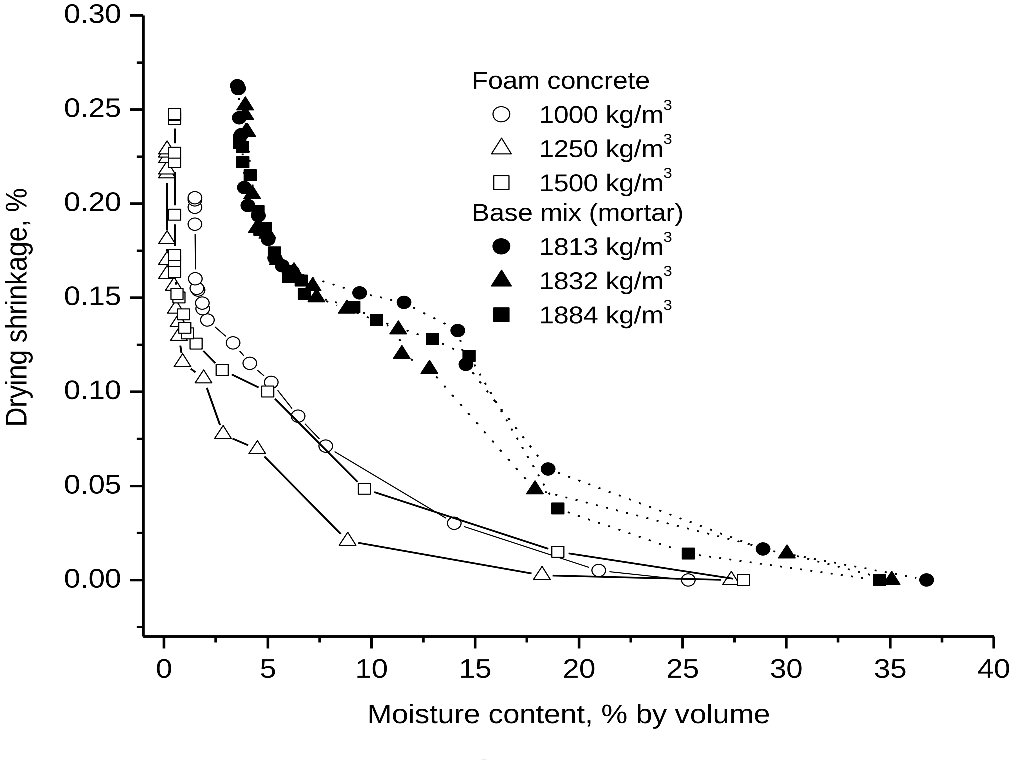

(b) SLES

Fig 7.9 Variation of shrinkage with moisture content for different design densities

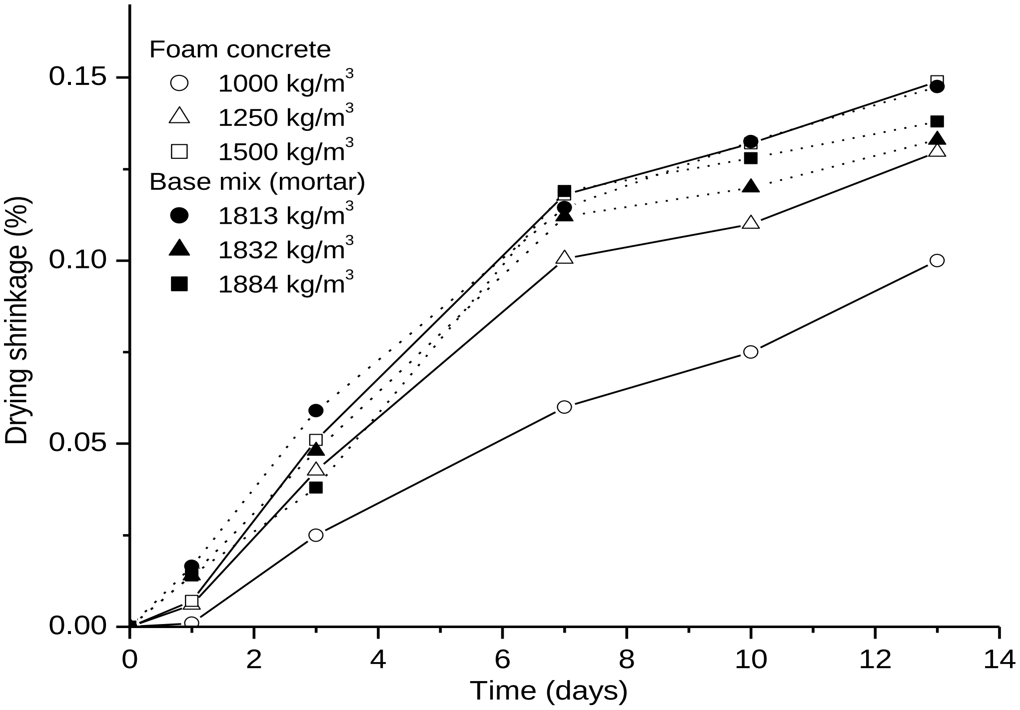

(a) SLS

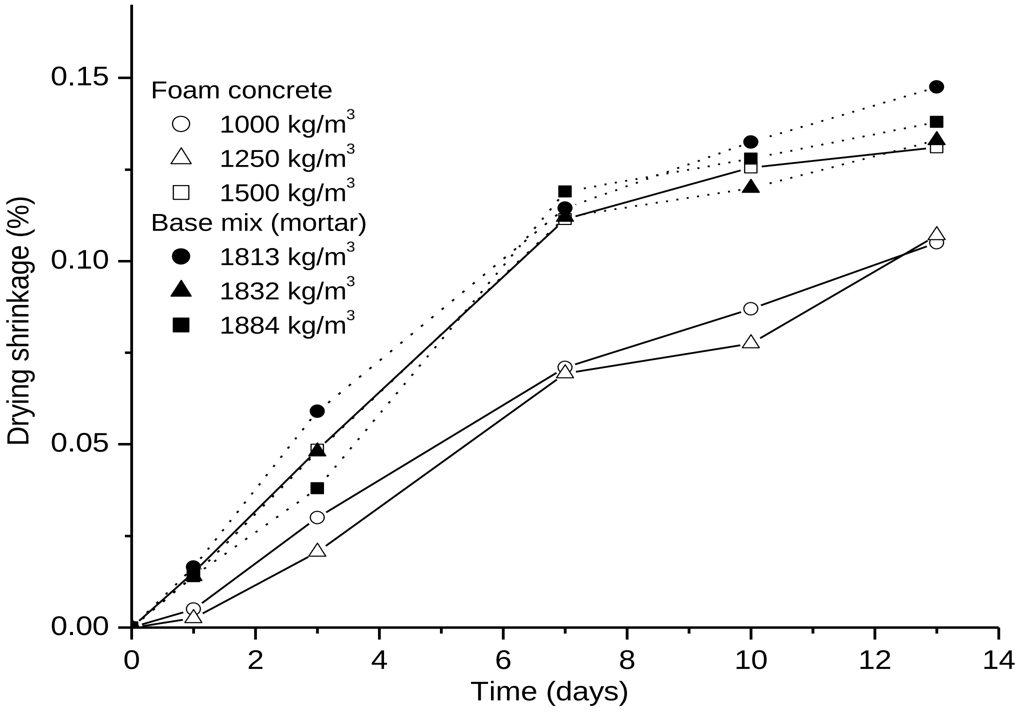

(b) SLES

Fig 7.10 Effect of density on variation of drying shrinkage with time for foam concrete

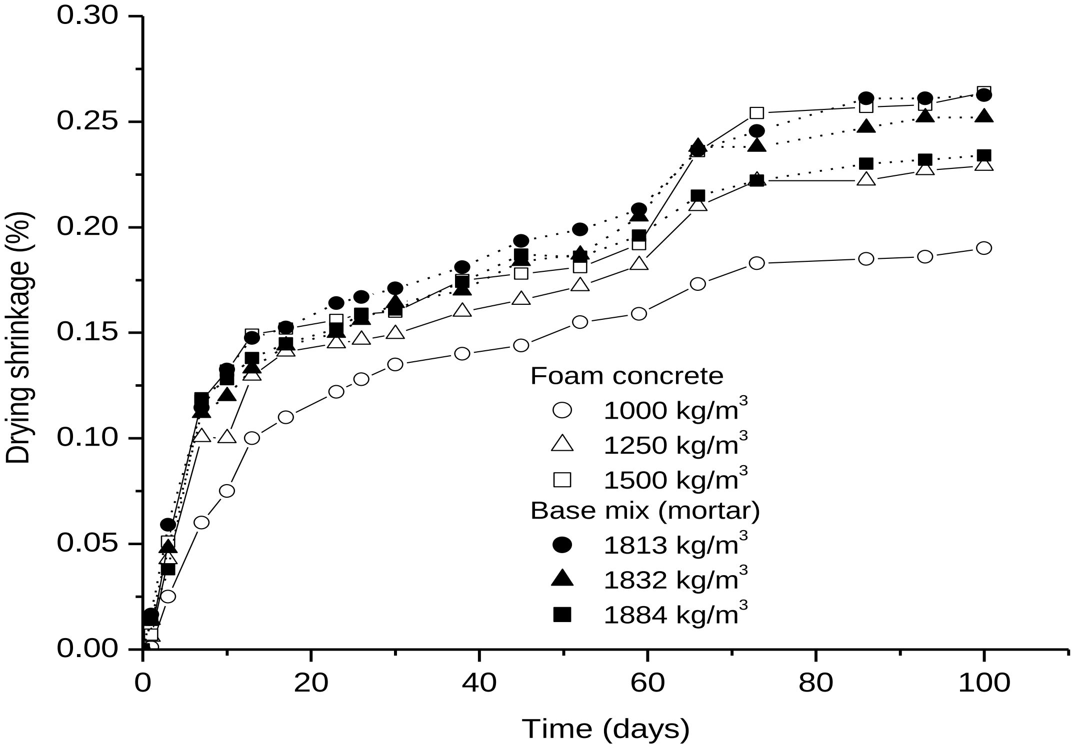

(a) SLS

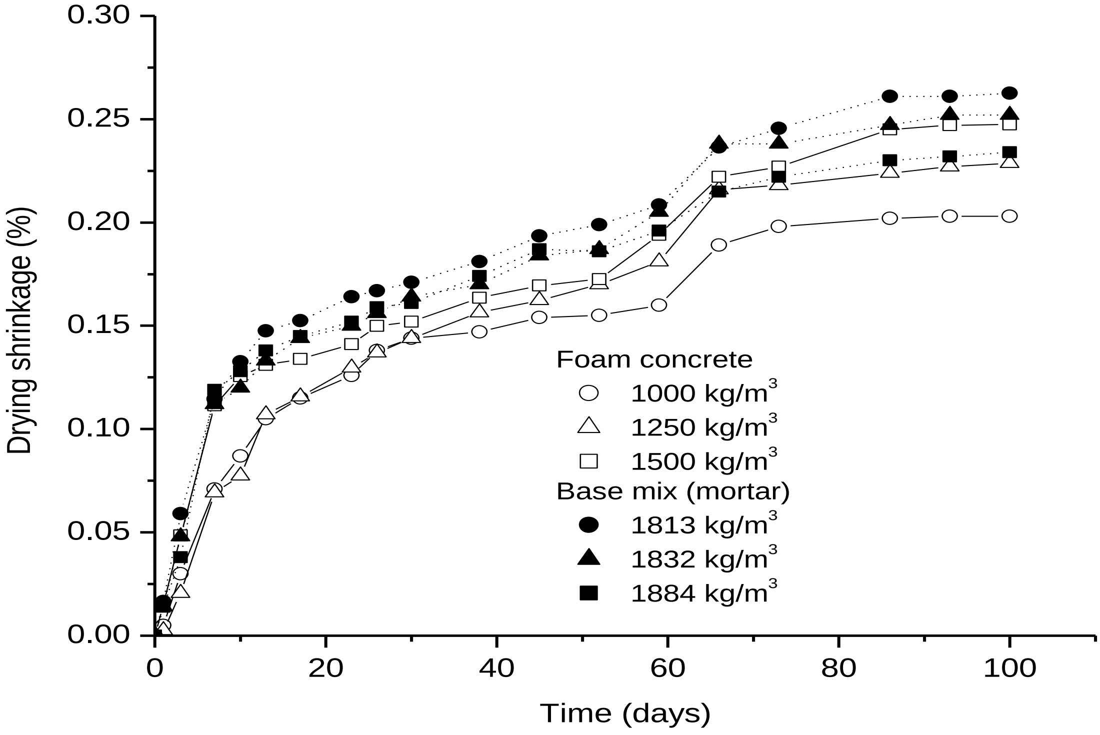

(b) SLES

Fig 7.11 Effect of density on variation of drying shrinkage with time

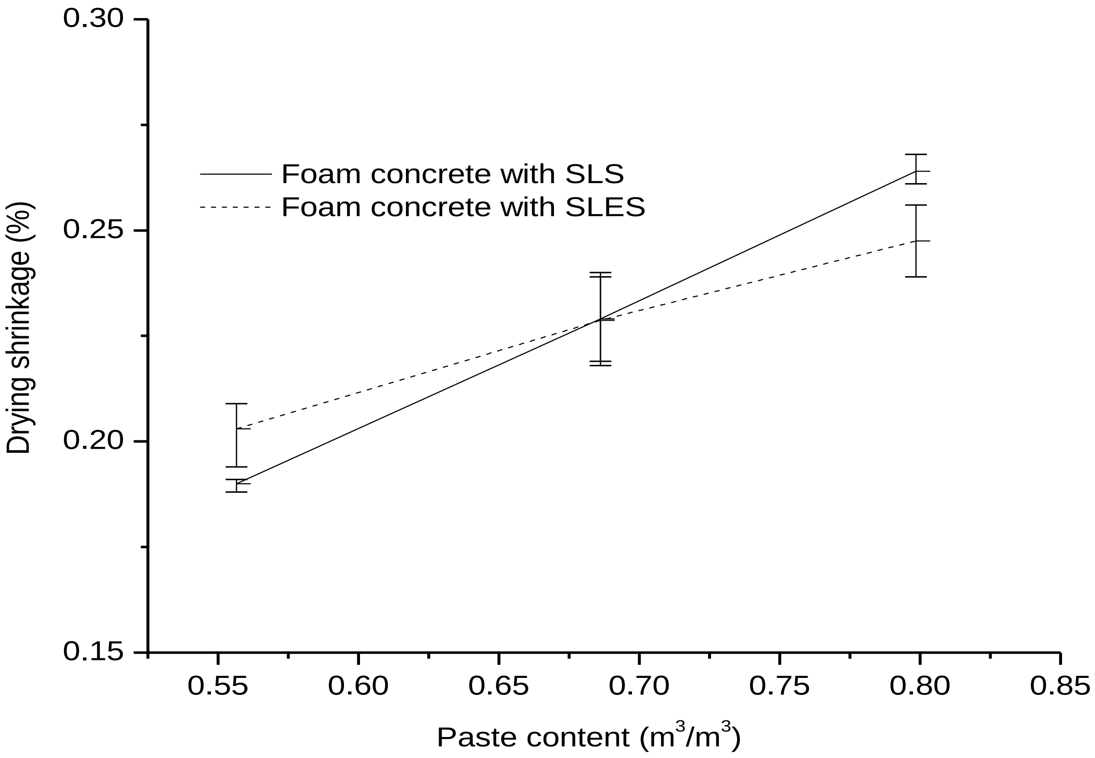

Fig 7.12 Variation of drying shrinkage with paste content

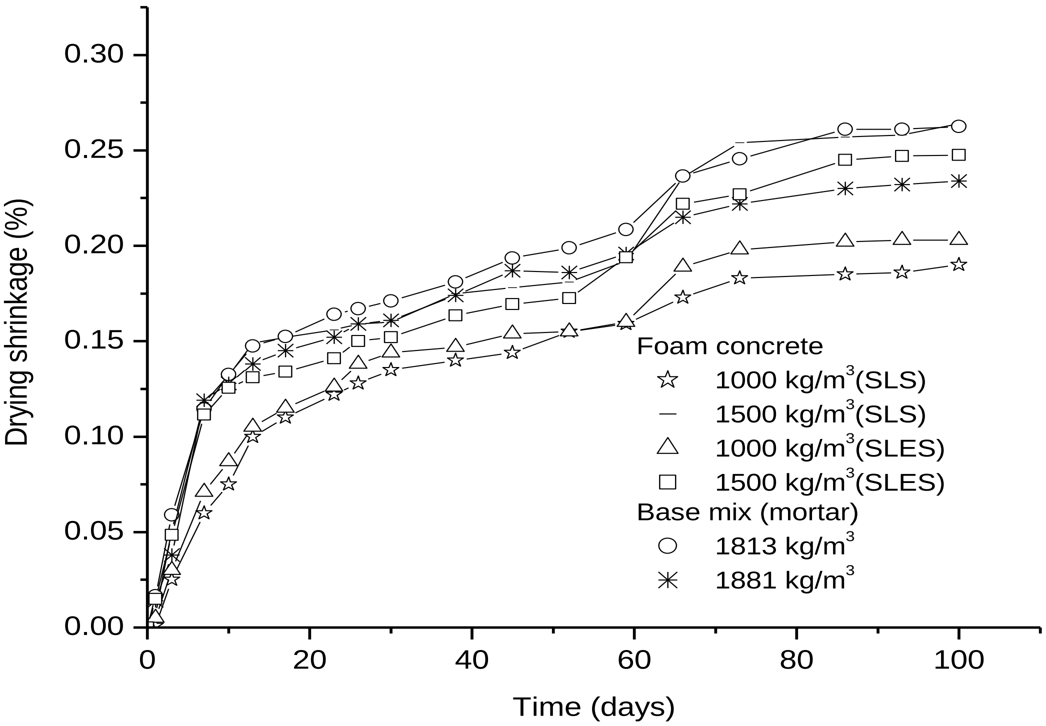

Fig 7.13 Comparison of drying shrinkage of foam concrete for two surfactants

7.7 SUMMARY

Water absorption by complete immersion, sorptivity and shrinkage behavior were studied for mixes with different design densities. Sorption and shrinkage have been observed to be lower than the corresponding base mixes (mortar without foam) for both the surfactants, the reduction being proportional to the amount of foam added. Hence the moisture movement in foam concrete depends on the pores in the paste content and not on the entrained air voids which are not interconnected. Also the effect of curing on the sorption behavior has been investigated and concluded that the sorptivity of air cured foam concrete is 2.5 times higher than that of water cured concrete. When the two surfactants are compared, the sorptivity of foam concrete with Sodium lauryl ether sulfate is 8 to 18% greater than that of Sodium lauryl sulfate when calculated based on cumulative sorption and depth of penetration. But the difference in percentage shrinkage between two surfactants is less than 6%.

CHAPTER 8

BEHAVIOUR OF FOAM CONCRETE UNDER SULPHATE ENVIRONMENT

8.1 GENERAL

Deterioration of concrete due to exposure to sulphate environment is encountered when structures are exposed to ground water containing sulphate or are placed in sulphate bearing soils. The nature of sulphate attack is well known to depend on type of cation present and the concentration of sulphate ion in the solution. The commonly reported forms of sulphate attack involve viz., (i) removal of hydrated cement paste due to formation of gypsum, (ii) formation of ettringite resulting in failure by expansion and (iii) decomposition of CSH gel into non-cementitious magnesium silicate hydrate affecting the strength (Cohen and Arnon, 1988; Al-Amoudi 2002; Prasad et al, 2006). Several test methods are necessary to assess the damage due to the above mentioned mechanisms. This chapter focuses on the investigations on the effects of different concentrations of sodium and magnesium sulphate solutions on the durability of foam concrete produced with two synthetic surfactants for a period of 1 year. The progressive deterioration and the relative sulphate resistance of different mixes were evaluated through the measurements of change in length, mass, strength and through chemical analysis.

8.2 SULPHATE ATTACK MECHANISM

Mechanism of sulphate attack is more complex as it depends on various factors like type of cement, presence of mineral admixtures, water-cement ratio, permeability, type of cation associated with sulphate ion, concentration of sulphate, time and duration of exposure and environment (Prasad et al, 2006; Brown et al, 2004; Sahmaran et al, 2007; CaO et al, 1997). Many researchers have documented the reactions involving the attack of magnesium and sodium sulphate solutions (Cohen and Arnon, 1988; Mehta and Monteiro, 1993; Al-Amoudi et al, 1995; Shannag and Shaia, 2003; Prasad et al, 2006) and Santhanam et al. (2003) developed models representing the mechanism of attack for plain and blended cement mortars exposed to different concentration of sulphate solution and to different temperatures.

It has been observed that sulphate solutions can attack most of the hydration products of cement. It turns out that each individual hydration product can give rise to a new compound as a result of sulphate attack.

Sodium sulphate ($N\bar{S}$) and Magnesium sulphate ($M\bar{S}$) can react with Calcium Hydroxide (CH) to produce gypsum ($C\bar{S}H_2$), sodium hydroxide (NH) and Magnesium Hydroxide (MH or brucite) according to the following approximate reactions

$CH + N\bar{S} + 2H$ -----------> $C\bar{S}H_2 + NH$ (8.1)

$CH + M\bar{S} + 2H$ ------------> $C\bar{S}H_2 + MH$ (8.2)

This phenomenon is often termed as gypsum corrosion. The formation of gypsum renders the structure soft, which leads to decrease in strength of the structure. The gypsum formed can react further with hydrated calcium aluminates (i.e C_4AH_{13}), hydrated calcium sulfoaluminates (i.e monosulphate – $C_4A\bar{S}H_{12\text{-}18}$), or unhydrated tricalcium aluminate (C_3A) according to the following equations:

$C_4AH_{13} + 3C\bar{S}H_2 + 14H$ -------------> $C_6A\bar{S}_3H_{32} + CH$ (8.3)
(ettringite)

$C_4A\bar{S}H_{12\text{-}18} + 2C\bar{S}H_2 + (10\text{-}16)H$ ------> $C_6A\bar{S}_3H_{32}$ (8.4)

$C_3A + 3C\bar{S}H_2 + 26H$ --------------------> $C_6A\bar{S}_3H_{32}$ (8.5)

(CaO- C, SiO_2 – S, Al_2O_3 –A, H_2O- H, Na_2O- N, MgO – M, SO_3- $\bar{S}$)

This phenomenon is called ettringite corrosion and the formation of ettringite is said to be expansive due to crystal growth and crystallization pressure. Two different mechanisms, one based on swelling theory and the other based on topochemical reaction theory have been reported to associate with the expansion of concrete due to formation of ettringite (Kurtis et al, 1998).

Presently there are rising concerns about the changes in strength of concrete material under long-term exposure to sulphate environment. The higher loss in strength was attributed to decalcification of C-S-H gel and formation of more quantum of gypsum. The reaction proceeds as shown below in the equation (8.6)

$C_3S_2H_X + 3M\bar{S} + (X+21)H$ -------> $3C\bar{S}H_2 + 3MH + 3SH_Y + (12+X-2Y)H$ (8.6)

Thus this reaction produces more gypsum that could go through another cycle of the reactions to produce more ettringite. Moreover the MH and the silica hydrate formed in this reaction can further react to produce magnesium silicate hydrate, which is reported to be non – cementitious, as indicated by the reaction shown below in equation 8.7

$4MH + SH_Y \text{-------}\rightarrow M_4SH_{8.5} + (4.5\text{-}Y)H$ (8.7)

The damaging effects on the CSH gel are only due to the action of magnesium sulphate. Thus the nature of deterioration in specimens placed in sodium and magnesium sulphate environment are different indicating that the mechanisms of deteriorations are not similar.

8.2.1 Linear Expansion Behaviour

The expansion resulting from sulphate attack is generally attributed to the formation of ettringite and gypsum. The influence of sulphate concentration and water-cement ratio on the magnitude of evolution of ettringite and gypsum in sodium sulphate solution was detected using X-ray diffraction analysis by Chen and Jiang (2008). The quantity of ettringite and gypsum as measured by Differential Scanning Calorimetry was found to increase with the time of immersion in the sulphate solution (Santhanam et al, 2003). In a study by Tian and Cohen (2000), the effect of gypsum formation on the resulting expansion of C_3S paste and mortar prisms was investigated. Ferraris et al (1997) observed that the pH and concentration of sulphate solution played an important role in the rate of expansion. In sodium sulphate, the increase in temperature accelerated the rate of expansion (Lawrence 1990). Prasad et al (2006) and Al-Amoudi et al (1995) presented the results of expansion of concrete under sodium, magnesium and mixed sulphate solution for a period of 1 year and identified that in mixed sulphate environment, the mode of deterioration was predominantly controlled by magnesium sulphate. Higher expansion was observed for specimens placed in sodium sulphate environment which may be attributed to formation of more quantum of delayed ettringite (Al-Amoudi et al, 1995). Jones and McCarthy (2005c) studied the performance of foam concrete exposed to Design sulphate Class 2 (DS2) and Class 4 (DS4) chemical solutions in terms of length change and chemical analysis for a period of 1 year. It was observed from their studies that the net expansion caused by chemical environment was lesser indicating good resistance of foam concrete.

8.2.2 Mass and Strength Variation

From the studies conducted by Justnes (2003) on resistance of mortar specimens to 5% sodium sulphate solution, it was observed that there was significant increase in mass until 6 months (which was associated with expansion) and decrease in mass from 10 months as the material started degrading. A steady rate of mass gain was also observed by Santhanam et al. (2003) for Portland cement and C_3S mortars when exposed to 4.44 mass % sodium sulphate solution for a period of 41 weeks. The gain in mass was reported to be associated with deposition of sulphate attack products in the pores (Thokchom et al. (2010). Park et al. (1999b) assessed the variation in mass and strength of high strength concrete under 10% sulphate solution for a period of 270 days and reported that the compressive strength and mass showed a greater tendency for decrease in magnesium sulphate solution than that in sodium sulphate solution. A mass loss of nearly 6% and drop in strength of 40% under 10% magnesium sulphate solution was reported by the authors based on their results (Park et al. 1999b). Mirza and Al-Noury (1986) observed a drop in strength of nearly 40% when autoclaved aerated concrete was subjected to 5% magnesium sulphate solution for a period of 90 days and concluded that the résistance to sulphate environment could be improved by surface treatment. There have been several investigations on mass and strength loss of normal weight concrete. But only limited information is available on the behavior of foam concrete in sulphate environment.

8.3 MATERIALS AND METHODOLOGY

The materials, their properties and mix proportioning described in the earlier Section 5.2 have been adopted for this study. Table 8.1 summarizes the different test solutions adopted for the study. The mass percentages of magnesium sulphate ($MgSO_4$) and sodium sulphate (Na_2SO_4) chosen were different with the objective of maintaining the same SO_4^{2-} concentration in both sodium and magnesium sulphate solutions. The solutions were changed at regular intervals to maintain the concentration level throughout the test period.

Table 8.1 Concentration of different test solutions used

Exposure	Type of cation associated with sulphate	Mass % of corresponding sulphate solution	Equivalent SO_4^{2-}, ppm
Severe	Sodium	0.5%	3380
Severe	Magnesium	0.424%	3380
Very Severe	Sodium	5%	33800
Very Severe	Magnesium	4.24	33800

For each mix, six prismatic specimens of size 40 mm X 40 mm X 160 mm were cast for exposure to each type of chemical and concentration of exposure. After 28-day water curing, steel balls were fixed at top and bottom of the specimen, initial length measurement was made using a length comparator and then the specimens were kept immersed in solutions of different sulphate environment. Periodical length measurement was done up to a period of one year.

To monitor the overall extent of deterioration due to both expansion cracking and softening types of sulphate attack, the deterioration has to be evaluated by change in strength and mass. Hence along with length measurement the mass of the prismatic specimens were also determined to assess any mass loss due to disintegration. To evaluate the variation of strength with period of immersion in sulphate solution, 180 cubes of 50 mm size were cast for each mix for testing 6 cubes at different ages for a period of one year. Out of 180 cubes, 150 cubes were immersed in different sulphate solutions and 30 cubes were water cured to serve as reference specimen for comparison. The strength loss was measured by sulphate deterioration factor (SDF) which is the percentage difference in strength of cubes after immersion in sulphate solution and in water at age “t” (Moon et al., 2002; Rasheeduzzafar et al, 1990).

For better understanding of the damage, the deteriorated parts namely the edges and corners of the mortar specimens were examined by XRD on a X-ray diffractometer using CuKα radiation with a wavelength of 1.54 Å at a voltage of 30 kV, scanning speed of 1 deg/min and current of 30 mA. The samples, which had been washed in acetone, were finely ground by hand and sieved through a 75 µm sieve. The powdered samples were then stored in airtight plastic containers. The samples used for investigation were fractured sections taken from the edge of foam concrete specimens.

8.4 LINEAR EXPANSION BEHAVIOUR

The present study presents the analysis of the results of linear expansion and chemical analysis of foam concrete produced with two synthetic surfactants subjected to attack by sodium and magnesium sulphate environment. The parameters identified for this study are density, type of cation associated with sulphate ion, concentration of sulphate and time of exposure. A comparison of behavior of foam concrete of different densities and the corresponding base mixes of mortar without foam has also been reported.

8.4.1 Expansion with Time in Sodium Sulphate Environment

8.4.1.1 Early age behaviour up to 28 days

The early age expansion up to 28 days in sodium sulphate (Na_2SO_4) environment and water for foam concrete with density 1000 kg/m^3 are presented in Fig.8.1. The expansion of foam concrete is marginally lower than that of base mix (mortar). Expansion of order of 0.035% is observed for foam concrete under water which is attributed mainly due to absorption of solution. The expansion of foam concrete under sodium sulphate environment is higher than that in water. For foam concrete in severe exposure sodium sulphate environment, the greatest expansion (up to 55% of expansion reported at the end of test period) has occurred during initial 28 days. The specimens in very severe sodium sulphate show a gradual expansion until 28 days (up to 11% of expansion is reported at the end of test period).

8.4.1.2 Long term behaviour up to 1 year

Figs. 8.2 to 8.4 show the long term (1 year) behaviour of foam concrete under water and sulphate environment. For foam concrete in water, there is no significant increase in expansion after 50 days. This confirms that the initial expansion observed in water is only from swelling due to absorption. The expansion of foam concrete in sodium sulphate environment is marginally higher than that in water. For foam concrete under severe exposure conditions, the net expansion (excluding the absorption due to water) is less than 0.02% and also lack of visual evidence of chemical attack indicates that the length change due to sulphate exposure is not significant (Jones and McCarthy, 2005c). Under very severe sodium sulphate environment, beyond 75 days, the specimens expands steeply till the end of 1 year. The expansion under very severe sodium sulphate environment is 4 to 4.5 times higher than those under severe exposure environment. Figs 8.5 and 8.6 shows the comparison of XRD patterns of foam concrete subjected to different concentrations of sodium sulphate and water at the end of 1 year. The comparison of XRD patterns of foam concrete exposed to severe and very severe concentration of sodium sulphate indicate that the intensity of Portlandite (marked as 18 and 21 in Fig 8.6) peak is higher in severe concentration exposed specimens for foam concrete with both the surfactants. This is because when subjected to lesser sulphate concentration, sulphate available is not sufficient to convert all portlandite (calcium hydroxide) into gypsum and ettringite. However in very severe exposure most of the calcium hydroxide is converted into gypsum and ettringite. Hence the intensity of ettringite (marked as 7 in Fig 8.6) and gypsum (marked as 8 and 11 in Fig 8.6) is relatively higher in very severe exposure than the ettringite (marked as 15 in Fig 8.6) and gypsum peaks (marked as 16 and 19 in Fig 8.6) in concrete under severe sulphate exposure conditions. The above observation is more evident in foam concrete with design density 1500 kg/m^3 (Fig 8.6). Also the calcite (marked as 12 in Fig 8.6) peaks are predominant in specimens exposed to very severe exposure conditions indicating that these specimens are subjected to high degree of leaching.

The variation of expansion with density under very severe exposure conditions is presented in Fig 8.7. For a given exposure, up to 5% increase in expansion is observed when the fresh density of foam concrete varies from 1000 to 1500 kg/m^3. The larger variation in density of concrete with paste content variation of 40% does not result in significant variation in expansion because it is complex to differentiate the mechanism of expansive sulphate reactions with respect to density. For a given volume of foam concrete with reduction in density the foam volume increases and hence the paste content reduces and this can be attributed to the marginal reduction in expansion observed.

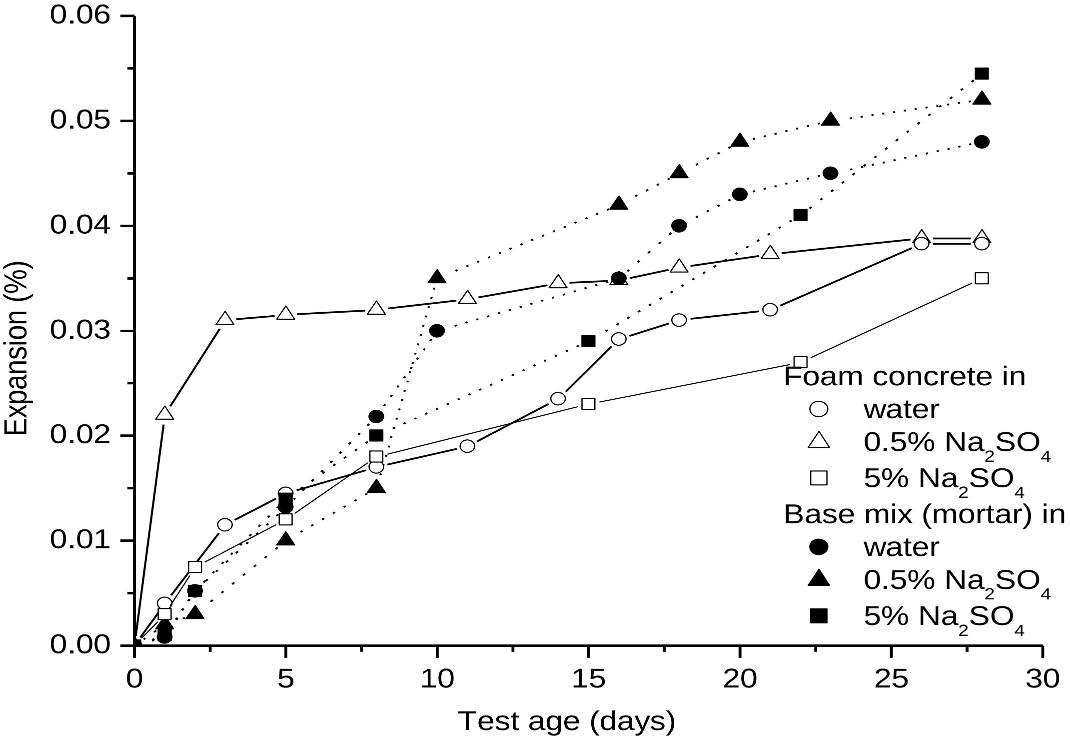

(a) SLS

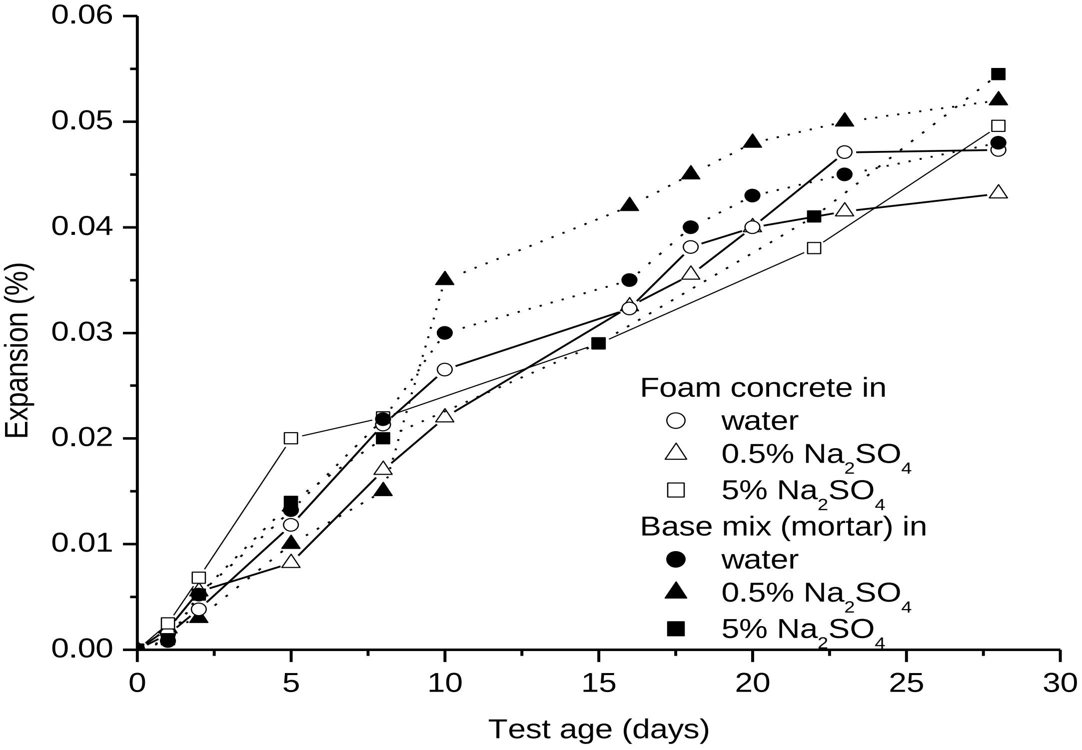

(b) SLES

Fig 8.1 Expansion with time during initial 28 days in Na_2SO_4 (1000 kg/m^3)

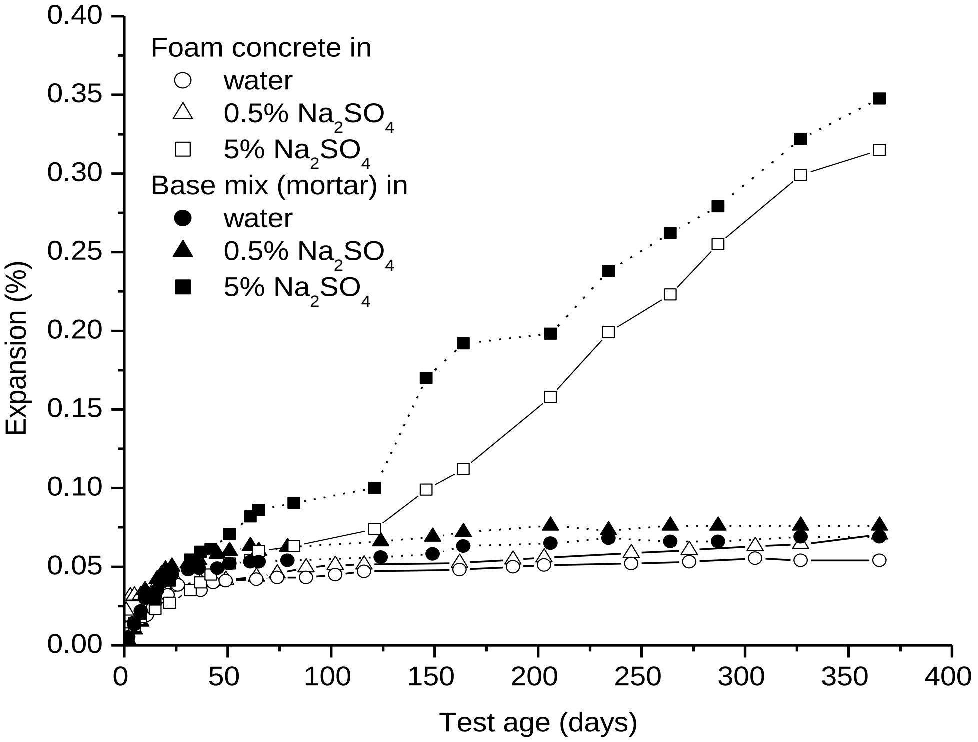

(a) SLS

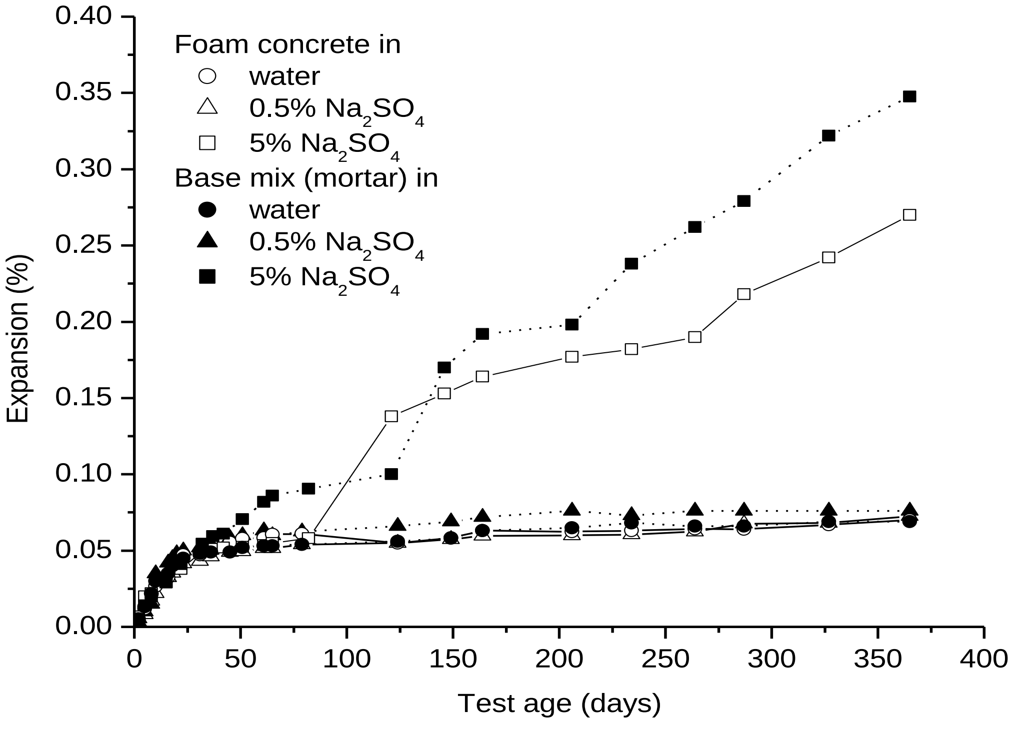

(b) SLES

Fig 8.2 Variation of expansion with time in Na_2SO_4 (1000 kg/m^3)

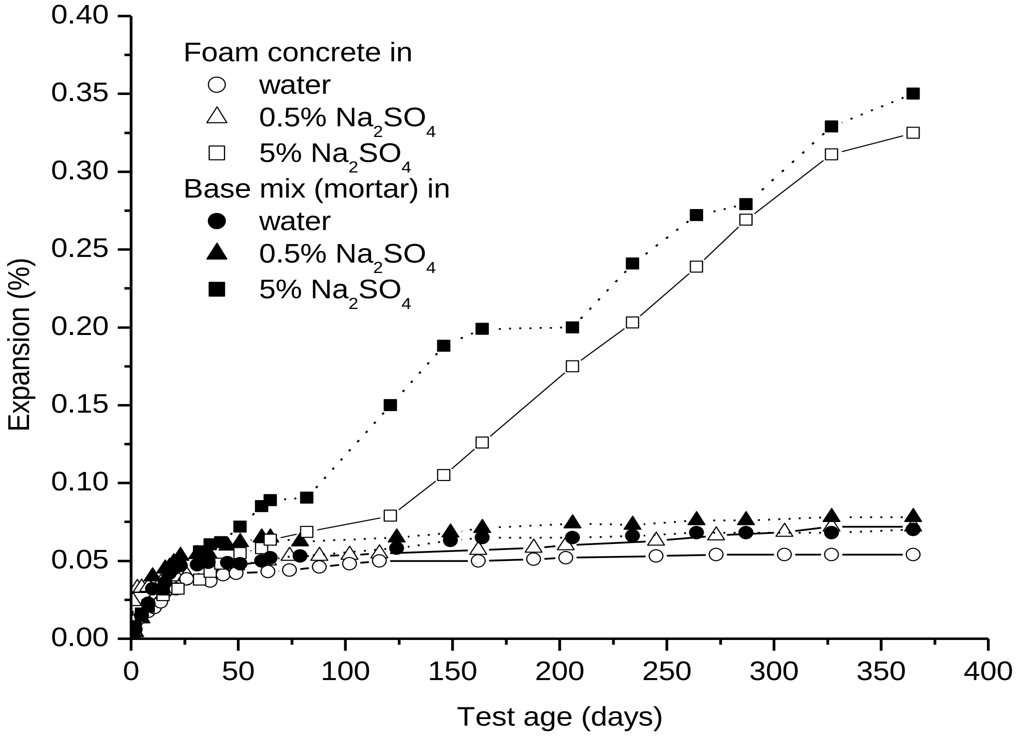

(a) SLS

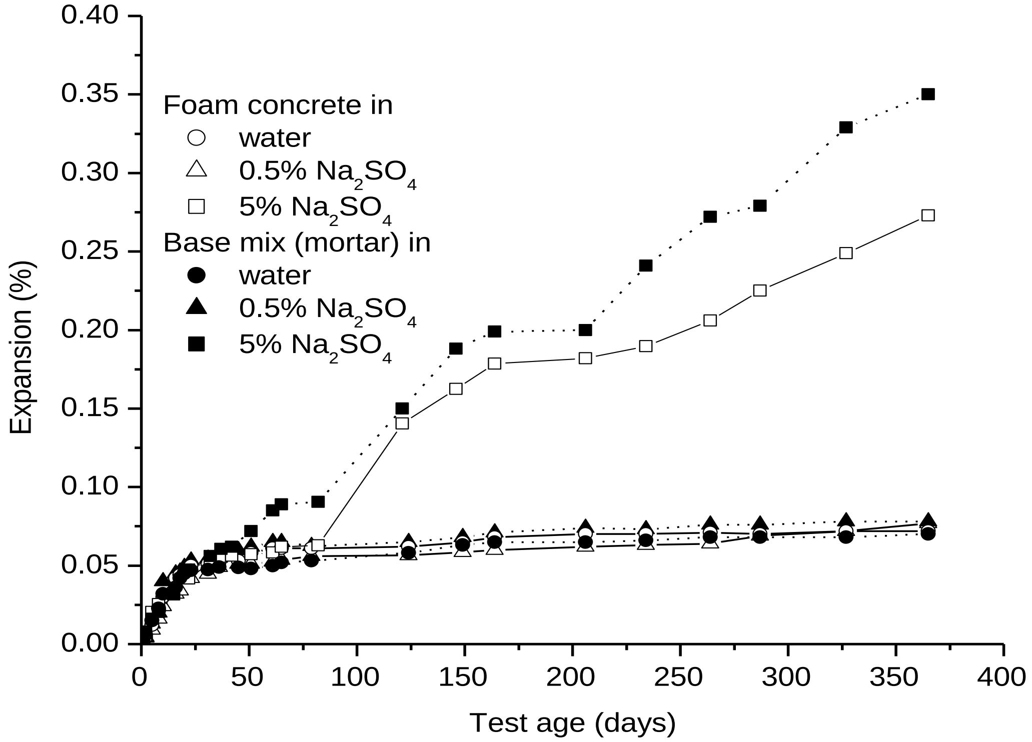

(b) SLES

Fig 8.3 Variation of expansion with time in Na_2SO_4 (1250 kg/m^3)

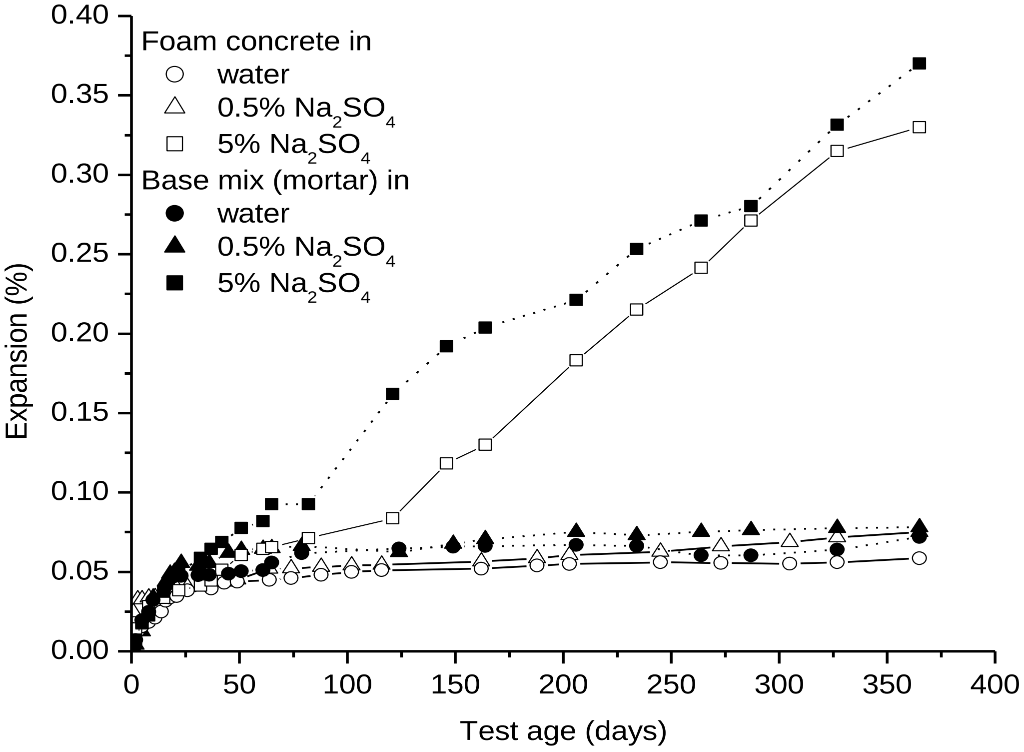

(a) SLS

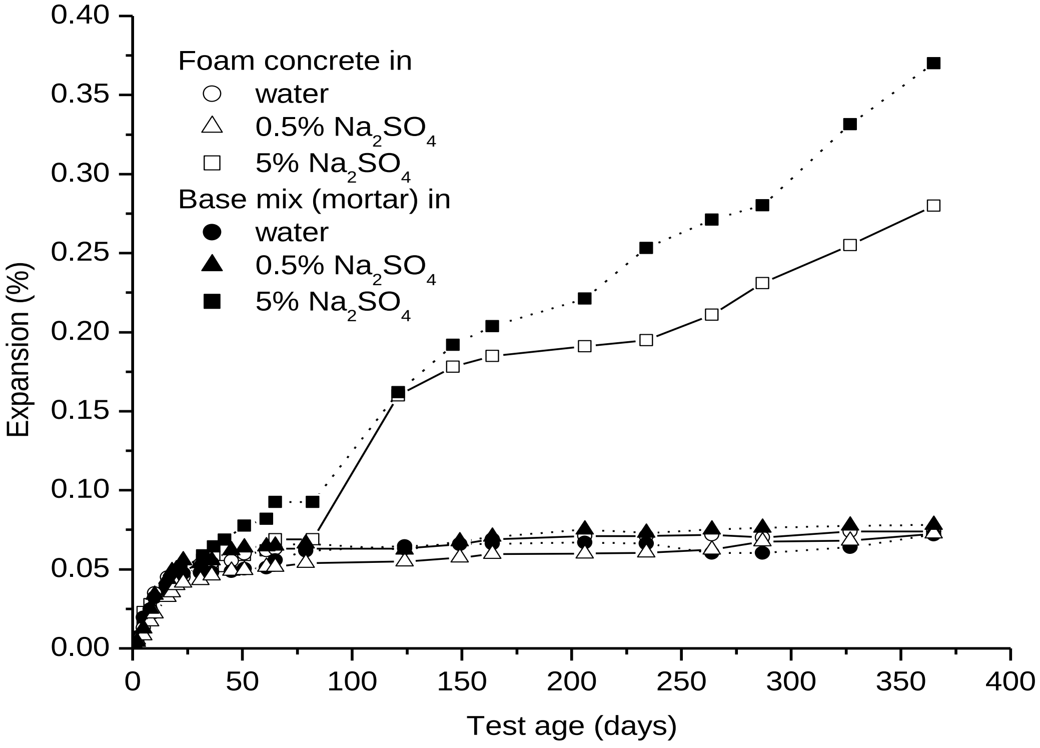

(b) SLES

Fig 8.4 Variation of expansion with time in Na_2SO_4 (1500 kg/m^3)

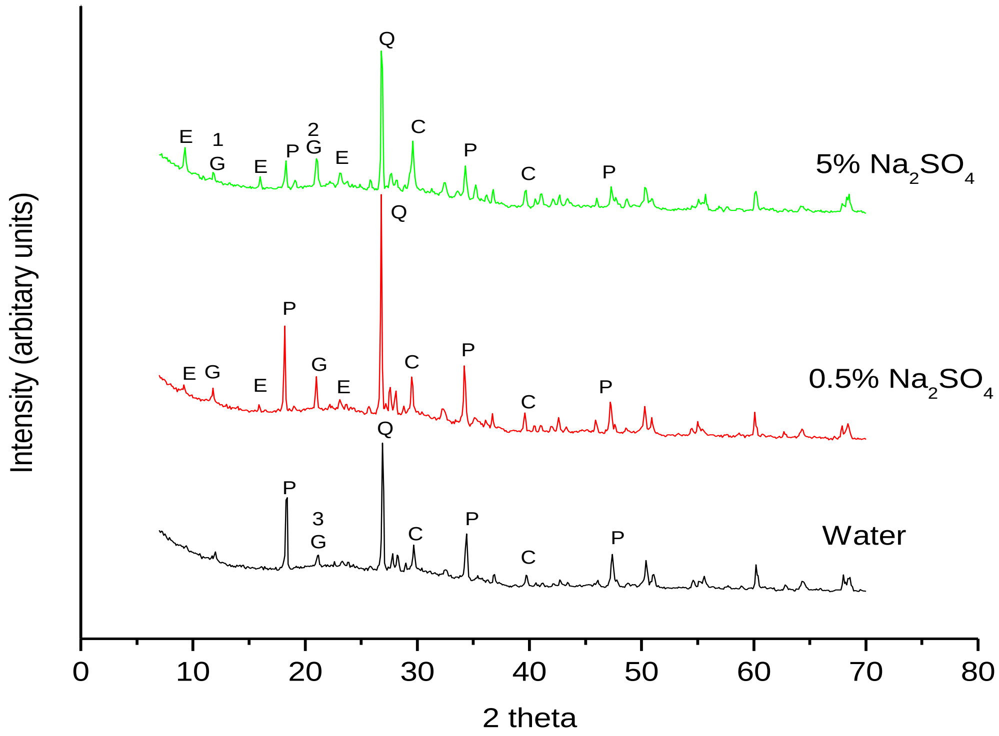

(a) SLS

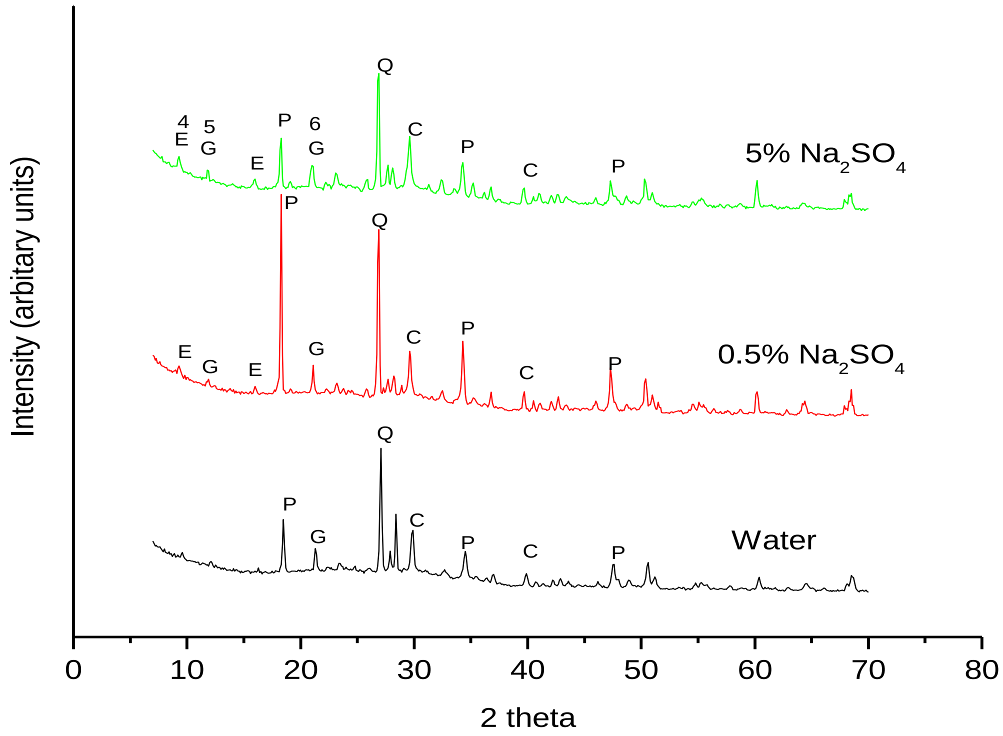

(b) SLES

E- Ettringite ($6CaO.Al_2O_3.3SO_3.32H_2O$), G-Gypsum ($CaSO_4. 2H_2O$), P-Portlandite ($Ca (OH)_2$), Q-Quartz (SiO_2), C-Calcite ($CaCO_3$)

Fig 8.5 XRD patterns of samples under Na_2SO_4 (1000 kg/m^3)

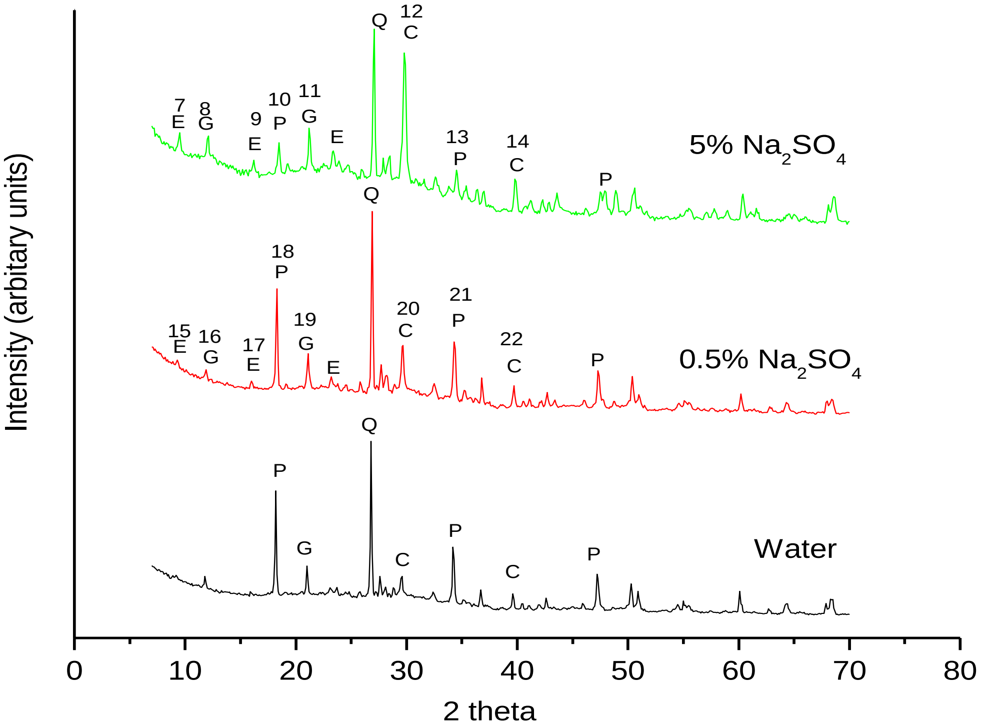

(a) SLS

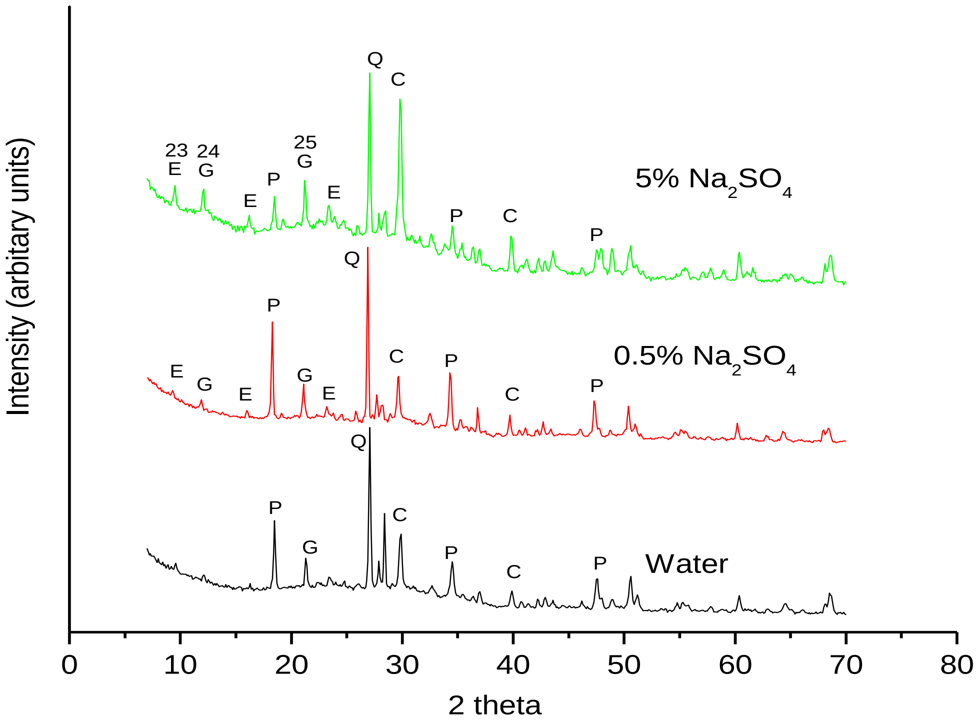

(b) SLES

Fig 8.6 XRD patterns of samples under Na_2SO_4 (1500 kg/m^3)

The comparison of XRD patterns of foam concrete of two densities indicate that the intensity of gypsum peaks (marked as 28, 29, 34 and 35 in Fig 8.8) in foam concrete with density 1500 kg/m^3 is higher than gypsum peaks (marked as 26, 27, 32 and 33 in Fig 8.8) in concrete with density 1000 kg/m^3. Irrespective of the density of foam concrete, the expansion of foam concrete is marginally lower than that of base mix (mortar) under severe exposure conditions. But for concrete exposed to very severe exposure conditions, the foam concrete with SLS and SLES is 10 and 29% respectively lower than that of the base mix (mortar). This is reflected in the XRD patterns of base mix specimens (mortar without foam) immersed in very severe sodium sulphate environment in which the intensity of peaks of gypsum (marked as 30 and 36 in Fig 8.8) are higher than the gypsum peaks (marked as 26 and 32 in Fig 8.8) for foam concrete with SLS and SLES.

8.4.2 Expansion with Time in Magnesium Sulphate Environment

8.4.2.1 Early age behaviour up to 28 days

The variation of expansion showing the early age behaviour up to 28 days in magnesium sulphate ($MgSO_4$) environment and water for foam concrete with density 1000 kg/m^3 is presented in Fig 8.9. The expansion of foam concrete under magnesium sulphate environment is (i) higher than that under water and (ii) lower than that of base mix (mortar). For foam concrete under severe exposure magnesium sulphate environment, the greatest expansion (up to 60% of expansion reported at the end of test period) has occurred during the initial 28 days. Under very severe exposure conditions the early age development of expansion is gradual similar to that observed under sodium sulphate environment.

8.4.2.2 Long term behaviour up to 1 year

Figs. 8.10 to 8.12 shows the long term behaviour of foam concrete under water and sulphate environment. The expansion of foam concrete in magnesium sulphate environment is higher than that in water. For foam concrete under severe exposure conditions, the increase in expansion beyond 75 days is not significant. Under very severe magnesium sulphate environment, beyond 75 days the specimens expands steeply. For a given density of foam concrete, the expansion is 3.5 to 4 times higher than that in severe exposure environment.

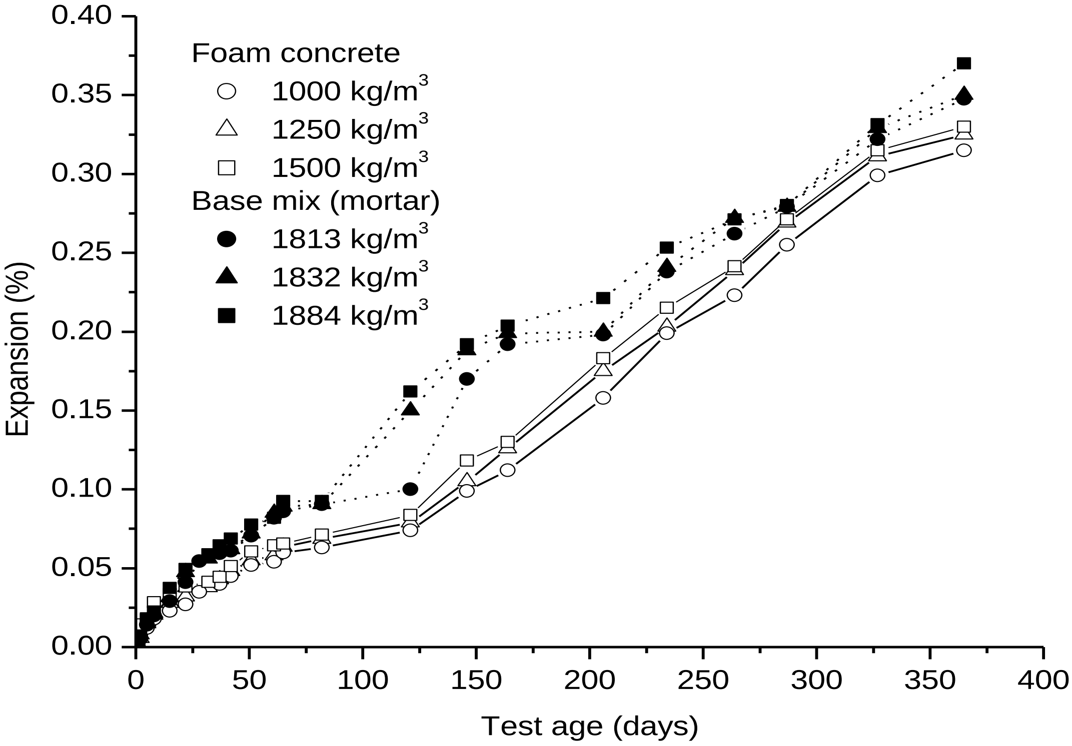

(a) SLS

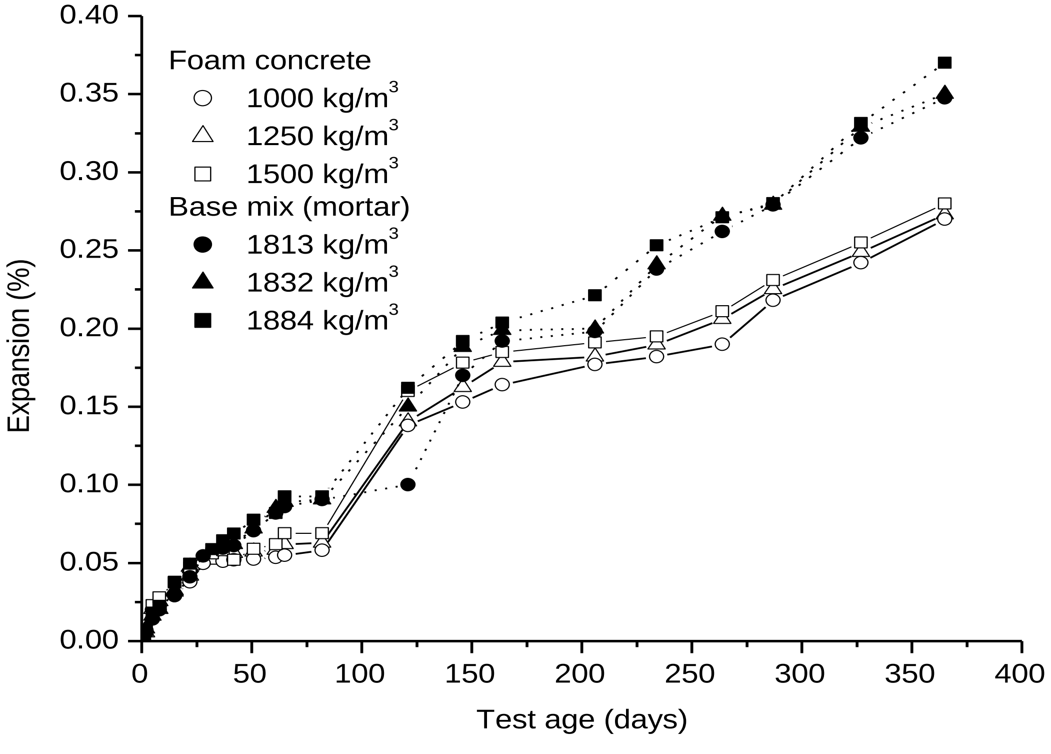

(b) SLES

Fig 8.7 Variation of expansion with density under very severe exposure Na_2SO_4

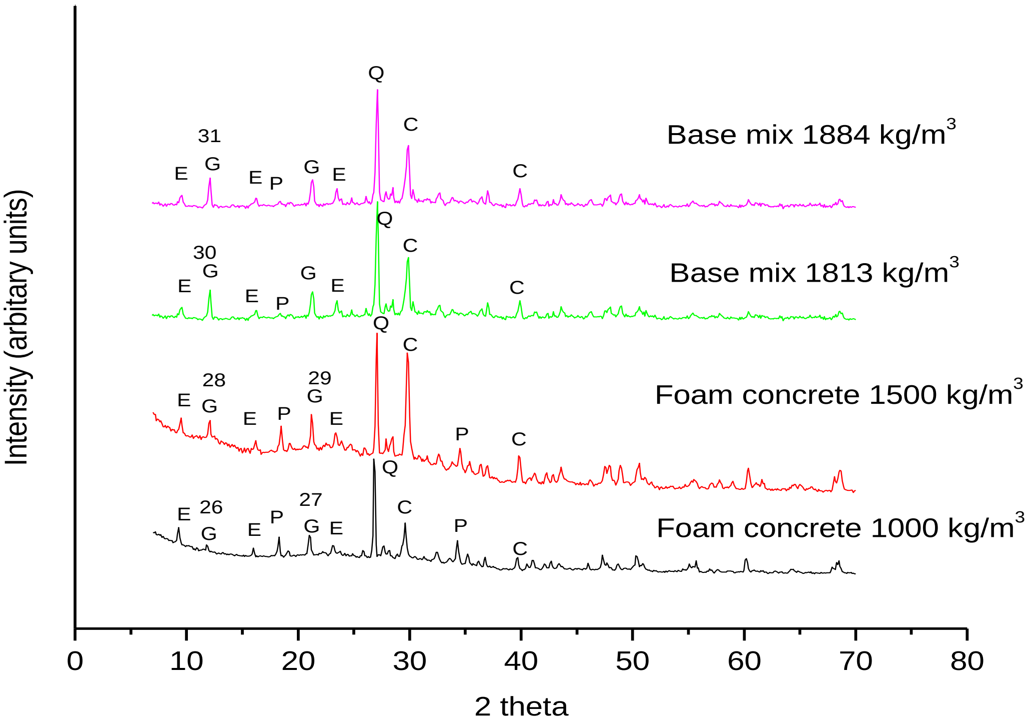

(a) SLS

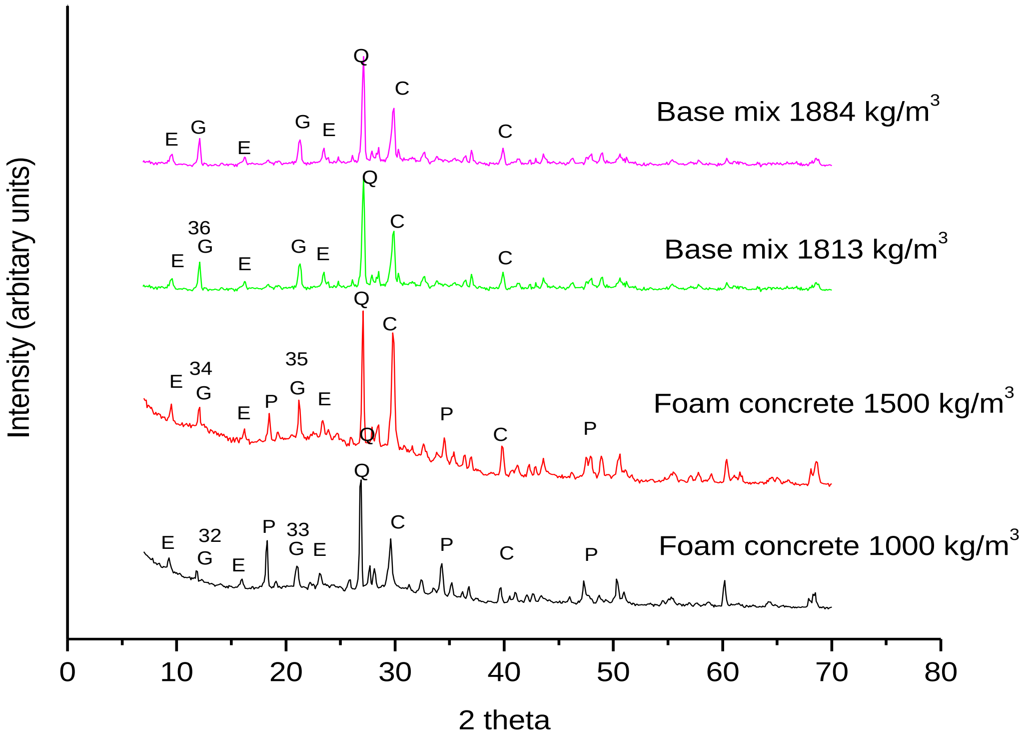

(b) SLES

Fig 8.8 XRD patterns of samples of different densities under very severe Na_2SO_4

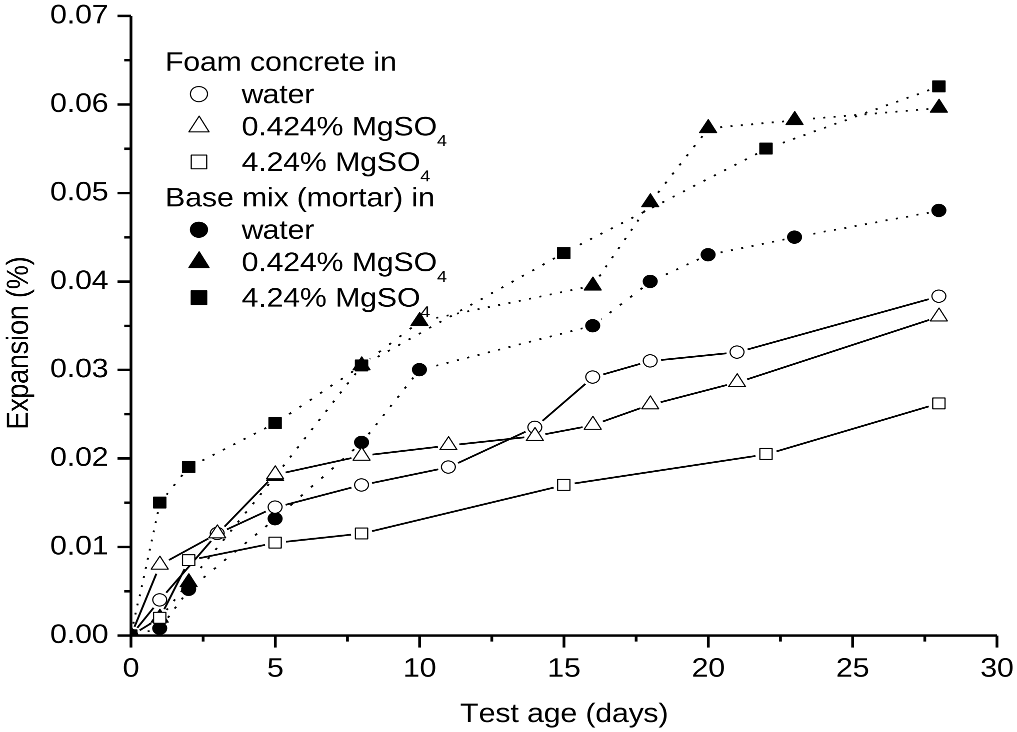

(a) SLS

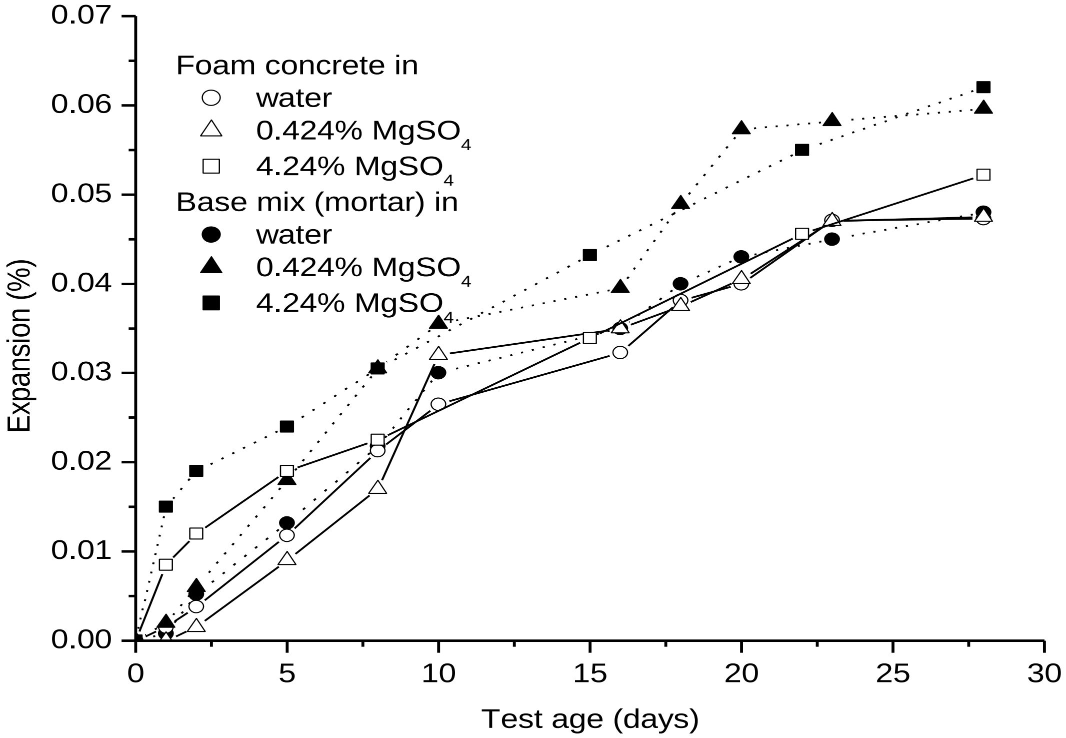

(b) SLES

Fig 8.9 Expansion with time during initial 28 days in $MgSO_4$ (1000 kg/m^3)

The comparison of XRD patterns of foam concrete exposed to different concentrations of magnesium sulphate and water at the end of 1 year is presented in Figs 8.13 and 8.14.The XRD patterns show that the intensity of Calcium hydroxide (marked as 48 in Fig 8.14) is relatively higher in foam concrete specimens subjected to severe exposure condition. In very severe exposure most of the calcium hydroxide (marked as 43 in Fig 8.14) is converted into gypsum and ettringite indicating that the dominant sulphate chemical reactions involved the conversion of portlandite (calcium hydroxide) into gypsum and etringite. Hence the intensity of ettringite (marked as 41 in Fig 8.14) and gypsum (marked as 42 and 44 in Fig 8.14) are relatively higher under very severe exposure than ettringite (marked as 46 in Fig 8.14) and gypsum (marked as 47 and 49 in Fig 8.14) in foam concrete subjected to severe exposure sulphate environment (Fig 8.14). Also the calcite peaks (marked as 45 in Fig 8.14) are predominant in specimens exposed to very severe exposure condition.

The variation of expansion with density under very severe exposure conditions is presented in Fig 8.15. For a given exposure, the difference in expansion observed in foam concrete with different densities (1000 to 1500 kg/m^3) is only 5%. The expansion of foam concrete is 30% and 47% lower than that of base mix (mortar) respectively under severe and very severe exposure conditions. For a constant density of foam concrete the mixes with surfactant Sodium lauryl ether sufate has relatively higher expansion than that of Sodium lauryl sulfate.

8.4.3 Behaviour under Sodium and Magnesium Sulphate Environment

Figs. 8.16(a) and 8.16(b) shows the comparison between expansion of foam concrete in sodium and magnesium sulphate environments. For a constant density, the expansion of foam concrete under sodium sulphate environment is higher than that exposed to magnesium sulphate environment. The difference in percentage of expansion observed is approximately 13% for foam concrete under severe exposure conditions. The above difference in expansion is noted to be 28% and 4% for foam concrete with SLS and SLES respectively under very severe exposure conditions. The chemical analysis shows that the sodium sulphate specimens has a higher amount of ettringite (marked as 51 in Fig 8.17) as compared to specimens subjected to magnesium sulphate wherein the gypsum peak (marked as 50 in Fig 8.17) is high in particular for foam concrete with SLS. Hence the relatively higher expansion in sodium sulphate environment can be attributed to the dominant chemical reaction between gypsum and hydrated calcium aluminate resulting in the formation of ettringite which is characterized by expansion and cracking (Al-Amoudi et al, 1995; Jones and McCarthy, 2005c).

8.5 MASS AND STRENGTH VARIATION

The present study focuses on variation in strength and mass of foam concrete produced with two synthetic surfactants with density when subjected to different concentrations and type of sulphate environment for a period of 1 year.

8.5.1 Variation in Mass under Sodium Sulphate Environment

The variation of mass from the initial state of saturated surface dry condition with time under water and sodium sulphate environment is presented in Figs. 8.18 to 8.20. An increase in mass of up to 4% is observed for foam concrete under water and this gain in mass is due to swelling from absorption of solution. The gain in mass of base mix (mortar) (BM) is higher than that of foam concrete. For foam concrete under sulphate solution, a continuous increase in mass is observed up to a period of 1 year when compared to the expansion which got leveled off beyond 28 days of exposure. This shows that variation in mass could be associated with expansion only during the initial period (Justnes, 2003). Hence the measurement of linear expansion is not reliable measure for foam concrete. The final gain in mass is as high as 5% and 10% under severe and very severe exposure conditions respectively. The probable reason of mass gain at later stages can be associated with the deposition of sulphate attack products namely gypsum and ettringite in the pores (Al-Dulaijan et al, 2003). The mass gain under sulphate environment is higher than that under water. The increase in mass under very severe sodium sulphate environment is 1.5 to 3.5 times higher than that in severe exposure environment for surfactants Sodium lauryl sulfate and Sodium lauryl sulfate respectively. The greater mass gain in very severe exposure environment can be attributed to more quantum of deposition of gypsum in the pores of concrete.

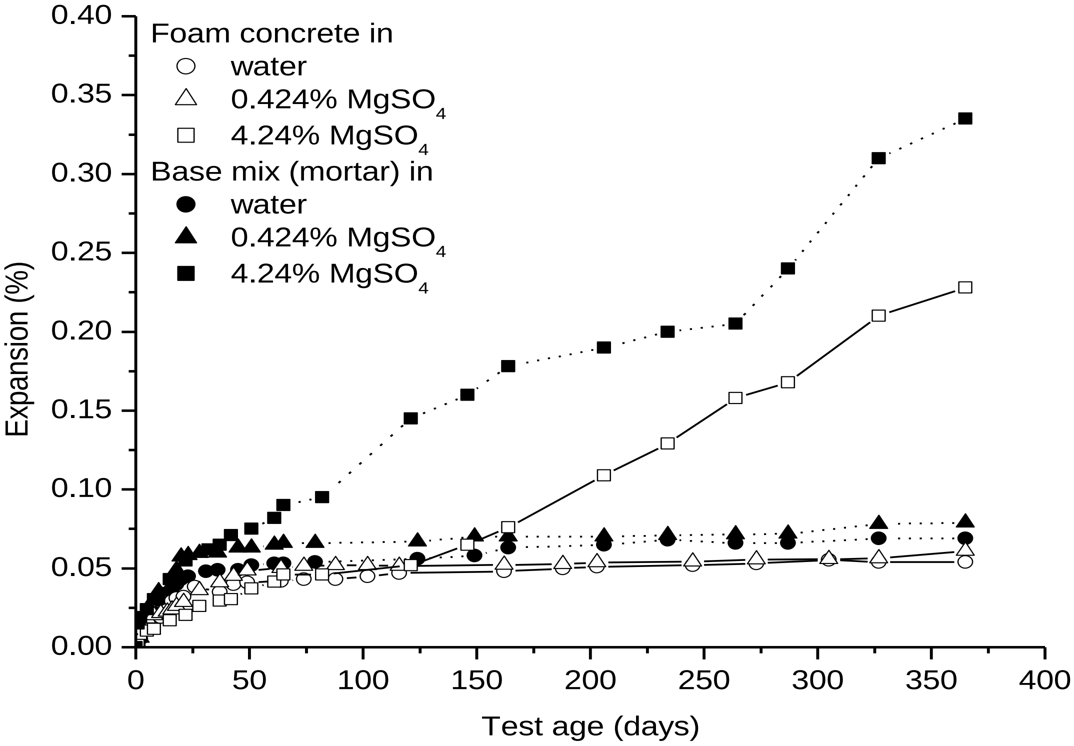

(a) SLS

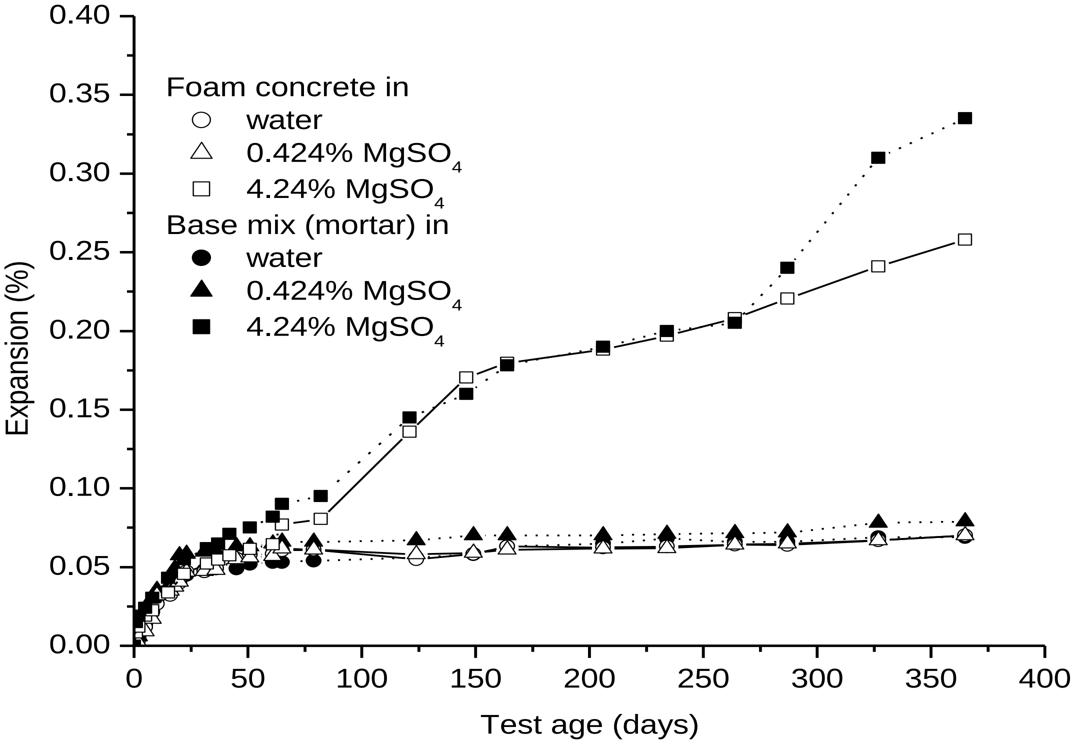

(b) SLES

Fig 8.10 Variation of expansion with time in $MgSO_4$ (1000 kg/m^3)

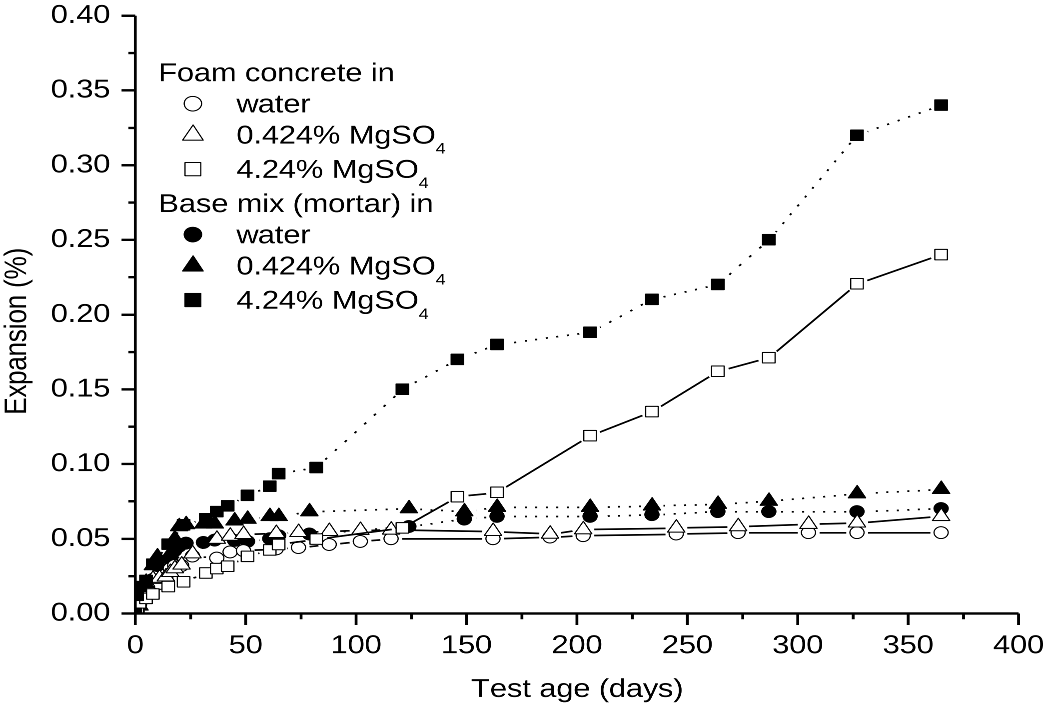

(a) SLS

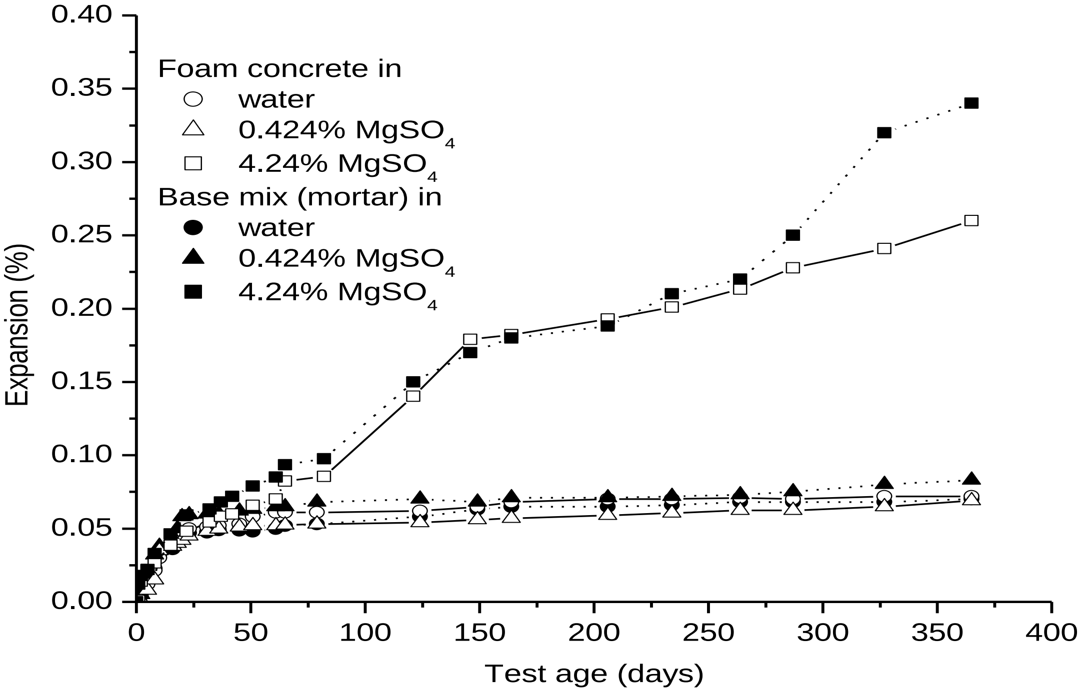

(b) SLES

Fig 8.11 Variation of expansion with time in $MgSO_4$ (1250 kg/m^3)

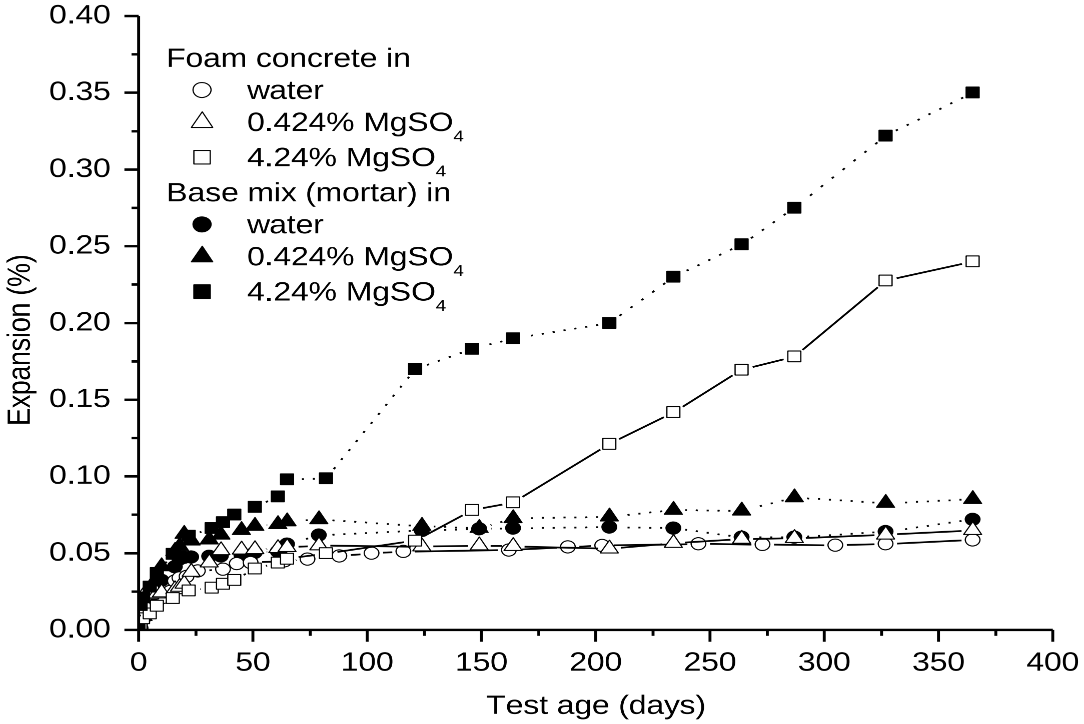

(a) SLS

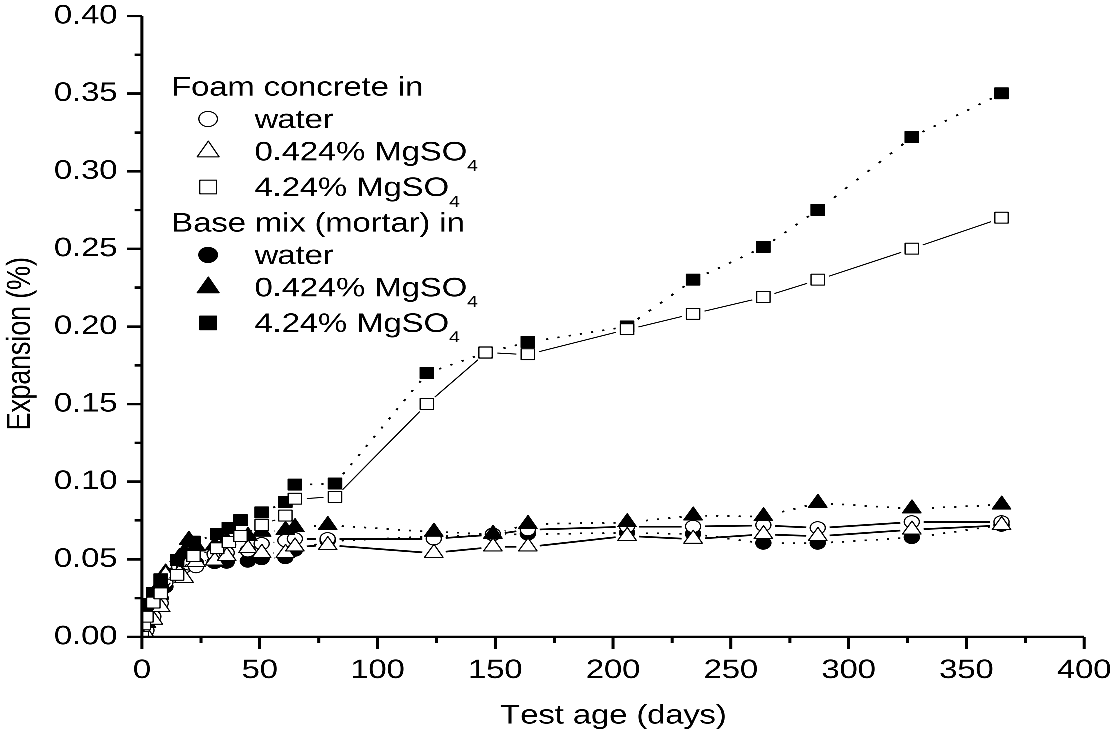

(b) SLES

Fig 8.12 Variation of expansion with time in $MgSO_4$ (1500 kg/m^3)

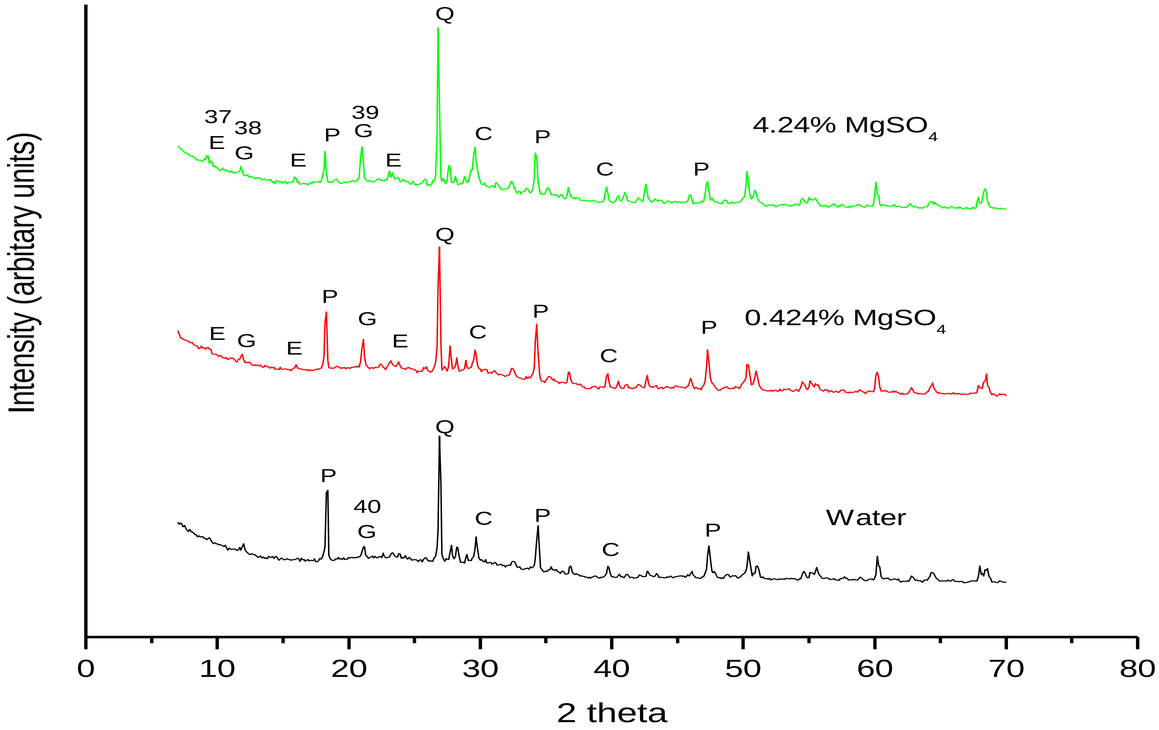

(a) SLS

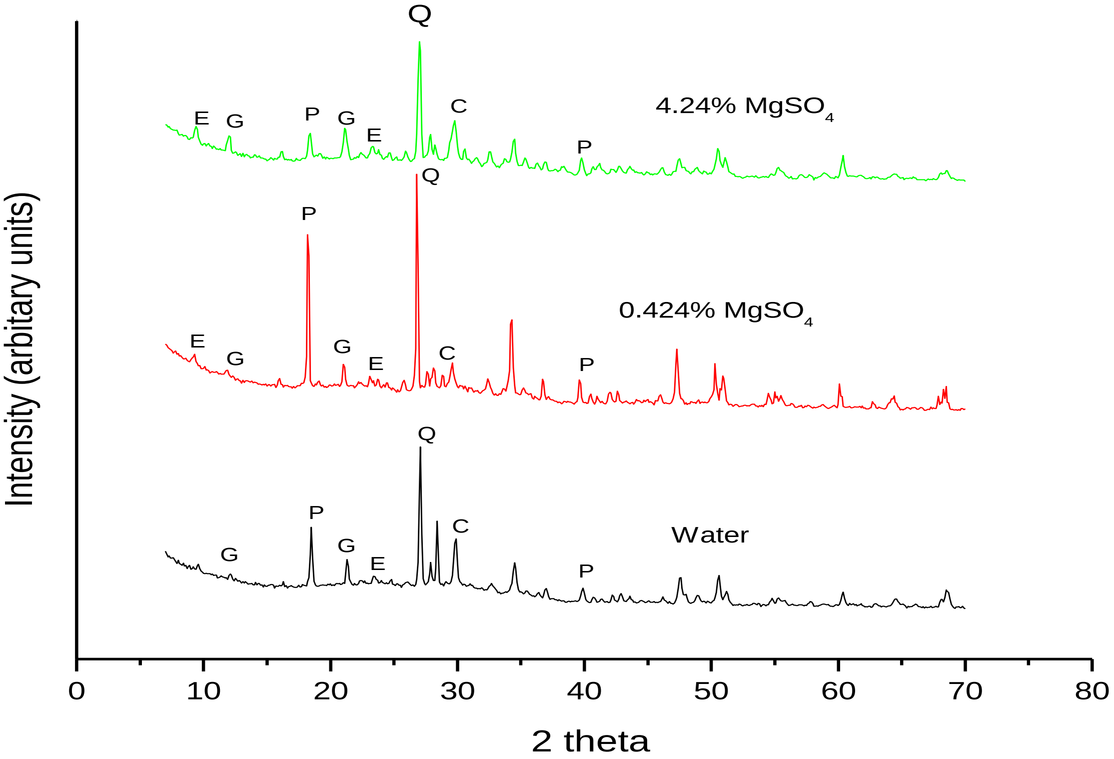

(b) SLES

Fig 8.13 XRD patterns of samples under $MgSO_4$ (1000 kg/m^3)

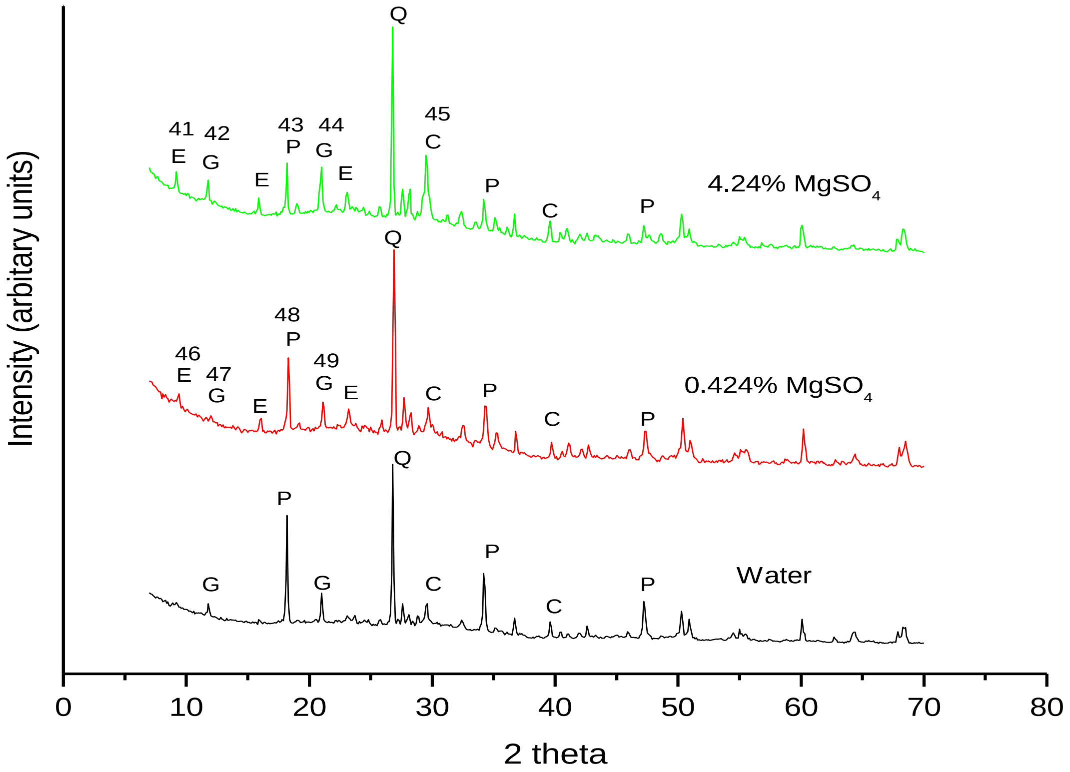

(a) SLS

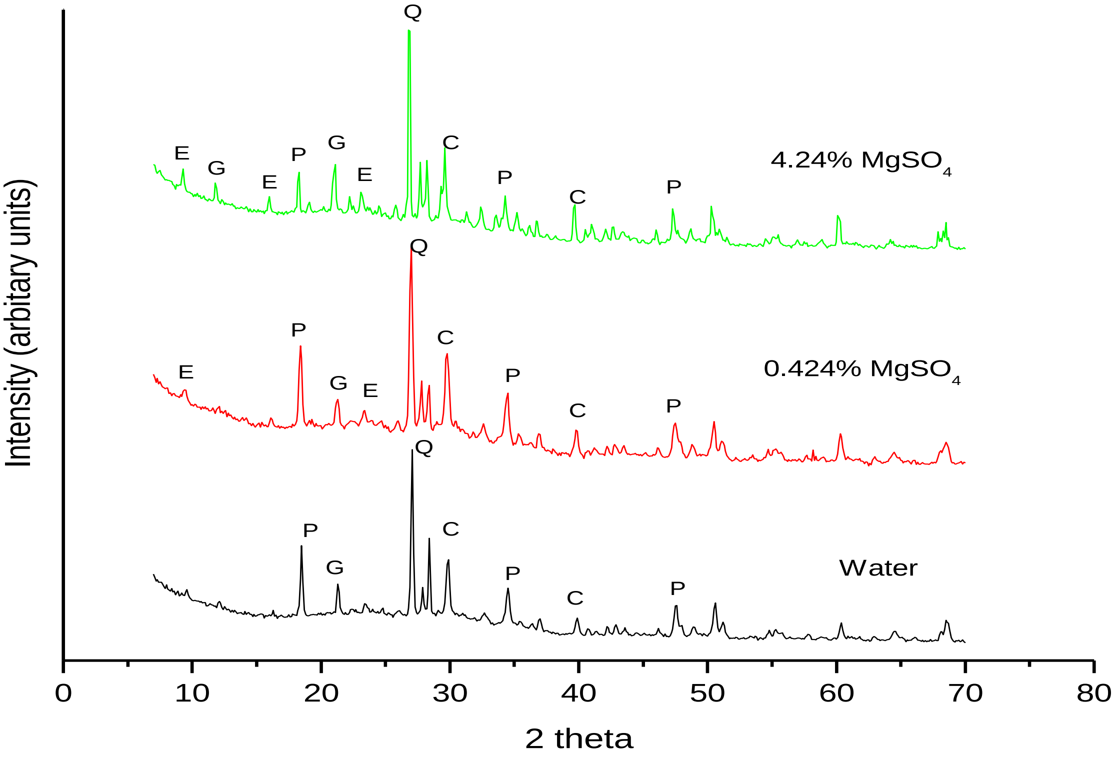

(b) SLES

Fig 8.14 XRD patterns of samples under $MgSO_4$ (1500 kg/m^3)

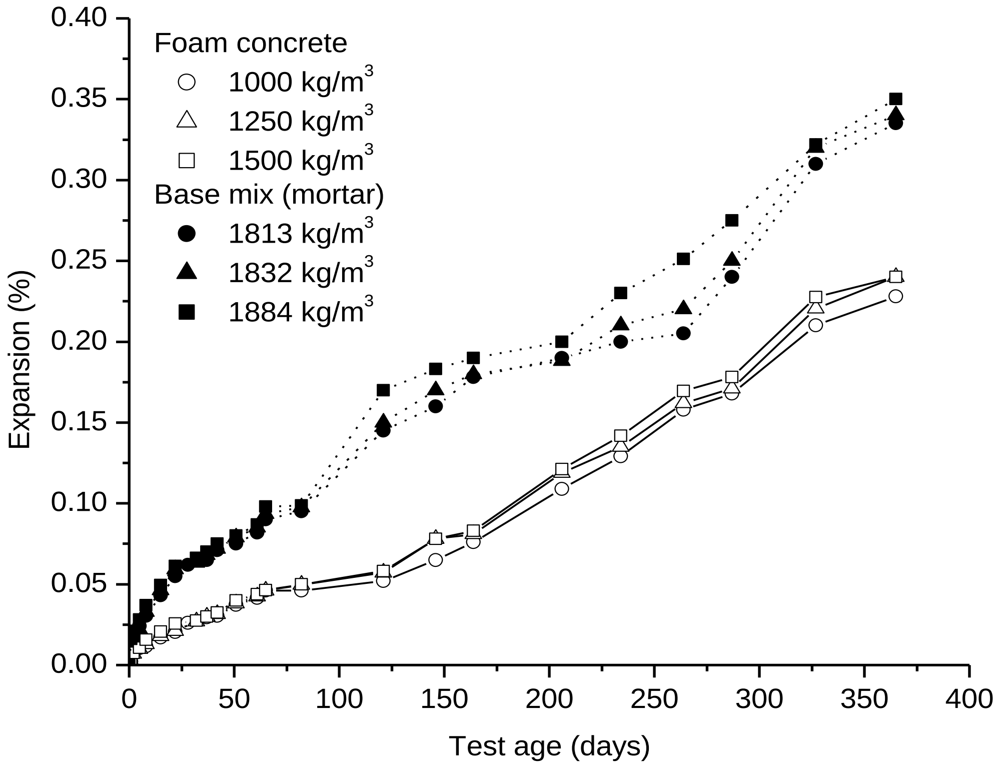

(a) SLS

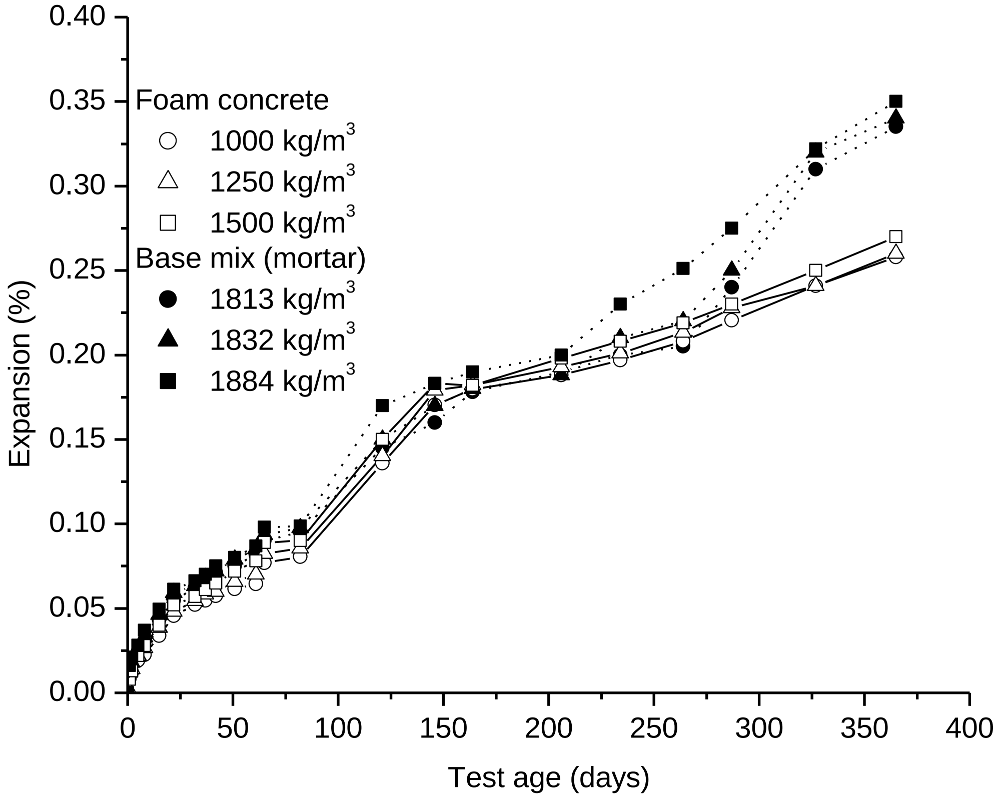

(b) SLES

Fig 8.15 Variation of expansion with density under very severe exposure $MgSO_4$

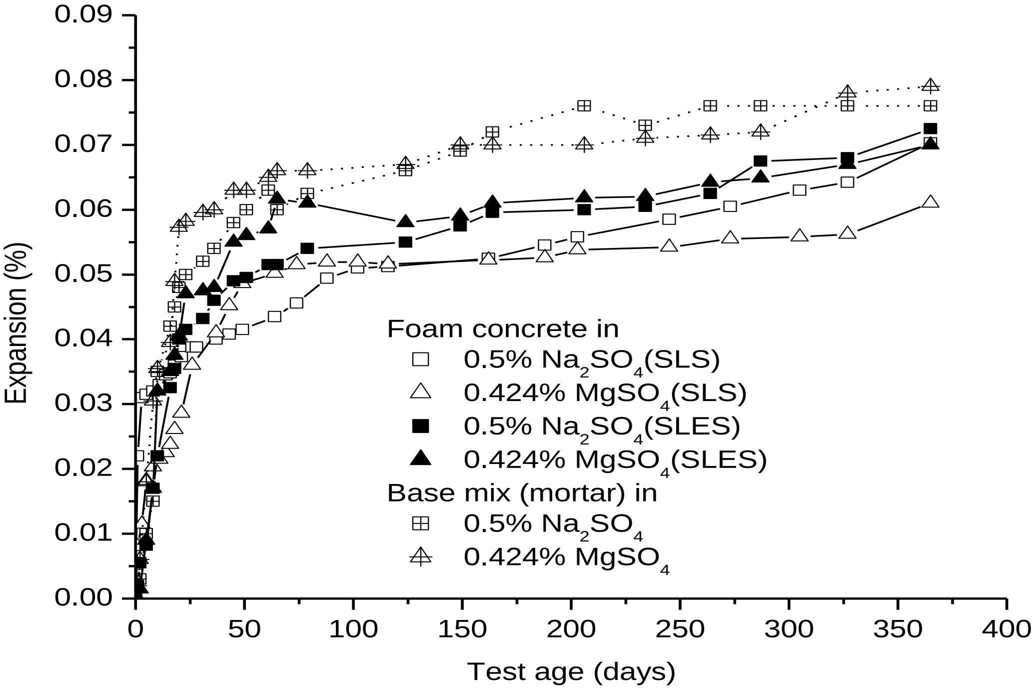

(a) Severe exposure

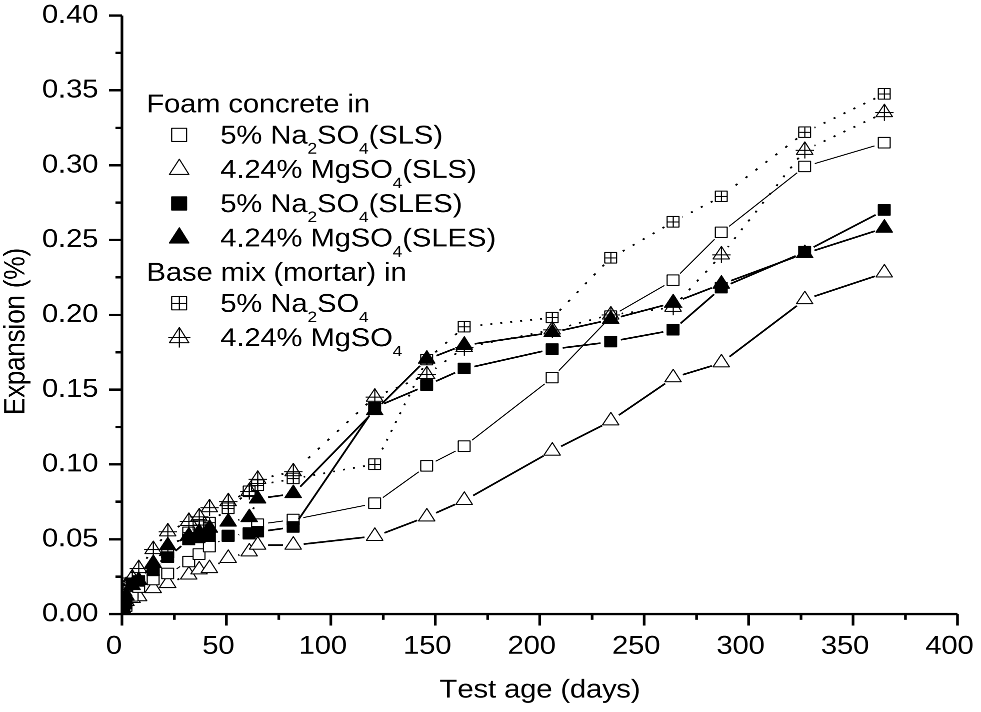

(b)Very severe exposure

Fig 8.16 Comparison of expansion under two sulphate environments (1000 kg/m^3)

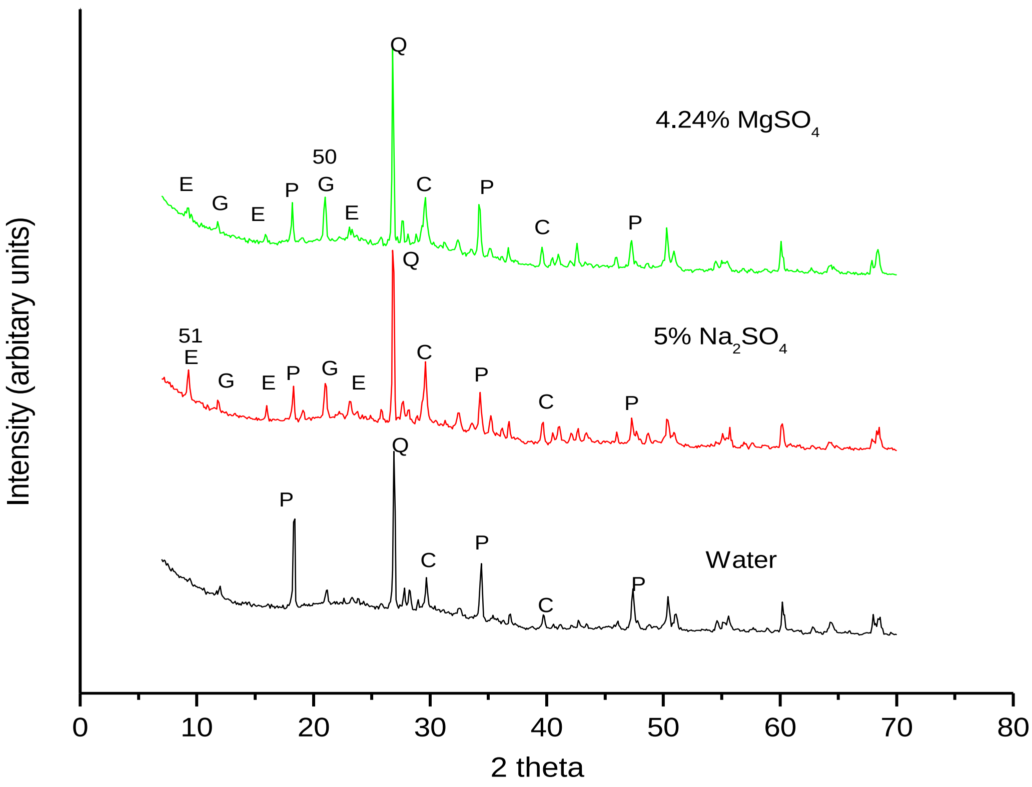

(a) SLS

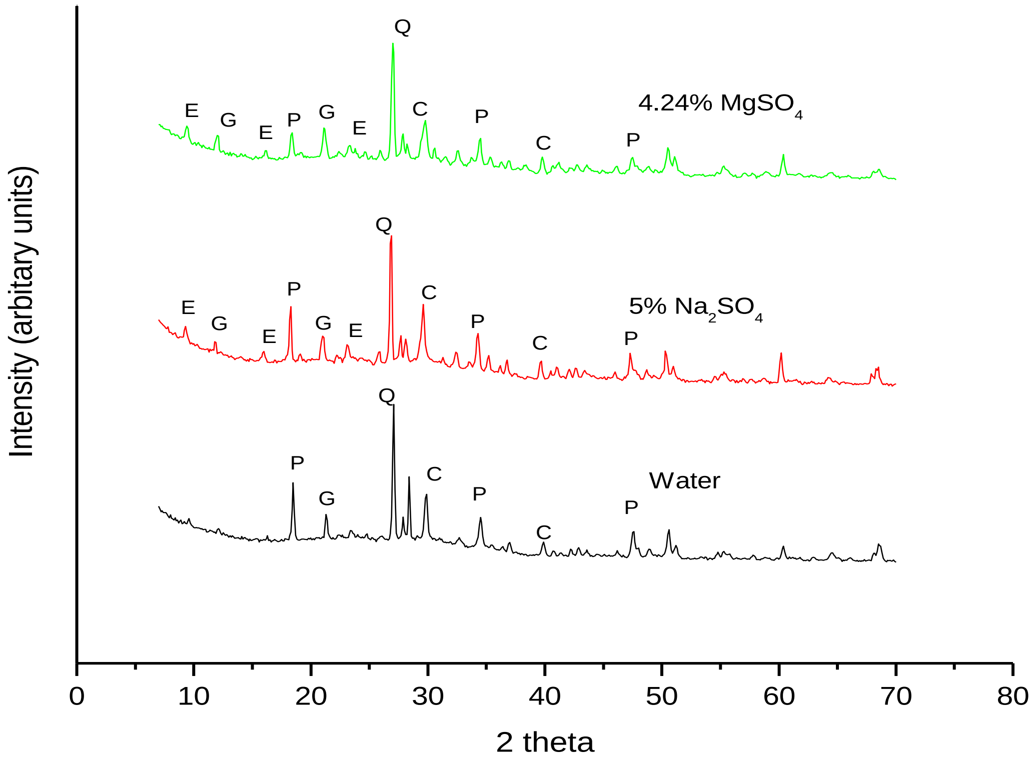

(b) SLES

Fig 8.17 XRD patterns of samples under two sulphate environments (1000 kg/m^3)

The comparison of XRD patterns of foam concrete exposed to severe and very severe concentration of sodium sulphate indicate that the intensity of ettringite (marked as 7 in Fig 8.6) and gypsum (marked as 8 and 11 in Fig 8.6) are relatively higher in very severe exposure than the ettringite (marked as 15 in Fig 8.6) and gypsum peaks (marked as 16 and 19 in Fig 8.6) in concrete under severe sulphate exposure conditions. The above observation is more evident in foam concrete with design density 1500 kg/m^3 (Fig 8.6).

The variation of mass with density under very severe exposure conditions is presented in Fig 8.21. Under very severe exposure conditions, 12% and 15% increase in mass is observed for the variation in density studied for foam concrete with surfactants SLS and SLES respectively (Fig 8.21). The increase in volume of paste content for foam concrete with higher density can be attributed to higher mass gain. The comparison of XRD patterns of foam concrete of two densities indicate that the intensity of gypsum peaks (marked as 28, 29, 34 and 35 in Fig 8.8) in foam concrete with density 1500 kg/m^3 is higher than gypsum peaks (marked as 26, 27, 32 and 33 in Fig 8.8) in concrete with density 1000 kg/m^3. Irrespective of the density of foam concrete, the gain in mass of foam concrete is marginally lower than that of base mix (mortar) under severe exposure conditions. But for concrete exposed to very severe exposure conditions, the mass gain of foam concrete with SLS and SLES is 35 and 2% respectively lower than that of the base mix (mortar).

8.5.2 Variation in Mass Under Magnesium Sulphate Environment

The variation in mass of foam concrete under water and magnesium sulphate environment is presented in Figs 8.22 to 8.24. The variation in mass under severe and very severe exposure conditions follows different trend. For specimens exposed to severe exposure conditions increase in mass with time is observed till the end of exposure period. Specimens immersed in 4.24% magnesium sulphate environment exhibit gain in mass up to 150 days. Beyond this period, the deterioration is so rapid which resulted in the spalling of edges and corners and thus the mass started reducing with time. The reason for loss in mass can be attributed to formation of more quantum of gypsum and decalcification of CSH gel in concrete under very severe exposure conditions which resulted in softening, loss of cementitious structure and thus led to disintegration of specimens (Cohen and Arnon, 1988).

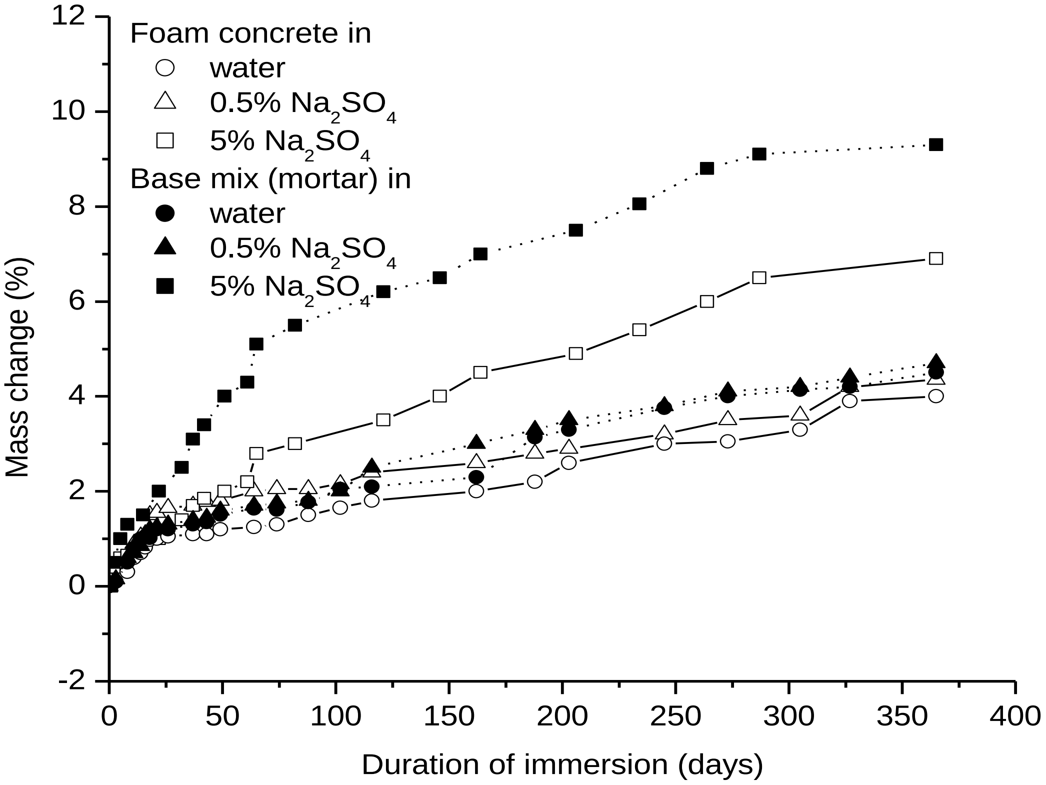

(a) SLS

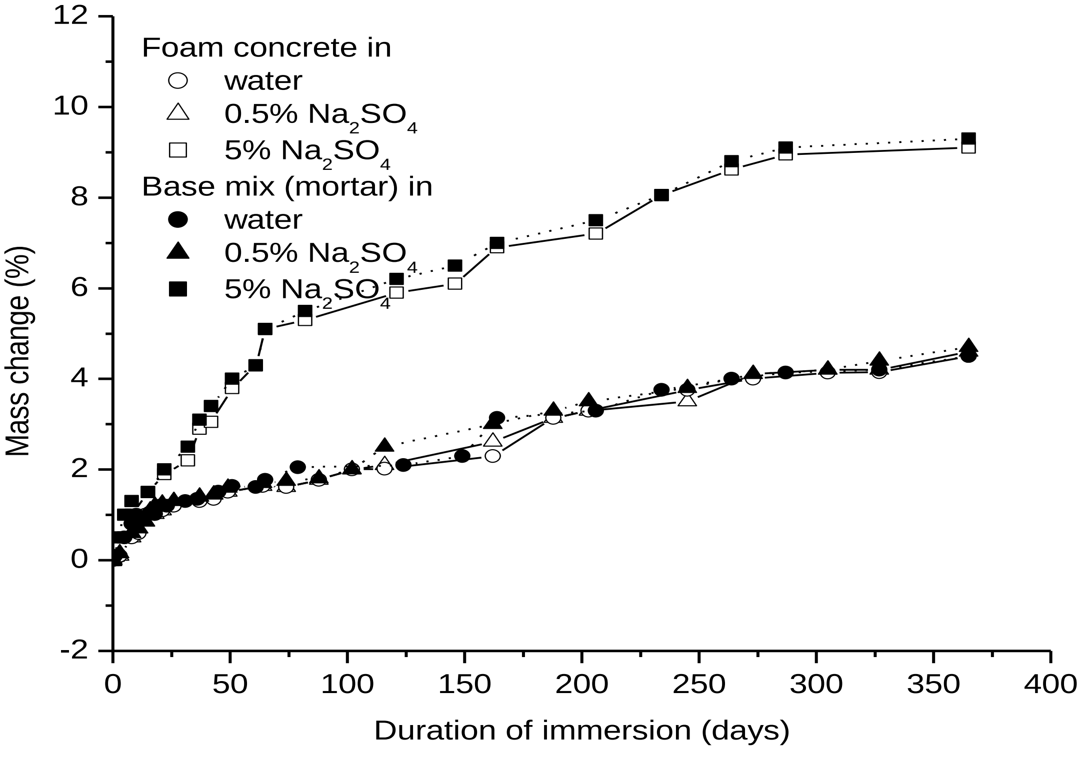

(b) SLES

Fig 8.18 Variation of mass with time in $NaSO_4$ (1000 kg/m^3)

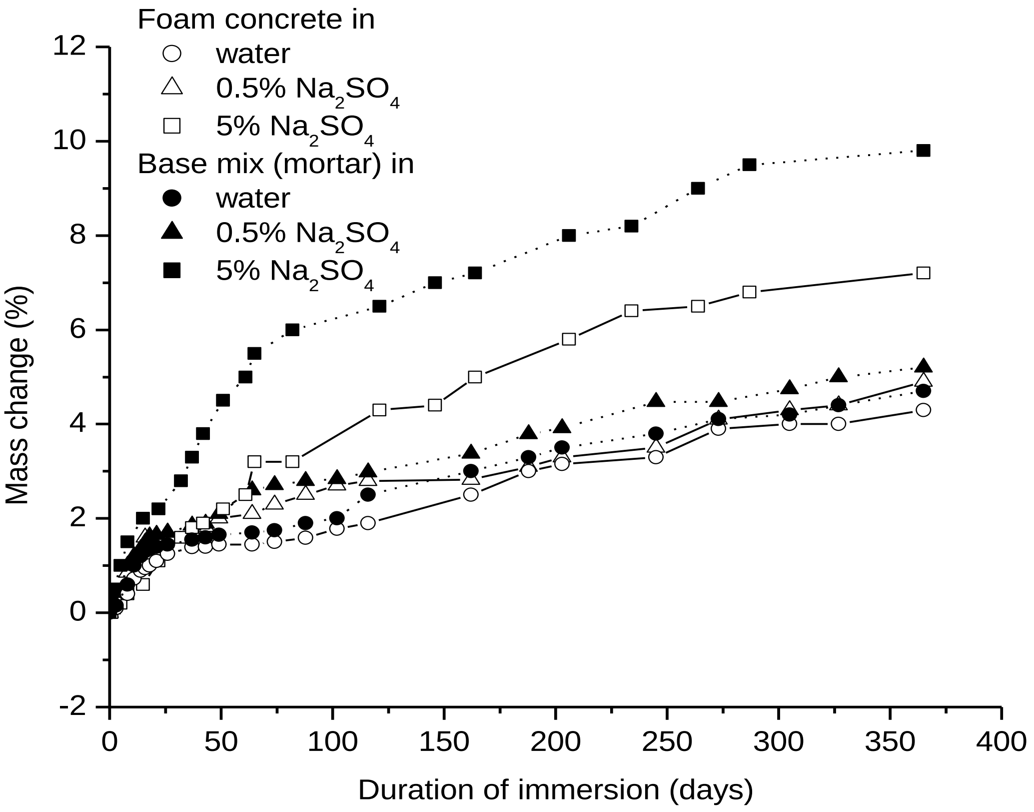

(a) SLS

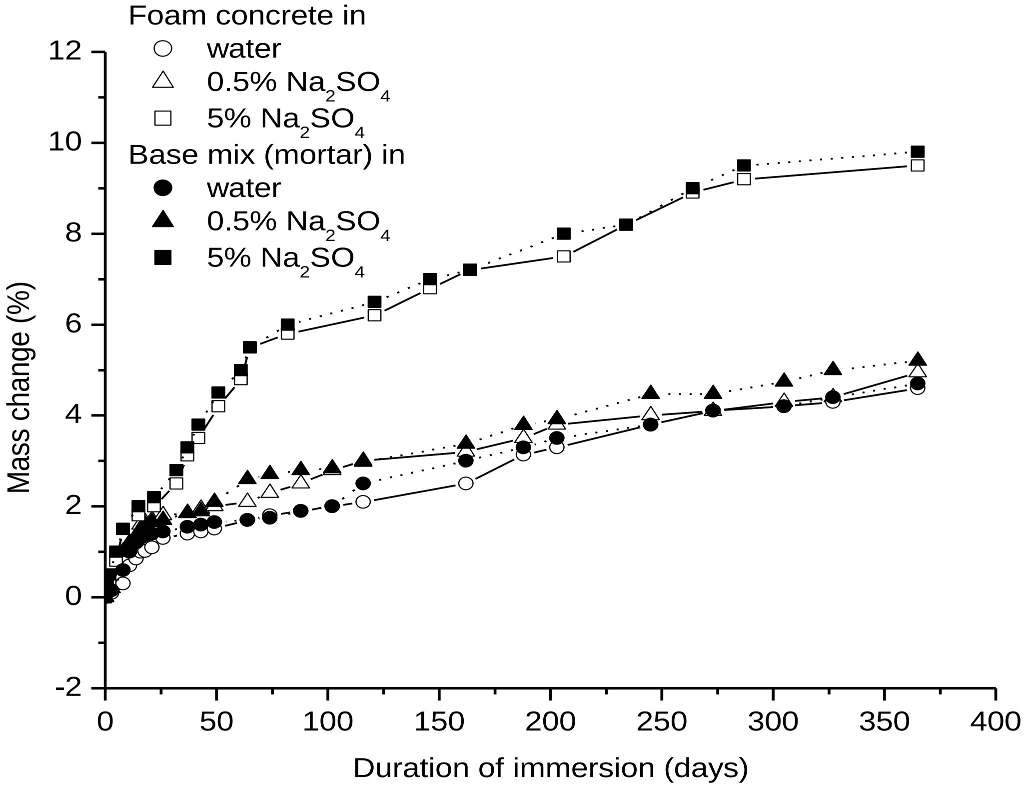

(b) SLES

Fig 8.19 Variation of mass with time in $NaSO_4$ (1250 kg/m^3)

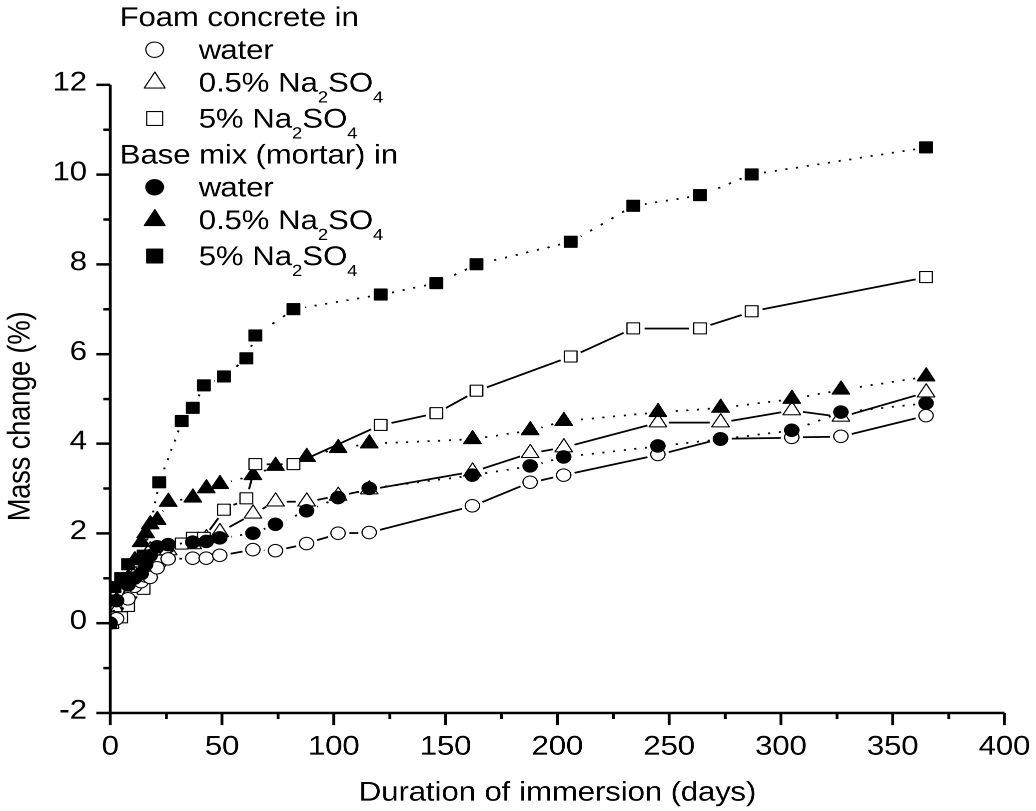

(a) SLS

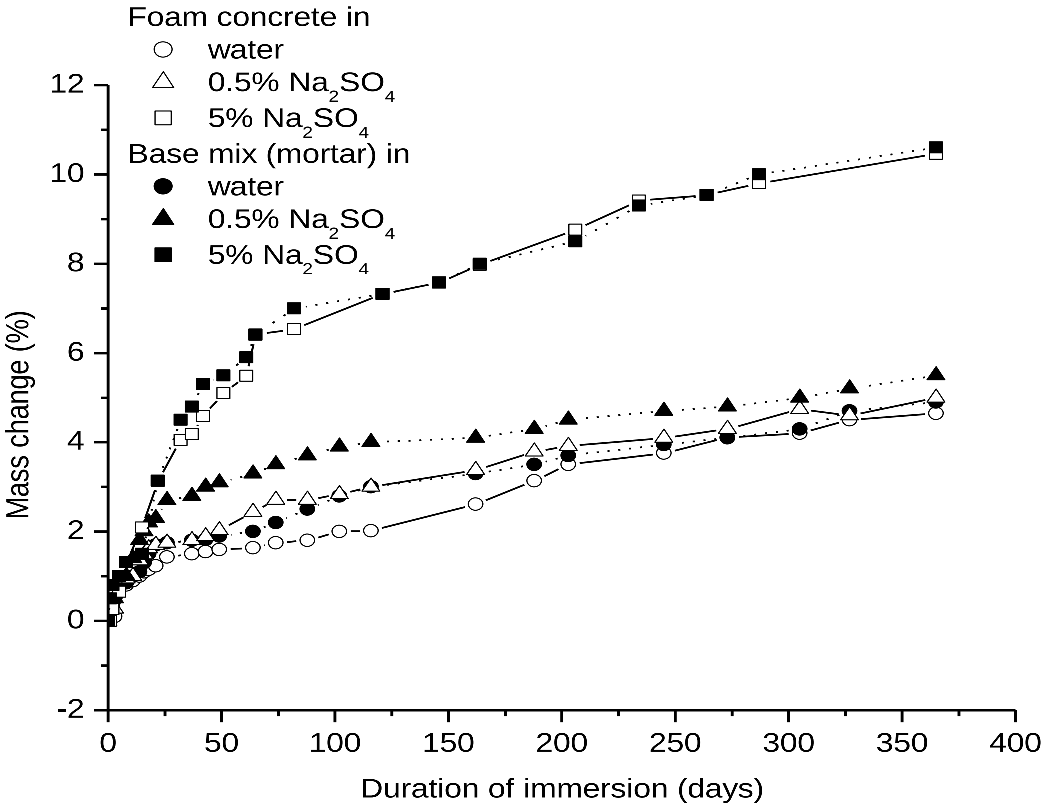

(b) SLES

Fig 8.20 Variation of mass with time in $NaSO_4$ (1500 kg/m^3)

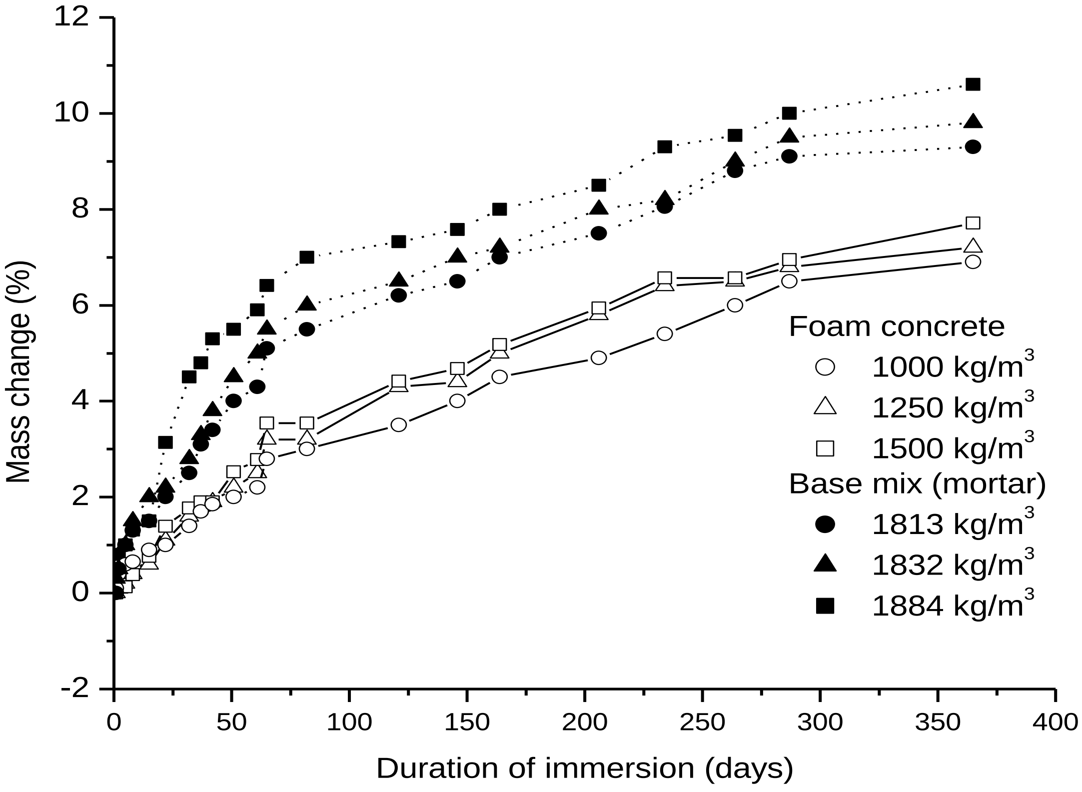

(a) SLS

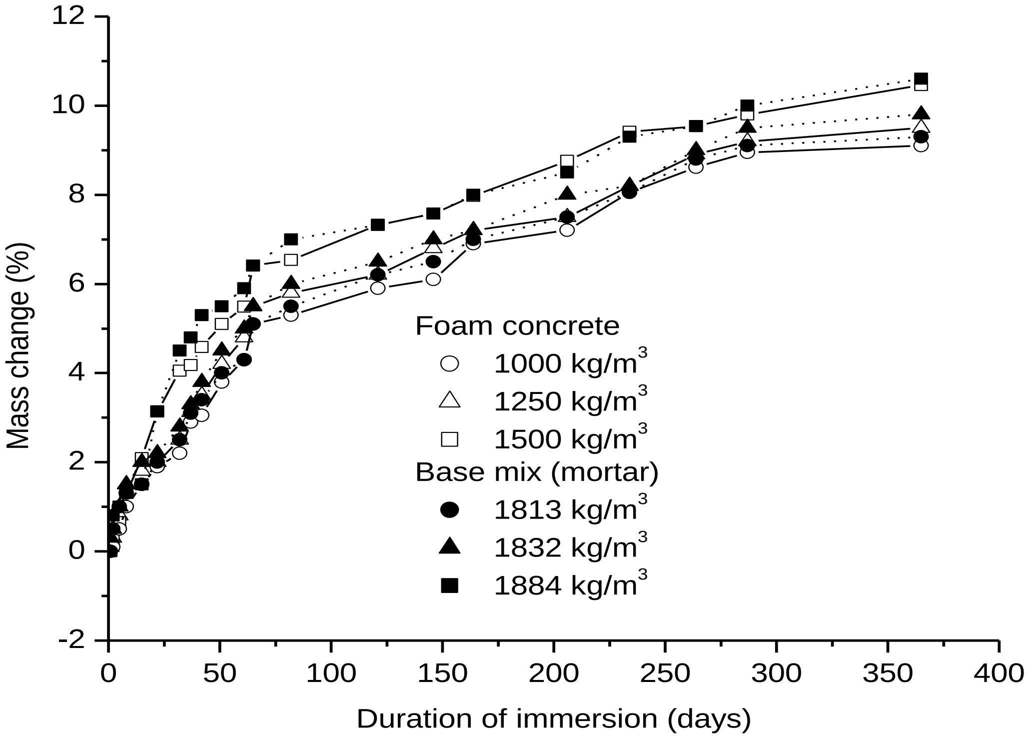

(b) SLES

Fig 8.21 Variation of mass with density under very severe exposure $NaSO_4$

Comparison of XRD patterns indicate that the intensity of gypsum peak (marked as 42 and 44 in Fig 8.14) is high in very severe exposure when compared to concrete under severe exposure conditions.The variation of mass with density under very severe exposure conditions is presented in Fig 8.25. The variation in mass loss with variation in density is 10% and 4% for foam concrete with surfactants SLS and SLES respectively. The mass loss of base mix is 20% higher than that of foam concrete.

8.5.3 Behaviour under Sodium and Magnesium Sulphate Environment

Figs. 8.26(a) and 8.26(b) shows the comparison between variation in mass of foam concrete under sodium and magnesium sulphate environment of severe and very severe exposure conditions respectively. For a constant density it is observed that the increase in mass of foam concrete in magnesium sulphate environment is 8 to 12% higher than that in sodium sulphate environment under severe exposure conditions.

Under very severe exposure condition loss in mass is observed in magnesium sulphate environment (due to disintegration of specimens) against the gain in mass observed for sodium sulphate environment. This observation is consistent with results of earlier researchers in normal weight concrete (Cohen and Arnon, 1988; Moon et al, 2002).

8.5.4 Sulphate Deterioration Factor under Sodium Sulphate Environment

Figs. 8.27 to 8.29 show the variation in SDF of foam concrete under sodium sulphate environment. For a given density, SDF of foam concrete under very severe exposure sodium sulphate environment is 20 to 25% and 6 to 12% higher than that under severe exposure conditions for surfactants SLS and SLES respectively. The SDF of base mix is up to 25% higher than that of foam concrete. The variation of SDF with density under very severe exposure conditions is presented in Fig 8.30. Up to 13% increase in strength deterioration is observed when the fresh density of foam concrete varied from 1000 to 1500 kg/m^3. The greater volume of sorbing paste at the higher densities leads to higher sorptivity (Jones and McCarthy, 2005c) and thus resulted in rapid permeation of water containing sulphate ions.

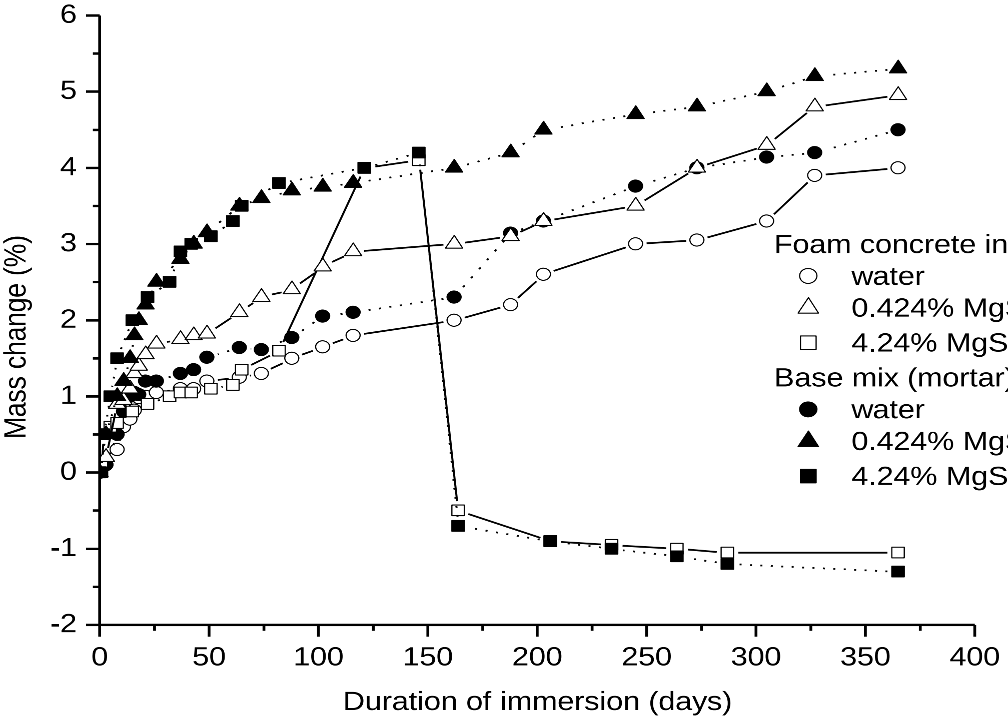

(a) SLS

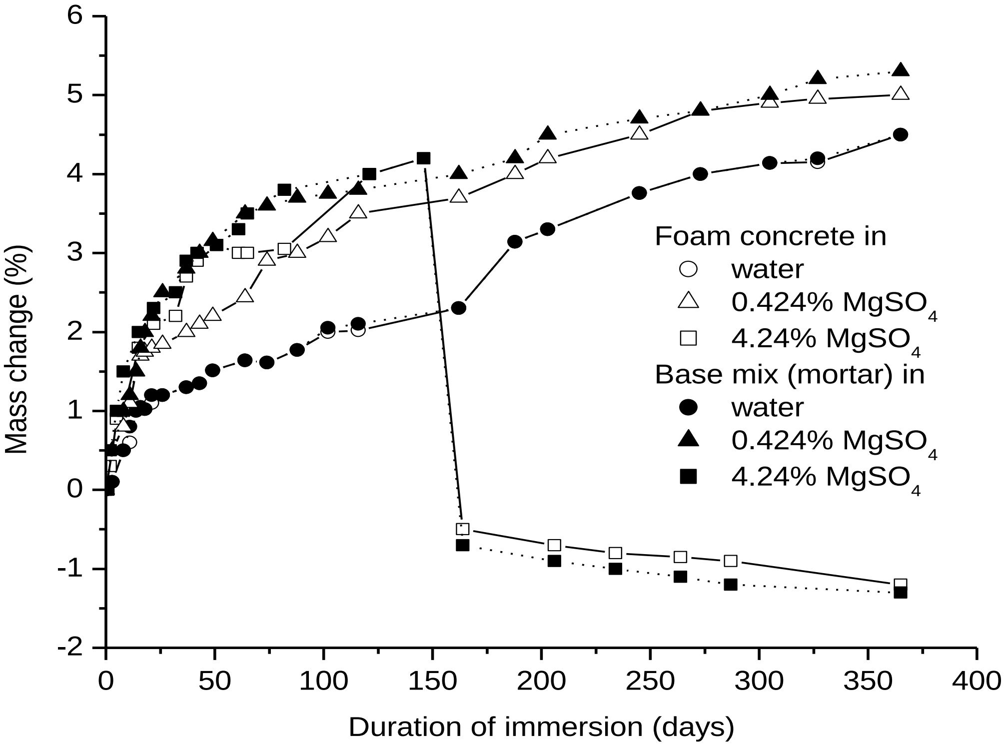

(b) SLES

Fig 8.22 Variation of mass with time in $MgSO_4$ (1000 kg/m^3)

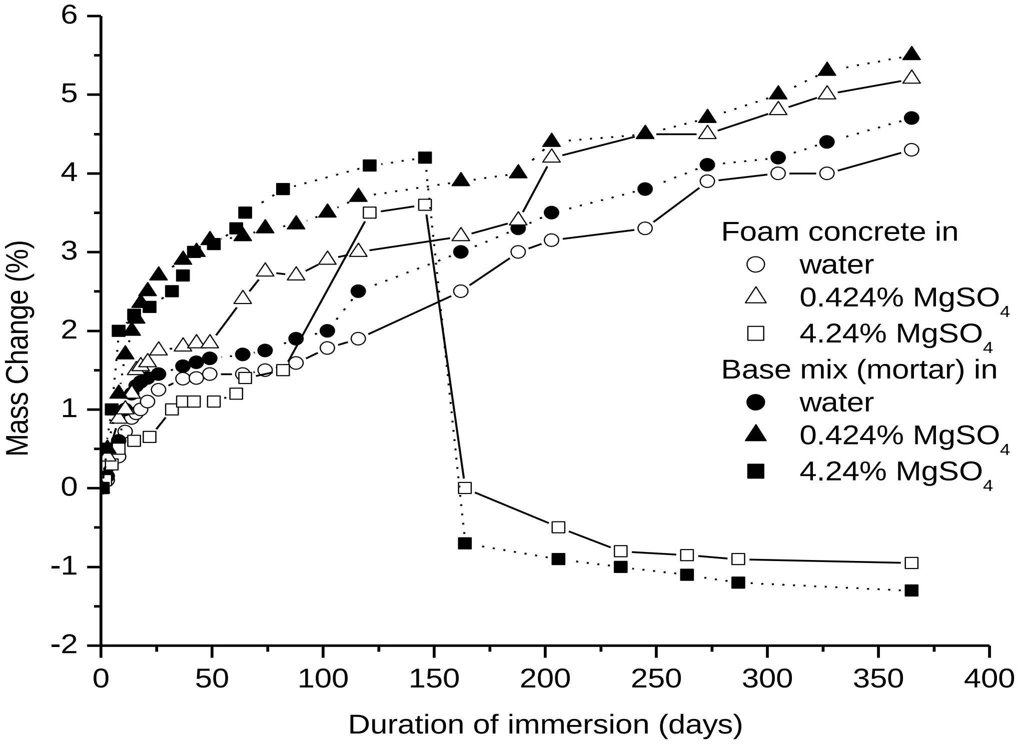

(a) SLS

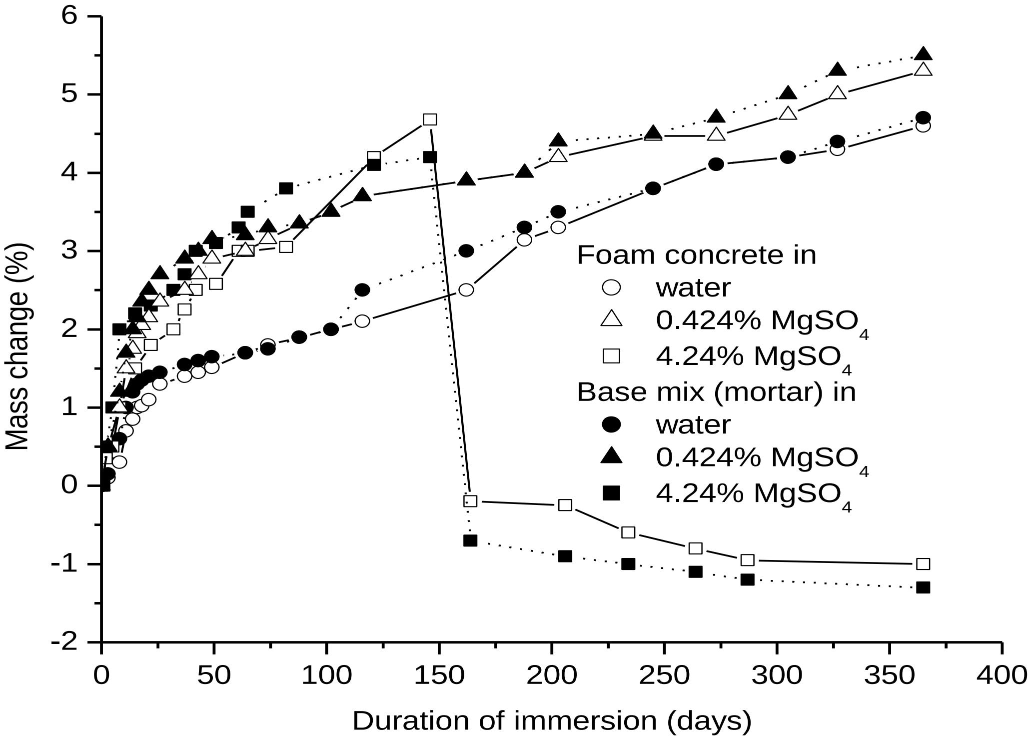

(b) SLES

Fig 8.23 Variation of mass with time in $MgSO_4$ (1250 kg/m^3)

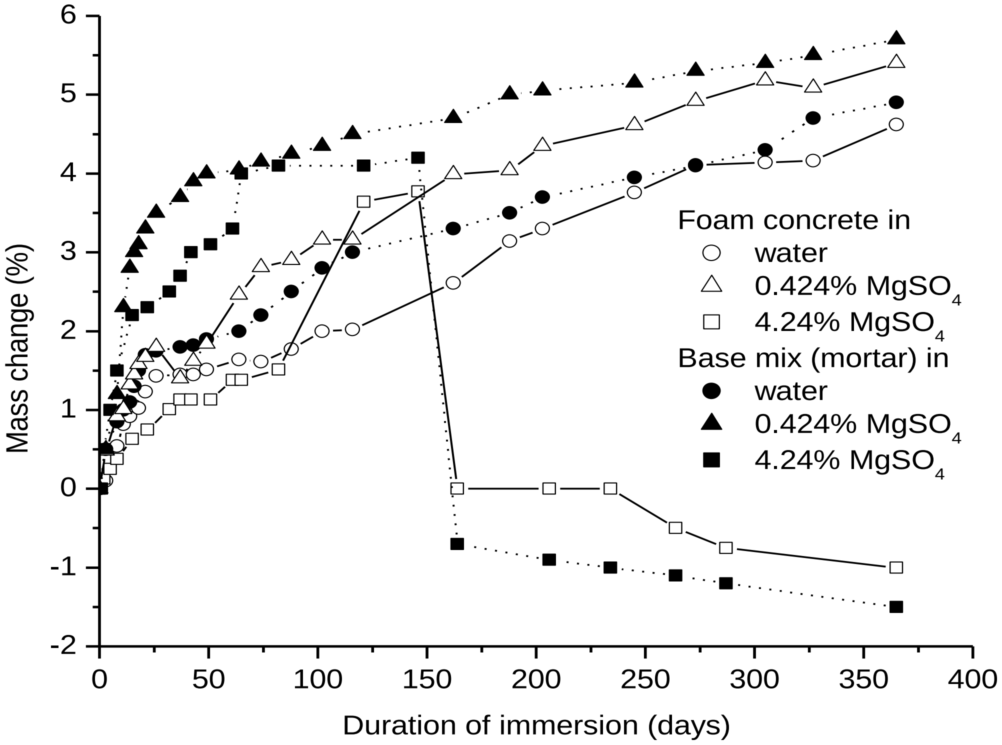

(a) SLS

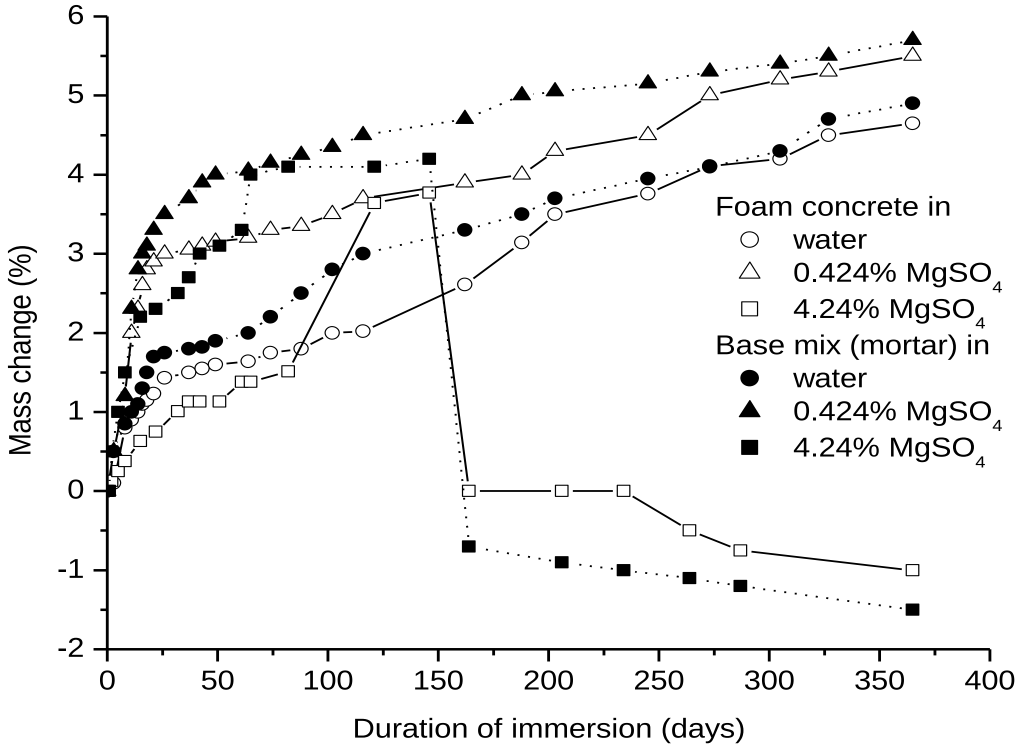

(b) SLES

Fig 8.24 Variation of mass with time in $MgSO_4$ (1500 kg/m^3)

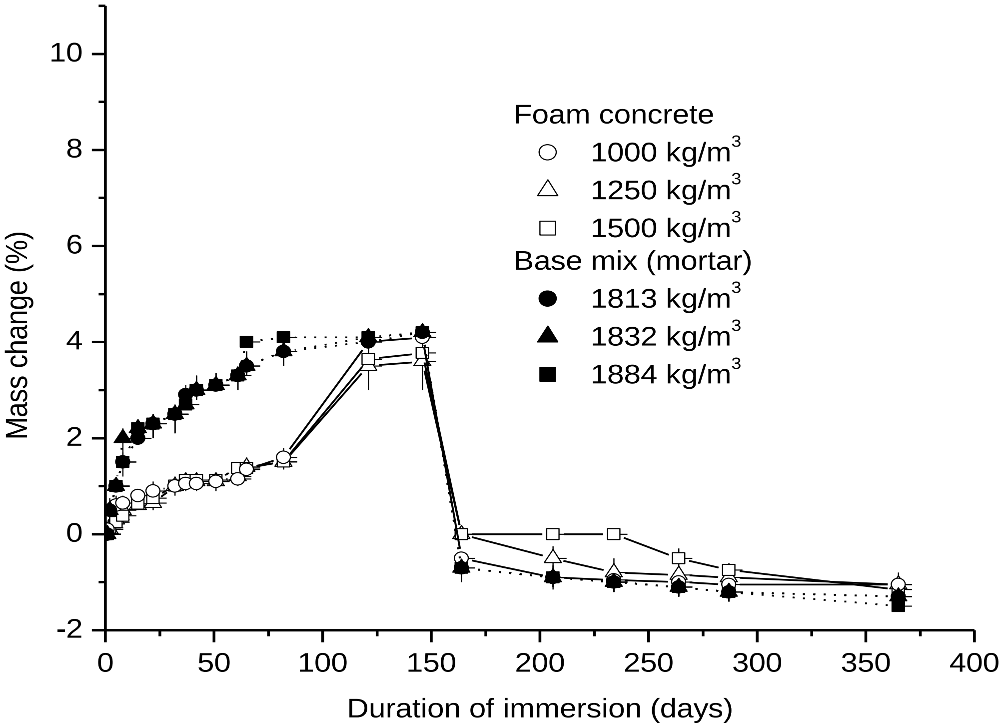

(a) SLS

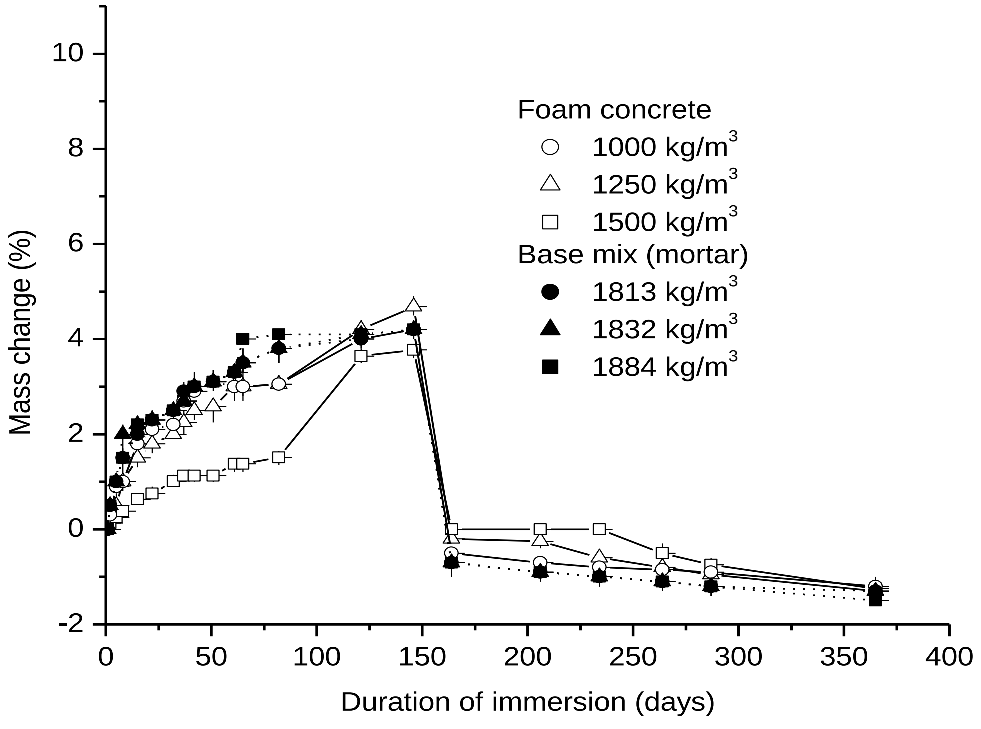

(b) SLES

Fig 8.25 Variation of mass with density under very severe exposure $MgSO_4$

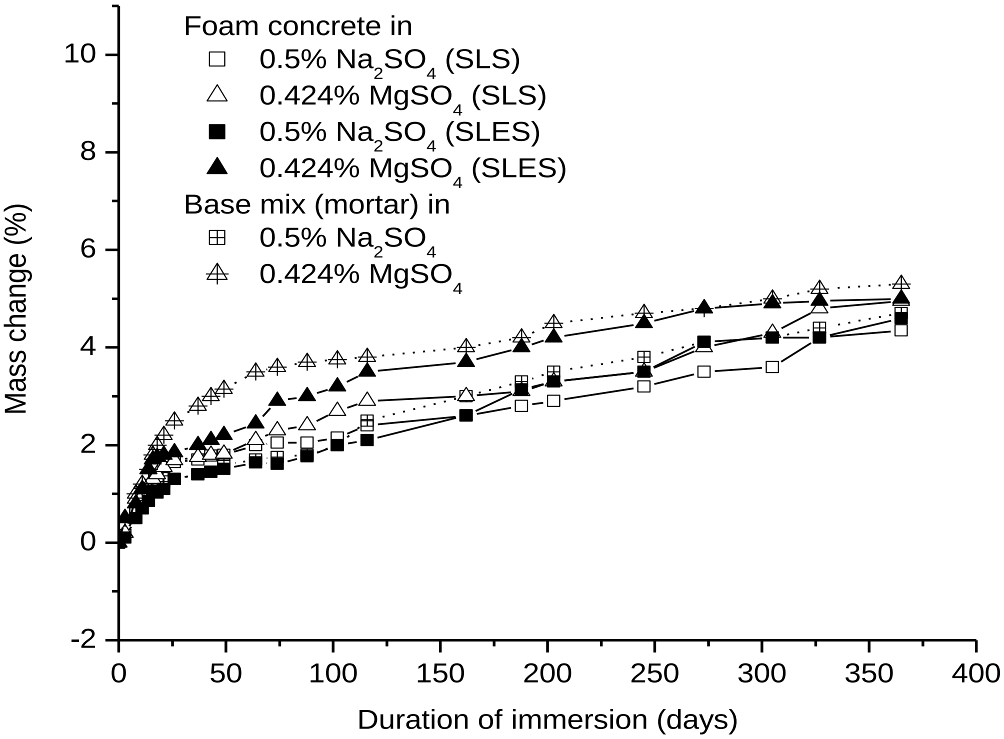

(a) Severe exposure

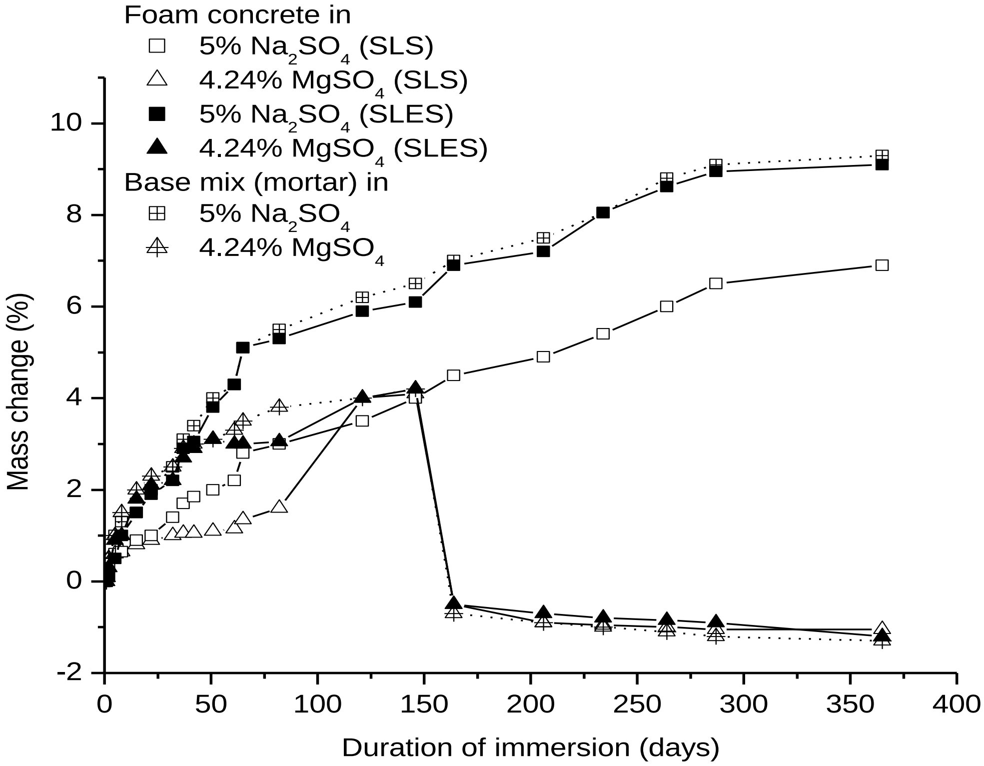

(b) Very severe exposure

Fig 8.26 Comparison of mass variation under two sulphate environments (1000 kg/m^3)

8.5.5 Sulphate Deterioration Factor under Magnesium Sulphate Environment

The sulphate deterioration factor of concrete under very severe exposure magnesium sulphate environment is 70% and 62% higher than that under severe exposure conditions for surfactants SLS and SLES respectively (Figs 8.31 to 8.33). This greater loss in strength of nearly 40% obtained in very severe exposure magnesium sulphate environment conditions can be attributed to more quantum of gypsum formation which leads to softening of structure under very severe exposure conditions (Cohen and Arnon, 1988). This observation is supported by XRD patterns which shows higher intensity of gypsum peaks (marked as 42 and 44 in Fig 8.14) in foam concrete under very severe exposure condition when compared to gypsum (marked 47 and 49 as in Fig 8.14) in foam concrete under severe exposure condition. The SDF of base mix is 13% to 20% higher than that of foam concrete. The increase in SDF with variation in density is less than 3% under very severe exposure conditions (Fig 8.34).

8.5.6 Behaviour under Sodium and Magnesium Sulphate Environment

Figs. 8.35(a) and 8.35(b) show the comparison between change in SDF of foam concrete with SLS and SLES respectively under sodium and magnesium sulphate environment. For a constant density, it is observed that the SDF of foam concrete under magnesium sulphate environment is 13% and 63% higher than that under sodium sulphate environment when subjected to severe and very severe exposure conditions respectively. This is because the major deterioration mechanism in magnesium sulphate environment is softening and disintegration of cementing material as the magnesium sulphate can react with cementitious C-S-H gel and form the non cementitious M-S-H. This reaction produces more gypsum which renders the cementitious structure soft and thus results in reduction in strength (Cohen and Arnon, 1988; Al-Amoudi et al, 1995). The XRD analysis shows that the specimens subjected to magnesium sulphate has higher intensity of gypsum peaks (marked 50 in Fig 8.17) as compared to that under sodium sulphate environment. The variation in strength deterioration between sodium and magnesium sulphate environment is higher under very severe exposure conditions. This can be attributed to mass loss due to spalling of edges and corners of specimens which contributed to significant strength loss under very severe exposure conditions.

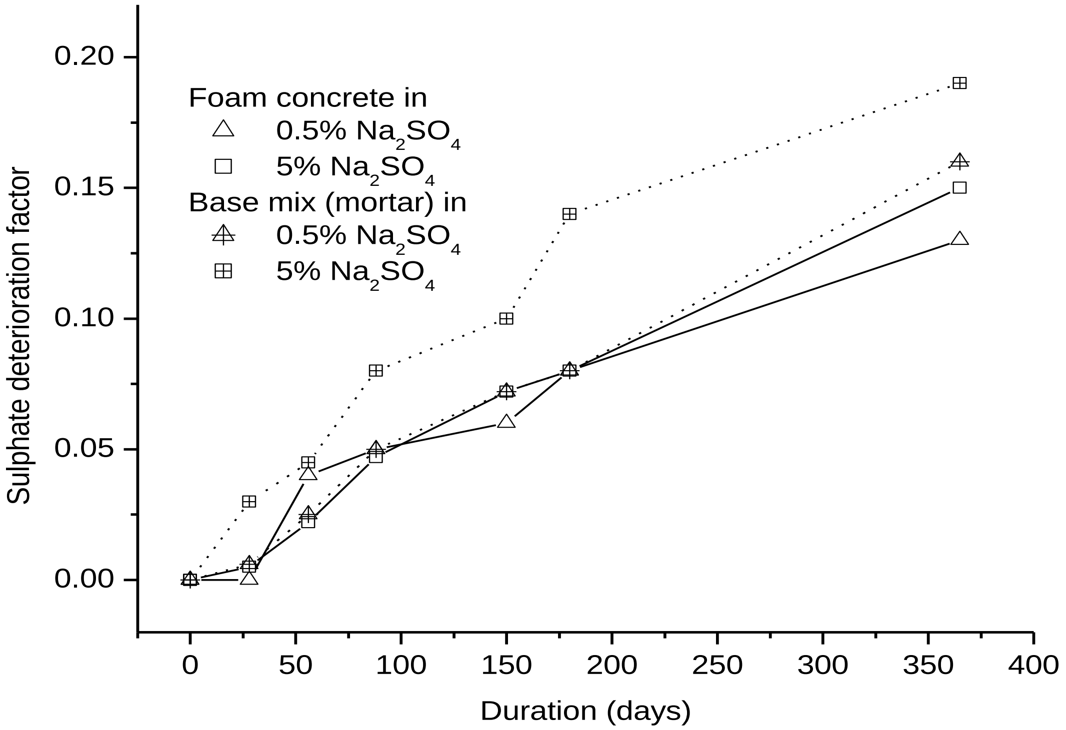

(a) SLS

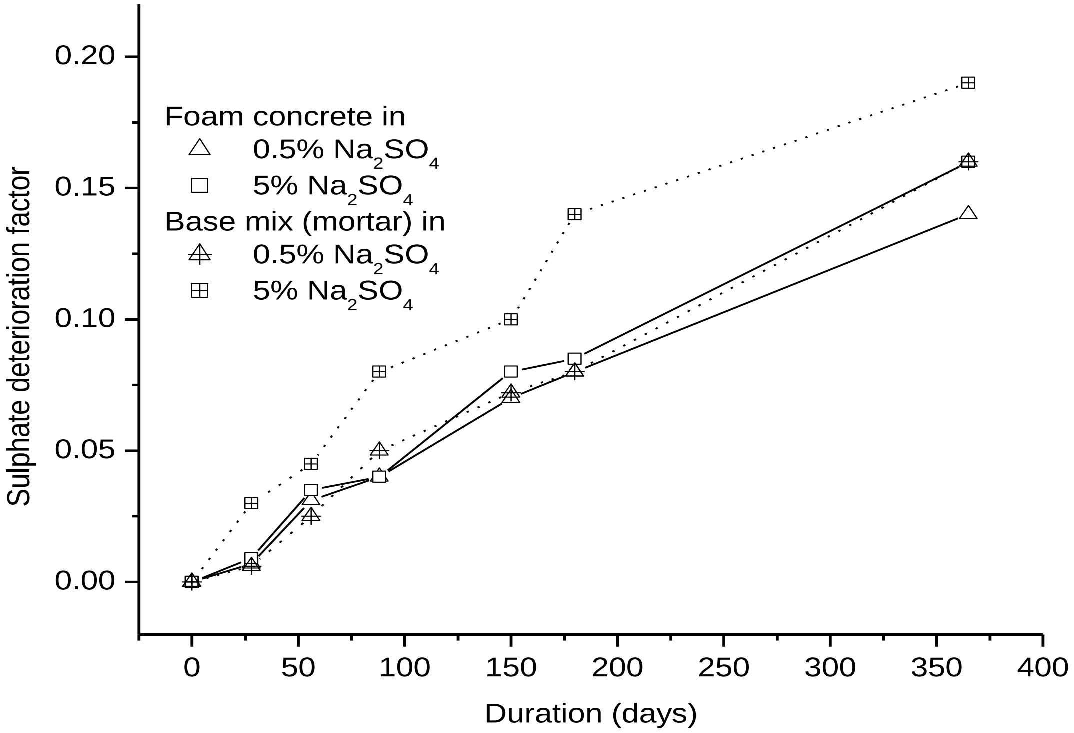

(b) SLES

Fig 8.27 Variation of SDF with time under Na_2SO_4 (1000 kg/m^3)

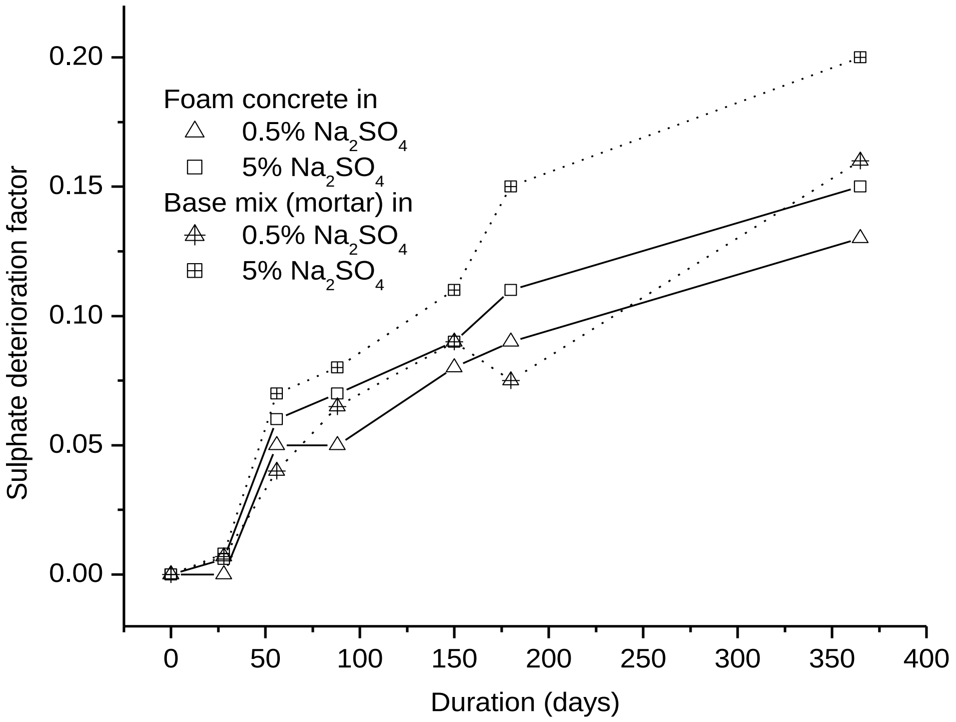

(a) SLS

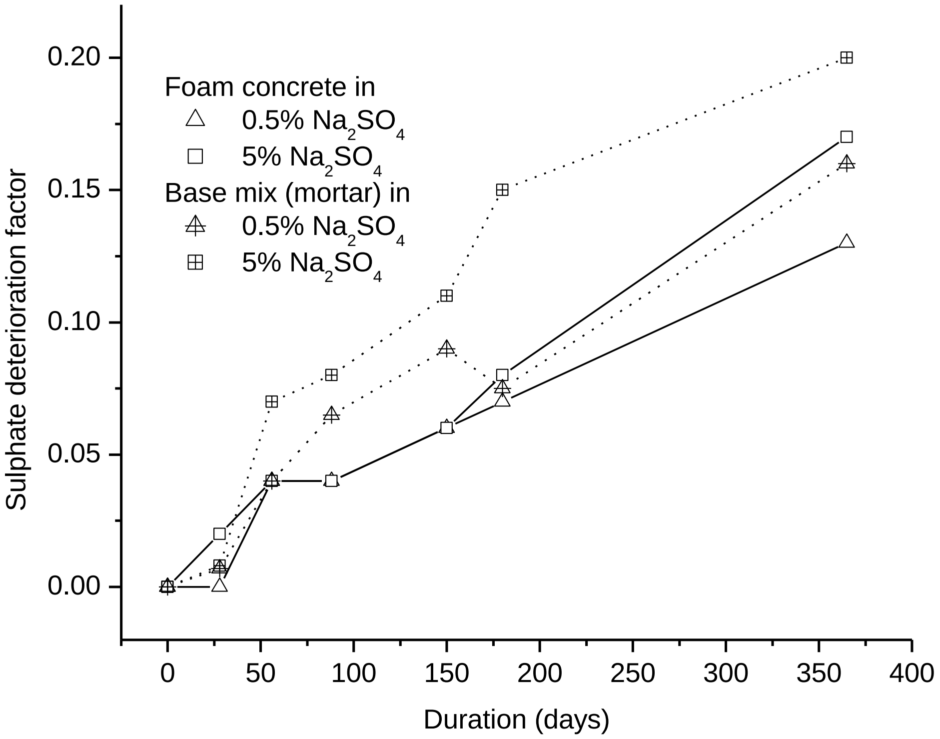

(b) SLES

Fig 8.28 Variation of SDF with time under Na_2SO_4 (1250 kg/m^3)

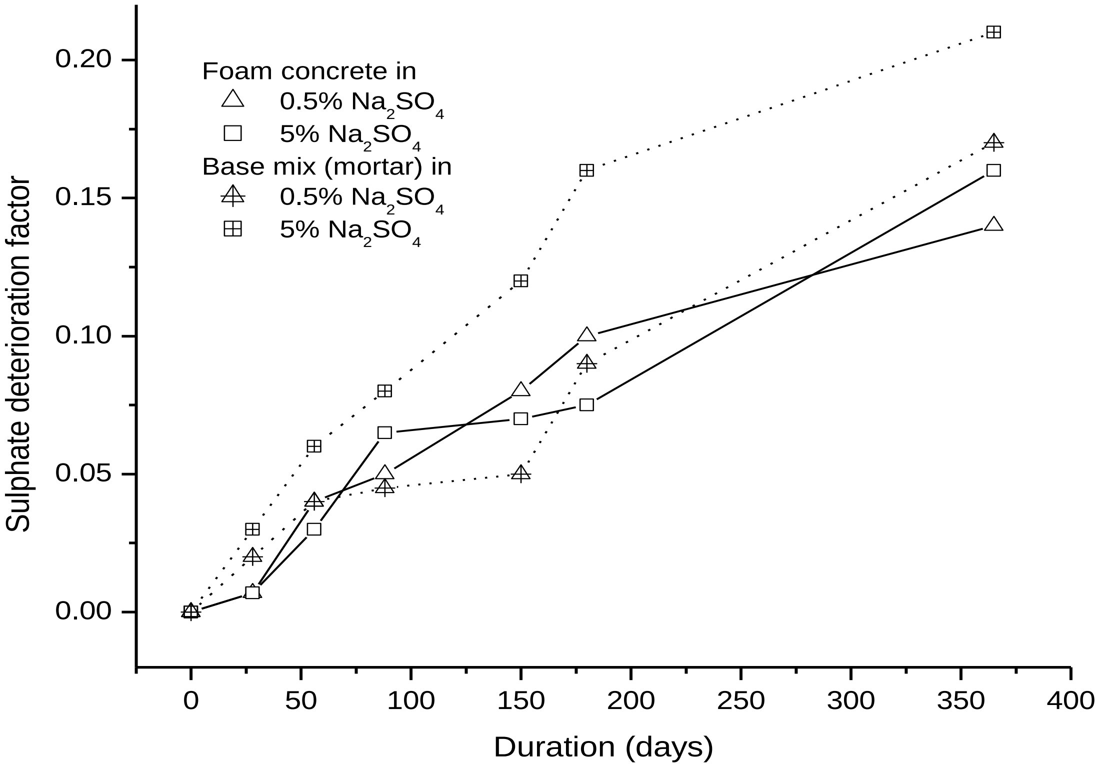

(a) SLS

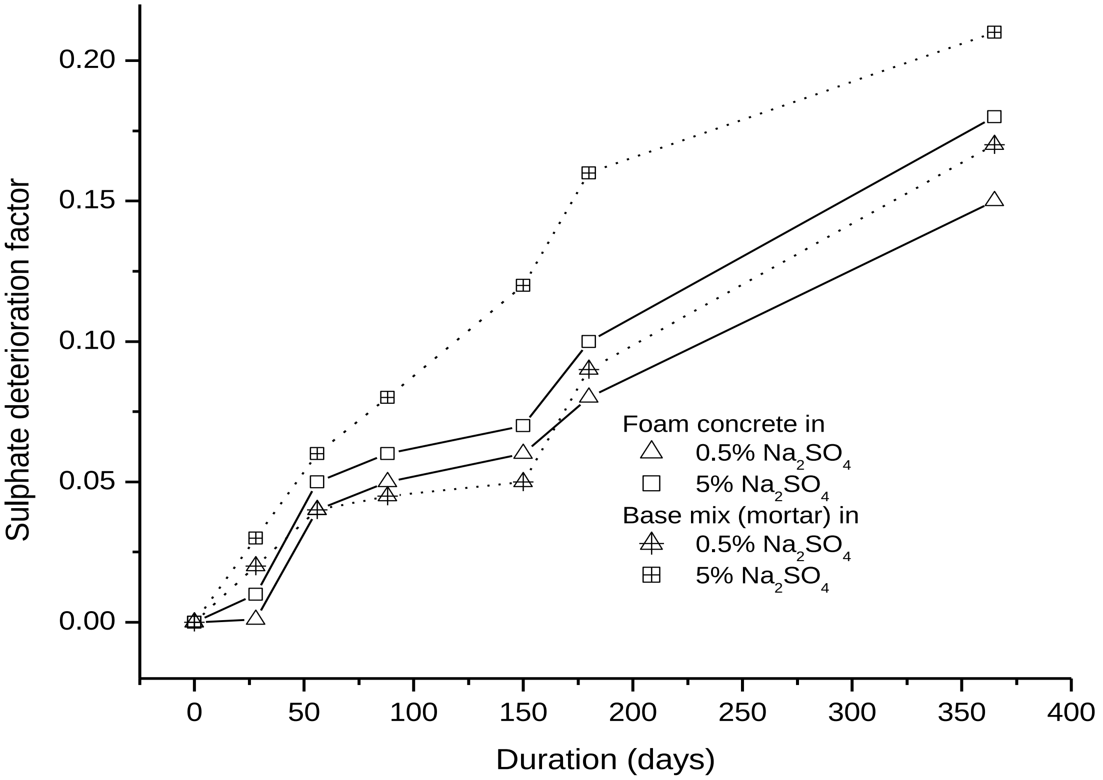

(b) SLES

Fig 8.29 Variation of SDF with time under $NaSO_4$ (1500 kg/m^3)

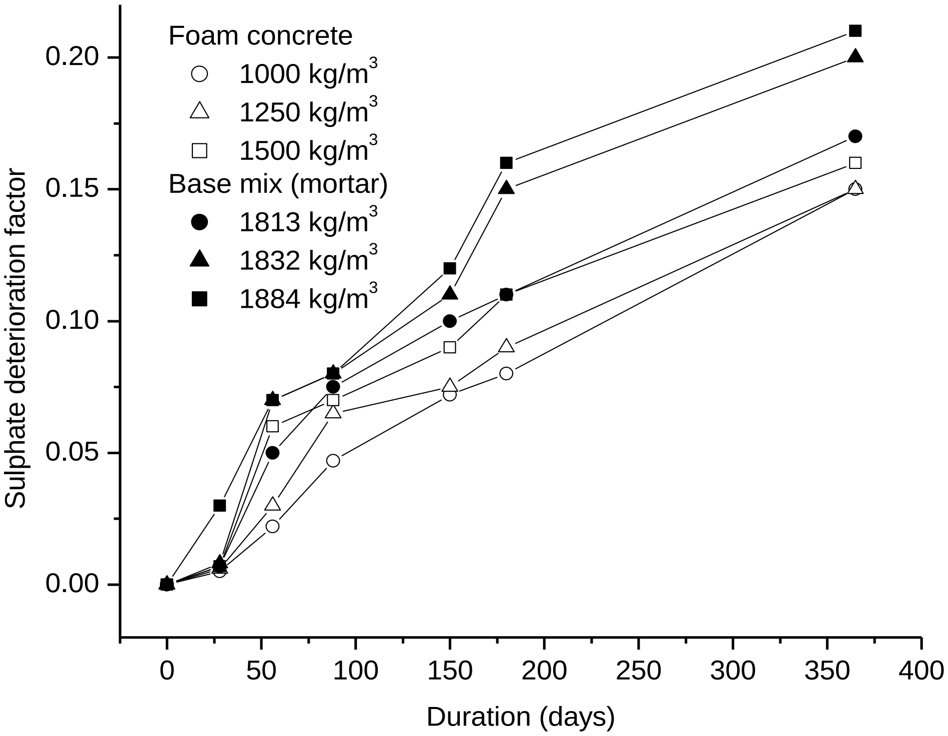

(a) SLS

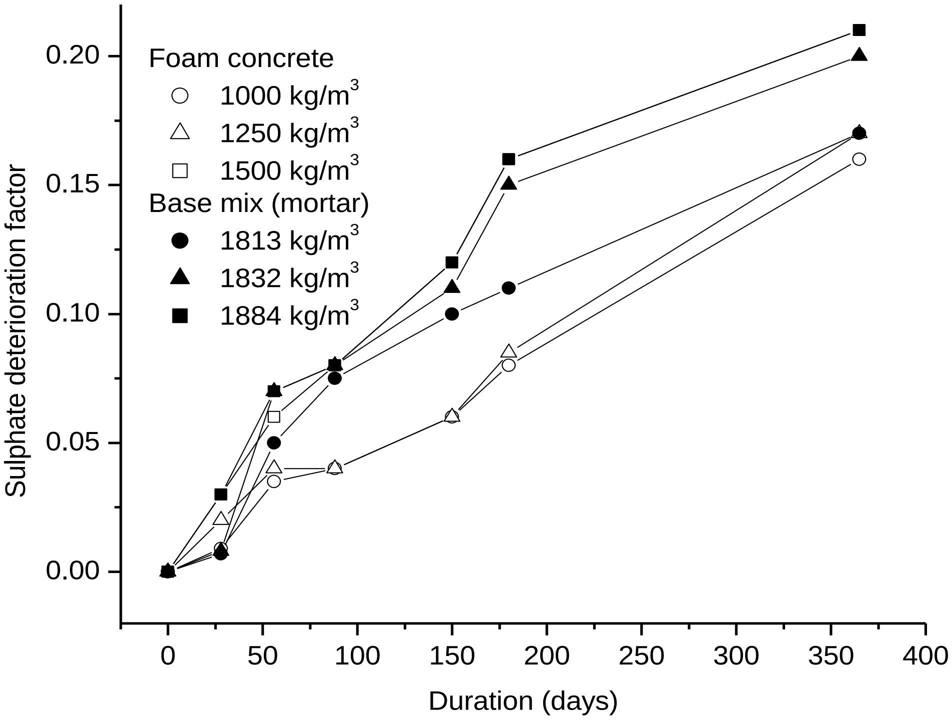

(b) SLES

Fig 8.30 Variation of SDF with density under very severe exposure Na_2SO_4

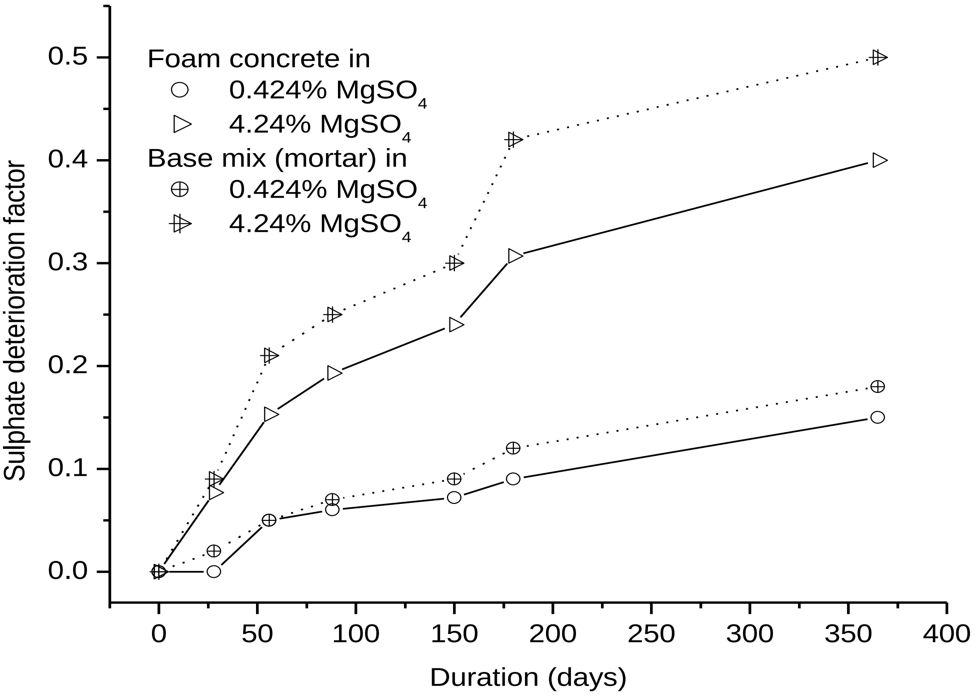

(a) SLS

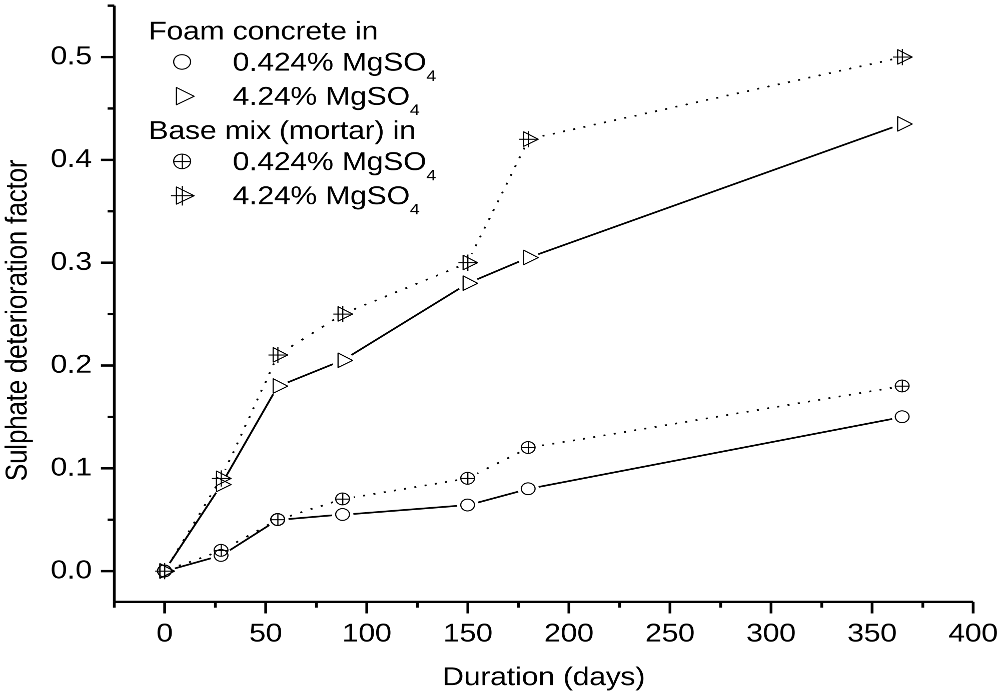

(b) SLES

Fig 8.31 Variation of SDF with time under $MgSO_4$ (1000 kg/m^3)

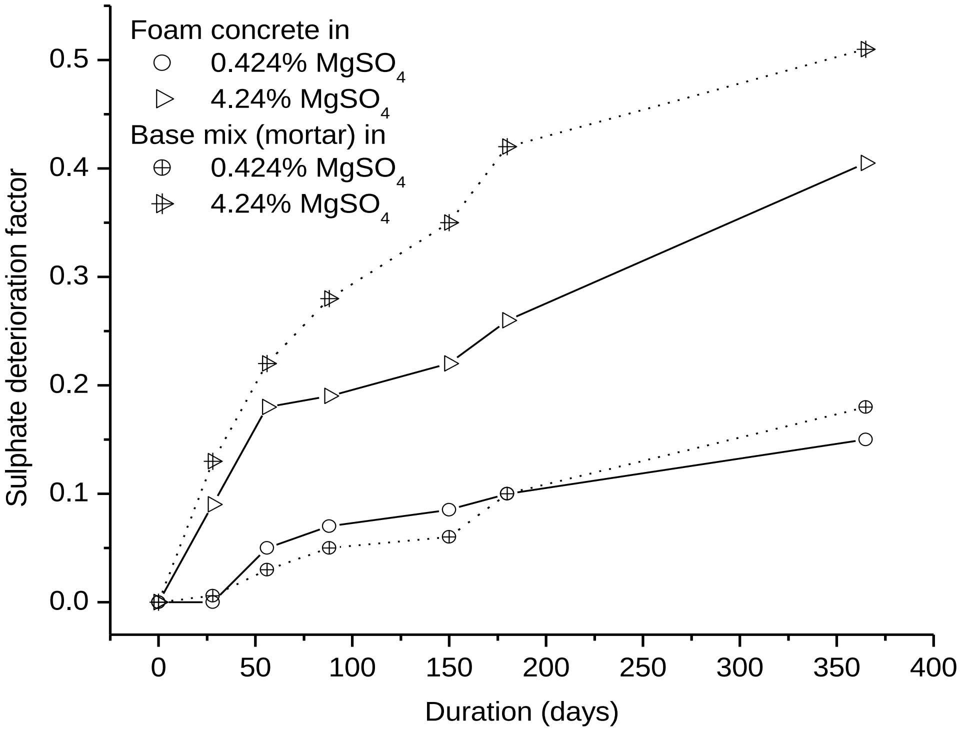

(a) SLS

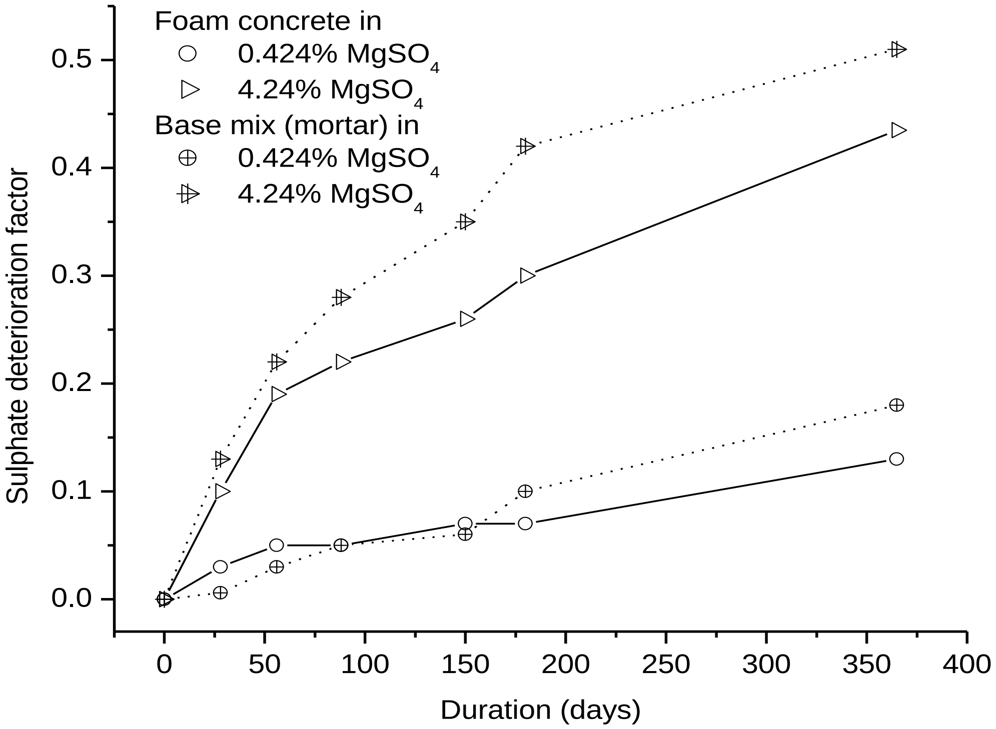

(b) SLES

Fig 8.32 Variation of SDF with time under $MgSO_4$ (1250 kg/m^3)

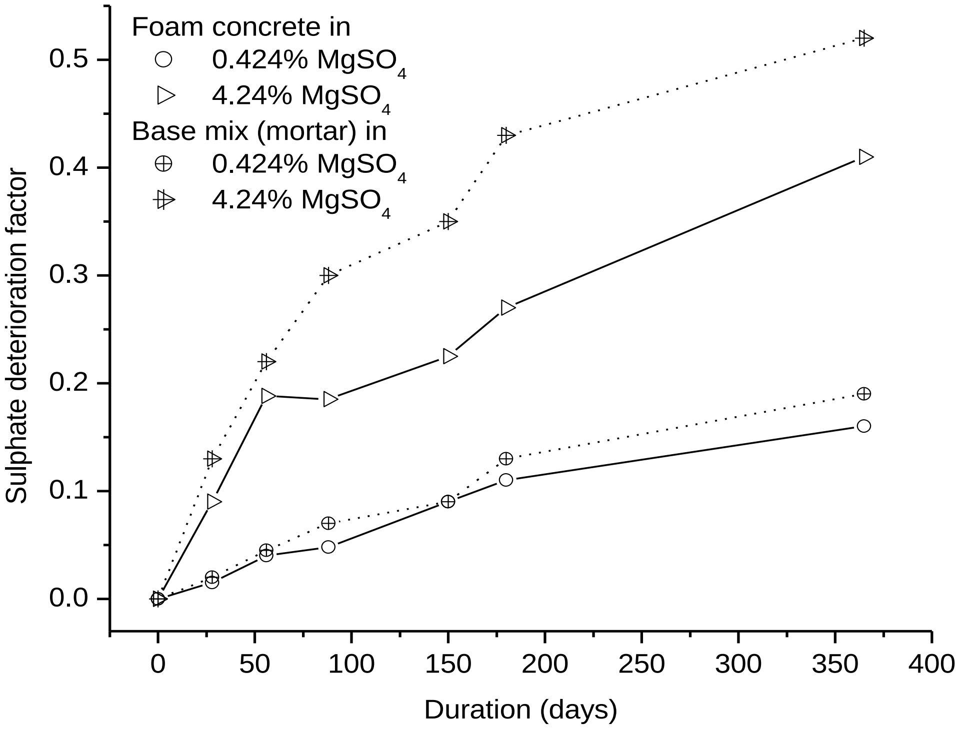

(a) SLS

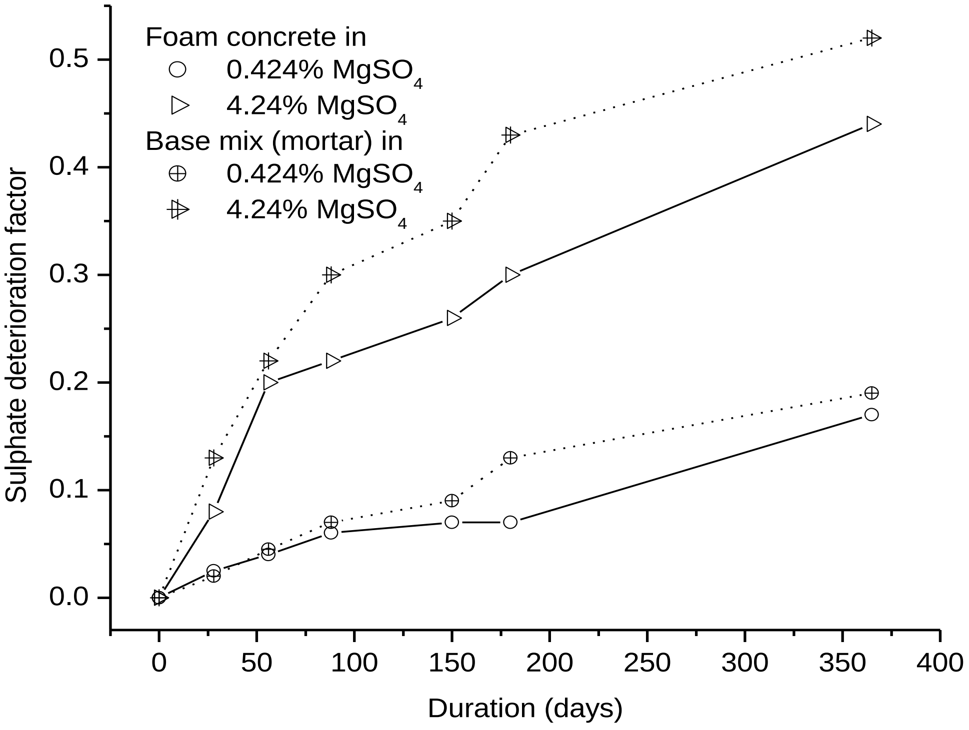

(b) SLES

Fig 8.33 Variation of SDF with time under $MgSO_4$ (1500 kg/m^3)

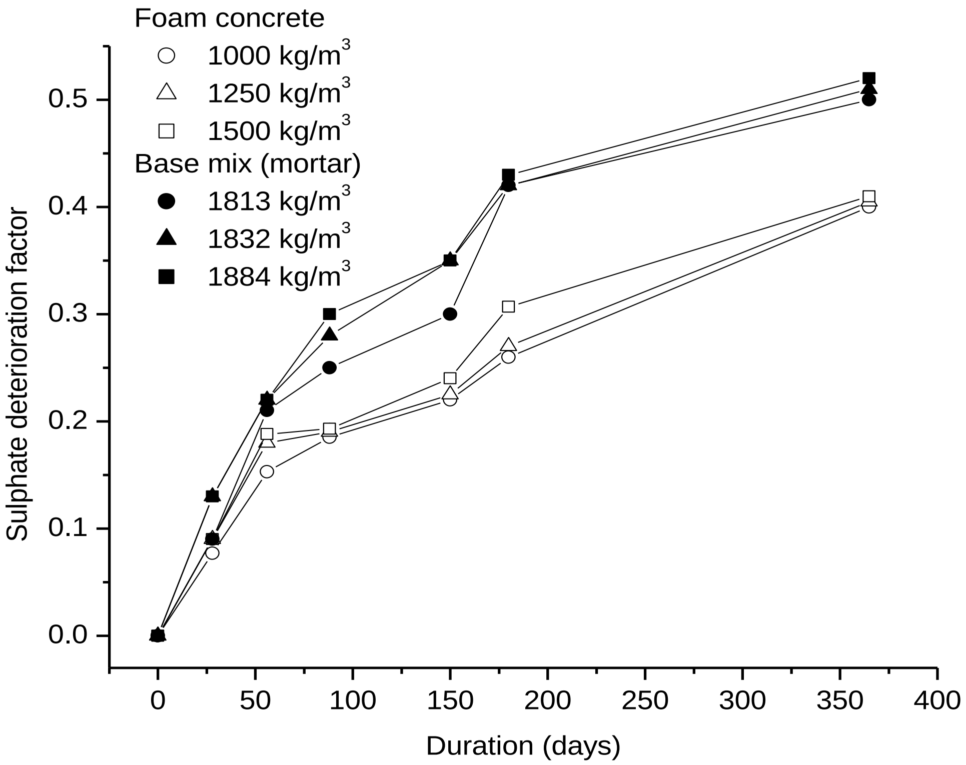

(a) SLS

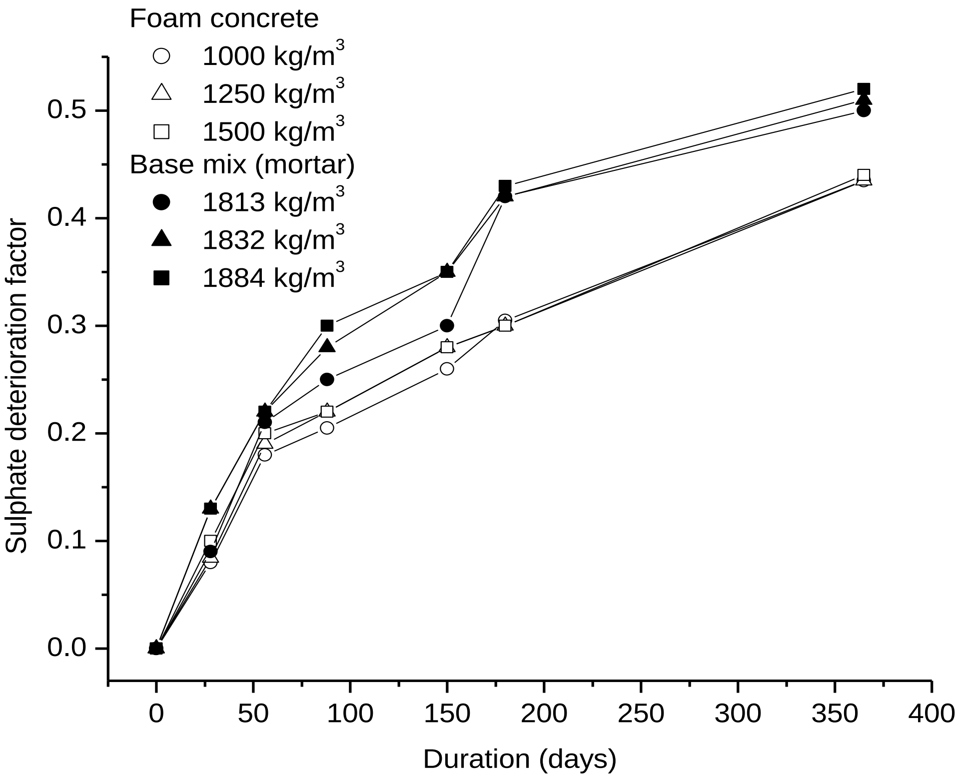

(b) SLES

Fig 8.34 Variation of SDF with density under very severe exposure $MgSO_4$

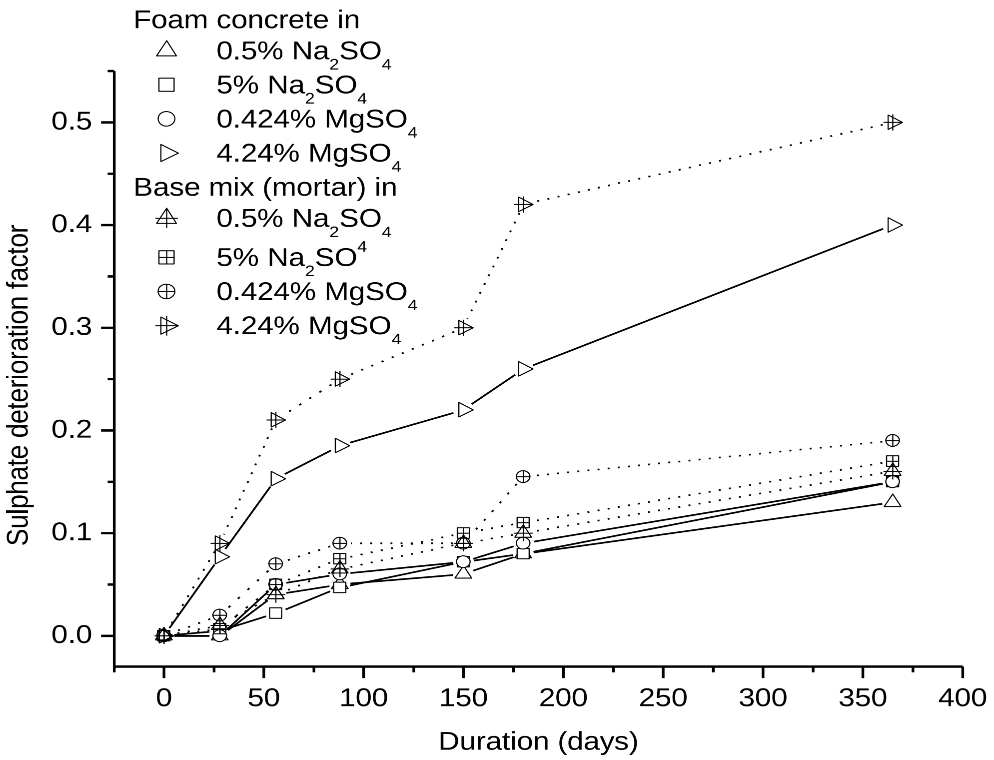

(a) SLS

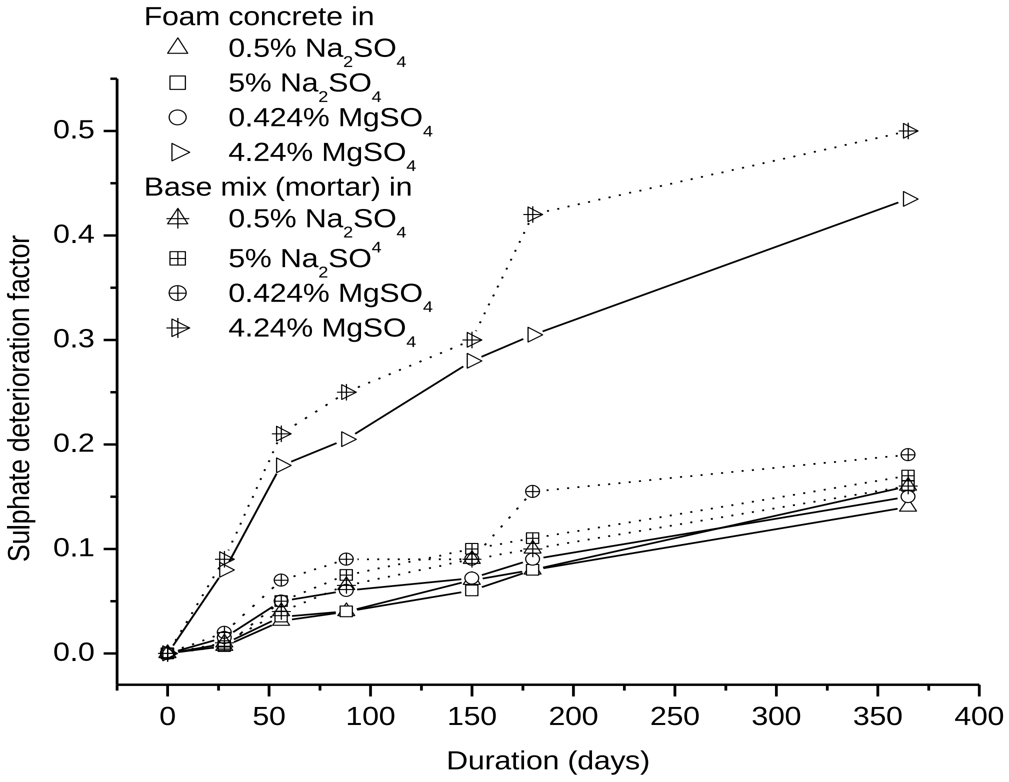

(b) SLES

Fig 8.35 Comparison between SDF under two sulphate environments (1000 kg/m^3)

8.6 SUMMARY

The investigations indicated that the nature of sulphate attack depends on the type of cation present and the concentration of sulphate ion in the solution. The expansion under very severe sulphate environment is 3.5 to 4.5 times higher than that under severe exposure environment due to availability of more sulphate for the expansive sulphate reactions. Hence the intensity of ettringite peak is relatively higher and portlandite peak is lower for foam concrete subjected to very severe sulphate exposure conditions. The sulphate deterioration factor of concrete under very severe exposure magnesium sulphate environment is 70% and 62% higher than that under severe exposure conditions for surfactants SLS and SLES respectively. The XRD analysis indicated the presence of higher intensity of gypsum peaks for specimens under very severe exposure magnesium sulphate environment is responsible for higher SDF and loss in mass of specimens. The nature of deterioration in specimens placed in sodium and magnesium sulphate environment are different indicating that the mechanisms of deteriorations are not similar. Sodium sulphate attacks the structure by causing deleterious expansion as a result of formation of ettringite and hence the expansion % of foam concrete under sodium sulphate environment is 13% and 28% higher than that under magnesium sulphate in severe and very severe exposure conditions respectively. But the major deterioration mechanism in magnesium sulphate environment is softening and disintegration of cementing material and this contributed to higher SDF for specimens in 4.24% magnesium sulphate environment. Under very severe exposure condition loss in mass is observed in magnesium sulphate environment (due to disintegration of specimens) against the increase in mass observed for sodium sulphate environment. Irrespective of the concentration and type of sulphate environment, the expansion, SDF and loss in mass of foam concrete is lower than that of base mix (mortar without foam). Hence it can be concluded that the cell like structure of foamed concrete and possible porosity of the cell walls do not necessarily make the foam concrete less resistant to penetration of aggressive ions. These results still need to be correlated with full scale, long term durability tests.

CHAPTER 9

CONCLUSIONS AND SCOPE FOR FURTHER WORK

9.1 CONCLUSIONS

The salient conclusions arising out of this research work are summarised in this section. The studies on foam concrete described here basically comes under five stages viz.; (i) performance evaluation of different synthetic surfactants; (ii) fresh and hardened properties of foam concrete; (iii) air-void characteristics of foam concrete; (iv) moisture movement behaviour and (v) behaviour under sulphate environment. The conclusions from the experimental investigations are grouped under these five sections, which are applicable to the characteristics of the materials used and the range of parameters investigated.

9.1.1 Performance Evaluation of Different Synthetic Surfactants

i) For all the synthetic ionic surfactants used, the foam density increases with an increase in foam generation pressure and decreases with an increase in surfactant concentration up to a dosage of 4%.

ii) For the non ionic surfactant Cocodiethanolamide the initial foam density increases with an increase in surfactant concentration at lower foam generation pressure with a reverse trend at higher foam generation pressure. Also at higher surfactant concentration the foam density decreases with an increase in foam generation pressure unlike ionic surfactants.

iii) The drainage is proportional to the initial foam density for all the surfactant concentration for ionic surfactants at different foam generation pressures.

iv) At very low surfactant concentration and higher foam generation pressure, though the foam possess high initial density, the stability is poor due to higher drainage. Hence apart from foam density, foam drainage is also an important parameter in the selection of the foaming agent.

v) The optimum surfactant concentration values are 2% and 5% when economy is considered as one of the factors for ionic and non ionic surfactants respectively and the optimum foam generation pressure ranges between 110-120 kPa.

9.1.2 Fresh and Hardened Properties of Foam Concrete

i) For mixes with higher foam volume the adhesion between bubbles and solid particles increases the stiffness of the mix which results in higher water requirement to avoid breakage of bubbles during mixing.

ii) For each foam volume there exists an optimal superplasticiser dosage which results in a mix of desired density (± 50 kg/m^3) with a reduction in water-solids ratio. This optimum dosage of superplasticiser reduces with increase in foam volume as the mixes become unstable at higher dosages of superplasticiser.

iii) Though the addition of superplasticiser results in considerable reduction in water-solids ratio, it does not result in proportionate enhancement in strength because the strength of foam concrete is mainly influenced by the entrained air voids.

iv) The specific strength of foam concrete is higher than the corresponding base mix which indicates that that the increase in modulus of elasticity with strength is proportional for foam concrete than that of the base mix.

v) Tensile strength values of foam concrete of dry densities from 850 to 1215 kg/m^3 ranges between 6 to 9% (split cylinder) and 6 to 13% (flexural) of compressive strength. These lower values of strength is due to the lesser interlocking effect of the hydrated cement paste with the finer sand used.

9.1.3 Air-void Characteristics of Foam Concrete

i) The median circularity varies from 0.65 to 0.9 indicating that practically most of the air-voids are nearly spherical. However a few lower values of 0.2 to 0.3 represents irregular pores produced due to merging of bubbles at higher foam volume.

ii) The median air-void size in foam concrete varies between 106 to 345 microns for foam concrete with fresh density ranging from 1500 to 1000 kg/m^3 and this did not deviate much from the median bubble diameter in foam of 280 microns. This implies that there was not much error in measurement of air voids and also the foam was stable in concrete.

iii) Modified Rosin-Rammler distribution can be evaluated as a method providing easy means of describing the size distribution of air void and bubble in foam concrete and foam. The void sizes when determined based on modified Rosin rammler distribution are higher than the median void sizes calculated based on D50 derived from the plot of cumulative % oversize.

iv) A linear relationship between spacing factors SP50 and SP90 with density and strength are observed for both the surfactants. In general when the density and strength are lower, the spacing between the air voids also reduces due to the increase in foam volume.

v) All the air void parameters studied viz., size factors, shape factors and spacing factors have influence on strength and density. It is observed that the smaller, circular and larger the spacing between voids, the greater is the strength of foam concrete.

9.1.4 Sorption and Shrinkage Behaviour

- Water absorption, sorptivity and drying shrinkage of foam concrete is lower than that of corresponding base mix (mortar without foam) and it reduces with density of foam concrete. This reduction observed in mixes with lower density of foam concrete can be attributed to reduced volume of paste content and thus reduced volume of micro and macro capillary pores which is responsible for above moisture transport mechanisms. The entrained air voids are not interconnected and hence do not contribute to the above transport mechanisms.

- The sorptivity of air-cured foam concrete is 2.5 times higher than that of water cured concrete. Hence the method of curing has significant influence on sorptivity.

- The rate of increase in shrinkage is rapid when the moisture content reduces below 2.5% due to removal of water from very small pores and adsorbed water from gel surface at later stage of drying.

9.1.5 Behaviour under Sulphate Environment

- The expansion under very severe sulphate environment is 3.5 to 4.5 times higher than that under severe exposure environment due to availability of more sulphate for the expansive sulfate reactions. Hence the intensity of ettringite peak is relatively higher and portlandite peak is lower for foam concrete subjected to very severe sulphate exposure conditions.

- The sulphate deterioration factor of concrete under very severe exposure magnesium sulphate environment is 70% and 62% higher than that under severe exposure conditions for surfactants SLS and SLES respectively. The XRD analysis indicates the presence of higher intensity of gypsum peaks for specimens under very severe exposure magnesium sulphate environment, which is responsible for higher SDF and loss in mass of specimens.

- Sodium sulphate attacks the structure by causing deleterious expansion as a result of formation of ettringite and hence the expansion % of foam concrete under sodium sulphate environment is 13% and 28% higher than that under magnesium sulphate in severe and very severe exposure conditions respectively.

- The major deterioration mechanism in magnesium sulfate environment is softening and disintegration of cementing material and this contributed to higher SDF for specimens in 4.24% magnesium sulphate environment. Under very severe exposure condition loss in mass is observed in magnesium sulphate environment (due to disintegration of specimens) against the increase in mass observed for sodium sulphate environment.

- Irrespective of the concentration and type of sulphate environment, the expansion, SDF and loss in mass of foam concrete is lower than that of base mix (mortar without foam). The higher deterioration of base mix can be attributed to higher paste content which is more susceptible to permeation mechanism of sulphate ions.

9.2 SCOPE FOR FURTHER WORK

This study forms an initial part in the ensuing long-term investigations on foam concrete. The areas on which continued research can be undertaken to provide better understanding of the material and thus be of more use to the construction industry are:

i) Investigations on new additives that could enhance the performance of foam in terms of density and stability can be carried out.

ii) Investigations on functional characteristics of foam concrete namely thermal conductivity and sound transmission can be undertaken. The effect of density of foam concrete on the functional characteristics and its comparison with normal weight concrete can be studied.

iii) Methods of reducing shrinkage of foam concrete by incorporation of light weight coarse aggregates can be investigated. A comparative study on the shrinkage of autoclaved concrete and moist cured foam concrete can be made.

iv) Studies on optimum dosage of fibres to enhance the performance with respect to tensile and flexural strength of foam concrete without affecting the fresh state behaviour can be carried out.

v) Studies on identification of more compatible chemical admixtures in foam concrete to reduce the water-solids ratio requirement can be carried out. Also the effect of superplasticiser on shrinkage and sorption behaviour can be analysed.

vi) Standard test methods available to test the resistance of normal weight concrete to chloride environment can be checked for its suitability to foam concrete. Also studies on resistance of foam concrete to acidic environment can be conducted.

vii) In order to integrate foam concrete into residential concrete, studies can be made on properties of light weight blocks, wall panels and lightweight reinforced foam concrete.

REFERENCES

1. **ACI 318-99** Building code requirements for structural concrete. *American Concrete Institute*., Farmington hills, Michigan, USA, 1999.

2. **ACI 523.1R-1992** Guide for Cast-in-place low density concrete. *American Concrete Institute*, 1992.

3. **ACI committee 523** (1975) Guide for cellular concretes above 50 pcf, and for aggregate concretes above 50 pcf with compressive strengths less than 2500 psi. *ACI Journal*, **72**. 50-66.

4. **Al-Amoudi, O.S.B.** (2002) Attack on plain and blended cements exposed to aggressive sulfate environments. *Cement and Concrete Composites*, **24**, 305-316.

5. **Al-Amoudi, O.S.B., M. Maslehuddin and M. Saadi** (1995) Effect of magnesium sulfate and sodium sulfate on the durability performance of plain and blended cements. *ACI Material Journal*, **92**, 15-24.

6. **Aldridge, D.** (2000) Foamed concrete. *Concrete*, **34**, No.4, 20-22

7. **Aldridge, D. and T. Ansell** (2001) Foamed concrete: Production and equipment design, properties, applications and potential, Proceedings of *One Day Seminar on Foamed Concrete: Properties. Applications and Latest Technological Developments*, Loughborough University, July, 1-11.

8. **Aldridge, D.** *Introduction to foamed concrete What, Why, and How?* pp. 1-14 *In* **R.K. Dhir, M.D. Newlands,** and **A. McCarthy** (eds.) *Use of Foamed Concrete in Construction*, Thomas Telford, London, 2005.

9. **Al-Dulaijan, S.U., M. Maslehuddin, M.M. Al-Zahrani, A.M. Sharif, M. Shameen and M. Ibrahim** (2003) Sulphate resistance of plain and blended cements exposed to varying concentrations of sodium sulphate. *Cement and Concrete Composites*, ***25,*** 429-437.

10. **ASTM C 1202** (1997) Standard test method for electrical indication of concrete’s ability to resist chloride ion penetration. *American Society of Testing and Materials*, Philadelphia.

11. **ASTM C 230** (1998) Specification for flow table for use in tests of hydraulic cement. *American Society of Testing and Materials*, Philadelphia.

12. **ASTM C 469** (1994) Test method for Static Modulus of Elasticity and Poisson’s Ratio of Concrete in compression. *American Society of Testing and Materials*, Philadelphia.

13. **ASTM C 495** (1991) Test method for compressive strength of lightweight insulating concrete. *American Society of Testing and Materials*, Philadelphia.

14. **ASTM C 496** (1996) Test method for splitting tensile strength of cylindrical concrete specimens. *American Society of Testing and Materials*, Philadelphia.

15. **ASTM C 596** (2009) Standard test method for drying shrinkage of mortar containing hydraulic cement *American Society of Testing and Materials*., Philadelphia.

16. **ASTM C 642** (1997) Standard test method for density, absorption, and voids in hardened concrete. *American Society of Testing and Materials*, Philadelphia.

17. **ASTM C 796** (1997) Standard test method for foaming agents for use in producing cellular concrete using preformed foam. *American Society of Testing and Materials*, Philadelphia.

18. **ASTM C 869 (**1991) Specification for foaming agents used in making preformed foam for cellular concrete. *American Society of Testing and Materials*, Philadelphia.

19. **Attiogbe, E.K.** (1993) Mean spacing of air voids in hardened concrete. *ACI Material Journal*, **90,** 174-181.

20. **Basiurski, J. and D. Wells** (2001) The use of foamed concrete in construction and civil Engineering, *Conspectus* 2001, 64-73.

21. **Beningfield, N., R. Gaimster, and P. Griffin**. *Investigation into the air-void characteristics of foamed concrete*. pp. 51-60 *In* **R.K. Dhir, M.D. Newlands,** and **A. McCarthy** (eds.) *Use of Foamed Concrete in Construction*, Thomas Telford, London. 2005.

22. **Brown, P., R.D. Hooton and B. Clark** (2004) Microstructural changes in concretes with sulfate exposure. *Cement and Concrete Composites*, **26**, 993-999.

23. **BS 1881 Part: 118** (1983) Method for determination of flexural strength. *British Standard Institution*, London.

24. **Byun, K.J., H.W. Song and S.S. Park (1998)** Development of structural lightweight foamed concrete using polymer foam agent. *ICPIC-98*.

25. **Cabrillac, R. and Z. Malou** (2000) Mechanical modelization of anisotropic porous materials with a homogenization method. Application to aerated concretes. *Construction and Building Materials*, **14**, 25-33.

26. **Cabrillac, R., B. Fiorio, A. Beaucour, H. Dumontet and S. Ortola** (2006) Experimental study of the mechanical anisotropy of aerated concrete and of the adjustment parameters on the induced porosity. *Construction and Building Materials*, **20**, 286-95.

27. **Cao H.T., L. Bucea, A. Ray and S. Yozghatlian** (1997) The effect of cement composition and pH of environment on sulfate resistance of Portland cements and blended cements. *Cement and Concrete Composites*, **19**, 161-171.

28. **Chan, S.Y.N and X. Ji** (1998) Water sorptivity and chloride diffusivity of oil shale ash concrete. *Construction and building materials,* **12**, 177-183.

29. **Chatterji, S. and H. Gudmundsson** (1977) Characterization of entrained air bubble systems in concrete by means of an image analyzing microscope. *Cement and Concrete Research,* **7,** 423-428.

30. **Chen, J. and M. Jiang** (2008) Long–term evolution of delayed ettringite and gypsum in Portland cement mortars under sulfate erosion. *Construction and Building Materials,* **23**, 812-816.

31. **Cohen, M.D and B. Arnon** (1988) Durability of Portland Cement- Silica Fume Pastes in Magnesium sulfate and Sodium sulfate solutions. *ACI Material Journal,* **85-M3**, 148-157.

32. **Colak, A. (2000)** Density and strength characteristics of foamed gypsum. *Cement and Concrete Composites,* **22,** 192-200.

33. **Cox, L. and S. VanDijk** (2002) Foam concrete- a different kind of mix. *Concrete*, February, 54-55.

34. **De Rose, L. and J. Morris** *The influence of mix design on the properties of micro-cellular concrete,* pp. 185-197 *In* **R.K. Dhir** and **N.A. Handerson** (eds.) *Specialist Techniques and Materials for Construction,* Thomas Telford, London, 1999.

35. **Defence Standard 42-40** (2002) Foam liquids, Fire Extinguishing (Concentrates, foam, fire extinguishing), *Ministry of Defence*, United Kingdom..

36. **Dias, W.P.S.** (2000) Reduction of concrete sorptivity with age through carbonation. *Cement and Concrete Research,* **30**, 1255-1261.

37. **Dias, W.P.S.** (2004). Influence of drying on concrete sorptivity. *Magazine of Concrete Research,* **56**, 537-543.

38. **Durack, J.M. and L. Weiqing** (1998) The properties of foamed air cured fly ash based concrete for masonry production. Proceedings of 5th *Australian Masonry Conference,* Gladstone, Queensland, Australia, June. 129-138.

39. **Ferraris, C.F., J.R. Clifton, P.E. Stutzman and E.J. Garboczi** *Mechanisms of degradation of Portland-Cement based systems by sulfate attack*. pp. 185-192. *In:* **K.L. Scrivener and J.F. Young** (eds.) Mechanisms of chemical degradation of cement-based systems, E & FN Spon, London, 1997.

40. **Fujiwara, H., E. Sawada, and Y. Ishikawa** *Manufacturing of high strength aerated concrete containing silica fume.* pp.779-91. *In* **V.M. Malhotra**, (ed.) Proceedings of Fifth *International Conference on Fly ash, Silica fume, Slag and Natural pozzolana in concrete,* SP 153, V.2, American Concrete Institute, Farmington Hills, 1995.

41. **Giannakou, A and M.R. Jones** *Potentials of foamed concrete to enhance the thermal performance of low rise dwellings*, pp. 533-544 *In* **R.K. Dhir, P.C. Hewelett and L.J. Csetenyi** (eds.) *Innovations and Development in Concrete materials and Construction*, Thomas Telford, U.K, 2002.

42. **Goual, M.S., F.de. Barquin, M.L. Benmalek, A. Bali, and M. Queneudec** (2000) Estimation of the capillary transport coefficient of Clayey aerated concrete using gravimetric technique. *Cement and Concrete Research*, **30**, 1559-63.

43. **Hall, C.** (1989) Water sorptivity of mortar and concretes: A review. *Magazine of Concrete Research*, **41**, 51-61.

44. **Hamidah, M.S., I. Azmi, M.R.A. Ruslan, K. Kartini and N.M. Fadhil** *Optimisation of Foamed Concrete mix of Different Sand – cement ratio and curing conditions*. pp. 37-44. *In* **R.K. Dhir, M.D. Newlands,** and **A. McCarthy** (eds.) *Use of Foamed Concrete in Construction*, Thomas Telford, London, 2005.

45. **Hoff, G.C.** (1972) Porosity-strength considerations for cellular concrete. *Cement and Concrete Research*, **2**, 91-100.

46. **Hunaiti, Y.M.** (1996) Composite action of foamed and lightweight aggregate concrete. *Journal of Materials in Civil Engineering*, **8**, No.3, 111-113.

47. **Hunaiti, Y.M.** (1997) Strength of composite sections with foamed and lightweight aggregate concrete. *Journal of Materials in Civil Engineering*, **9**, No.2, 58-61.

48. **Hutzler.S., S.J. Cox** and **G. Wang** (2005) Foam drainage in two dimensions *Colloids and Surfaces: A Physico Chem.Eng.Aspects*, **263**, 178-183.

49. **Image J** http://rsb.info.nih.gov/ U.S. National Institutes of Health, Bethesda, MD, USA (visited on 1/08/2006).

50. **IS 12269** (1987), Specification for 53 grade Ordinary Portland Cement, *Bureau of Indian Standards*, BIS, New Delhi, India.

51. **Jalmes, A.S., M.L Peugeot, H. Ferraz and D. Langevin** (2005) Differences between protein and surfactant foams: Microscopic properties, stability and coarsening, *Colloids and Surfaces: A Physico Chem.Eng.Aspects*, **263**, 219-225.

52. **Jones, M.R.** (2001) Foamed concrete for structural use, Proceedings of *One Day Seminar on Foamed Concrete: Properties. Applications and Latest Technological Developments*, Loughborough University, July. 27-60.

53. **Jones, M.R. and A. McCarthy** (2005a) *Behaviour and assessment of foamed concrete for construction applications*. pp. 61-88. *In* **R.K. Dhir, M.D. Newlands, and A. McCarthy** (eds.) *Use of Foamed Concrete in Construction*, Thomas Telford, London, 2005.

54. **Jones, M.R. and A. McCarthy** (2005b) Preliminary views on the potential of foamed concrete as a structural material. *Magazine of Concrete Research*, **57**, 21-31.

55. **Jones, M.R. and A. McCarthy** (2005c) Utilising unprocessed low-lime coal ash in foamed concrete. *Fuel*, **84**, 1398-1409.

56. **Jones, M.R. and A. McCarthy** (2006) Heat of hydration in foamed concrete: Effect of mix constituents and plastic density. *Cement and Concrete Research*, **36**, No.6, 1032-41.

57. **Jones, M.R., A. McCarthy, and R.K. Dhir** (2005) Recycled and secondary aggregate in foamed concrete, *WRAP Research Report*, The Waste and Resources Action Programme, Banbury, Oxon OX16 0AH.

58. **Jones, M.R., M.J. McCarthy, and A. McCarthy** (2003) Moving fly ash utilization in concrete forward: a U K perspective, Proceedings of *the 2003 International Ash Utilisation Symposium*, Centre for Applied Energy Research, University of Kentucky, October. 20-22.

59. **Jones, R. and A. Giannakou** (2002) Foamed concrete for energy-efficient foundations and ground slabs. *Concrete*, March, 14-17.

60. **Justnes, H.** (2003) Thaumasite followed by sulphate attack on mortar with limestone filler. *Cement and Concrete Composites*, **25**, 955-959.

61. **Karl, S. and J.D. Worner** *Foamed concrete – mixing and workability*. pp 217-224. ***In*** **P.J.M. Bartos** (ed.) *Special Concrete – Workability and Mixing*, E&FN Spon, London, 1993.

62. **Kearsely, E.P. and H.F. Mostert** (1997) Use of Foam concrete in Southern Africa, Proceedings from *The ACI International Conference on High Performance Concrete*, SP 172-48, 919-934.

63. **Kearsely, E.P. and M. Visagie** *Micro-properties of foamed concrete*. pp 173-184. *In* **R.K. Dhir and N.A. Handerson** (eds.) *Specialist Techniques and Materials for Construction*, Thomas Telford, London, 1999.

64. **Kearsley, E.P. and H.F. Mostert** *Designing mix composition of foamed concrete with high fly ash contents*. pp 29-36. *In* **R.K. Dhir, M.D. Newlands, and A. McCarthy** (eds.) *Use of Foamed Concrete in Construction,* Thomas Telford, London, 2005a.

65. **Kearsley, E.P. and H.F. Mostert** *The use of foamed concrete in refractories*. pp 89-96 *In* **R.K. Dhir, M.D. Newlands, and A. McCarthy** (eds.) *Use of Foamed Concrete in Construction*, Thomas Telford, London, 2005b.

66. **Kearsley, E.P. and P.J. Booyens** (1998) Reinforced foamed concrete, can it be durable. *Concrete/Beton*, **91**, 5-9.

67. **Kearsley, E.P. and P.J. Wainwright** (2001a) The effect of high fly ash content on the compressive strength of foamed concrete. *Cement and Concrete Research*, **31**, 105-112.

68. **Kearsley, E.P. and P.J. Wainwright** (2001b) Porosity and permeability of foamed concrete. *Cement and Concrete Research*, **31**, 805-812.

69. **Kearsley, E.P. and P.J. Wainwright** (2002a) Ash content for optimum strength of foamed concrete. *Cement and Concrete Research*, **32**, 241-246.

70. **Kearsley, E.P. and P.J. Wainwright** (2002b) The effect of porosity on the strength of foamed concrete. *Cement and Concrete Research*, **32**, 233-239.

71. **Kearsley, E.P.** *Just foamed concrete – an overview*. pp. 227-237. *In* **R.K. Dhir and N.A. Handerson** (eds.) *Specialist Techniques and Materials for Construction*, Thomas Telford, London, 1999.

72. **Kearsley, E.P.** *The use of foamed concrete for affordable development in third world countries*. pp 233-243. *In* **R.K. Dhir and M.J. McCarthy** (eds.) *Appropriate Concrete Technology*, E&FN Spon, London, 1996.

73. **Khatri, R.P., V. Sirivivatnanon and L.K. Yu** (1977) Effect of curing on water permeability of concretes prepared with normal Portland cement and with slag and silica fume. *Magazine of Concrete Research*, 49, 167-172.

74. **Koudriashoff, I.T.** (1949) Manufacture of reinforced foam concrete roof slabs. *Journal of the American Concrete Institute*, 37-48.

75. **Kurtis, K.E., P.J.M. Monteiro, J.T. Brown, W. Meyer-Ilse** (1998) Mechanisms of concrete damage caused by sulfate attack examined through Transmission X-ray Microscopy. http://www.als.lbl.gov/als/compendium/ (visited on 17/02/2011)

76. **Kyle, D.** (2001) Manufacture and supply of Ready mix C4 top foamed concrete, Proceedings of *One Day Seminar on Foamed Concrete: Properties. Applications and Latest Technological Developments*, Loughborough University, July. 19-26.

77. **Lange, A.D.** (1994) Image analysis techniques for characterization of pore structure of cement – based materials. *Cement and Concrete Research*, **24**, 841-853.

78. **Laukaitis, A., R. Zurauskas** and **J. Keriene** (2005) The effect of foam polystyrene granules on cement composite properties, *Cement and Concrete Composites*, **27**, 41-47.

79. **Laukitis, A. and B. Fiks** (2006) Acoustical properties of aerated autoclaved aerated concrete. *Applied acoustics*, **67,** 284-96.

80. **Laundess, A.J., M.S. Rayson, B.Z. Dlugogorski and E.M. Kennedy** (2009) Small-scale test protocol for fire fighting foams DEF (AUST) 5706: Effect of bubble size distribution and Expansion ratio. *Fire Technology*. doi: 10.1007/s10694-009-0136-2.

81. **Lawrence, C.D.** (1990) Sulphate attack on concrete. *Magazine of Concrete Research* **42**, 249-264.

82. **Lee, Y.L. and Y.T. Hung** *Exploitation of Solid Wastes with Foamed Concrete*. pp. 15-22. *In* **R.K. Dhir, M.D. Newlands,** and **A. McCarthy** (eds.) *Use of Foamed Concrete in Construction*, Thomas Telford, London, 2005.

83. **Liew, A.C.M** *New innovative lightweight foam concrete technology*. pp. 45-50. *In* **R.K. Dhir, M.D. Newlands,** and **A. McCarthy** (eds.) *Use of Foamed Concrete in Construction*, Thomas Telford, London, 2005.

84. **Lohaus, L. and J.U. Pott** (2003) Structural Lightweight Concrete with combined grain and matrix porosity. Proceedings of the *International Symposium Celebrating Concrete- Role of Concrete in Sustainable development*, Dundee, September. 547-555.

85. **Luping, T.** (1986) A study of the quantitative relationship between strength and pore size distribution of porous materials. *Cement and Concrete Research,* **16,** 87-96.

86. **Madjoudj, M., M. Quenendec, and R.M. Dheilly** *Water capillary absorption of cellular clayed concrete obtained by proteinic foaming*. pp. 513-521. *In* **R.K. Dhir, P.C. Hewelett** and **L.J. Csetenyi** (eds.) Innovations and Development in Concrete materials and Construction, Thomas Telford, U.K, 2002.

87. **Magrabi, S.A., B.Z. Dlugogorski, G.J. Jameson** (2001) Free drainage in aqueous foams: Model and Experimental study. *AIChE Journal*, **47,** 314-327.

88. **Magrabi, S.A, B.Z. Dlugogorski, G.J. Jameson** (2002) A comparative study of drainage characteristics in AFFF and FFFP compressed-air fire-fighting foams. *Fire Safety Journal*, **37**, 21-52.

89. **Malou, Z., R. Cabrillac, A. Beaucour, B. Fiorio and H. Dumontet** *Experimental study of the lightening phenomenon and the mechanical anisotropy in aerated concretes.* pp. 503-512. *In* **R.K. Dhir, P.C. Hewelett** and **L.J. Csetenyi** (eds.) *Innovations and Development in Concrete materials and Construction,* Thomas Telford, U.K, 2002

90. **Marze S.P.L., A.S. Jalmes and D. Langeven** (2005) Protein and surfactant foams: linear rheology and dilatancy effect. *Colloids and Surfaces A:Physicochem.Eng.Aspects,* **263**, 121-128.

91. **McCarter, W.J., H. Ezirim and M. Emerson** (1992) Absorption of water and chloride into concrete. *Magazine of Concrete Research,* **44**, 31-37.

92. **McCormick, F.C.** (1967) Rational proportioning of preformed foam cellular concrete. *ACI Material Journal*, **64**, 104-109.

93. **Mehta, P.K. and P.J.M. Monteiro** *Concrete: Structure, Properties and Materials*, Prentice Hall, New Jersey, 1993.

94. **Mirza, H.W. and S. Al-Noury** (1986) Utilisation of Saudi sands for aerated concrete production. *The International Journal of Cement Composites and Lightweight concrete*, **8**, 81-85.

95. **Montgomery, D.C.** (2001) *Design and analysis of experiments*. Wiley, New York.

96. **Moon, H., S. Lee , H. Kim and S. Kim** (2002**)** Experimental study on the sulfate resistance of concrete blended Ground granulated blast furnace slag for recycling. *Geosystem Engineering*, 5, 67-73.

97. **Myers**, D. *Surfactant Science and Technology*. VCH Publishers, NewYork, 1998.

98. **Nambiar** (2006). Influence of composition and pore parameters on properties of preformed foam concrete, *PhD Thesis, Indian Institute of Technology, Madras.*

99. **Nambiar, E.K.K. and K. Ramamurthy** (2006a) Influence of filler type on the properties of foam concrete. *Cement and Concrete Composites*, **28**, 475-480.

100. **Nambiar, E.K.K. and K. Ramamurthy** (2006b) Models relating mixture composition to the density and strength of foam concrete using response surface methodology. *Cement and Concrete Composites*, **28**, 752-760.

101. **Nambiar, E.K.K. and K. Ramamurthy** (2006c) Air-void characterization of foam concrete. *Cement and Concrete Research*, **37**, 221-30.

102. **Nambiar, E.K.K. and K. Ramamurthy** (2007) Sorption characteristics of foam concrete. *Cement and Concrete Research*, **37,** 1341-47.

103. **Nambiar, E.K.K. and K. Ramamurthy** (2008a). Fresh state characteristics of foam concrete. *ASCE Materials in Civil Engineering*, **20**, 111-117.

104. **Nambiar, E.K.K. and K. Ramamurthy** (2008b). Models for strength prediction of foam concrete. *Materials and Structures*, **41**, 247-54.

105. **Nambiar, E.K.K. and K. Ramamurthy** (2009). Shrinkage behaviour of foam concrete. *Journal of Materials in Civil Engineering*, **21**, 631-636.

106. **Narayanan, N. and K. Ramamurthy** (2000) Microstructural investigations on aerated concrete. *Cement and Concrete research*, **30,** 457-64.

107. **Nehdi, M., Y. Djebbar, and A. Khan** (2001) Neural Network Model for preformed foam cellular concrete. *ACI Material Journal*, **98**, 402-409.

108. **Nmai, C.K., F. McNeal, and D. Martin** (1997) New foaming agent for CLSM applications. *Concrete International*, April. 44-47.

109. **Papayianni, I. and I.A. Milud** *Production of Foamed Concrete with High Calcium Fly Ash*. pp. 23-28. *In* **R.K. Dhir, M.D. Newlands,** and **A. McCarthy** (eds.) *Use of Foamed Concrete in Construction*, Thomas Telford, London, 2005.

110. **Park, S.B., E.S Yoon** and **B.I. Lee** (1999a) Effects of processing and materials variations on mechanical properties of lightweight composites, *Cement and Concrete Research,* **29**, No.2, 193-200.

111. **Park, Y., J. Suh , J. Lee and Y. Shin** (1999). Strength deterioration of high strength concrete in sulfate environment. *Cement and Concrete Research*, **29**, 1397-1402.

112. **Paul**, Aqueous foam–Technology and Systems development http://www.aquafoam.com/NDIA2000.html (visited on 15/05/2007).

113. **Perez, L.E.B. and L.A.B. Cortez (1997)** Potential for use of pyrolytic tar from baggase in industry**,** *Biomass and Bioenergy,* **12**, 5,363-366.

114. **Petrov, I. and E. Schlegel** (1994) Application of automatic image analysis for the investigation of autoclaved aerated concrete structure. *Cement and Concrete Research,* **24**, 830-840.

115. **Philleo, R.E** (1983) A method for analyzing void distribution in air entrained concrete. *Cement, Concrete and Aggregates,* **5,** 128-130.

116. **Pickford, C. and S. Crompton** (1996) Foam concrete in bridge construction. *Concrete*, December, 14-15.

117. **Pleau, R., M. Pigeon and J. Laurencot** (2001) Some findings on the usefulness of image analysis for determining the characteristics of the air-void system on hardened concrete. *Cement Concrete and Composites,* **23**, 237-246.

118. **Pleau R., R. Plante, M. Gagne and Pigeon** (1990) Practical considerations pertaining to the microscopical determination of air-void characteristics of hardened concrete (ASTM C 457 standard), *Cement, Concrete and Aggregates,* **12,** 3-11.

119. **Prasad, J., D.K. Jain and A.K. Ahuja** (2006). Factors influencing the sulphate resistance of cement concrete and mortar. *Asian Journal of Civil Engineering. (Building & housing)*, **7,** 259-268.

120. **Prim and Wittmann** (1983) *Structure and water absorption of aerated concrete*. pp. 43-53. *In* **F.H. Wittmann** (ed.). *Autoclaved Aerated Concrete, Moisture and Properties*, Elsevier, Amsterdam, 1983.

121. **Proshin, A., V.A Beregovoi, A.M. Beregovoi and A. Eremkin** *Unautoclaved Foam concrete and its constructions, Adopted to the regional conditions.* pp.113-120. *In* **R.K. Dhir, M.D. Newlands** and **A. McCarthy** (eds.) *Use of Foamed Concrete in Construction*, Thomas Telford, London, 2005.

122. **Pugh, R.J.** (1996) Foaming, foam films, antifoaming and defoaming, *Advances in Colloid and Interface Science*, 64, 67-142.

123. **Quebaud S., M. Sibai and J.P Henry** (1998) Use of chemical foam for improvements in drilling by earth – pressure balanced shields in granular soils. *Tunnelling and Underground Space Technology,* **13**, 173-180.

124. **Ramakrishnan, K.N.** (2000) Modified Rosin Rammler equation for describing particle size distribution of milled powders. *Journal of Material Science and letters,* **19**, 1903-1906.

125. **Ramamurthy, K., E.K.K. Nambiar and G.I.S Ranjani** (2009) A Classification of studies on properties of foam concrete. *Cement and Concrete Composites,* **31**, 6, 388-396.

126. **Ranjani, G.I.S. and K. Ramamurthy** (2010) Relative assessment of density and stability of foam produced with four synthetic surfactants. *Materials and Structures,* **43**, 1317-1325.

127. **Rasheeduzzafar, F.H. Dakhil, S. Al-Gahtani , SS. Al-Saadoun and M.A. Bader** (1990) Influence of cement composition on the corrosion of reinforcement and sulfate resistance of concrete. *ACI Material Journal,* **87**, 114-122.

128. **Regan, P.E. and A.R. Arasteh** (1990) Lightweight aggregate foamed concrete. *Structural Engineer*, **68**, No.9, 167-173.

129. **Richard, T.G.** (1977) Low temperature behaviour of cellular concrete. *ACI Journal*, **74**, 173-178.

130. **Richard, T.G., J.A. Dobogai, T.D. Gerhardt, and W.C. Young** (1975) Cellular concrete - A potential load-bearing insulation for cryogenic applications. *IEEE Transactions on Magnetics*, **11**, No.2, 500-503.

131. **Rudnai, G.** *Lightweight concretes*. Budapest, Akademikiado, 1963.

132. **Sahmaran, M., O. Kasap , K. Duru and I.O. Yaman** (2007) Effect of mix composition and water-cement ratio on the sulfate resistance of blended cements. *Cement and Concrete Composites,* **29,** 159-167.

133. **Santhanam. M., M.D. Cohen and J. Olek** (2003) Effects of gypsum formation on the performance of cement mortars during external sulphate attack. *Cement and Concrete Research*, **33**, 325-332.

134. **Sarma, D.S.H.S., J. Pandit, K.C. Khilar** (1988) Enhancement of stability of aqueous foams by addition of water soluble polymers – Measurement and Analysis. *Journal of Colloids and Interface Sciences*, **124,** 339-348.

135. **SAS Release 8.02**, SAS Institute Inc., Cary, NC, USA.

136. **Schubert, P.** *Shrinkage behaviour of aerated concrete.* pp 207-217. *In* **F.H. Wittmann** (ed.). *Autoclaved Aerated Concrete, Moisture and Properties*, Elsevier. Amsterdam, 1983.

137. **Shannag, M.J. and H.A. Shaia** (2003) Sulfate resistance of high performance concrete. *Cement and Concrete Composites*, **25**, 363-369.

138. **Short, A. and W. Kinniburgh** *Lightweight concrete*. Asia Publishing House, 1963.

139. **Shrivastava, O.P**(1977) Lightweight aerated concrete-a review. *Indian Concrete Journal*, **51**, 10-23.

140. **Singh, G.B.** (2002) Fast and economical housing using cellular lightweight concrete. http://www.techno-preneur.Net/timeis/technology/SciTechFeb02/economocal.html. (visited on 12/08/2007).

141. **Snyder, K.A.** (1998) A numerical test of air void spacing equations. *Advances in cement based materials*, **8**, 28-44.

142. **Soroushian, P. and M. Elzafraney** (2005) Morphological operations, planar mathematical formulations, and stereological interpretations for automated image analysis of concrete microstructure. *Cement and Concrete Composites*, **27,** 823-833.

143. **Tada, S.** (1986) Material design of aerated concrete-an optimum performance design. *Materials and Construction*, **19**, 21-26.

144. **Tada, S. and S. Nakano** (1983) *Microstructural approach to properties of mist cellular concrete*. pp 71-88 *In* **F.H. Wittmann** (ed.). *Autoclaved Aerated Concrete, Moisture and Properties*, Elsevier, Amsterdam, 1983.

145. **Tam, C.T., T.Y. Lim, and S.L. Lee** (1987) Relationship between strength and volumetric composition of moist-cured cellular concrete. *Magazine of Concrete Research*, **39**, 12-18.

146. **Tan, S.N., D. Fornaseiro, R. Sedev** and **J. Ralston** (2005) The role of surfactant structure on foam behaviour. *Colloids and Surfaces : A Physico Chem.Eng.Aspects*, **263** , 233-238.

147. **Tasdemir C.** (2003). Combined effects of mineral admixtures and curing conditions on the sorptivity coefficient of concrete. *Cement and Concrete Research* **33**, 1637-1642.

148. **Taylor W.H.** *Concrete Technology and Practice*. Angus and Robertson, London, 1969.

149. **Thokchom, S., P. Ghosh and S. Ghosh** (2010) Performance of fly ash based geopolymer mortars in sulphate solution. *Journal of Engineering Science and Technology review*, **3**, 36-40.

150. **Tian, B. and M.D. Cohen** (2000) Does gypsum formation during sulfate attack on concrete lead to expansion? *Cement and Concrete Research*, **30**, 117-123.

151. **Tikaisky, P.J., J. Pospisil, and W. MacDonald** (2004) A method for assessment of the freeze-thaw resistance of preformed foam cellular concrete. *Cement and Concrete Research*, **34**, No.5, 889-893.

152. **Turner, M.** (2001) Fast set foamed concrete for same day reinstatement of openings in highways, Proceedings of *One Day Seminar on Foamed Concrete: Properties. Applications and Latest Technological Developments*, Loughborough University, July. 12-18.

153. **Valore, R.C.** (1954a) Cellular concrete Part 1 Composition and methods of production. *ACI Journal*, **50**, 773-796.

154. **Valore, R.C.** (1954b) Cellular concrete Part 2 Physical properties. *ACI Journal*, **50**, 817-836.

155. **Van Deijk, S.** (1991) Foam concrete. *Concrete*, August, 49-53.

156. **Visagie, M. and E.P. Kearsely** (2002) Properties of foamed concrete as influenced by air-void parameters. *Concrete/Beton*, **101**, 8-14.

157. **Watson, K.L**.(1980) Autoclaved aerated concrete from slate waste Part 2: Some property/porosity relationship. *The International Journal of Lightweight Concrete*, **2**, No.3, 121-123.

158. **Wee, T.H., D.S. Babu, T. Tamilselvan and H.S. Lin** (2006) Air-void systems of foamed concrete and its effect on mechanical properties. *ACI Materials Journal*, **103**, No.1, 45-52.

159. **Weigler, H. and S. Karl** (1980) Structural lightweight aggregate concrete with reduced density – Lightweight aggregate foamed concrete. *The International Journal of Lightweight Concrete*, **2**, 101 – 104.

160. **Wilde, P.J.** (1996) Foam measurement by the micro-conductivity technique: An assessment of its sensitivity to interfacial and environmental factors. *Journal of Colloids and Interface Sciences*, **178,** 733-739.

161. **Wilson, M.A., W.D. Hoff, and C. Hall** (1991) Water movement in porous building materials - Absorption from a small cylindrical cavity. *Building and Environment*, **26**, 143-152.

162. **Yamamoto M., Y. Honda, A. Ogawa and K. Rokugo** *Fiber Reinforced Foamed Mortar with Multiple Cracks in Flexure.* pp.75-82G. *In* **Fischer** and **V. C. Li** (eds.) International RILEM Workshop on *High Performance Fiber Reinforced Cementitious Composites in Structural Applications* , RILEM Publications SARL, Japan,1999.

163. **Ziembicka, H**. (1977). Effect of micropore structure on cellular concrete shrinkage. *Cement and Concrete Research,* **7,** 323-332.

LIST OF PAPERS SUBMITTED ON THE BASIS OF THIS THESIS

1. **K. Ramamurthy, E.K. Kunhanandan Nambiar and G. Indu Siva Ranjani** (2009). A Classification of studies on properties of foam concrete. *Cement and Concrete Composites,* **31**, 6, 388-396.

2. **G. Indu Siva Ranjani and K. Ramamurthy** (2010). Analysis of foam generated using surfactant Sodium lauryl sulfate. *International Journal of Concrete Structures and Materials,* **4**, 55-62

3. **G. Indu Siva Ranjani and K. Ramamurthy** (2010). Relative assessment of density and stability of foam produced with four synthetic surfactants. *Materials and Structures,* **43**, 1317-1325.

4. **G. Indu Siva Ranjani G and K. Ramamurthy**. Evaluation of synthetic based preformed foam concrete. Proceedings of *4th International Conference & Exhibition on ICI-IWC,* New Delhi, 2008.

5. **G. Indu Siva Ranjani and K. Ramamurthy**. Linear expansion behaviour of foam concrete under sulphate environment. *Cement and Concrete Composites* (under review).

6. **G. Indu Siva Ranjani and K. Ramamurthy**. Investigations on mass and strength reduction in foam concrete under sulphate environment. *Cement and Concrete Composites* (under review).

7. **G. Indu Siva Ranjani and K. Ramamurthy**. Analysis of air-void system in foam concrete with two synthetic surfactants using image analysis technique. *Magazine of concrete research* (under review).

8. **G. Indu Siva Ranjani and K. Ramamurthy**. Sorption and shrinkage behavior of moist-cured preformed foam concrete with synthetic surfactants. *Materials and Structures* (under review).